HMGB1 Controls ARTD1 Function during Stress Signaling

Dissertation

zur

Erlangung der naturwissenschaftlichen Doktorwürde

(Dr. sc. nat.)

vorgelegt der

Mathematisch-naturwissenschaftlichen Fakultät

der

Universität Zürich

von

Anneli Andersson

aus

Schweden

Promotionskomitee

Prof. Dr. Dr. Michael O. Hottiger

(Vorsitz und Leitung der Dissertation)

Prof. Dr. Anne Müller

PD Dr. Hans-Dietmar Beer

Prof. Dr. Marco Bianchi

Zürich 2016

Summary

Protein ADP-ribosylation is a post-translational modification involved in multiple biological processes, such as differentiation, inflammatory signaling, metabolism and cancer. The best studied ADP-ribosyltransferase (ART), nuclear protein ARTD1, catalyzes the addition of poly-ADP-ribose (PAR) onto target proteins, which influences local chromatin condensation and thereby affects transcription, replication and DNA repair. Furthermore, ARTD1 interacts with the histone-like protein HMGB1, an abundant protein that affects chromatin organization through its ability to bend DNA. ARTD1 is strongly activated upon genotoxic stress, commonly attributed to the DNA strand breaks induced. It is not clear to which extent the activity and function of ARTD1 is controlled by other molecular mechanisms. Thus, the aim of this thesis was to investigate if HMGB1 regulates ARTD1 function during different stress conditions.

Upon oxidative stress induced by H_2O_2, we found ARTD1-mediated PAR formation to be strongly dependent on intracellular calcium release and the activation of the calcium-dependent kinase PKCα. However, phosphorylation of ARTD1 by this kinase did not affect its *in vitro* ADP-ribosylation activity. Since HMGB1 is also a modification target of PKCα, we tested whether phosphorylation of HMGB1 by PKCα may be involved in H_2O_2-induced PAR formation. Indeed, while non-phosphorylated HMGB1 represses ARTD1 activity, the PKCα-mediated phosphorylation of HMGB1 is required to allow induction of PAR formation by ARTD1 upon H_2O_2.

Moreover, we investigated whether the transcriptional co-factor function of ARTD1 is regulated by HMGB1. We could show that ARTD1 and HMGB1 co-regulated the LPS-induced gene expression of the NF-κB-target gene *IP-10*, but not that of *IL-6*. However, we show that ARTD1 can influence the chromatin flavor around the promoter of the pro-inflammatory gene *IL-6* by repressing MLL1-mediated trimethylation of H3K4, resulting in attenuated transcription.

The findings of this thesis demonstrate how HMGB1 controls the activity of ARTD1 during oxidative stress, and how ARTD1 regulates NF-κB-dependent gene expression. This underlines the important involvement of ARTD1 and HMGB1 in the cellular stress response, and could be medically relevant for targeting oxidative stress-related conditions and inflammation.

Zusammenfassung

ADP-Ribosylierung von Proteinen ist eine posttranslationale Modifikation, die in multiplen biologischen Prozessen vorkommt, wie zum Beispiel bei inflammatorischen Signalübermittlungen, Stoffwechselprozessen und Krebserkrankungen. Die am besten untersuchteste nukleäre ADP-Ribosyltransferase (ART) ist ARTD1. ARTD1 katalysiert den Anhang von Poly-ADP-Ribose (PAR) an Zielproteine, wodurch die lokale Chromatin-Kondensation moduliert und dadurch Transkription, Replikation und DNS Reparatur beeinflusst wird. Außerdem interagiert ARTD1 mit dem häufig vorkommenden Histon-ähnlichen Proteinen HMGB1, das durch seine Eigenschaft die DNS zu biegen die Chromatin Organisation mitgestaltet.

ARTD1 wird bei genotoxischem Stress, der mit Schäden der DNS einhergeht, stark aktiviert. Es ist unklar, inwiefern die Aktivierung und Funktion von ARTD1 durch andere molekulare Mechanismen kontrolliert wird. Diese Dissertation untersucht, ob und wie HMGB1 die Funktionsweise von ARTD1 während unterschiedlichen Stressbedingungen reguliert.

Wir zeigen, dass die durch H_2O_2-vermittelten oxidativen Stress-induzierte und durch ARTD1 ausgeführte PAR-Bildung sowohl von der intrazellulären Calciumfreisetzung als auch von der Calcium-abhängigen Kinase PKCα abhängt. Die Phosphorylierung von ARTD1 durch diese Kinase hatte jedoch keinen Einfluss auf die ADP-Ribosylierung *in vitro*. Währendem HMGB1, ebenfalls Zielprotein von PKCα, im nicht-phosphorylierten Zustand die Aktivität von ARTD1 hemmt, ist die PKCα vermittelte Phosphorylierung von HMGB1 nötig, um H_2O_2-induzierte PAR-Bildung zu erlauben.

Außerdem untersuchten wir, ob die transkriptionelle Cofaktorfunktion von ARTD1 durch HMGB1 reguliert wird. Wir konnten zeigen, dass ARTD1 und HMGB1 nach LPS-Stimulierung das NF-κB Ziel-Gen *IP-10*, jedoch nicht *IL-6* regulieren. Ferner konnten wir zeigen, dass ARTD1 die Chromatin-Eigenschaften am Promoter des pro-inflammatorischen Gens IL-6 dahingehend verändert, dass die MLL1-abhängige Trimethylierung von H3K4 unterdrückt und dadurch die Transkription gehemmt wird.

Die Ergebnisse dieser Arbeit zeigen, wie HMGB1 die Aktivität von ARTD1 während oxidativen Stresses kontrolliert und wie ARTD1 die NF-κB abhängige Genepression reguliert. Dies unterstreicht die Wichtigkeit von ARTD1 und HMGB1 in der zellulären Stressantwort und könnte darüberhinaus von medizinischer Relevanz sein.

Table of Contents

Abbreviations

8-oxoG	7,8-Dihydro-8-oxoguanine
aa	Amino acid
ADPr	Adenosine diphosphate ribose
AP sites	Apurinic/apyrimidinc sites
ARH	ADP-ribosyl hydrolase
ART	ADP-ribosyltransferase
ARTD	ADP-ribosyltransferase diphtheria toxin-like
ARTC	ADP-ribosyltransferase cholera toxin-like
ATM	Ataxia telangiectasia mutated
ATP	Adenosine triphosphate
BER	Base excision repair
bp	Base pair
BRCT	BRCA1 carboxy-terminal domain
CaMK	Ca^{2+}/calmodulin-dependent protein kinase
CBP	CREB-binding protein
ChIP	Chromatin immunoprecipitation
CTCF	CCCTC-binding factor
DAG	Diacylglycerol
DBD	DNA-binding domain
DAPI	4',6-diamidino-2-phenylindole
DNA	Deoxyribonucleic acid
DNMT	DNA methyltransferase
DSB	Double-strand break
eEF2	Eukaryotic elongation factor 2
ER	Endoplasmic reticulum
ERK	Extracellular signal-regulated kinase
ET	Endotoxin tolerance
GSH	Glutathione
HDAC	Histone deacteylase
H_2O_2	Hydrogen peroxide
H3K4me1	Histone H3 lysine 4 monomethylation
H3K4me2	Histone H3 lysine 4 dimethylation
H3K4me3	Histone H3 lysine 4 trimethylation
H3K9me3	Histone H3 lysine 9 trimethylation
H3K27me3	Histone H3 lysine 27 trimethylation
H3K36me3	Histone H3 lysine 36 trimethylation
H3K79me3	Histone H3 lysine 79 trimethylation
HMG	High-mobility group protein
HMGB1	High-mobility group protein box 1
HR	Homologous recombination
HP1	Heterochromatin protein 1
IKK	IκB kinase
IL6	Interleukin 6
IP10	Interferon gamma-induced protein 10
IP_3	Inositol-1,4,5-triphosphate
IP3R	IP3 receptor
JNK	c-Jun N-terminal kinase

LPS	Lipopolysaccharide
MAPK	Mitogen-activated protein kinase
MAR	Mono-ADP-ribose
MARylation	Mono-ADP-ribosylation
MEF	Mouse embryonic fibroblast
MIP2	Macrophage inflammatory protein 2
MLL1	Myeloid/lymphoid or mixed-lineage leukemia protein 1
NAD	Nicotinamide adenine dinucleotide
NAM	Nicotinamide
NE	Nuclear extract
NEIL	NEI-like endonucleases
NER	Nucleotide excision repair
NHEJ	Non-homologous end joining
NMNAT	NMN adenylyltransferase
NF-κB	Nuclear factor of kappa light polypeptide gene enhancer in B-cells
NFAT	Nuclear factor of activated T-cell
NTH1	Endonuclease III homologue
$O_2^{\bullet -}$	Superoxide radical
•OH	Hydroxyl radical
OGG1	8-oxoguanine glycosylase 1
PAR	Poly-ADP-ribose
PARG	Poly-(ADP-ribose)-glycohydrolase
PARP	Poly-(ADP-ribose)-polymerase
PARPi	PARP inhibitor
PARylation	Poly-ADP-ribosylation
PBM	PAR-binding motif
PBS	Phosphate-buffered saline
PBZ	Poly-ADP-ribose-binding zinc finger
PHE	1,10-phenanthroline
PIP_2	Phosphatidylinositol 4,5-bisphosphate
PKC	Protein kinase C
PLC	Phospholipase C
PNKP	Polynucleotide kinase-phosphatase
Pol β	DNA polymerase β
PRC	Polycomb repressory complexes
PRD	PARP regulatory domain
PTEN	Phosphatase and tensin homolog
PTM	Post-translational modification
RAGE	Receptor for advanced glycation end products
RB	Retinoblastoma
RNA	Ribonucleic acid
ROS	Reactive oxygen species
SIRT	Sirtuin
SOD	Superoxide dismutase
SSB	Single-strand break
TNFα	Tumor necrosis factor α
XRCC1	X-ray repair cross-complementing protein 1

1 Introduction

1.1 Oxidative Stress

Reactive oxygen species (ROS), such as superoxide radical ($O_2^{\bullet -}$), hydrogen peroxide (H_2O_2) and hydroxyl radical ($^{\bullet}OH$), are continuously formed endogenously by partial reduction of oxygen during cell metabolism [1]. ROS are released by macrophages in the inflammatory response, as well as formed by NADPH oxidases in other cell types upon growth factor or cytokine stimulation [2, 3]. Exogenous stimuli such as ionizing radiation and cigarette smoke can also cause an increase in intracellular ROS [1]. ROS induces oxidation of cellular biomolecules, which influences their function and can lead to severe cellular damage. Intracellular ROS levels thus need to be kept at a minimum. The total cellular ROS levels at any given point depends on the antioxidant defense capacity of the cell. The cellular antioxidant defense system consists of several enzymes such as superoxide dismutase (SOD), which converts $O_2^{\bullet -}$ to H_2O_2, catalase, which breaks down H_2O_2 to H_2O and oxygen, and glutathione peroxidase, which catalyzes the breakdown of peroxides, including H_2O_2, via the reductant glutathione (GSH) [2, 4]. Similarly, thioredoxins catalyze the breakdown of H_2O_2 via its own oxidation [3]. Oxidative stress results from the increased levels of ROS and induces oxidation of various cellular biomolecules, such as lipids, proteins and nucleic acids [5]. Lipid peroxidation primarily cause damage to the lipid-rich cell membrane, but can also mediate further cell damage via reactive aldehydes and lipoproteins [6]. Protein oxidation leads to either protein degradation, or altered protein function due to oxidation of essential cysteine residues [5]. ROS also induce oxidative damage to nucleic acids such as DNA, which can cause mutations when not properly repaired [1].

1.1.1 Oxidative stress-induced signaling

Protein oxidation has been shown to play an important role in cellular signaling of oxidative stress, since the oxidation of many signaling enzymes, such as kinases and phosphatases, leads to altered catalytic function [2, 3, 7]. For example, mitogen-activated protein kinase kinase kinase (MAPKKK) is activated by H_2O_2 via oxidation of thioredoxin [3, 8]. In turn, activated MAPKK activates Jun N-terminal kinase (JNK), extracellular signal-regulated kinase (ERK) and p38 MAPK, which induce cellular responses such as inflammation, proliferation and DNA repair [3]. Ataxia

telangiectasia mutated (ATM) kinase can also be oxidized and activated by H_2O_2, which leads to dimer formation, auto-phosphorylation and subsequent phosphorylation of target proteins, such as p53 and Chk2 [9].

Increased intracellular ROS can lead to the oxidation of protein tyrosine kinases, such as phosphatase and tensin homolog (PTEN). The oxidation of PTEN leads to its inactivation, which in turn activates phospholipase C (PLC) at the membrane. PLC-dependent cleavage of phosphatidylinositol 4,5-bisphosphate (PIP_2) generates the secondary messengers inositol-1,4,5-triphosphate (IP_3) and diacylglycerol (DAG), of which IP_3 regulates the release of Ca^{2+} from the ER via the IP3 receptor (IP3R) [10]. Ca^{2+} acts as an activator and cofactor of multiple proteins with a wide range of biological functions, such as kinases (e.g. protein kinase C [PKC], Ca^{2+}/calmodulin-dependent protein kinases [CaMK] and MAPK), transcription factors (e.g. nuclear factor of activated T-cell [NFAT] and CREB-binding protein [CBP]), nitric oxide synthases, and multiple membrane channels and pumps [11].

1.1.2 Ca^{2+} signaling

Intracellular Ca^{2+} levels can increase up to 10-fold upon oxidative stress, and Ca^{2+} has been described as a potent signaling molecule involved in processes such as cell proliferation, gene transcription and tumor progression [11-14]. The elevated Ca^{2+} levels can enhance the initial oxidative signaling via increased Ca^{2+} uptake by the mitochondria, which stimulates the TCA (Krebs) cycle and thereby increases oxygen consumption and subsequent ROS generation [15]. The increased levels of Ca^{2+} upon H_2O_2 stimulation have been attributed the dynamic release of Ca^{2+} from the major intracellular Ca^{2+} storage, the endoplasmic reticulum (ER) [10, 11].

1.1.3 Oxidative DNA-damage

ROS cause oxidative damage to the DNA, resulting in modified bases or sugars, DNA-protein cross-links, strand breaks, apurinic/apyrimidinc (AP) sites or tandem lesions [1]. The exact mechanism by which H_2O_2 induces DNA damage is not known, but it has been suggested that the highly reactive •OH is formed through the Fenton reaction in close proximity to the DNA target, with transition metal ions (copper or iron) as catalyst [2]. The oxidative damage of sugar backbone can generate single-stranded breaks (SSB), due to the displacement of the ribose [16]. Over 20 different types of oxidative lesions to DNA bases can be formed by ROS, which may result in

mutations if not repaired properly [1]. 7,8-Dihydro-8-oxoguanine (8-oxoG) is one of the most common oxidative base lesion observed in tissues and cells, and by far the most studied oxidative lesion, both biochemically and pathologically, due to the availability of measuring techniques and its mutagenic properties [4, 16, 17].

1.1.4 Repair of oxidative DNA lesions by BER and DNA glycosylases

ROS-induced DNA lesions are mainly repaired by the base excision repair (BER) pathway, which replaces the single damaged base stepwise with an undamaged base [4]. In the first step, a DNA glycosylase excises the modified base from the DNA by hydrolyzing the N-glycosidic bond between the modified base and the backbone, generating an AP site [18]. Thereafter, endonucleases with an AP lyase activity cleave the 3′-phosphodiester bond to remove the ribose, causing a single-stranded nick. The single nucleotide is replaced by DNA polymerase β (pol β) and finally the backbone sealed by DNA ligase III in complex with X-ray repair cross-complementing protein 1 (XRCC1) (Figure 1) [19].

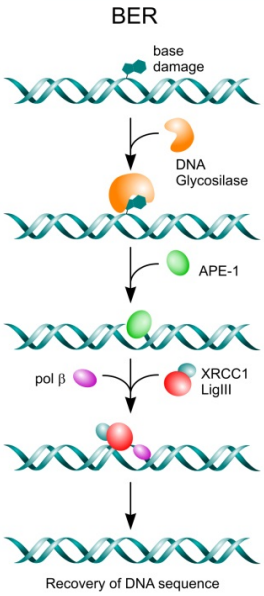

Figure 1. The base excision repair pathway [19]

The main DNA glycosylase that excises 8-oxoG is 8-oxoguanine glycosylase 1 (OGG1), which is also the best studied enzyme [20]. However, a few other DNA glycosylases with different specificities towards oxidative DNA lesions have also received attention in recent years, such as NEI-like endonucleases (NEIL) 1-3 and endonuclease III homologue (NTH1) [4, 21, 22]. What mechanism activates the specific DNA glycosylases has not been fully elucidated and needs further investigation.

1.2 Protein ADP-ribosylation

Protein ADP-ribosylation is a reversible post-translational modification (PTM) catalyzed by a class of enzymes called ADP-ribosyltransferases (ARTs). They use nicotinamide adenine dinucleotide (NAD^+) as substrate to covalently attach adenosine diphosphate ribose (ADPr) to specific amino acid side chains of a protein and consequently release nicotinamide (NAM) as byproduct [23]. Protein ADP-ribosylation is a widely spread PTM in eukaryotes, although absent in yeast, but was originally identified as the functional mechanism of bacterial toxins such as the *Corynebacterium diphteriae* toxin [24, 25]. Several amino acids (aa) have been reported to be acceptors of ADPr in eukaryotic cells: arginine (R), glutamate (E), aspartate (D), lysine (K), diphtamide (Dph), phospho-serine (pS), asparagine (N) and cysteine (C) [26-28]. Protein mono-ADP-ribosylation (MARylation) is the addition of one ADPr unit to a specific aa. The first ADPr can be extended through a glycosidic ribose-ribose bond and can by further extension give rise to an oligomer and eventually a polymer of ADPr, a process termed protein poly-ADP-ribosylation (PARylation) [29]. Polymers of ADPr (PAR) can be linear or branched and can reach a length of 400 moieties *in vitro* [30], but it is currently unknown how the polymer length and the branching frequency of the polymers is controlled *in vivo*.

Identification of eukaryotic ADP-ribosylated proteins has long been limited by the lack of appropriate methods, but has vastly progressed in the last few years due to technical advances [31-33]. Endogenous basal levels of cellular ADP-ribosylation are very low and difficult to detect, but higher detectable levels can be induced by mitogenic or genotoxic stress, which cause activation of various ARTs [23]. The presence of the large size and the bulkiness of the branched polymers, as well as the markedly negative charge of ADPr, change the nature of the modified target proteins. Thus, PARylation of a target protein can modulate its activity [34, 35], localization [36] or other functions, depending on the context and the role of the protein modified.

1.2.1 Substrate NAD^+

NAD^+ is a universal energy-carrying molecule that acts as a cofactor in multiple cellular redox reactions and is reversibly oxidized (NAD^+) or reduced (NADH) by various oxidoreductases [37]. NAD^+ is de novo synthesized from L-tryptophan or via the salvage pathway from nucleobases and nucleosides [38]. The salvage pathway can recycle the byproduct of ARTs NAM into NAD^+, and thereby restore the NAD^+-

levels, providing NAD^+-dependent enzymes with new substrate. In the nucleus, NMN adenylyltransferase (NMNAT) 1 is responsible for the final step of the salvage synthesis [39, 40], and since NMNAT1 KO in mice is embryonic lethal, NAD^+ levels from other cellular compartments do not seem to be able to compensate the loss of NAD^+ in the nucleus [41]. However, the lack of *in vivo* detection methods for NAD^+ makes it difficult to assess how the NAD^+ pools of specific compartments change upon activation of NAD^+-consuming enzymes.

The consumption of NAD^+ by ARTs upon high activity can lead to depletion of cellular NAD^+ contents, and a consequent drop in ATP levels, leading to cell death [37, 38]. Upon excessive ADP-ribosylation, the nuclear member of the NAD^+-dependent deacetylases sirtuins SIRT1 is inhibited by limited nuclear NAD^+ [42, 43]. The balancing act of NAD^+ consumption by nuclear ARTs and SIRT1 have been described for several cellular functions, such as metabolism, aging and inflammation [40]. However, whether ARTs and SIRTs compete for the same NAD^+-pool remains to be shown.

1.2.2 ARTD family members

Cellular ARTs are subdivided into two large families, the membrane-associated cholera toxin-like ARTCs, facing the extracellular space, and the intracellular diphtheria toxin-like ARTDs [28]. The human ARTD subclass, formerly known as poly-ADP-ribose polymerases (PARPs), consists of 18 family members, which all contain the characteristic catalytic ART domain [28]. It has been postulated that the H-Y-E motif sequence, located in the catalytic domain of ARTD1-6, determines the ability of ARTDs to form PAR, while ARTDs lacking this motif only form mono-ADP-ribose (MAR) [44]. However, although the NAD^+-binding pocket of ARTD3 and ARTD4 contain this motif, they have only been described to have MARylation activity so far [44, 45]. ARTD5 and ARTD6 synthesize oligo-ADP-ribose of around 20 ADPr moieties, while ARTD1 and ARTD2 can form PAR of up to hundreds of ADPr units, both linear and branched [46]. ARTD7-17 are mono-ADP-ribosylatransferases, except for ARTD9 and ARTD13, which have been described to be inactive in spite of harboring a catalytic domain [27, 44, 47]. The activity of ARTD18 has not yet been determined. ARTD1 is located exclusively in the nucleus, ARTD7, ARTD12, ARTD13, ARTD15-17 in the cytoplasm, and ARTD2-6, ARTD8-11 and ARTD14 have a nuclear and a cytoplasmic localization [29, 38].

1.2.3 Readers of protein ADP-ribosylation

ADP-ribosylation acts as a scaffold to recruit specific proteins and induce complex formation. There are several known ADP-ribose-binding motifs and domains [48-51]. Macrodomains are highly conserved globular modules with a preferential binding to terminal ADP-ribose, whereas the poly-ADP-ribose-binding zinc finger (PBZ) domains recognize two adjacent ADP-ribose moieties, and WWE-domains bind to *iso*-ADP-ribose and PAR [29, 52]. The PAR-binding motif (PBM), which consists of 20 amino acids with clusters of basic and hydrophobic residues, has been suggested to bind to highly negative long polymers, and is found in several proteins involved in DNA damage repair [29, 52].

Several cellular processes, such as DNA repair, transcription, differentiation, RNA maturation and degradation, as well as chromatin remodeling have been shown to be influenced by non-covalent binding of PAR-binding proteins [29]. The most studied process in the context of protein recruitment by interaction with PAR has been DNA repair. Several DNA repair factors have been described to bind to PAR via their PBMs, such as XRCC1, XPA, Chk1, p53 and WRN [53-56]. The scaffold feature of PAR not only recruits single factors, but can also facilitate 'droplet' formation of low complexity region proteins (e.g. FUS). The PAR chains provide a transient scaffold for nucleation of these intrinsically disordered proteins via interaction between their positively charged RGG repeats and the highly negatively charged PAR, a process described to be involved in orchestrating the initiation of DNA repair [57].

Additionally, the highly negative charge of the polymers have been suggested early on to compete with DNA for binding of the histones and thereby function as a histone chaperone, regulating nucleosome displacement from the chromatin [58]. However, this view has been recently challenged and other mechanisms by which PAR regulates nucleosome sliding and chromatin remodeling have been suggested. For example, the SNF2 ATPase chromatin remodeler ALC1 is rapidly recruited to nucleosomes by macrodomain-mediated binding to PAR, to increase chromatin accessibility [59, 60]. Conversely, the binding of macrodomains from histone macroH2A1.1, which localizes to DNA damage sites, can lead to the compaction of chromatin [48].

1.2.4 Erasers of protein ADP-ribosylation

The majority of protein ADP-ribosylation has a half-life of less than 40 seconds up to a few minutes, depending on the stimulus used, while a small fraction of the modification has a half-life of several hours [61, 62]. The rapid turnover of ADP-ribosylation is mainly due to the hydrolysis of the modification by ADP-ribose protein hydrolases, such as poly-(ADP-ribose)-glycohydrolase (PARG), ADP-ribosyl hydrolases (ARH) 1 and 3, or, as was recently discovered by our group and others, macrodomain hydrolases (MDO1, MDO2 and C6orf130/TARG) [63-67]. These different classes of hydrolases have distinct modes of action: Whereas PARG and ARH3 seem to mainly remove poly-ADP-ribose (PAR), ARH1 and the macrodomains remove the mono-ADP-ribose (MAR) of different acceptor sites [52, 64, 65].

1.2.5 PARP inhibitors

Most ARTD inhibitors, also named PARP inhibitors (PARPis), are NAD^+-analogues and inhibit the catalytic activity of ARTs by competing with the binding of NAD^+ to the catalytic cleft [68]. Although the development of new, more specific PARPis than the initial low-potency 3-aminobenzamide has largely progressed, no compound currently on the market is specific for a certain ARTD family member [68, 69]. Additionally, it is not well known which members are inhibited and to which extent by particular compounds. Clinical studies with PARPi have mainly been focusing on ARTD1, which has been shown to have a dual role in the response to genotoxic stress and DNA damage. ARTD1 has a pro-survival function by promoting DNA repair, but upon excessive DNA damage, ARTD1 is strongly activated, leading to NAD^+-depletion, drastic ATP reduction, resulting in cell necrosis [70, 71].

Monotherapy with PARPi is used for tumors with BRCA1/2 mutations, hence deficient in homologous recombination (HR). The treatment is thought to result in the accumulation of high levels of unrepaired DNA breaks, due to BER inhibition or trapping of catalytically inactive ARTD1 at the site of damage, which accumulate SSB, leading to double-stranded breaks (DSB) after replication, causing synthetic lethality [72, 73]. An alternative model describes how the presence of PARPis, in the absence of HR favors the more error-prone non-homologous end joining (NHEJ) repair pathway, which results in cytotoxic mutations and chromosomal rearrangements [73]. Combinational therapy, such as PARPi together with

chemotherapy or radiation therapy, targets ARTD1 to prevent efficient DNA repair, causing lethal levels of DNA breaks [68]. Although there are still many challenges in the development of more efficient PARPis, a recent important advancement is the approval of the PARPi olaparib (Lynparza) for treatment of advanced ovarian cancer in patients with *BRCA* mutations [68].

Lately, the interest in the alternative use of PARPi outside of the field of genotoxic stress has grown. Multiple studies have shown a protective effect of PARPis towards a number of inflammatory conditions [74-76], and have also been investigated as a strategy to treat inflammation-related diseases, such as myocardial infarction and stroke [72]. The studies on PARPi treatment in non-cancerous diseases are promising, but the precise protective mechanisms of PARPis in these diseases need further investigations.

1.3 ARTD1

The best-studied member of the ARTD family is ARTD1, which is exclusively localized in the nucleus and responsible for most of the nuclear PAR formed upon genotoxic stress [77]. Its role in genome stability is supported by studies based on ARTD1 KO mice, which are viable, but sensitive to genotoxic stress [78-80].

1.3.1 Protein structure of ARTD1

ARTD1 has a molecular weight of 116 kDa and contains several functional domains (Figure 2) [81]. ARTD1 consists of a DNA-binding domain (DBD), an automodification domain, a protein-interacting domain (BRCT), a WGR domain and

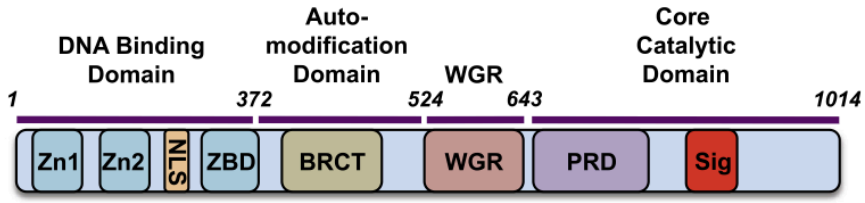

Figure 2. The structural domains of ARTD1 [81]

the characteristic core catalytic domain. The DBD is required for the activation of ARTD1 by DNA and contains three zinc-finger domains that mediate the binding of ARTD1 to DNA. The DBD is necessary and sufficient for binding to nucleosomes, yet the DBD alone is unable to promote ARTD1 functions, such as chromatin compaction [82]. ARTD1 was initially described to modify mainly itself on glutamic

acids in the auto-modification domain, a view that has recently been challenged by our group, by providing evidence that also lysines in this domain can serve as ADPr acceptor sites [83, 84]. The BRCT domain is important for several protein–protein interactions [84]. The WGR domain is essential for the correct folding of the enzyme upon activation by DNA strand breaks, but is not very well characterized [85]. The core catalytic domain consists of the α-helical PARP regulatory domain (PRD) and the characteristic ART domain containing the signature motif (Sig), which together are required for the binding of NAD^+ and the catalytic activity of ARTD1 [85]. Recent studies describe primarily lysines, arginines, glutamic and aspartic acids to be the targeted amino acids of ARTD1, although the main acceptor site of ARTD1-mediated ADP-ribosylation has not yet been determined [26, 31, 32, 86].

1.3.2 Regulation of ARTD1's enzymatic activity in a DNA-dependent manner

The activity of ARTD1 has most commonly been studied during genotoxic stress. DNA alkylating and oxidative agents have been extensively used to trigger nuclear PAR formation in cell culture experiments [71]. *In vitro*, ARTD1 activity is mainly induced by linear stretches of DNA or DNA containing nicks and breaks. Both zinc-finger 1 and 2 in the DBD of ARTD1 have been described to be important for its binding to DNA breaks [87, 88]. The binding of ARTD1 to sites of DNA damage facilitates its dimerization and induces its trans-automodification [88], which in turn is required for efficient SSB repair and enables recruitment of ARTD2 and XRCC1 to sites of damage [56, 89]. However, the dependency of the recruitment of BER factors on ARTD1 has been challenged. Alternative models suggest that ARTD1 stabilize SSB and repair intermediates, and is mainly important to extend the repair capacity of BER upon excessive DNA damage [90].

DNA breaks can be triggered by topoisomerase IIβ upon activation by hormonal stimuli, and can serve as activator of ARTD1 on specific loci [91]. Intracellular Ca^{2+} positively regulates PARylation in cells treated with the reactive nitrogen species peroxynitrite, and has also been shown to regulate ARTD1 activity upon treatment of cells with the NQO1 co-substrate β-lapachone, through the activity of ROS-producing NQO1 [92, 93].

Although most studies have focused on the activation of ARTD1 by DNA breaks, many recent reports provide evidence for an additional type of regulation and alternative activation mechanisms of ARTD1 activity.

ARTD1 has been shown to be activated by DNA-dependent, but DNA break-independent mechanisms. *In vitro* studies using chromatin and histones have shown that ARTD1 is more strongly activated by polynucleosomes than by sheared DNA [94]. ARTD1 incubated with chromatinized plasmids forms a compact chromatin structure *in vitro*, and upon the sole addition of NAD^+, ARTD1 is activated, leading to a relaxed chromatin structure [94]. In line with this DNA break-independent, but DNA-dependent activation, ARTD1 binds to three- and four-way junctions, stably unpaired regions in double-stranded DNA and recognizes distortions in the DNA helical backbone (bent DNA), which all also cause an activation of ARTD1 [95].

1.3.3 Regulation of ARTD1's enzymatic activity by protein interactions and post-translational modifications

Induction of ARTD1 enzymatic activity has also been observed by protein–protein interactions as well as by posttranslational modifications of ARTD1. The nuclear NAD^+-catalyzer NMNAT-1 has, apart from promoting ARTD1 activity by substrate supply, been described to stimulate PARylation by direct interaction of ARTD1 and PAR [96]. The interaction with MAPK has been described to activate ARTD1 as well. For example in cortical neurons stimulated with nerve growth factors, ARTD1 is activated by the interaction with ERK2 [97]. Another MAPK that has been shown to enhance PAR formation is JNK1. After 30 minutes of stimulation with H_2O_2, JNK has translocated from the cytoplasm to the nucleus, where it interacts with ARTD1, leading to an enhanced ARTD1 activity [98].

The most commonly studied PTM of ARTD1, beside auto-ADP-ribosylation, is phosphorylation. A variety of kinases have been reported to phosphorylate and thereby modulate the activity of ARTD1, including ERK1/2, CKII, CDK5, JNK1, CaMKII and PKCα/β [75, 99-105]. The phosphorylation of ARTD1 by PKCα/β *in vitro* has been shown to reduce its DNA binding and enzymatic activity [104]. In line with this, activation of PKC in thymocytes by phorbol esters (PMA) suppresses MNNG-induced ARTD1 activation, while PKC inhibition leads to enhanced ARTD1 activation [103]. CDK2 is activated upon progesterone exposure in certain breast cancer cells and phosphorylates ARTD1 in the catalytic cleft to enhance its enzymatic activity [102]. The MAPK signaling pathways have also been shown to regulate ARTD1 activity by phosphorylation. Several studies have revealed that inhibition of ERK1/2 reduces PAR formation [75, 99-101]. In neuronal differentiation,

phosphorylation of ARTD1 by CaMKIIδ occurs at the chromatin and leads to an activation of ARTD1 [106]. Although the cell types and stimuli differ between these studies, an overall conclusion is that the phosphorylation of ARTD1 by PKCs generally reduces ARTD1 activity, while phosphorylation mediated by CDK2, MAPK or CaMKIIδ generally enhance ARTD1 activity.

In addition, acetylation has also been shown to affect the catalytic activity of ARTD1. For example, PCAF-dependent acetylation of ARTD1 upon physical stress of cardiomyocytes activates ARTD1 in a DNA-independent manner [42]. In line with this, the deacetylation of ARTD1 by SIRT1 reduces its activity, and *Sirt1* KO cells show enhanced H_2O_2-induced PAR formation [42, 107]. Furthermore, a crosstalk between ADP-ribosylating enzymes has been described, where ARTD3 and SIRT6 can stimulate ARTD1 activity [45, 108].

1.3.4 ARTD1 in transcription

Most chromatin rearrangements induced by ARTD1 result in transcriptional changes. ARTD1 can affect transcription by its function as a cofactor for DNA sequence-specific transcription factors [70, 97, 109-111]. Both co-activator and co-repressor functions have been described, some of which are dependent on PAR activity (e.g. Sp1, NFAT and Elk1), while others are not (e.g. NF-κB and B-Myc). Additionally, the interaction of ARTD1 with the mediator complex has been described upon stimulation with different stimuli, such as retinoic acid or lipopolysaccharide (LPS), which thereby enhances transcription of RAR or NF-κB target genes, respectively [112, 113]. Additionally, activation of transcription could be observed upon PARylation of the lysine deacetylase KDM5B, due to a consequent inhibition of H3K4me3 demethylation [35]. Taken together, the current data show that ARTD1 protein and in some cases its enzymatic activity play an important role in the regulation of transcription.

1.4 Chromatin

Cellular DNA is wrapped around nucleosomes to be structurally packaged within the nucleus. The nucleosome forms the fundamental unit of chromatin, composed of the four core histones (H2A, H2B, H3, H4) in an octameric configuration, around which 147 base pairs of DNA are wrapped [114, 115]. The chromatin creates a 10 nm fiber in a beads-on-a-string formation, and can be further compacted to a 40 nm fiber by

the binding of linker histone H1, a structure called solenoid. Linker histone H1 binds the nucleosomal core particle close to the DNA entry–exit point, where it protects the linker DNA between adjacent nucleosomes [114, 115]. The compaction of nucleosomes into higher-order chromatin structures is regulated by nucleosome occupancy, nuclear localization, replacement by histone variants, DNA methylation and histone PTMs (Figure 3) [115]. The chromatin can be divided in euchromatin and heterochromatin. Euchromatin is generally associated with an open chromatin structure and active gene transcription, while heterochromatin is a repressive

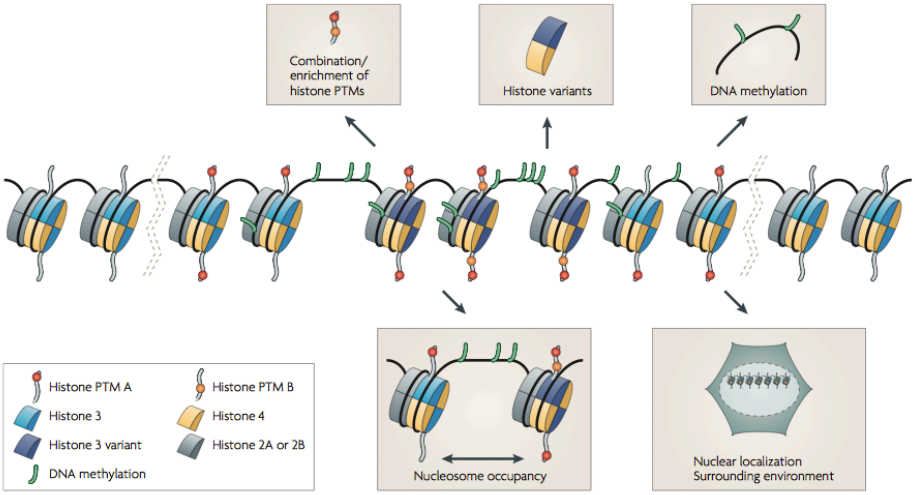

Figure 3. Various factors regulating chromatin structure [115]

chromatin environment with reduced transcriptional activity. Another silencing factor on these regions is the methylation of cytosine at CpG dinucleotides, which is highly stable and not easily reversible, as opposed to the histone modifications [115-117]. DNMT3A and DNMT3B are the main enzymes performing *de novo* DNA methylation, while DNMT1 is responsible for maintaining DNA methylation through cell division to maintain a repressive chromatin after replication [115-117].

In addition to compaction of the DNA, the nuclear localization and arrangement of chromatin plays also a role in the dynamic regulation of appropriate gene expression and activation of cellular pathways. Studies on the long distant interactions between enhancers and promoters, DNA-looping and insulation of topological associated domains, have highlighted the relevance of the chromatin localization within the nucleus [118].

1.4.1 Histone variants

The incorporation of structurally distinct non-typical histone variants into the nucleosomes also regulates the chromatin structure. The incorporation of variant forms of H3 (e.g. H3.3) and H2A (e.g. H2A.Z) at specific loci can influence nucleosome positioning and gene transcription [119, 120]. The H2A variant H2A.X, when phosphorylated, marks double-stranded DNA damage, while macroH2A contains a macro-domain and is mainly associated with compact chromatin [119, 121]. Linker histone H1 has 11 subtypes, which all mediate a different level of chromatin condensation, highlighting their role as highly diverse constituents of chromatin [122].

1.4.2 Histone modifications

Histone PTMs mark the chromatin and participate in protein complex recruitment and chromatin organization during transcription, replication and DNA repair [123]. The N-terminal tail of the histones is the most accessible domain and is a target for alterations by multiple PTMs, including acetylation, methylation, SUMOylation, phosphorylation, ubiqutination, and ADP-ribosylation [26, 123].

Histone acetylation is mainly present at euchromatic regions and is mediated by histone acetyltransferases such as CBP/p300, Tip60 and HAT1 [123]. Moreover, histone deacetylases (HDACs) and SIRTs reverse the modification and consequently cause a more compact chromatin [124].

Histone methylation has distinct functions on chromatin depending on which residue is modified. H3K4me3, H3K36me3, and H3K79me3 are histone marks associated with euchromatin and can be mediated by MLL, SET2D or DOT1 [123]. The best studied writer of euchromatin-associated histone methylation is MLL1, responsible for H3K4me2/3 [125]. MLL1 is active in a core complex consisting of four proteins, which are essential for protein and chromatin interactions [125, 126]. H3K27me3, H3K9me3 and H4K20me3 are associated with heterochromatin, and are mediated by different methyltransferases depending on the targeted region [127]. H3K27me3 is found on the rather temporary silenced state, facultative heterochromatin, while H3K9me3 and H4K20me3 mark constitutive heterochromatin at pericentric and telomeric regions [128], Histone methylation can be removed by various lysine demethylases with different specificity for the different marks [129].

The acetylation and phosphorylation of histone H1 generally seems to correlate with increased replication and cellular growth [130]. H1.4K34 acetylation is enriched at active genes, where it recruits general transcription factors, suggesting that H1 is a fine tuner of chromatin condensation, rather than solely a repressor [119, 130].

Histone marks can be recognized by readers specific for the different modifications. Proteins containing chromodomains or PHD-domains have been described to bind to methylated lysines, while bromodomains and tandem PHD-domains bind to acetylated lysines [131]. For example, chromodomain-containing heterochromatin protein (HP) 1 binds to H3K9me3 to propagate the heterochromatic state [127], while chromatin remodeler CHD1 binds via its chromodomain to H3K4me3 to provide an accessible chromatin and facilitate transcription [131]. The PRC2 has been described to bind its own mark, H3K27me3, to sustain heterochromatin. Likewise, the PHD3 domain of MLL1 binds to its own mark, H3K4me3 [126, 128].

Considering that lysines are the acceptor site of most modifications, and in certain cases even the same residue is target for several modifications, a functional crosstalk between different PTMs exists [26, 132, 133].

ADP-ribosylation by ARTD1 of multiple sites on all core histones and the linker histone H1 has been described [26, 32, 134]. How these modifications influence chromatin by their negative charge, binding of macrodomain-containing protein ALC1 and macroH2A [48, 55, 60], or via crosstalk with other histone modifications, is an interesting issue that needs further investigation.

1.4.3 ARTD1 in the chromatin context

The function of ARTD1 on the chromatin is to modulate chromatin condensation, nucleosome positioning, DNA damage repair efficiency and other nuclear functions [60, 135, 136]. Whether ARTD1 acts as a repressor or activator depends on the surrounding proteins and the signal given. Thus, the main function of ARTD1 seems to be to arrange the chromatin environment in an optimal way for other chromatin-associated proteins to perform their function.

Chromatin decondensation by ARTD1 can be induced *in vivo* by various cellular stress and results in an increased transcription of stress-related genes [137-139]. Upon inflammasome signaling, ARTD1 is cleaved at the chromatin by inflammasome-dependent caspases, leading to a locally decondensed chromatin and

activation of cytokine gene transcription [139]. In Drosophila, it has recently been shown that ARTD1 is activated by the acetylation of H2AK5 in combination with phosphorylation on H2AvS137 (homologous to the human H2AX and H2AZ) in response to heat shock, leading to eviction of nucleosomes and increased *Hsp70* gene transcription [137, 138].

The trigger and biological relevance for the specific ADP-ribosylation of histones is also being increasingly studied. In response to hormone stimulation, topoisomerase IIβ cleaves DNA at estrogen, androgen, retinoic acid and thyroid receptor binding sites, which in turn activates ARTD1 to PARylate itself and histone H1, leading to histone H1 displacement from the chromatin and a consequently more permissive environment and increased transcription [140].

ARTD1 activity has been described to influence DNA methylation, although there are contradictory data on how ARTD1 affects DNMT1 activity. PARylated ARTD1 has been shown to interact with DNMT1 and repress its activity, promoting an unmethylated DNA [141, 142]. However, more recent work suggests that ARTD1 regulates UHRF1 and DNMT1 to promote the re-establishment of silencing at heterochromatic regions after replication [143, 144].

The association of ARTD1 with CCCTC-binding factor (CTCF), a protein involved in gene insulation and chromatin barrier function [113, 145], induces PARylation of CTCF, which has been shown to be important for maintaining CTCF function [141, 146]. Hundreds of common chromatin-binding sites of CTCF and ARTD1 have been identified, speaking for a genome wide co-regulatory function between CTCF and ARTD1 [145, 147, 148].

1.5 HMGB1

The high mobility group (HMG) proteins modulate chromatin structure by binding to the chromatin in a non-sequence specific manner [149]. The HMG proteins are subdivided into three distinct structural families: HMGA (HMG-AT-hook), HMGB (HMG-box), and HMGN (HMG-nucleosome binding) [150]. In humans and mice, the HMGB family consists of four isoforms; HMGB1-3, which share more than 80% sequence identity and mainly differ in the C-terminal last few amino acids, and HMGB4, which is slightly shorter and completely lacks the C-terminal tail [151]. HMGB1 is an abundant nuclear protein associated with the chromatin and its amino

acid sequence is conserved across mammals, with approximately 99% identity between different species [152, 153]. HMGB1 contains two AT-hook DNA-binding domains, commonly referred to as the A-box and B-box, which are structurally highly similar (Figure 4) [151]. These DNA-binding boxes are L-shaped and consist of three α-helices, out of which helix I and II together form the short arm, while helix III forms the longer arm [154, 155]. At the C-terminus, HMGB1 has an acidic tail, consisting exclusively of aspartic and glutamic acids, which is important for protein–protein interactions [153].

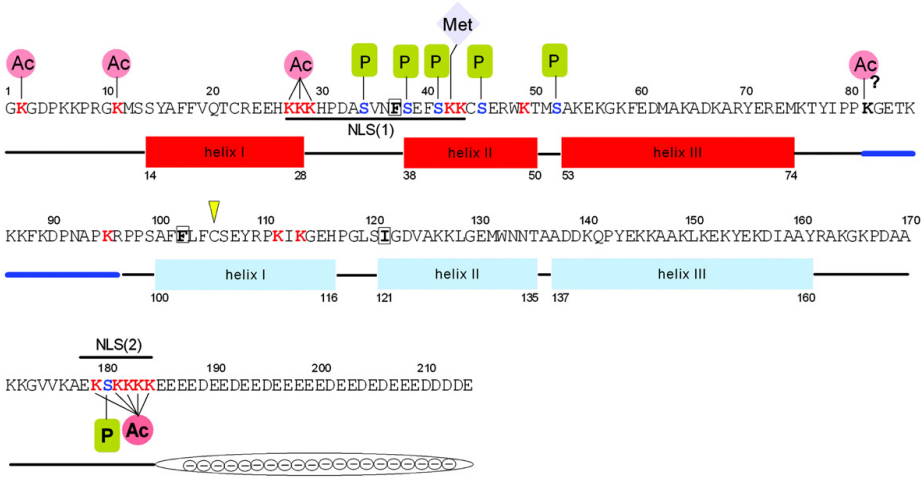

Figure 4. The structure of HMGB1, including most known sites of post-translational modifications. [151]

1.5.1 HMGB1 – A chromatin architectural protein

HMGB1 has been described as a histone-like protein, but rather than stably binding to the DNA, it interacts with the DNA in a highly dynamic manner [156, 157]. No specific sequence is known which HMGB1 preferentially binds to, HMGB1 rather recognizes specific DNA structures, such as cisplatin adducts [158] and cruciformed, bent [159] or single-stranded DNA [160]. At the chromatin, HMGB1 binds to the linker DNA at the exit/entry point of the nucleosomes close to where the H3 tail stabilizes the nucleosomes by exiting between the two gyres of DNA, via the recruitment of H3 [161, 162]. HMGB1 has the ability to bend the DNA it binds to [163, 164]. HMGB1 has been shown to facilitate nucleosome sliding by binding to DNA proximate to the nucleosome and bend it, and nucleosome incorporation into the chromatin by reducing the rigidity of the DNA wrapped around the nucleosome [164-166]. Moreover, HMGB1 seems to be important for the correct placement and spacing of nucleosomes, and cells lacking HMGB1 have fewer nucleosomes in the

chromatin, potentially due to HMGB1's function to facilitate nucleosome assembly [167]. Additionally, the reduced number of nucleosomes affects global transcription output and the relative expression of about 10% of all genes [167].

Moreover, histone H1 and HMGB1 interact via their C-terminal tails, resulting in the mutual replacement of H1 and HMGB1 at the chromatin [168], where these two proteins have rather opposite functional effects. While HMGB1 has been implicated in situations where the chromatin structure might need to be loosened, or in which the DNA is distorted, H1 binds more tightly and is required for the formation of a stable, well-ordered chromatin structure [169].

1.5.2 Function of HMGB1

HMGB1 has been linked to DNA damage repair due to the fact that it preferentially binds to damaged DNA [170, 171]. The high affinity binding of HMGB1 to cisplatin-DNA adducts causes a delay in the repair of these lesions [171]. Interaction with the nucleotide excision repair (NER) proteins RPA [170], XPC and XPA [172] has been demonstrated. The function of HMGB1 in NER, and whether it enhances or reduces repair activity is still under debate [153]. HMGB1 has been shown to positively regulate base excision repair (BER) by enhancing the activity of APE1 and FEN1, and HMGB1 has been shown to interact with the BER factors APE1, Polβ and FEN1 [173].

HMGB1 also interacts with and regulates transcription factors in different cell types upon stimulation with various stimuli [174-178]. In the breast cancer cell line MCF-7, HMGB1 interacts with retinoblastoma (RB), where HMGB1 enhances the ability of RB to repress transcription of E2F and cyclin A, leading to cell growth inhibition [174]. HMGB1 facilitates p53 recruitment to the DNA [175, 176], where the levels of p53/HMGB1 complexes at the DNA regulate the balance between autophagy and apoptosis in cells [177]. The interaction between HMGB1 and the NF-κB subunit p50 has been described to enhance the binding of p50/p50 and p50/p65 dimers to their target sites on DNA and increase TNFα-induced *VCAM* expression [178]. These studies therefore describe that HMGB1 modulates different cellular stress responses, such as DNA damage, proliferation and inflammation.

1.5.3 Post-translational modifications of HMGB1

HMGB1 has been shown to be a target of phosphorylation, acetylation, methylation and ADP-ribosylation [36, 179-188] (Figure 4).

Several reports have shown that PKC phosphorylates HMGB1 [189-191], and PKC and HMGB1 have been shown to interact with each other in monocytes stimulated with LPS [189]. The phosphorylation by PKC has been described to enhance the DNA-bending ability of HMGB1, as well as increase its binding to cis-platinated DNA [190]. Additionally, TNFα-induced phosphorylation of HMGB1 in monocytes targets several amino acids in the NLS, which results in the exclusion of HMGB1 from the nucleus, finally leading to its secretion [180]. Ca^{2+} chelation inhibits activation of the Ca^{2+}-dependent kinases PKCα and CamKIV, thus preventing phosphorylation of HMGB1 and its subsequent nuclear release [189, 192, 193].

Similarily, acetylation has been described to affect both the DNA-binding specificity and the release of HMGB1 [181, 182, 194-197]. The constitutive monoacetylation of HMGB1 at K2 increases the affinity of the protein to distorted and negatively supercoiled DNA [181, 194]. This leads to enhanced binding of HMGB1 to nucleosomes containing linker DNA and thus facilitates nucleosome sliding [195]. The most prominent targets for post-translational modification on HMGB1 are the two NLSs [151, 180, 182]. In LPS-stimulated monocytes, NLS1 and 2 have been shown to be heavily acetylated, which leads to nuclear to cytoplasmic translocation, thus, the hyperacetylation of HMGB1 is required for its active nuclear release during inflammation [182, 196, 197].

The methylation of HMGB1 is thought to cause its release, as in neutrophils and clear cell renal cell carcinoma, the cytoplasmic HMGB1 was found to be constitutively mono-methylated [183, 184]. However, further investigations are required to elucidate the functional role of HMGB1 methylation.

HMGB1 was also described to be ADP-ribosylated over 30 years ago [185, 186]. Several publications have described how ADP-ribosylation is important for the release of HMGB1 from the nucleus upon DNA damage or inflammatory stimuli, inhibiting efferocytosis and increasing autophagy [36, 187, 188]. However, the site of modification, as well as the effect of ADP-ribosylation on the DNA-binding activity of HMGB1, has not been identified so far.

Taken together, these observations show that a low degree of phosphorylation or acetylation of HMGB1 results in an enhancement of its DNA-bending ability, while extensive modification of HMGB1 by phosphorylation, acetylation or ADP-ribosylation, leads to its release.

1.6 ARTD1 and HMGB1 in inflammation

Inflammation is a protective response of the body to tissue irritation, injury or infection, which is characterized by pain, swelling, heat, redness, and/or loss of function [198]. The purpose of inflammation is to eliminate the initial cause of cell injury, clear out necrotic cells and tissues damaged from the original insult and the inflammatory process itself, and to initiate tissue repair [199]. While an insufficient host response leads to unresolved tissue damage and infection, the over-activation of the inflammatory response can also lead to tissue damage and ultimately to septic shock, which both compromise the survival of the organism [198]. Thus, the system needs to be tightly regulated at many different levels to keep the inflammatory response in check.

1.6.1 Transcriptional regulation by NF-κB

The transcription factor nuclear factor-κB (NF-κB) has been extensively studied for its role in inflammation, immunity and cell proliferation [200]. The NF-κB/Rel family of transcription factors consists of p50, p52, p65 (RelA), c-Rel and RelB, which in the absence of stimuli reside as dimers in the cytoplasm [201]. The IκB-proteins bind NF-κB dimers in the cytoplasm, and phosphorylation of IκB by IκB kinases (IKKs) and subsequent ubiquitination and degradation are required for the induction of NF-κB and dimer translocation to the nucleus (Figure 5) [201, 202]. The most studied and best described pathways of NF-κB activation and nuclear translocation are those induced by cytokines, TLRs, TNFRs or virus-stimulation (canonical), or CD40L, BAFF, LTβR or TNFR (non-canonical) signaling [203]. The canonical pathway preferentially induces nuclear translocation of p50/p65 heterodimer and transcriptional regulation by binding to κB-sites at promoters and enhancers of genes that code for cytokines, chemokines and adhesion molecules [204]. The non-canonical pathway leads to the activation and nuclear translocation of p52/RelB dimers, and subsequent transcriptional regulation of genes mainly involved in adaptive immunity and autoimmunity [205, 206].

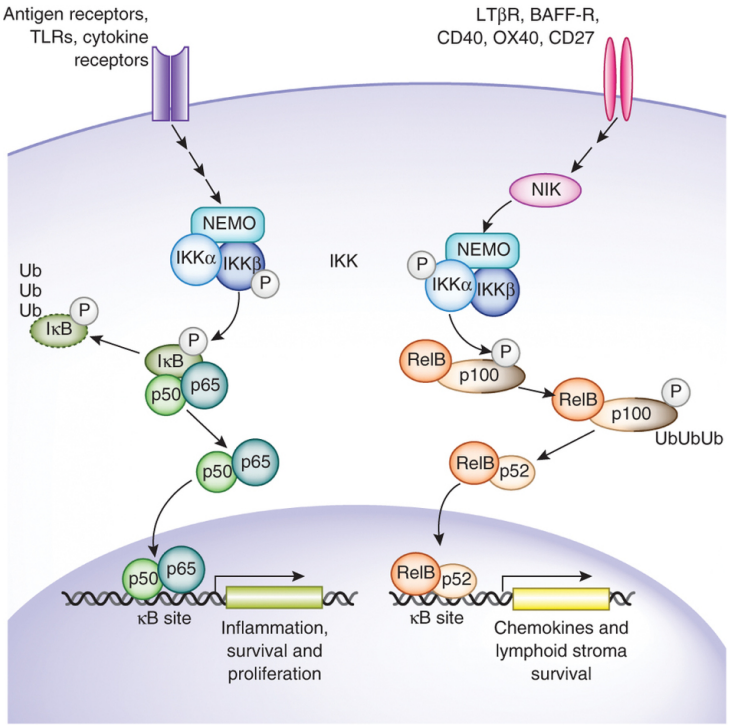

Figure 5. The canonical and non-canonical signaling pathways of NF-κB. [202]

To control the specificity of the signaling and consequent expression of NF-κB-target genes, several chromatin-associated proteins are involved in NF-κB regulation. The regulations and interactions of NF-κB at the chromatin level are important to control the final inflammatory response induced by the various cellular stimuli. The post-translational modifications of NF-κB are crucial for NF-κB-mediated transcription, by their influence on stability, DNA-binding, and interaction with transcriptional co-factors [204]. Association with other inflammatory-activated transcription factors and enhancers has been shown to be important for NF-κB-binding to its target sites [207]. Moreover, the transcription of canonical p65 target genes, such as *IL-6*, *IL-1*, *TNF-α*, *ICAM*, *VCAM*, and *IP-10*, has been shown to rely on cofactors such as CBP/p300, PRMT, HDACs and CDK6, as well as nucleosome remodelers (e.g. SWI/SNF), to increase the accessibility of p65 to κB-binding sites [113, 207-210].

1.6.2 NF-κB and ARTD1

One of the most striking phenotypes of the ARTD1 KO mice is their resistance to LPS-induced septic shock and lethality [211]. NF-κB transcriptional activation is impaired in ARTD1 KO mice, and consequently the *in vivo* release of inflammatory mediators is reduced upon LPS stimulation, as compared to wt mice [211, 212]. LPS-induced expression of inflammatory response genes such as *TNF-α*, *IL-6*, *IFN-γ, MIP-2, ICAM* and *iNOS* has been observed to be considerably lower in cells lacking

ARTD1 [70]. Some studies have suggested a role of ADP-ribosylation in NF-κB dependent transcription, while studies from our group show that the interaction between NF-κB subunits p50/p65 and ARTD1 trigger enhanced NF-κB-dependent transcription upon LPS, independent of the enzymatic activity and DNA-binding of ARTD1 [213, 214]. Furthermore, histone methyltransferase PRMT1 and acetyltransferase p300/CBP both interact with ARTD1 and p65 to synergistically influence p65-dependent transcription [208]. The acetylation of ARTD1 by p300/CBP is required for its coactivator function with NF-κB and p300 and the association with the mediator complex, resulting in increased expression of inflammatory genes [113]. Not only does p300/CBP regulate ARTD1 coactivator function, ARTD1 has also been shown to up-regulate the levels of these acetyltransferases upon LPS stimulation in macrophages [187]. Moreover, ARTD1-dependent down-regulation of HDACs 1 and 4 can be observed upon LPS-stimulation, adding another layer by which ARTD1 regulates transcription upon inflammatory signaling.

PARPi treatment has been shown to have a protective effect against inflammatory diseases, suggesting that ARTD activity has an important role in tissue inflammation [72]. During inflammation, the levels of ROS rise and ARTD1 is highly activated, which leads to depletion of intracellular NAD^+ and ATP levels, resulting in necrotic cell death, tissue damage and sustained inflammation [70, 199]. Changes in NAD^+ levels due to high ARTD1 activity also inhibit SIRT1 activity, by virtue of the lack of available substrate. The acetylation of p65 partially regulates its activity, and can be reversed by SIRT1-mediated deacetylation [215]. Consequently, PARPi treatment maintains p65 in a deacetylated state and thereby reduces p65-mediated gene transcription [215]. Recent studies have proposed that ARTD1 activity influences inflammatory signaling by promoting the release of the inflammatory mediator HMGB1 [187, 188]. Thus, ARTD1, in addition to its function as co-activator of NF-κB, enhances inflammation by necrosis-induced tissue damage, which could potentially also be attenuated by PARPi treatment.

1.6.3 HMGB1 in inflammation

HMGB1 can be actively secreted during inflammation, or be passively released from cells upon necrosis [216]. Upon injection of a lethal dose of LPS in mice, high levels of HMGB1 have been detected in the serum after 8 hours, and were sustained up to 32 hours [217]. Treatment of mice with an anti-HMGB1 antibody has been shown to

drastically increase the survival rate of LPS-challenged mice [217]. Furthermore, the administration of recombinant HMGB1 to mice causes septic shock [217], and increased serum levels of HMGB1 have been detected in human patients of numerous diseases, such as hepatic ischemia/reperfusion, cerebral ischemia, myocardial ischemia, arthritis and septic shock [217-221].

Released HMGB1 mediates inflammation by acting as a cytokine or chemokine [216]. A range of receptors have been described to interact with HMGB1, including the receptor for advanced glycation end products (RAGE), TLR4, TLR2, TLR9, syndecan-3, certain integrins and CXCR4 [222, 223]. The specificity by which receptor HMGB1 signals through during inflammation is governed by formation of complexes with other soluble inflammatory molecules to achieve a synergistic enhancement of the danger response [224]. The canonical receptors of the molecules it complexes with dictate which pathways and cell types will be activated [222]. Recent findings show a highly important redox-mediated regulation of HMGB1, where its redox-state leads to different inflammatory responses [225]. When passively released, HMGB1 is mainly in a reduced state, making it a chemoattractant due to CXCL12 complex formation, and resultant signaling through CXCR4 [224]. The mildly oxidized form of HMGB1 makes it a cytokine, thus stimulating TNF-α release from macrophages via TLR4-signaling, while complete oxidation renders HMGB1 inactive [225]. Thus, the redox-state of HMGB1, determined by the microenvironment, orchestrates its participation in the resolution of inflammation.

2 Aim of the thesis

ADP-ribosylation in general and ARTD1 specifically have been implicated in various diseases and are involved in multiple biological processes, such as differentiation, inflammatory signaling, metabolism and genomic maintenance. ARTD1 and its activity have been shown to regulate gene transcription and DNA repair by rearranging chromatin, resulting in a permissive environment. The chromatin architectural protein HMGB1, which has been shown to associate with ARTD1, bends DNA and facilitates the sliding of nucleosomes, increasing access of transcription factors or DNA repair machinery to the DNA. The overlapping cellular functions and regulatory roles of ARTD1 and HMGB1 suggest that these two proteins may co-regulate nuclear processes which need chromatin rearrangements.

We thus hypothesized that HMGB1 regulates the function of ARTD1 under stress. The aim of this thesis was to focus on; i) investigating the role of ARTD1 and HMGB1, separately and together, in NF-κB-mediated transcription in the context of chromatin regulation, ii) and to study the regulation of ARTD1-induced PAR formation by HMGB1 upon oxidative stress.

3 Results

3.1 Submitted manuscript

3.1.1 PKCα controls oxidative stress-induced poly-ADP-ribose formation by phosphorylating HMGB1

Authors: **Andersson A.***, Bluwstein A.*, Kumar N., Teloni F., Traenkle J., Baudis M., Altmeyer M. and Hottiger MO.
*equal contribution

Contribution: Planning, performing and evaluating the experiments for Fig. 1d, 2c, 3a-f, 3j, 4c-g, S1c, S3d-e, S4b, S4f, S4i-k. Preperation of all figures, and writing and revising of manuscript.

3.2 Published results

3.2.1 ARTD1 Supresses Interleukin 6 Expression by Repressing MLL1-Dependent Histone H3 Trimethylation

Authors: Minotti R.*, **Andersson A.*** and Hottiger MO.
*equal contribution

Journal: Molecular and Cellular Biology, 2015

Contribution: Planning, performing and evaluating the experiments for Fig. 1D, 2A, 5D and replicates of Fig. 5E and 6C. Preperation of figures and revising of manuscript.

3.2.2 SET7/9-dependent methylation of ARTD1 at K508 stimulate poly-ADP-ribose formation after oxidative stress

Authors: Kassner, I., **Andersson A.**, Fey, M., Tomas M., Ferrando-May E. And Hottiger MO.

Journal: Open Biology, 2013

Contribution: Planning, performing and evaluating the experiments for Fig. 3b, 3c and S3C.

3.1 Submitted manuscript

PKCα controls oxidative stress-induced poly-ADP-ribose formation by phosphorylating HMGB1

Anneli Andersson[1,3†], Andrej Bluwstein[1,2†], Nitin Kumar[4], Federico Teloni[1,3], Jens Traenkle[5], Michael Baudis[4], Matthias Altmeyer[1] and Michael O. Hottiger[1*]

Running title: PKCα regulates nuclear poly-ADP-ribose formation

[1]Institute of Veterinary Biochemistry and Molecular Biology, University of Zurich, Winterthurerstrasse 190, 8057 Zurich, Switzerland
[2]Cancer Biology PhD Program, Life Science Zurich Graduate School, University of Zurich, Winterthurerstrasse 190, CH-8057 Zurich, Switzerland
[3]Molecular Life Sciences PhD Program, Life Science Zurich Graduate School, University of Zurich, Winterthurerstrasse 190, CH-8057 Zurich, Switzerland
[4]Institute for Molecular Life Science (IMLS) and Swiss Institute of Bioinformatics (SIB), University of Zurich, Winterthurerstrasse 190, Zurich, Switzerland
[5]Bayer Technology Services GmbH, Leverkusen, Germany

†These authors have contributed equally to this work
*Corresponding author: Email: hottiger@vetbio.uzh.ch

Abstract

Harmful oxidation of proteins, lipids, and nucleic acids is observed when reactive oxygen species (ROS) are produced excessively and/or the antioxidant capacity is depleted, causing 'oxidative stress'. Nuclear poly-ADP-ribose (PAR) formation is thought to be induced in response to oxidative DNA damage and to promote cell death under sustained stress conditions. However, what exactly triggers PAR induction in response to oxidative stress is incompletely understood. Using reverse phase protein array (RPPA) and in-depth analysis of key oxidative stress signaling components, we observed that calcium signaling leads to DNA lesions and was responsible for H_2O_2-dependent PAR formation by ARTD1. However, these DNA lesions were not sufficient for inducing PAR formation, but required the activation of PKCα, as well as the phosphorylation-dependent eviction of HMGB1 from chromatin. Consistently, the lack of PAR formation in the absence of PKCα was recovered by simultaneous knockdown of HMGB1. Together, these results identify PKCα as an important regulator of the chromatin modulation involved in oxidative stress-induced PAR formation, a finding that may have important medical relevance for oxidative stress-associated pathophysiological conditions.

INTRODUCTION

Reactive oxygen species (ROS) are a group of chemical species that consist of at least one oxygen atom, but display stronger reactivity than molecular oxygen. ROS can typically arise from exogenous sources such as UVA or γ-irradiation, drugs, heavy metals (1-3), or from endogenous sources e.g. oxidative metabolism, apoptosis, bystander cells or enzymatic activity (4-7). When ROS are produced excessively or antioxidant capacity is depleted, indiscriminate oxidation of proteins, lipids, and nucleic acid elicits harmful effects, known as 'oxidative stress'. ROS as well as the more stable and less reactive by-product of ROS production, hydrogen peroxide (H_2O_2), are more than toxic products of respiratory burst, they are also effectors for a plethora of signaling pathways inducing innate and adaptive immune cell recruitment, proliferation, tissue healing, cell survival or apoptosis (8-11).

ADP-ribosylation is a post-translational protein modification that consists of mono- and poly-ADP-ribose (PAR) molecules covalently linked to specific residues of target proteins (12). The linear or branched PAR polymer consists of 200-400 ADP-ribose moieties linked by *O*-glycosidic 1'-2' ribose-ribose bonds. These modifications are synthesized by a subfamily of ADP-ribosyltransferases (ARTs), which use NAD^+ as a substrate and belong to the ADP-ribosyltransferase diphtheria toxin-like (ARTD, originally PARP) family. In mammals, the ARTD family is comprised of 18 members, which contain a catalytic ART domain conferring enzymatic activity (13).

The best-characterized ARTD family member is ARTD1 (originally PARP1), a 116 kDa nuclear enzyme consisting of an N-terminal DNA-binding domain (DBD), a central automodification domain (AMD), and a C-terminal catalytic domain (CAT) (14). ARTD1 modifies itself in cis at the automodification domain (15) and other target proteins such as histones, transcription factors and DNA-repair proteins in trans, which points at an important function of ADP-ribosylation in epigenetics, transcriptional regulation and repair (16). Indeed, ADP-ribosylation is implicated in the regulation of a plethora of cellular processes, biological phenomena and medical conditions (14,16,17). ARTD1 has recently been termed a "cellular rheostat", because it integrates different types and levels of stress signals (14). In response to mild or moderate stresses, it regulates transcription and DNA repair, while upon severe and sustained stress conditions, hyper-activation of ARTD1 leads to apoptosis

or necrosis (18,19). Interestingly, a series of studies has shown that ARTD1 is automodified in the presence of specific DNA structures such as cruciform hairpins (20). In line with these results, nucleosomes (intact DNA wrapped around core histones) are sufficient and even more strongly induce ARTD1 than damaged DNA does (21). Moreover, ARTD1 activity can also be stimulated by polyamines (spermine) or core histones (H1 and H3), or in combination, indicating that DNA-independent mechanisms can activate ARTD1 *in vitro* (22). The phosphorylation of $H2Av^{Ser137}$ can also stimulate ARTD1 activity, and the acetylation of $H2A^{Lys5}$ further enhances the ARTD1 activity (23). The fact that nucleosomes, single histones as well as modified histones can stimulate PAR formation, suggests that chromatin is involved in the activation of ARTD1. However, by which mechanism chromatin activates PAR formation *in vivo* has not been elucidated.

Cellular signaling pathways have the potential to directly regulate ARTD1 activity independently of DNA damage by post-translational modification. Positive and direct regulation of ARTD1 activity has been described for the extracellular signal-regulated kinase (ERK) (24-26) as well as for c-Jun N-terminal kinase (JNK) (27), while opposing roles for the involvement of protein kinase C (PKC) signaling in the regulation of ARTD1 have been reported (28-31). The activation of ARTD1 independent of DNA lesions adds an additional layer to the traditional view that considers ARTD1 as part of the DNA damage response, which is induced upon genotoxic or oxidative stress. Upon oxidative stress, ROS are believed to induce oxidative DNA damage and cause DNA strand breaks in the nucleus, which then strongly stimulates the enzymatic activity of ARTD1 and induces the formation of PAR (12). However, it has not been determined until now whether ARTD1 is activated by DNA damage *in vivo* or if the stimulation of ADP-ribosylation in response to oxidative stress is the result of signaling events that are not directly linked to DNA damage.

In this work, we deliberately interrupted the cellular signaling pathways induced early upon stimulation of oxidative stress by H_2O_2 to elucidate the molecular mechanisms involved in PAR formation. Using a systematic reverse phase protein array (RPPA) approach and in-depth molecular analysis of the key signaling components, we identified activation of the PLC/IP3R/calcium signaling axis as a key regulator of PAR formation. While calcium-dependent signaling induced DNA lesions, which alone were not able to activate ARTD1, calcium-dependent signaling

mediated by PKCα did not induce DNA lesions, but was nevertheless required to stimulate PAR formation. Our results show that PKCα activation and the consecutive phosphorylation of HMGB1, which leads to its chromatin eviction, is a major so far underappreciated mechanism by which oxidative stress stimulates PAR formation.

MATERIAL and METHODS

Cell culture, siRNA transfection, lysis and proliferation assay

MRC-5 and IMR-90 human lung fibroblasts (32,33) were obtained from the American Type Culture Collection (ATCC) and cultured in supplemented MEM (Invitrogen). NIH/3T3 were obtained from American Type Culture Collection (ATCC) and cultured in supplemented DMEM (Invitrogen). MEFs were cultivated in supplemented DMEM. Cells were preincubated with inhibitors or activators (stocks dissolved in DMSO) for 1 h prior to H_2O_2 treatment in FCS-free media, which was also used as a vehicle for H_2O_2. All inhibitors were obtained from Enzo Life Sciences, except from Olaparib (AstraZeneca), PD98059 (Santa Cruz), IKK VII and KN-93 and PMA (Merck Millipore) and used at a final concentration as indicated in the figures or figure legends. To reduce isoform specific ARTD1, PKCα/δ, PKC pan or HMGB1 expression, $2x10^5$ NIH/3T3, $1x10^5$ MRC-5 cells or $2.5x10^4$ MEFs were transfected using mouse siARTD1 (QIAGEN, SI02731428), siPKCα (QIAGEN, SI01388583), siPKCδ (QIAGEN, SI01388744), siHMGB1 (Microsynth) or siMock (QIAGEN, scrambled sequence), or human siARTD1 (Microsynth), siPKC pan (Santa Cruz Biotechnology, sc-29449), siHMGB1 (QIAGEN, SI03650374), lacking significant homology to any known human or mouse gene sequence) with Lipofectamine RNAiMAX transfection reagent (Invitrogen) according to manual's instructions over 3-4 days, prior to H_2O_2 treatment. Whole cell extracts were prepared with standard RIPA lysis buffer (50 mM Tris/pH8, 400mM NaCl, 0.5% NP-40, 1% DOC, 0.1% SDS supplemented with proteinase inhibitor cocktail (Roche), 10 mM β-glycerolphosphate, 1mM NaF and DTT) and total protein concentration determined using standard Lowry method. Cytoplasmic/chromatin fraction was prepared as described in (34). Cell viability was determined by the MTT assay (Sigma).

Reverse phase protein arrays (RPPA)

RPPA were prepared as described (35,36). In brief, whole cell extracts were spotted onto hydrophobically coated Zeptosens Chips (Bayer Technology Services GmbH). Serially diluted lysates (100, 75, 50 and 25%) were arrayed in duplicates onto hydrophobic Zeptosens Chips using the Nanoplotter NP2.0 (GeSiM), followed by blocking in an ultrasonic nebulizer (ZeptoFOG, Bayer Technology Services GmbH). Antibody incubation (Invitrogen), microarray data acquisition (ZeptoREADER, Bayer

Technology Services GmbH) and data analysis (ZeptoVIEW version 3.1.0.2, Bayer Technology Services GmbH) was performed exactly as described (37). The eight data points (100, 75, 50, 25% lysate amount in duplicates) were fitted using a weighted linear least squares fit (38) and the relative fluorescence intensity determined by interpolating at the median protein concentration or modification. To correct for small variations in protein content, relative intensities were normalized to the signals of β-Catenin, which did not show any significant variation (ANOVA, $p < 0.05$) in response to H_2O_2 over 10-60 min.

Significance and clustering analysis

To identify significant proteome changes in response to H_2O_2, relative fluorescence intensities were imported to MeV version 4.6 (39). Relative fluorescence intensities were log2 transformed and normalized, before performing statistical analysis using One-way ANOVA as described in (40). The mean transformed fluorescence intensities for group 1 (biological duplicates of untreated_10 min), group 2 (biological duplicates of 0.5 mM_10 min), group 3 (biological duplicates of 0.5 mM_60 min) were compared using F-statistics with $p < 0.05$. For fold-change analysis, transformed means of the biological replicates were normalized to the untreated sample (set as 1) and proteome changes were filtered (cut off set at 1x SD equal to log2 > 0.77 / < -0.77 for 0.5 mM). Significant proteome changes in response to H_2O_2 were selected for clustering analysis (Fig. S2a) if significant by one-way ANOVA ($p < 0.05$). To correct for potential false negatives or positives, significance analysis was performed using fold change cut off with thresholds described above or performing a quality control analysis by visualization (V.C.) for clustering analysis as shown Fig. S2c. Similar profiles of the fold changes over time were identified by clustering analysis using the k-means clustering algorithm and default parameters of MeV version 4.6 (39). K-means based clustering analysis in Fig. 1f comprises significant proteome changes, identified by ANOVA ($n=2$, $p<0.05$), Fold change cut off (1 S.D.) and/or visual control (V.C.) and thus might slightly differ from the results obtained by k-means clustering using only ANOVA ($n=2$, $p<0.05$) in Fig. S2a.

Pathway and network analysis

Gene pathway membership data was obtained from protein interaction database, PID (41) and KEGG (42). A total of 200 and 211 pathways were obtained from PID and

KEGG, respectively. For statistical analysis all analyzed proteins in this study (unique IDs) were set as the background list and all pathways consisting of more than 5 proteins from the background list were considered for statistical analysis by Fisher's exact test, resulting in a total of 93 pathways from PID and 63 from KEGG. Fisher's exact test was performed to identify pathways significantly affected by proteins (modifications) altered in response to H_2O_2 (significant by ANOVA and fold-change) using the R statistical framework (43). To account for multiple testing, p values were corrected for false discovery rates (FDRs) using Benjamini-Hochberg correction. We have used an FDR corrected p value cut off of 0.1 to identify pathways significantly affected by proteome changes.

Significant proteome changes, identified by statistical (ANOVA) and fold-change analysis (log2 cut off) were subjected to protein-protein interaction analysis using STRING (v 9.0) (44). Only interactions with a STRING score of at least 0.7 were further analyzed using Cytoscape (http://www.cytoscape.org/) (45).

Immunoblotting

For Western Blot analysis, proteins were separated by SDS PAGE gel electrophoresis and bands were visualized by either using horseradish peroxidase-conjugated antibodies (1:5000, GE Healthcare) and ECL detection (GE Healthcare) or by using IR-Dye-conjugated antibodies (1:15000, LI-COR) and detection by the Odyssey infrared imaging system (LI-COR). For quantification, bands were analyzed by ImageJ 1.46 (35) and the Odyssey imaging software (LI-COR).

Antibodies used for Western blotting were anti-ARTD1 (Santa Cruz), anti-CREB Phospho (pS133)/ATF-1 Phospho (CST), anti-JNK1/2 (CST), anti-JNK1/2 Phospho (CST), anti-PAR (10H, homemade), anti-PKCα (CST), antiPKC-δ (CST), anti-Tubulin (1:10'000, Sigma), anti-HMGB1 (1:5000 abcam), anti-H3 (1:5000 abcam). If not else stated, antibody dilution was 1:1000.

Immunofluorescence (IF) microscopy

For PAR IF analysis $1.5x10^5$ NIH/3T3 or $2.5x10^4$ MEF, MRC-5, or IMR-90 cells were grown on cover slips overnight prior to inhibitor/activator preincubation and H_2O_2 treatment. Afterwards cells were washed with PBS (1x), fixed with ice-cold methanol and acetic acid (3:1) for 10 min at 4°C, washed with PBS (3x), blocked in 5% milk/0.05% Tween-20 in PBS for 30 min and stained immunohistochemically

with primary mouse anti-poly(ADP-ribose) IgG, 1:250 (10H, homemade). Next, cells were washed with PBS (3x) before hybridization with a secondary antibody (1:250 Cy3 conjugated anti-mouse IgG, Jackson ImmunoResearch or 1:250 Alexa Fluor 488 ocnjugated anti-rabbit IgG, Invitrogen). Eventually, cells were mounted on glass slides using DAPI-containing VECTASHIELD (Vector Labs) and images acquired using an inverted fluorescence microscope at 40x, oil immersion (Leica). Fluorescence intensity or foci number were quantified using ImageJ (v. 1.46r) or Imaris (v. 7.6.0, Bitplane) and equal set-up between the images and experiments.

Image-based cell cycle staging

For quantitative image-based cell cycle staging, automated wide-field microscopy was performed on a Leica DMI 6000 inverted microscope equipped with a motorized stage, a Tri-band bandpass filter (DAPI/FITC/TX; BP387/11/BP 494/20/BP 575/20) and a 12-bit monochrome EMCCD camera (Leica DFC 350 FX, 1392x1040 pixels, 6.4µm pixel size). All images were acquired under non-saturating conditions and unbiased, automated image acquisition was performed using the Leica Matrix Screening Software. Images were imported to the Olympus ScanR Image Analysis Software Version 2.5.1, a dynamic background correction was applied, and nuclei segmentation was performed using an integrated intensity-based module. Pulsed 5-ethynyl-2'-desoxyuridine (EdU) incorporation, PAR levels, and DAPI intensities were measured. G1 cells were identified based on their low EdU and low DAPI content, S phase cells based on their high EdU content, and G2 cells based on their low EdU and high DAPI content.

***In vitro* kinase and ARTD1 automodification assay**

For PKCδ kinase assay, experiment was performed using 0.2 µl recombinant PKC catalytic subunit of the PKCδ isoform from rat brain (Sigma, P1609) and 1 µg ARTD1 fl. or ARTD1 fr. in PKCδ kinase buffer (120 mM Tris/pH 7.5, 40 mM MgCl2, 2 mM CaCl2, 2 mM DTT) and 20 nM ATP (Sigma) spiked with 0.74 MBq gamma-labeled ATP (20 nM) and reaction time as indicated in the figure or figure legend. For PKCα kinase assay 100 ng recombinant PKCα (Enzo, BML-SE494-0005) were incubated in PKCα kinase buffer (25 mM MOPS/pH 7.2, 12.5 mM β-glycerophosphate, 25 mM $MgCl_2$, 5 mM EGTA, 2 mM EDTA and 0.25 mM DTT) with 100 µM ATP (Sigma) spiked with 0.74 MBq gamma-labeled ATP (20 nM) /

reaction and 1 µg recombinant ARTD1 fl., ARTD1 deletion fragments (ARTD1 fr.), HMGB1 or histone-mix (Roche) for 15 min. For ARTD1 automodification assay, the kinase assay reaction was supplemented with PARP reaction buffer (50 mM Tris-HCl/pH 8, 4 mM $MgCl_2$, 250 µM DTT, 1 µg pepstatin/bestatin/leupeptin), 100 µM or 100 nM NAD (Sigma) spiked with 100 nM gamma-labeled NAD and in some cases 0.5 pmol of EcoRI dsDNA linker to induce ARTD1 activity *in vitro*.

RESULTS

H_2O_2 rapidly induces nuclear PAR and in a cell cycle-independent manner

To study the signaling mechanisms by which oxidative stress induces PAR formation and to obtain kinetic and dose response information on this process, MRC-5 primary human fibroblasts were treated for different periods of times (10 to 60 min) with increasing concentrations of H_2O_2 (0.1 to 2 mM), and PAR formation was analyzed by immunofluorescence (Fig. 1a, S1a) or Western blotting (Fig. 1b). These experiments revealed that H_2O_2 transiently induced strong nuclear PAR formation already at 10 min after treatment, with levels returning to baseline after 60 min, and that maximum PAR formation was observed already at 0.5 mM H_2O_2. Nuclear PAR formation was prevented when cells were preincubated with either the ARTD inhibitor ABT-888, olaparib, or PJ-34, indicating that it was formed by intracellular ARTDs (Fig. 1b, S1b). PAR formation coincided with activation of ARTD1, as shown by the automodification of ARTD1 in nuclei isolated from mouse embryonic fibroblasts (MEFs) treated with H_2O_2 for 10 min and incubated with radioactively labeled NAD^+ (Fig. S1c). Moreover, knockdown of ARTD1 by siRNA confirmed that H_2O_2-induced PAR formation was predominantly mediated by ARTD1 (Fig. 1c). H_2O_2-induced nuclear PAR formation occurred during all cell cycle stages (Fig. 1d, S1d), indicating that PAR formation was not a result of potential H_2O_2-induced changes in the cell cycle, but due to direct cell cycle-independent signaling. To investigate the early H_2O_2-induced signaling events under sub-lethal, mild oxidative stress conditions, cell viability was assessed 24 h after treatment of cells with different concentrations of H_2O_2 (Fig. S1e). While cells treated with 0.5 mM H_2O_2 were still viable 24 h later (a dose at which PAR formation was already maximal), cell viability was markedly reduced when cells had been treated with 2 mM H_2O_2 (Fig. S1e). Interestingly, H_2O_2-induced PAR formation did not coincide with 53BP1 foci formation or γH2A.X staining, which was observed only after 60 min (Fig. S1f), suggesting that during the first 10 min no double strand breaks were generated.

H_2O_2 treatment induces dynamic proteomic changes

To investigate the early H_2O_2-induced signaling events that potentially regulate PAR formation, a proteomics screen using reverse phase protein arrays (RPPA) focusing on intracellular signaling cascades (i.e. kinases and their substrates) was performed on

MRC-5 cells treated with a sublethal concentration of H_2O_2 (i.e. 0.5 mM) for either 10 or 60 min, respectively (Fig. 1e-f, S2a, b). The two different time-points were chosen because strong PAR formation is observed at 10 min, while PAR is no longer detectable at 60 min after H_2O_2 treatment (Fig. 1a). Significant changes in protein level or in posttranslational modification in the RPPA analysis were determined by statistical analysis using ANOVA ($p<0.05$, $n=2$). Untreated samples were used as a control group (Fig. 1f, S2a-d). The significant changes were clustered based on their temporal changes upon H_2O_2 treatment using k-means clustering algorithm (Fig. S2a-d). The majority of significant signal reductions concerned total protein levels, while increases in response to H_2O_2 treatment were often observed for phosphorylation events (Fig. S2d). Interestingly, early activation clusters 1-3 comprised kinases exclusively found in the cytoplasm and known to be activated directly by either stress stimuli (p-p38, p-JNK) or growth factor signaling (ErbB-2, p-Akt). Calcium signal transducers were also found among the early-induced proteome changes (p-PLCγ, p-PKC, p-CaMKII, p-CREB, p-PLA2) (Fig. 1f, 1g, S2d). The majority of late activated signaling events (cluster 4) included DNA damage response and cell cycle players such as p-aurora A, p-Chk1, p-cyclin D, p-p53, p-p27 and γH2AX (Fig. 1g). Downregulated proteins or phosphorylation (cluster 5) contained many factors involved in cell death. However, the main hubs (Akt, p38, ERK2) in the protein-protein interaction network were rather cytoplasmic signaling components (except for p53) mostly induced at the early time point, indicating cytoplasmic signaling events as the initial signaling events upon oxidative stress (Fig. 1h). In summary, our systematic RPPA analyses of the early H_2O_2-induced proteome changes have identified several cytoplasmic kinases and signaling components, which may potentially be involved in PAR formation.

Sublethal H_2O_2 treatment induces several cellular signaling pathways, which however do not regulate PAR formation

Some of the observed proteomic changes strongly correlated in their kinetics with PAR formation, pointing at possible candidates for regulating PAR formation. To further validate the H_2O_2-induced early signaling proteomic changes potentially responsible for PAR formation, a screen with small molecule inhibitors for a sub-set of the identified early-activated cytoplasmic kinases was performed. Both human IMR-90 and mouse NIH/3T3 fibroblasts were treated with inhibitors against either

ARTDs (olaparib, as control, ARTDi), IKK (IKK VII, IKKi), AMPK (dorsomorphin, AMPKi), p38 (SB203580, p38i), JNK (SP600125, JNKi) or MEK (PD985059, MEKi), and PAR formation assessed by IF analysis or western blotting using the 10H anti-PAR antibody (Fig. 2a). Even though the kinetics of the H_2O_2-mediated activation of AMPK, p38 and IKK (IκBα phosphorylation) correlated with the enhanced PAR formation, their inhibition did not, or only weakly affect PAR levels (Fig. 2a, S3a), suggesting that these pathways do not regulate PAR formation. While inhibition of JNK with SP600125 significantly reduced PAR formation (Fig. 2a, S3b), we could not confirm this observation with JNK1/2 KO MEFs or siRNA experiments, indicating an off-target effect of SP600125 (Fig. S3c-d). Interestingly, H_2O_2 treatment does not only seem to induce positive, but also negative regulators of PAR formation. Thus, pretreatment of IMR-90 cells with MEK inhibitor (MEKi) lead to enhanced PAR formation (Fig. 2a). However, pre-treatment with MEKi in MEFs as well as knockdown of ERK1 and/or ERK2 in the same cells, had no significant effect on PAR formation (Fig. S3e), suggesting that ERK1/2 signaling is not involved in H_2O_2-induced PAR formation. In conclusion, although H_2O_2-induced PAR formation correlated with the activation of several signaling pathways, they do not regulate PAR formation.

Activation of membrane-associated phospholipase C and calcium signaling from the ER by IP3 are important for nuclear PAR formation

To further investigate how H_2O_2 induces nuclear PAR formation, additional pathways were explored with small molecular inhibitors for their role in PAR formation. One of the earliest changes observed by the RPPA was enhanced phosphorylation of membrane-associated phospholipase C (PLCγ) (Fig. 1f). To investigate the involvement of PLCγ in H_2O_2-induced PAR formation, IMR-90 fibroblasts were treated with the PLC inhibitor (PLCi) U-73122 (Fig. 2b). Treatment of cells with PLCi before inducing oxidative stress significantly reduced PAR formation, revealing that PLC contributes to PAR formation. PLC is known to stimulate the inositol triphosphate receptor (IP3R) at the ER through the synthesis of IP3. We thus extended the inhibitor screen including inhibitors against IP3R. The IP3R inhibitor 2-APB (IP3Ri) significantly reduced PAR formation, supporting the notion that PLC induces cytoplasmic signaling through IP3 and stimulation of the IP3R at the ER membrane. Activation of IP3R is known to release calcium (Ca^{2+}) from the ER.

Indeed, pre-treatment of cells with the cell membrane-permeable Ca^{2+} chelator BAPTA-AM (Ca^{2+}i) significantly reduced H_2O_2-induced PAR formation (Fig. 2b and S3f), indicating that calcium signaling positively regulates PAR formation. Moreover, Ca^{2+}i inhibited nuclear PAR formation in all cell cycle phases, indicating that the Ca^{2+}-dependency of PAR formation is cell cycle-independent (Fig. 2c). Extensive uptake of Ca^{2+} by the mitochondria, could lead to the opening of the mitochondrial permeability transition pore (mPTP) and a subsequent release of high levels of NAD^+, which has been suggested to activate PAR formation upon ischemia-reperfusion injury (17). However, inhibition of the mPTP controlling protein cyclophilin D (CypDi) did not affect the H_2O_2-induced PAR formation, suggesting that the calcium-induced opening of mPTP does not play a role in H_2O_2-induced PAR formation.

PKCα controls oxidative stress-induced PAR formation

Another early change observed in the RPPA analysis was the phosphorylation of PKC substrates. The PKC family of protein kinases consists of the conventional, calcium-dependent enzymes, as well as the novel and atypical calcium-independent kinases (46). In mammals, the PKC protein family consists of four conventional (PKCα, -βI/II and -γ), four novel (PKCδ, -ε, -η and -θ) and two atypical (PKCζ and -ι) isozymes (46). Interestingly treatment of MRC-5 cells with the PKC inhibitor (PKCi) led to enhanced H_2O_2-induced PAR formation (Fig. 2d). Similar results were obtained with IMR-90 cells (Fig. S3g). However, the PKC inhibitor-enhanced H_2O_2-induced PAR formation was completely abolished by the calcium chelator BAPTA-AM (Ca^{2+}i), suggesting that Ca^{2+}-dependent signaling is essential for the induction of nuclear PAR formation by H_2O_2 and more dominant than the negative regulatory effect mediated by PKC inhibition. To confirm PKC-dependent regulation of oxidative stress-induced PAR formation, MRC-5 cells were transfected with a pan siPKC against all PKC family members. In contrast to the PKC inhibitor effect, knockdown of PKC isoforms, including PKCα and PKCδ, led to a strong reduction in the number of H_2O_2-induced PAR foci (Fig. 2e and 2f), suggesting that different PKC family members may regulate PAR formation in opposite ways. Thus, to dissect the positive and negative regulatory effects observed by PKC inhibition and down-regulation, NIH/3T3 cells were transfected with siPKCα and/or siPKCδ. In line with the PAR-reducing effect of BAPTA-AM, knockdown of PKCα resulted in

significantly lower H_2O_2-induced PAR formation as compared to control siRNA (Fig. 2g, S4a). This effect was confirmed using PKCα KO MEFs, which showed significantly less H_2O_2-induced PAR formation as compared to WT MEF (Fig. S4b, S4c). In contrast, knockdown of PKCδ resulted in enhanced PAR formation, comparable to that with the PKC inhibitor. Double knockdown of PKCα and PKCδ caused a reduction in PAR levels similar to that by knockdown of PKCα only, suggesting a dominant effect of PKCα on PAR formation (Fig. 2g). Knockdown of the conventional PKC family members β and γ showed no effect on PAR formation (Fig. S4d). Together, these results demonstrate both stimulating and attenuating functions of PKC isoforms in H_2O_2-treated fibroblasts, although PKCα seems to dominate over PKCδ.

PKCα does not regulate calcium-induced DNA lesions, but neither do OGG1 or APE1

To further investigate the positive regulatory function of PKCα in H_2O_2-induced PAR formation, we studied whether PKCα translocates to the nucleus in response to H_2O_2 and potentially regulates ARTD1 activity in this compartment. Indeed, 10 min after treatment of MEFs with H_2O_2, PKCα levels were ~2.5-fold increased in the nucleus, with a corresponding decrease in the cytoplasm (Fig. 3a). Genetic complementation of WT or ARTD1 KO MEFs with WT ARTD1, an ARTD1 mutant with only mono-ADP-ribosylation activity (E988K), or a mutant that lacks zinc fingers I and II (aa215-1014), revealed that the presence of zinc fingers and thus the binding to DNA is important for the ARTD1-mediated PAR formation in vivo (Fig. 3b). Since ARTD1 is strongly activated by DNA damage, we tested whether PKCα-dependent formation of DNA lesions is responsible for the activation of ARTD1. Thus, MEF cells were treated with siPKCα, stimulated with H_2O_2 and DNA integrity assessed by the comet assay. While H_2O_2 induced DNA tail formation in a dose and time-dependent manner (Fig. S4e), DNA tail formation was still present in cells treated with siPKCα (Fig. 3c), suggesting that PKCα does not regulate PAR formation by affecting H_2O_2-induced DNA damage and that the induced DNA damage is not sufficient to induce PAR formation (Fig. 3c upper panel). Similarly, H_2O_2-induced activation of ARTD1 (measured by automodification activity in nuclear extracts) was not affected by siPKCα treatment (Fig. 3d). Intriguingly, however, treatment of cells

with BAPTA-AM caused a marked reduction in H_2O_2-induced DNA lesions (Fig. 3e) and activation of ARTD1 (Fig. 3f), suggesting that Ca^{2+}-dependent signaling is important for the observed DNA tail formation. Interestingly, neither knockdown of the calcium-dependent DNA-glycosylase OGG1 nor APE1 affected PAR formation or induced DNA tail formation after 10 min of oxidative stress (Fig. S4f), suggesting that the observed DNA lesions may not be 8oxoG modifications or abasic sites. The dependency on Ca^{2+} was specific for H_2O_2-induced DNA lesions, since DNA damage induced by either $KBrO_3$ or MNNG was much less affected, if at all, by treatment with BAPTA-AM (Fig. 3g).

PKCα regulates oxidative stress-induced PAR formation independently of ARTD1 phosphorylation

To assess a potential direct regulation of ARTD1 activity through phosphorylation by PKCα in the nucleus, full-length ARTD1 was incubated with PKCα and radioactively labeled ATP in vitro. DNA polymerase beta (Polβ), known to be phosphorylated by PKC (47) was included as positive control in the reaction containing PKCα (Fig. 3h), indicating that PKCα is able to directly phosphorylate ARTD1 *in vitro*. Incubation of different ARTD1 fragments with PKCα indicated that ARTD1 was phosphorylated indiscriminately at various sites across the whole protein (Fig. 3i). To assess whether the enzymatic activity of ARTD1 is affected by PKCα-mediated phosphorylation, ARTD1 pre-phosphorylated by PKCα was incubated with radioactively labeled NAD^+ in the presence or absence of ATP and different amounts of DNA (Fig. 3j). ARTD1 activity was essentially the same whether ARTD1 was phosphorylated by PKCα or not, thus excluding direct PKCα-dependent phosphorylation of ARTD1 as the mechanism by which PAR formation is induced in a calcium-dependent manner upon H_2O_2 treatment and suggest an indirect mechanism by which PKCα activates ARTD1. Interestingly, comparable experiments with the calcium-independent PKCδ isoform revealed that PKCδ phosphorylates ARTD1 at the N-terminus (amino acids 1-214) and phosphorylation of ARTD1 by PKCδ inhibited DNA-induced PAR formation by ARTD1 *in vitro* (Fig. S4g, h), suggesting that the observed stimulatory effect of the PKCi on PAR formation is likely due to inhibition of PKCδ.

Oxidative stress-induced PKCα-dependent phosphorylation of HMGB1 is essential for PAR formation

To investigate additional PKCα targets that could potentially positively influence PAR formation, histones were phosphorylated by PKCα *in vitro* and subjected to an *in vitro* ADP-ribosylation assay (Fig. 4a, b). Neither phosphorylated, nor non-phosphorylated histones showed any enhancing effect on the ARTD1 autocatalytic activity, excluding that PKCα mediates PAR formation by the phosphorylation of histones.

Another known PKCα target within the chromatin landscape that could potentially affect PAR formation is the ubiquitously expressed histone-like protein high mobility-group protein box 1 (HMGB1). HMGB1 has been described to alter its DNA binding-affinity when phosphorylated by PKC (48,49). To study the consequences of HMGB1 phosphorylation by PKCα, recombinant HMGB1 was incubated with PKCα and radioactively labeled ATP. A strong signal corresponding to phosphorylated HMGB1 was observed (Fig. 4c), confirming that HMGB1 is a target of PKCα *in vitro*. Phosphorylation of HMGB1 by PKCα did not show an enhanced ARTD1 autocatalytic activity *in vitro* (Fig. 4d). However, these *in vitro* studies are not in the context of chromatin, which could be an important factor for the activity of ARTD1. Thus, further studies were conducted in MEFs lacking HMGB1. We knocked down HMGB1 together with PKCα in WT MEF cells to further investigate a possible contribution of HMGB1 to PAR formation. Surprisingly, knockdown of HMGB1 and PKCα rescued the inhibitory effect of PKCα single knockdown on H_2O_2-induced PAR formation (Fig. 4e). In HMGB1 KO MEFs, the inhibitory effect of PKCα knockdown was also greatly attenuated (Fig. S4i).

To test, whether the observed rescue of PKCα knockdown on PAR formation by HMGB1 was based on protein/protein interactions only or required Ca^{2+} signaling-induced DNA lesions, MEFs were treated with BAPTA-AM after knockdown of HMGB1 alone or after HMGB1/PKCα double-knockdown (which showed the partial rescue) and PAR formation assessed after H_2O_2 treatment (Fig. 4e). Under the tested conditions, treatment with BAPTA-AM abrogated PAR formation in MEFs, but also in cells with knocked-down HMGB1 and HMGB1 KO MEFs (Fig. S4j), suggesting that Ca^{2+} signaling-induced DNA lesions are important, but not sufficient for PAR formation.

To investigate whether HMGB1 contributes to the effect of PKC knockdown also in human cells (cf. Fig. 2e), the effect of PKC knockdown was tested in MRC-5 cells knocked-down for HMGB1 and compared to cells with proficient HMGB1 levels (Fig. 4f). Also in this case, the attenuating effect of PKC knockdown on PAR formation was reversed in cells depleted of HMGB1. These results provide strong evidence that the positive effect of PKCα on PAR formation is mediated through HMGB1.

To study how the H_2O_2-induced phosphorylation by PKCα affects the chromatin association of HMGB1, H_2O_2-treated MEFs were fractionated into chromatin and cytoplasmic fraction. While an increased amount of HMGB1 could be detected in the cytoplasmic fraction of H_2O_2-treated as compared to non-treated MEFs, the levels in the chromatin fraction remained unaffected (Fig. 4g). The cytoplasmic increase of HMGB1 was absent in MEFs lacking PKCα, indicating that phosphorylation of HMGB1 by PKCα reduces its chromatin association.

These results suggest that the presence of HMGB1 at the chromatin represses PAR formation during H_2O_2-induced DNA lesions, until the H_2O_2-stimulated Ca^{2+} release activates PKCα, leading to phosphorylation of HMGB1 and consequential decreased affinity of HMGB1 for the chromatin, revealing an intriguing interplay between PAR stimulating and inhibiting mechanisms.

DISCUSSION

Our results indicate two main molecular mechanisms that regulate ARTD1 activity upon oxidative stress. Oxidative stress induces intracellular Ca^{2+} release which not only induces PAR-stimulating DNA lesions, but also releases the inhibitory effect of HMGB1 by PKCα-mediated HMGB1 phosphorylation and chromatin eviction to successfully induce full PAR formation in the nucleus (Fig. S4k).

Oxidative stress is a potent activator of PAR formation in different cell types, but a coherent picture of the molecular events that lead to ARTD1 activation and PAR formation has not existed so far. Although ARTD1 appears to be activated by oxidative stress indirectly via the induction of DNA lesions, a mechanism providing evidences for such a direct activation *in vivo* has not been reported and ample evidence suggests additional possibilities of controlling ARTD1 enzymatic activity. To elucidate the activated signaling pathways during oxidative stress, we applied a proteomics screen using reverse phase protein arrays (RPPA) focusing on the major intracellular signaling cascades (i.e. kinases and their substrates) in MRC-5 cells treated with a sublethal concentration of H_2O_2. Overall, the majority of significant signal reductions concerned total protein levels, while increases in response to H_2O_2 treatment were often observed for phosphorylation events. This could be explained by the H_2O_2-induced inhibition of translation, which causes a general reduction of the protein half-life (50). Moreover, this analysis revealed the kinetics of the H_2O_2-mediated activation of several pathways. The bioinformatics analysis of the samples treated with 0.5 mM did not significantly differ from samples treated with a lethal dose (i.e. 2 mM, data not shown), suggesting that the initiated signal pathways are the same, independent on the cell fate. Interestingly, validation of several pathways with inhibitors revealed that many of the induced pathways did not, or only weakly, affect PAR formation, suggesting that these pathways do not regulate nuclear PAR formation. Only inhibition of signaling pathways involving JNK, MEK and PKC altered the PAR intensity significantly which is in agreement with previous observations (27,29,51). However, validation of these results by siRNA or using KO MEFs revealed that the JNK and MEK pathway are unlikely to regulated PAR formation and that the observed effect of the inhibitors on PAR formation could be due to off target effects, as in the case with the JNK_i.

From the other tested signaling events, Ca^{2+} release from the endoplasmatic reticulum and Ca^{2+}-dependent signaling was confirmed to play a major role during

oxidative stress and for PAR formation. This finding is in agreement with studies that have implicated calcium signaling in the activation of ARTD1 (52-54). Our findings revealed that Ca^{2+} release is initiated at the cellular plasma membrane through the activation of phospholipase C (PLC). This is in agreement with earlier publications reporting that phosphorylation and activation of PLC by a sulfhydryl oxidation-dependent mechanisms, which leads to increased IP3 synthesis and subsequent activation of the IP3 receptor to induce the release of Ca^{2+} from intracellular stores (55,56). Chelation of Ca^{2+} by BAPTA-AM strongly inhibited H_2O_2-induced PAR formation, suggesting that this event is important for PAR formation. Ca^{2+} activated mainly two different molecular processes that seemed to regulate nuclear PAR formation, the induction of DNA lesions and the activation of PKCα, respectively. The nature of the detected Ca^{2+}-induced DNA lesions needs further investigation, since the performed experiments allow the detection of double-stranded, single-stranded DNA breaks, but also abasic sites. Although we did observe a very strong correlation between Ca^{2+} release and the induction of DNA lesions, we cannot conclude to which extent the induced lesions are required for PAR formation, since the molecular mechanism responsible for the induction of the observed lesions is currently not known. Interestingly, neither knockdown of OGG1 nor APE1 affected PAR formation or induced DNA tail formation after 10 min of oxidative stress, suggesting that the initial H_2O_2-induced DNA lesions (i.e. within the first 10 min) may not be 8oxoG or abasic DNA sites. Ca^{2+} also activated the Ca^{2+}-dependent PKC isoform PKCα, which upon oxidative stress localized to the nucleus. Interestingly, PKCα has so far not been linked to the regulation of PAR metabolism and ARTD1 activity and was only studied as a factor affected by PARP inhibition (57). At the molecular level we found that PKCα was able to phosphorylate ARTD1. Previous studies have already shown ARTD1 phosphorylation by PKCα and PKCβ, and identified Ser504, Ser519 and Trh656 as preferential phosphorylation targets of PKCβ in full length ARTD1 (58). Phosphorylation of ARTD1 by PKCα *in vitro* did not alter ARTD1 enzymatic activity. In contrast, oxidative stress also activated the Ca^{2+} independent PKC isoform PKCδ, which phosphorylated ARTD1 *in vitro* and reduced ARTD1-dependent DNA-induced PAR formation. We localized the phosphorylation by PKCδ to the N-terminal DBD of ARTD1, with a strong preference for the region encompassing the first two zinc fingers. Based on *in silico* analysis, sequence-stretches around Ser20 in the N-terminal DBD of ARTD1 match the consensus-motif

of the two Ca^{2+}-independent PKC isoforms PKCδ and PKCε (Motif Scan, ScanSite). Indeed, based on two recently published structures of ARTD1 zinc finger domains bound to DNA, Ser20 stabilizes the interaction with the DNA backbone by forming a hydrogen bond with a phosphate of a phosphodiester bond (59,60). It can thus be speculated that phosphorylation of Ser20 by PKCδ destabilizes the interaction of the first ARTD1 zinc finger with the DNA backbone due to the negative charge of the phosphorylation, eventually resulting in less activity in response to H_2O_2. This observation is in agreement with data obtained with inhibition of PKC signaling by the pan PKC inhibitor GF109203X that led to a significant increase in H_2O_2-induced PAR formation. Indeed, PKC has been previously shown to phosphorylate ARTD1 *in vitro* (30) and its inhibition resulted in increased PAR induction upon alkylation stress (29), indicating a general regulatory mechanism of ARTD1 activity by PKCs in response to genotoxic stress. In contrast, there are also studies that have reported a positive regulation of ARTD1 by PKCδ in response to histamine and we did not observe a stimulation of ARTD1 by PMA treatment alone (data not shown) (31,61). Thus the reported studies identified so far two seemingly opposing (positively and negatively), calcium-dependent and -independent regulatory mechanisms for PAR formation upon oxidative stress within the PKC family of proteins in human primary fibroblasts as well as in murine NIH/3T3 cells and MEFs. However, since the double knockdown of PKCα and PKCδ in our studies caused in the analyzed human and mouse fibroblast a reduction in PAR levels similar to that by knockdown of PKCα only, PKCα seems to play a dominant and more relevant role in PAR formation in the analyzed cell types.

PKCα was found to regulate PAR formation not by influencing H_2O_2-induced DNA damage, but its PAR-regulating mechanism is mainly through phosphorylation and subsequent release of the High mobility group box 1 (HMGB1) from chromatin. H_2O_2 treatment of cells has been described to influence the chromatin structure, possibly dependent on calcium signaling (62). HMGB1 is a chromatin-associated protein that plays a role in the organization, sliding and incorporation of nucleosomes (63-65), as well as the compaction of chromatin (66). There is evidence that the nucleosome occupancy in cells lacking HMGB1 changes globally over the genome and that the DNA is more accessible to MNase digestion (67). The release of HMGB1 from chromatin and nucleus into the cytoplasm is inhibited by chelation of calcium (68), showing the importance of calcium signaling in its dissociation from

chromatin. In HMGB1-deficient cells, we observed a stronger PAR formation in response to H_2O_2. Thus, there is a growing body of evidence that cellular signaling and chromatin-associated changes are involved in the activation of ARTD1 in a DNA damage-independent manner (69). Upon oxidative stress HMGB1 was released from chromatin, but only in the presence of PKCα. Interestingly, the regulatory effect of PKCα on PAR formation was reduced in cells lacking HMGB1, suggesting that HMGB1 is the principle PKCα target involved in controlling PAR formation. The impact of HMGB1 release on the chromatin structure, which chromatin domains (e.g. eu- or heterochromatin) are mainly affected and how the release allows for PAR formation needs further investigation. Whether the derepression of ARTD1 activity, due to Ca^{2+}-induced PKCα-dependent HMGB1 chromatin release includes additional proteins (e.g. H1 or HP1) or calcium-dependent processes *in vivo* remains to be determined.

In summary, the study presented here has identified the concurrent, H_2O_2-dependent activation of stimulatory and attenuating regulatory mechanism of nuclear PAR formation. Our findings thus highlight the complexity of the signaling network that regulate ARTD1-catalyzed PAR formation in the nucleus and identify key players that determine and fine-tune the nuclear PAR levels. Most importantly, the results presented here link cytoplasmic signaling components and pathways to the formation of PAR as a consequence of the calcium signaling. Furthermore, the calcium-dependent activation of PKCα leads to phosphorylation of HMGB1 and its subseuquent translocation from chromatin to cytoplasm, allowing for PAR formation to take place., These results thus identify PKCα as an important regulator of the chromatin modulation involved in oxidative stress-induced PAR formation, a finding that may have important medical relevance for oxidative stress-associated pathophysiological conditions.

REFERENCES

1. Shokolenko, I., Venediktova, N., Bochkareva, A., Wilson, G.L. and Alexeyev, M.F. (2009) Oxidative stress induces degradation of mitochondrial DNA. *Nucleic Acids Research*, **37**, 2539-2548.
2. Yoshida, H., Nishikawa, M., Kiyota, T., Toyota, H. and Takakura, Y. (2011) Increase in CpG DNA-induced inflammatory responses by DNA oxidation in macrophages and mice. *Free Radical Bio Med*, **51**, 424-431.
3. Zhang, Q., Itagaki, K. and Hauser, C.J. (2010) Mitochondrial DNA Is Released by Shock and Activates Neutrophils Via P38 Map Kinase. *Shock*, **34**, 55-59.
4. Brinkmann, V. and Zychlinsky, A. (2012) Neutrophil extracellular traps: Is immunity the second function of chromatin? *Journal of Cell Biology*, **198**, 773-783.
5. Collins, L.V., Hajizadeh, S., Holme, E., Jonsson, I.M. and Tarkowski, A. (2004) Endogenously oxidized mitochondrial DNA induces in vivo and in vitro inflammatory responses. *J Leukocyte Biol*, **75**, 995-1000.
6. Saxena, G., Chen, J.Q. and Shalev, A. (2010) Intracellular Shuttling and Mitochondrial Function of Thioredoxin-interacting Protein. *Journal of Biological Chemistry*, **285**, 3997-4005.
7. Yoshihara, E., Chen, Z., Matsuo, Y., Masutani, H. and Yodoi, J. (2010) Thiol Redox Transitions by Thioredoxin and Thioredoxin-Binding Protein-2 in Cell Signaling. *Method Enzymol*, **474**, 67-82.
8. Lane, T., Flam, B., Lockey, R. and Kolliputi, N. (2013) TXNIP shuttling: missing link between oxidative stress and inflannmasome activation. *Front Physiol*, **4**.
9. Kazak, L., Reyes, A. and Holt, I.J. (2012) Minimizing the damage: repair pathways keep mitochondrial DNA intact. *Nature reviews. Molecular cell biology*, **13**, 659-671.
10. Alexeyev, M., Shokolenko, I., Wilson, G. and LeDoux, S. (2013) The Maintenance of Mitochondrial DNA Integrity-Critical Analysis and Update. *Csh Perspect Biol*, **5**.
11. Suzuki, N., Kamataki, A., Yamaki, J. and Homma, Y. (2008) Characterization of circulating DNA in healthy human plasma. *Clin Chim Acta*, **387**, 55-58.

12. Hassa, P.O., Haenni, S., Elser, M. and Hottiger, M.O. (2006) Nuclear ADP-ribosylation reactions in mammalian cells: where are we today and where are we going? *Microbiol Mol Biol Rev*, **70**, 789-829.
13. Hottiger, M.O., Hassa, P.O., Lüscher, B., Schüler, H. and Koch-Nolte, F. (2010) Toward a unified nomenclature for mammalian ADP-ribosyltransferases. *Trends Biochem Sci*, **35**, 208-219.
14. Luo, X. and Kraus, W.L. (2012) On PAR with PARP: cellular stress signaling through poly(ADP-ribose) and PARP-1. *Genes Dev*, **26**, 417-432.
15. Altmeyer, M., Messner, S., Hassa, P.O., Fey, M. and Hottiger, M.O. (2009) Molecular mechanism of poly(ADP-ribosyl)ation by PARP1 and identification of lysine residues as ADP-ribose acceptor sites. *Nucleic Acids Res*, **37**, 3723-3738.
16. Krishnakumar, R. and Kraus, W. (2010) The PARP side of the nucleus: Molecular actions, physiological outcomes, and clinical targets. *Mol Cell*, **39**, 8-24.
17. Schiewer, M.J., Goodwin, J.F., Han, S., Brenner, J.C., Augello, M.A., Dean, J.L., Liu, F., Planck, J.L., Ravindranathan, P., Chinnaiyan, A.M. *et al.* (2012) Dual roles of PARP-1 promote cancer growth and progression. *Cancer Discov*.
18. Kraus, W.L. and Hottiger, M.O. (2013) PARP-1 and gene regulation: Progress and puzzles. *Mol Aspects Med*.
19. David, K.K., Andrabi, S.A., Dawson, T.M. and Dawson, V.L. (2009) Parthanatos, a messenger of death. *Front Biosci*, **14**, 1116-1128.
20. Lonskaya, I., Potaman, V.N., Shlyakhtenko, L.S., Oussatcheva, E.A., Lyubchenko, Y.L. and Soldatenkov, V.A. (2005) Regulation of poly(ADP-ribose) polymerase-1 by DNA structure-specific binding. *J Biol Chem*, **280**, 17076-17083.
21. Kim, M., Mauro, S., Gévry, N., Lis, J. and Kraus, W. (2004) NAD+-dependent modulation of chromatin structure and transcription by nucleosome binding properties of PARP-1. *Cell*, **119**, 803-814.
22. Kun, E., Kirsten, E., Mendeleyev, J. and Ordahl, C. (2004) Regulation of the enzymatic catalysis of poly(ADP-ribose) polymerase by dsDNA, polyamines, Mg2+, Ca2+, histones H1 and H3, and ATP. *Biochemistry*, **43**, 210-216.

23. Thomas, C.J., Kotova, E., Andrake, M., Adolf-Bryfogle, J., Glaser, R., Regnard, C. and Tulin, A.V. (2014) Kinase-Mediated Changes in Nucleosome Conformation Trigger Chromatin Decondensation via Poly(ADP-Ribosyl)ation. *Molecular Cell*, **53**, 831-842.
24. Cohen-Armon, M. (2007) PARP-1 activation in the ERK signaling pathway. *Trends Pharmacol Sci*, **28**, 556-560.
25. Cohen-Armon, M., Visochek, L., Rozensal, D., Kalal, A., Geistrikh, I., Klein, R., Bendetz-Nezer, S., Yao, Z. and Seger, R. (2007) DNA-independent PARP-1 activation by phosphorylated ERK2 increases Elk1 activity: a link to histone acetylation. *Mol Cell*, **25**, 297-308.
26. Kauppinen, T., Chan, W., Suh, S., Wiggins, A., Huang, E. and Swanson, R. (2006) Direct phosphorylation and regulation of poly(ADP-ribose) polymerase-1 by extracellular signal-regulated kinases 1/2. *Proc Natl Acad Sci USA*, **103**, 7136-7141.
27. Zhang, S., Lin, Y., Kim, Y.S., Hande, M.P., Liu, Z.G. and Shen, H.M. (2007) c-Jun N-terminal kinase mediates hydrogen peroxide-induced cell death via sustained poly(ADP-ribose) polymerase-1 activation. *Cell Death Differ*, **14**, 1001-1010.
28. Bauer, P.I., Farkas, G., Buday, L., Mikala, G., Meszaros, G., Kun, E. and Farago, A. (1992) Inhibition of DNA binding by the phosphorylation of poly ADP-ribose polymerase protein catalysed by protein kinase C. *Biochem Biophys Res Commun*, **187**, 730-736.
29. Hegedus, C., Lakatos, P., Olah, G., Toth, B.I., Gergely, S., Szabo, E., Biro, T., Szabo, C. and Virag, L. (2008) Protein kinase C protects from DNA damage-induced necrotic cell death by inhibiting poly(ADP-ribose) polymerase-1. *FEBS Lett*, **582**, 1672-1678.
30. Tanaka, Y., Koide, S.S., Yoshihara, K. and Kamiya, T. (1987) Poly (ADP-ribose) synthetase is phosphorylated by protein kinase C in vitro. *Biochem Biophys Res Commun*, **148**, 709-717.
31. Mizuguchi, H., Terao, T., Kitai, M., Ikeda, M., Yoshimura, Y., Das, A.K., Kitamura, Y., Takeda, N. and Fukui, H. (2011) Involvement of protein kinase Cdelta/extracellular signal-regulated kinase/poly(ADP-ribose) polymerase-1 (PARP-1) signaling pathway in histamine-induced up-regulation of histamine H1 receptor gene expression in HeLa cells. *J Biol Chem*, **286**, 30542-30551.

32. Jacobs, J.P., Jones, C.M. and Baille, J.P. (1970) Characteristics of a human diploid cell designated MRC-5. *Nature*, **227**, 168-170.

33. Nichols, W.W., Murphy, D.G., Cristofalo, V.J., Toji, L.H., Greene, A.E. and Dwight, S.A. (1977) Characterization of a new human diploid cell strain, IMR-90. *Science*, **196**, 60-63.

34. Mendez, J. and Stillman, B. (2000) Chromatin association of human origin recognition complex, cdc6, and minichromosome maintenance proteins during the cell cycle: assembly of prereplication complexes in late mitosis. *Mol Cell Biol*, **20**, 8602-8612.

35. Pawlak, M., Schick, E., Bopp, M.A., Schneider, M.J., Oroszlan, P. and Ehrat, M. (2002) Zeptosens' protein microarrays: a novel high performance microarray platform for low abundance protein analysis. *Proteomics*, **2**, 383-393.

36. Bluwstein, A., Kumar, N., Leger, K., Traenkle, J., Oostrum, J., Rehrauer, H., Baudis, M. and Hottiger, M.O. (2013) PKC signaling prevents irradiation-induced apoptosis of primary human fibroblasts. *Cell death & disease*, **4**, e498.

37. Voshol, H., Ehrat, M., Traenkle, J., Bertrand, E. and van Oostrum, J. (2009) Antibody-based proteomics: analysis of signaling networks using reverse protein arrays. *Febs J*, **276**, 6871-6879.

38. Bevington, P.R. (2002) *Data Reduction and Error Analysis for the Physical Sciences*. 3rd Ed. ed. McGraw-Hill, New York, NY.

39. Saeed, A.I., Sharov, V., White, J., Li, J., Liang, W., Bhagabati, N., Braisted, J., Klapa, M., Currier, T., Thiagarajan, M. *et al.* (2003) TM4: a free, open-source system for microarray data management and analysis. *Biotechniques*, **34**, 374-378.

40. Zar, J.H. (2009) *Biostatistical Analysis* 5th Ed. ed. Prentice Hall, Upper Saddle River, NJ.

41. Schaefer, C.F., Anthony, K., Krupa, S., Buchoff, J., Day, M., Hannay, T. and Buetow, K.H. (2009) PID: the Pathway Interaction Database. *Nucleic Acids Res*, **37**, D674-679.

42. Kanehisa, M., Goto, S., Furumichi, M., Tanabe, M. and Hirakawa, M. (2010) KEGG for representation and analysis of molecular networks involving diseases and drugs. *Nucleic Acids Res*, **38**, D355-360.

43. Ihaka, R. and Genleman, R. (1996) R. A language for data analysis and graphics. *J Comput Graph Stat*, **5**, 299-314.
44. Szklarczyk, D., Franceschini, A., Kuhn, M., Simonovic, M., Roth, A., Minguez, P., Doerks, T., Stark, M., Muller, J., Bork, P. *et al.* (2011) The STRING database in 2011: functional interaction networks of proteins, globally integrated and scored. *Nucleic Acids Res*, **39**, D561-568.
45. Shannon, P., Markiel, A., Ozier, O., Baliga, N.S., Wang, J.T., Ramage, D., Amin, N., Schwikowski, B. and Ideker, T. (2003) Cytoscape: a software environment for integrated models of biomolecular interaction networks. *Genome Res*, **13**, 2498-2504.
46. Newton, A.C. (2010) Protein kinase C: poised to signal. *Am J Physiol Endocrinol Metab*, **298**, E395-402.
47. Tokui, T., Inagaki, M., Nishizawa, K., Yatani, R., Kusagawa, M., Ajiro, K., Nishimoto, Y., Date, T. and Matsukage, A. (1991) Inactivation of DNA-Polymerase Beta by Invitro Phosphorylation with Protein-Kinase-C. *Journal of Biological Chemistry*, **266**, 10820-10824.
48. Ugrinova, I., Zlateva, S. and Pasheva, E. (2012) The effect of PKC phosphorylation on the "architectural" properties of HMGB1 protein. *Mol Biol Rep*, **39**, 9947-9953.
49. Oh, Y.J., Youn, J.H., Ji, Y., Lee, S.E., Lim, K.J., Choi, J.E. and Shin, J.S. (2009) HMGB1 Is Phosphorylated by Classical Protein Kinase C and Is Secreted by a Calcium-Dependent Mechanism. *J Immunol*, **182**, 5800-5809.
50. Vogel, C., Silva, G.M. and Marcotte, E.M. (2011) Protein expression regulation under oxidative stress. *Mol Cell Proteomics*, **10**, M111 009217.
51. Kauppinen, T.M., Chin, W.Y., Suh, S.W., Wiggins, A.K., Huang, E.J. and Swanson, R.A. (2006) Direct phosphorylation and regulation of poly(ADP-ribose) polymerase-1 by extracellular signal-regulated kinases 1/2. *P Natl Acad Sci USA*, **103**, 7136-7141.
52. Ju, B.-G., Solum, D., Song, E., Lee, K.-J., Rose, D., Glass, C. and Rosenfeld, M. (2004) Activating the PARP-1 sensor component of the groucho/ TLE1 corepressor complex mediates a CaMKinase IIdelta-dependent neurogenic gene activation pathway. *Cell*, **119**, 815-829.

53. Midorikawa, R., Takei, Y. and Hirokawa, N. (2006) KIF4 motor regulates activity-dependent neuronal survival by suppressing PARP-1 enzymatic activity. *Cell*, **125**, 371-383.

54. Bentle, M., Reinicke, K., Bey, E., Spitz, D. and Boothman, D. (2006) Calcium-dependent modulation of poly(ADP-ribose) polymerase-1 alters cellular metabolism and DNA repair. *J Biol Chem*, **281**, 33684-33696.

55. Sato, H., Takeo, T., Liu, Q., Nakano, K., Osanai, T., Suga, S., Wakui, M. and Wu, J. (2009) Hydrogen peroxide mobilizes Ca2+ through two distinct mechanisms in rat hepatocytes. *Acta pharmacologica Sinica*, **30**, 78-89.

56. Hong, J.H., Moon, S.J., Byun, H.M., Kim, M.S., Jo, H., Bae, Y.S., Lee, S.I., Bootman, M.D., Roderick, H.L., Shin, D.M. *et al.* (2006) Critical role of phospholipase Cgamma1 in the generation of H2O2-evoked [Ca2+]i oscillations in cultured rat cortical astrocytes. *J Biol Chem*, **281**, 13057-13067.

57. Bartha, E., Solti, I., Kereskai, L., Lantos, J., Plozer, E., Magyar, K., Szabados, E., Kalai, T., Hideg, K., Halmosi, R. *et al.* (2009) PARP inhibition delays transition of hypertensive cardiopathy to heart failure in spontaneously hypertensive rats. *Cardiovasc Res*, **83**, 501-510.

58. Gagne, J.P., Moreel, X., Gagne, P., Labelle, Y., Droit, A., Chevalier-Pare, M., Bourassa, S., McDonald, D., Hendzel, M.J., Prigent, C. *et al.* (2009) Proteomic investigation of phosphorylation sites in poly(ADP-ribose) polymerase-1 and poly(ADP-ribose) glycohydrolase. *J Proteome Res*, **8**, 1014-1029.

59. Langelier, M.F., Planck, J.L., Roy, S. and Pascal, J.M. (2012) Structural basis for DNA damage-dependent poly(ADP-ribosyl)ation by human PARP-1. *Science*, **336**, 728-732.

60. Ali, A.A., Timinszky, G., Arribas-Bosacoma, R., Kozlowski, M., Hassa, P.O., Hassler, M., Ladurner, A.G., Pearl, L.H. and Oliver, A.W. (2012) The zinc-finger domains of PARP1 cooperate to recognize DNA strand breaks. *Nat Struct Mol Biol*, **19**, 685-692.

61. Mizuguchi, H., Miyagi, K., Terao, T., Sakamoto, N., Yamawaki, Y., Adachi, T., Ono, S., Sasaki, Y., Yoshimura, Y., Kitamura, Y. *et al.* (2012) PMA-induced dissociation of Ku86 from the promoter causes transcriptional up-regulation of histamine H(1) receptor. *Sci Rep*, **2**, 916.

62. Konat, G.W. (2003) H2O2-induced higher order chromatin degradation: A novel mechanism of oxidative genotoxicity. *J Biosciences*, **28**, 57-60.
63. Osmanov, T., Ugrinova, I. and Pasheva, E. (2013) The chaperone like function of the nonhistone protein HMGB1. *Biochem Bioph Res Co*, **432**, 231-235.
64. Joshi, S.R., Sarpong, Y.C., Peterson, R.C. and Scovell, W.M. (2012) Nucleosome dynamics: HMGB1 relaxes canonical nucleosome structure to facilitate estrogen receptor binding. *Nucleic Acids Research*, **40**, 10161-10171.
65. Bonaldi, T., Langst, G., Strohner, R., Becker, P.B. and Bianchi, M.E. (2002) The DNA chaperone HMGB1 facilitates ACF/CHRAC-dependent nucleosome sliding. *Embo J*, **21**, 6865-6873.
66. Watson, M., Stott, K., Fischl, H., Cato, L. and Thomas, J.O. (2014) Characterization of the interaction between HMGB1 and H3-a possible means of positioning HMGB1 in chromatin. *Nucleic Acids Research*, **42**, 848-859.
67. Celona, B., Weiner, A., Di Felice, F., Mancuso, F.M., Cesarini, E., Rossi, R.L., Gregory, L., Baban, D., Rossetti, G., Grianti, P. *et al.* (2011) Substantial Histone Reduction Modulates Genomewide Nucleosomal Occupancy and Global Transcriptional Output. *Plos Biol*, **9**.
68. Shin, J.H., Lee, H.K., Lee, H.B., Jin, Y. and Lee, J.K. (2014) Ethyl pyruvate inhibits HMGB1 phosphorylation and secretion in activated microglia and in the postischemic brain. *Neurosci Lett*, **558**, 159-163.
69. Burkle, A. and Virag, L. (2013) Poly(ADP-ribose): PARadigms and PARadoxes. *Mol Aspects Med*.

AUTHOR CONTRIBUTIONS

A.A., A.B. and M.O.H. planned the experiments and wrote the manuscript. A.A. and A.B. performed and evaluated the data and M.O.H. supervised the study. JT supervised the RPPA study. F.T. and M.A. investigated cell cycle dependent PAR formation. N.K. performed the bioinformatics analysis and M.B. supervised the study. All authors reviewed the manuscript.

ACKNOWLEDGEMENT

We are grateful to Roger Davies (University of Massachusetts Medical School) for providing JNK1/2 WT and JNK1/2$^{-/-}$ MEFs, Peter J. Parker (Francis Crick Institute, UK) for PKCα KO MEFs, and Marco E. Bianchi (San Raffaele University, Milano, Italy) for immortalized HMGB1 KO MEFs. Markus Ehrat and Jan van Oostrum (Zeptosens - a division of Bayer (Schweiz) AG) are acknowledged for helpful input during the planning of the RPPA studies. Johann Grognux and Daniel Rechsteiner (Zeptosens) prepared the cell lysates for the Zeptosens Chips. Florian Freimoser and Stephan Christen (Institute of Veterinary Biochemistry and Molecular Biology, University of Zurich) provided valuable editorial assistance and critical input during the writing. We also thank Barbara van Loon, Nicole Grosse and Matthias Bosshard (Institute of Veterinary Biochemistry and Molecular Biology, University of Zurich) for help with the comet assay. The Center for Microscopy and Image Analysis at the University of Zurich is acknowledged for expert microscopy support.

Additional information

Funding: Research in the laboratory of M.A. is supported by the Swiss National Science Foundation (Grant PP00P3_150690/1) and by the University of Zurich Association Research Talent Development Fund. The work in the laboratory of M.O.H. was supported in part by the University Research Priority Program “Integrative Human Physiology” at the University of Zurich, the Swiss National Science Foundation Grant [310030B_138667 and 310030_157019], the Oncosuisse grant [KLS 02396-02-2009)] and the Kanton of Zurich (to M.O.H.).

Competing financial interests: JT was Zeptosens' Technology Manager at Bayer Technology Services GmbH and is currently Group Head for Process Analytical Technologies at the same company.

The other authors declare no competing financial interests.

FIGURE LEGENDS

Figure 1. Sublethal H_2O_2 treatment activates cytoplasmic kinases.

a) PAR immunofluorescence (IF) analysis of MRC-5 cells treated with 0.5 mM H_2O_2 for 10-60 min or left untreated (U).

b) Immunoblotting analysis of MRC-5 cells pretreated with 1 μM ABT-888 or DMSO (control) and H_2O_2 treatment for 10-60 min.

c) PAR IF analysis of MRC-5 cells transfected with siRNA against ARTD1 or mock, and treated with 0.1 mM H_2O_2 for 10 min or left untreated. Intensity in arbitrary units x 10^{-5}

d) MEFs incubated with EdU (10 μM) for 15 min prior to H_2O_2 (0.1 or 0.5 mM) treatment for 10 min, and fixation and staining. Quantification of the mean PAR signal intensity per nucleus in G1, S and G2 cells, displayed in arbitrary units.

e) Work flow for characterization of H_2O_2-induced proteome changes by reversed phase protein microarrays (RPPA).

f-g) Time profile clustering of 0.5 mM H_2O_2-induced proteome changes in MRC-5 cells (ANOVA, n=2, $p<0.05$) by k-means algorithm, showing increased protein expression / modification (green) or repression / de-modification (red). Modifications are indicated in brackets, antibodies that have been applied more than once are indicated by a 1-digit number at the end of the analyte name, antibodies from different vendors are indicated by a 3-digit number in brackets (e.g. 2-02).

h) *In silico* protein-protein interaction analysis of significant proteome changes induced in MRC-5 cells by 0.5 mM H_2O_2 using STRING with a score cut off > 0.7. Purple color indicates change in phosphorylation, while violet reflects change in total protein. Hubs (more ≥ 20 interactions) are enlarged.

Figure 2. Negative and positive modulation of ARTD1 activity by different PKC family members.

a) PAR IF analysis of IMR-90 human fibroblasts preincubated with selected kinase inhibitors or DMSO (control) prior to 0.1 or 0.5 mM H_2O_2 treatment for 10 min, or left untreated. Inhibitors against ARTDs (olaparib, 10 μM), IKK (IKK VII, 10 μM), AMPK (dorsomorphin, 50 μM), MEK (PD985059, 20 μM), JNK (SP600125, 50 μM), p38 (SB203580, 50 μM) were used at the indicated concentration. Experiments were also performed with NIH/3T3 mouse fibroblasts, with identical results.

Quantification performed on 10-20 nuclei analyzed per area (n=10), intensity in arbitrary units x 10^{-5}.

b) PAR IF analysis of IMR-90 preincubated with selected inhibitors or DMSO (control) prior to 0.1 mM H_2O_2 treatment for 10 min, or left untreated. Inhibitors against calcium (BAPTA-AM, 10 μ M), IP3R (2-APB, 100 μ M), PLC (U-73122, 1 μ M), cyclophilin D (cyclosporin A, 1 μ M). Quantification of 10-20 nuclei analyzed per area (n=10), intensity in arbitrary units x 10^{-5}.

c) MEFs pre-treated with 10 μM BAPTA-AM or DMSO were incubated with EdU (10 μM) for 15 min, stimulated for 10 min with H_2O_2 (0.1 or 0.5 mM), before fixation and staining. Quantification of the mean PAR signal intensity per nucleus in G1, S and G2 cells, displayed in arbitrary units.

d) PAR IF analysis of MRC-5 preincubated with 5 μM GF109203X (PKC inhibitor) or 10 μM BAPTA-AM (calcium chelator) or left untreated (U) prior to 0.1 mM H_2O_2 for 10 min. Intensity in arbitrary units x 10^{-5}.

e) PAR IF staining of MRC-5 cells transfected with siPKC (pan) prior to H_2O_2 treatment for 10 min (*left*). Quantification of PAR IF staining of MRC-5 cells transfected with siPKC (pan) prior to H_2O_2 treatment for 10 min (10-20 cells / condition, n=5) (*right*).

f) Knockdown confirmation of e) by immunoblotting with anti-ARTD1, anti-PKCα or anti-PKCδ using anti-tubulin as loading control.

g) PAR IF analysis of NIH/3T3 cells transfected with siPKCα and/or siPKCδ, siARTD1 (positive ctl) or siMock (negative control) prior to H_2O_2 (0.1 mM) treatment for 10 min (500 cells / condition, n=2).

Data are mean +/- SD by t-test with *p<0.05, **p<0.01, ***p<0.001, n.s. not significant.

Figure 3. PKCα regulates PAR formation in a DNA break-independent manner.

a) MEFs pre-treated with 10 μM olaparib or left untreated prior to 0.5 mM H_2O_2 treatment for 10 min. Nuclear and cytoplasmic extracts were analysed by immunoblotting. Quantification of PKCα levels was performed by densitometry, normalizing nuclear levels to ARTD1 and cytoplasmic levels to tubulin.

b) WT and ARTD1 KO MEFs transfected with myc-tagged WT ARTD1, ARTD1 E988K or aa215-1014 ARTD1 were treated with 0.5 mM H_2O_2 for 10 min and immunostained for myc and PAR.

c) Alkaline comet assay and PAR IF of siPKCα transfected MEFs or siMock (negative control) prior to 0.1 mM H_2O_2 treatment for 10 min. (100 nuclei analyzed / independent experiment, n=2.

d) MEFs transfected with scrambled siRNA or siRNA against PKCα were treated with 0.5 mM H_2O_2 for 10 min. Nuclear extracts (NE) were prepared and 10 µg incubated in an *in vitro* ADP-ribosylation assay using NAD (^{32}P) in the presence or absence of recombinant PKCα for 15 min at 30°C. Loading controlled by Coomassie blue staining of the gel (lower panel, CB).

e) Alkaline comet assay and PAR IF of MEFs pre-treated with 10 µM BAPTA-AM for 30 min or left untreated prior to 0.1 mM H_2O_2 treatment for 10 min (100 nuclei analysed / independent experiment, n=3.

f) MEFs were pre-incubated with either 10 µM olaparib, 10 µM BAPTA-AM or left untreated prior to 0.5 mM H_2O_2 for 10 min. Nuclear extracts (NE) were prepared and 10 µg incubated in an *in vitro* ADP-ribosylation assay using NAD (^{32}P) in the presence or absence of BAPTA-AM for 15 min at 30°C.

g) Alkaline comet assay of NIH/3T3 cells preincubated with BAPTA (20 µM) or DMSO prior to $KBrO_3$ (30 mM, 1 h) or MNNG (50 µM, 1 h) treatment (50 nuclei analyzed / independent experiment, n=6).

h) PKCα kinase assay using ARTD1 full length and Pol β (positive control) as substrates and radiolabeled ATP (^{32}P).

i) PKCα kinase assay using ARTD1 deletion fragments or full length ARTD1 as substrate and radiolabeled ATP (^{32}P).

j) ADP-ribosylation assay using radiolabeled NAD (^{32}P). PKCα was pre-incubated with ATP and/or ARTD1 for 30 min before adding PKC inhibitor (GF109203X, 5 µM), NAD (^{32}P) and 5, 0.5, 0.05, 0.005, or 0 pmol of EcoRI linker (ds DNA) and incubated for 15 min at 30°C.

Figure 4. PKCα-dependent phosphorylation of HMGB1 is required for oxidative stress-induced PAR formation.

a) PKCα kinase assay using radioactively labeled ATP (^{32}P) and histones as substrate.

b) ADP-ribosylation assay using ARTD1, radioactively labeled NAD (^{32}P) and histones as substrate.

c) PKCα kinase assay using radioactively labeled ATP (^{32}P) and HMGB1 as substrate.

d) ADP-ribosylation assay with ARTD1 and radioactively labeled NAD (^{32}P) (*every lane*), using HMGB1 pre-incubated with PKCα in the presence or absence of ATP.

e) MEFs treated with scrambled siRNA or siRNA against HMGB1 and/or PKCα were incubated 10 min with 0.5 mM H_2O_2, in the absence or presence of BAPTA-AM and stained for PAR (*left*). Quantification of PAR intensity (*right*), 200 nuclei analyzed/experiment, n=3.

f) Quantification of PAR intensity in MRC-5 cells treated with scrambled siRNA or siRNA against HMGB1 and/or PKC (pan), stained for PAR after 10 min of 0.5 mM H_2O_2 treatment (200 nuclei/independent experiment, n=3).

g) Western blot analysis of HMGB1 in chromatin and cytoplasmic fractions from MEFs transfected with scrambled siRNA or siRNA against PKCα, and treated with 0.5 mM H_2O_2 for 10 min, or left untreated.

Data are mean +/- SD analyzed by t-test with *p<0.05, **p<0.01, ***p<0.001, n.s. not significant.

Supplementary Figure Legends

Figure S1. Dose and time-dependent formation of PAR and loss of viability by H_2O_2.

a) Kinetic analysis of PAR formation in MRC-5 cells upon increasing concentrations of H_2O_2 by IF.

b) PAR IF analysis of MRC-5 cells preincubated with different ARTD inhibitors (1 μ M ABT-88, 1 μ M olaparib and 10 μ M PJ-34) prior to 0.5 mM H_2O_2 treatment.

c) MEFs were pre-incubated with 10 μM olaparib, or left untreated prior to 0.5 mM H_2O_2 for 10 min. Nuclear extracts (NE) were prepared and 10 μg were incubated in an *in vitro* ADP-ribosylation assay using NAD (^{32}P) for 15 min at 30°C.

d) Schematic presentation of image-based cell cycle staging through quantitative high-content microscopy for quantifying PAR intensities in the different cell cycle stages. The incorporated mean EdU signal was plotted vs. the total intensity of DAPI for every single cell. G1 cells were identified based on their low EdU and low DAPI content, S phase cells based on their high EdU content, and G2 cells based on their low EdU and high DAPI content.

e) MTT viability assay of MRC-5 cells treated with different concentrations of H_2O_2 for 10 min and recovery for 24 h (n=3).

f) IF analysis of MRC-5 cells treated with 0.5 mM H_2O_2 for 10-60 min followed by fixation and immunostaining with anti-PAR (red) and anti-γH2A.X (green) or anti-53BP1 (red) and counterstaining with DAPI (blue) (*left*). Quantification of PAR and γH2A.X foci number from e) (10-20 nuclei analyzed / area, n=5) (*right*).

Figure S2. RPPA analysis of H_2O_2-induced proteome changes in MRC-5 cells.

a) Relative fluorescence intensities (RFIs) (log2) for group 1 (biological duplicates for untreated (U)_10 min), group 2 (biological duplicates for 0.5_10 min), group 3 (biological duplicates for 0.5 mM_60 min) were compared using F-statistics (ANOVA) with $p < 0.05$.

b) Means of RFIs (replicates) were log2 transformed and fold changes (to U, group 1) were plotted individually for 0.5 mM H_2O_2 to determine the standard deviation, resulting in 1 S.D. = 0.77.

c) Statistical, fold change and quality control analysis of significant proteome changes in response to 0.5 mM H_2O_2 using ANOVA ($p < 0.05$, $n = 2$) (green) and cut off (1 S.D.) (dashed line). Proteome changes which passed the cut off filter (1 S.D.) and satisfied visual quality control are highlighted in yellow, proteome changes which only passed the cut off filter (1 S.D.) are highlighted in red, proteome changes which only passed the visual quality control are highlighted in orange.

d) Enrichment of pathways from the pathway interaction database (PID) with significant proteome changes (ANOVA, $p < 0.05$) induced by 0.5 mM H_2O_2 using Fisher's exact test. (FDR corrected p-value cut off = 0.05).

Figure S3. Identification of the H_2O_2-induced signaling players upstream of PAR formation.

a) PAR immunoblotting analysis of NIH/3T3 cells preincubated with AMPK inhibitor (dorsomorphin, 10 and 50 μM) for 1 h prior to 0.5 mM H_2O_2 treatment for 10 min.

b) PAR immunoblotting analysis of NIH/3T3 cells preincubated with either ARTD inhibitor (olaparib, 10 μM), JNK inhibitor (SP600125, 10 and 30 μM) or p38 inhibitor (SB203580, 10 μM) for 1 h prior to 0.5 mM H_2O_2 treatment for 10 min.

c) Immunoblotting analysis of JNK1/2 double KO or WT MEFs pretreated with JNK inhibitor SP600125 (30 μM) prior to 0.5 mM H_2O_2 treatment. Anisomycin (10 μM) treatment used as control for inducing JNK signaling. ARTD1 used as loading control and JNK1/2 to control absence of JNK in JNK1/2 double KO MEFs. PAR intensity normalized to tubulin and reported as percent of H_2O_2 + DMSO.

d) Intensity quantification of PAR IF in MEFs after 0.5 mM H_2O_2 for 10 min using MEFs transfected with scrambled siRNA (Mock) or siRNA targeting either JNK1 or JNK2, or 60 min pre-incubation with 50 μM JNK inhibitor SP600125 (*right*).

e) Experiment performed as in d), using MEFs transfected with scrambled siRNA, siRNA targeting ERK1 or ERK2, or both, or 60 min pre-incubation with 20 μM MEK1/2 inhibitor PD98059 (*right*), n=4.

f) PAR immunoblotting analysis of NIH/3T3 cells preincubated with Ca^{2+} chelator (BAPTA-AM, 10 μM) for 1 h prior to 0.5 mM H_2O_2 treatment for 10 min.

g) PAR IF analysis of IMR-90 preincubated with 5 μM GF109203X (PKC inhibitor) prior to 0.1 mM H_2O_2 for 10 min. Intensity in arbitrary units x 10^{-5}.

Data are mean +/- SD by t-test with *p<0.05, **p<0.01, ***p<0.001, n.s. not significant.

Figure S4. Principle role of PKCα isoform and HMGB1 in PAR formation

a) Knockdown control by western blot of NIH/3T3 cells treated with siRNA against ARTD1 (as control), PKCα and/or PKCδ.

b) WT and PKCα KO MEFs treated with 0.5 mM H_2O_2, immunostained for PAR and the intensity subsequently quantified, 200 nuclei / independent experiment, n=2.

c) PKCα and PKCδ levels in PKCα KO MEFs controlled by Western blot.

d) PAR IF analysis of NIH/3T3 cells transfected with siPKCα, siPKCβ, siPKCγ, siPKCδ, or siCtl (negative control) prior to H_2O_2 (0.1 mM) treatment for 10 min (50 cells / condition).

e) Alkaline comet assay of NIH/3T3 cells treated with increasing concentration of H_2O_2 for the indicated periods of time (50 nuclei analyzed / independent experiment, n=2).

f) MEFs were transfected with siRNA against Ogg1, Ape1 or mock control, and treated with 0.5 mM (left, middle) or 0.1 mM (right) H_2O_2 for 10 min. Analyzed by PAR IF and intensity quantified (left, middle) or the alkaline comet assay, 100 nuclei/condition (right).

g) PKC δ kinase assay using ARTD1 deletion fragments as substrate and radiolabeled ATP (^{32}P). Loading controlled by Comassie blue staining of the gel (lower panel, CB).

h) ADP-ribosylation assay using radiolabeled NAD (^{32}P) with PKC δ phosphorylated ARTD1, in the presence or absence of EcoRI linker (ds DNA) and incubation for 10 min at 30°C. Loading controlled by Comassie blue staining of the gel (lower panel, CB).

i) HMGB1 KO MEFs treated with scrambled siRNA or siRNA against PKCα were treated for 10 min with 0.5 mM H_2O_2 and stained for PAR. Quantification of PAR intensity (*right*), 200 nuclei analyzed/experiment, n=3.

j) Performed as in i), but pre-incubated with 10 μM BAPTA-AM.

k) Schematic representation of the signaling pathways involved in H_2O_2-induced PAR formation. Activation of ARTD1 by i) calcium-dependent formation of DNA strand breaks, ii) PKCα activation, translocation to the nucleus and subsequent

phosphorylation of HMGB1, which releases the repression of ARTD1. H_2O_2-induced PAR formation is negatively fine-tuned by phosphorylation of ARTD1 by PKCδ.

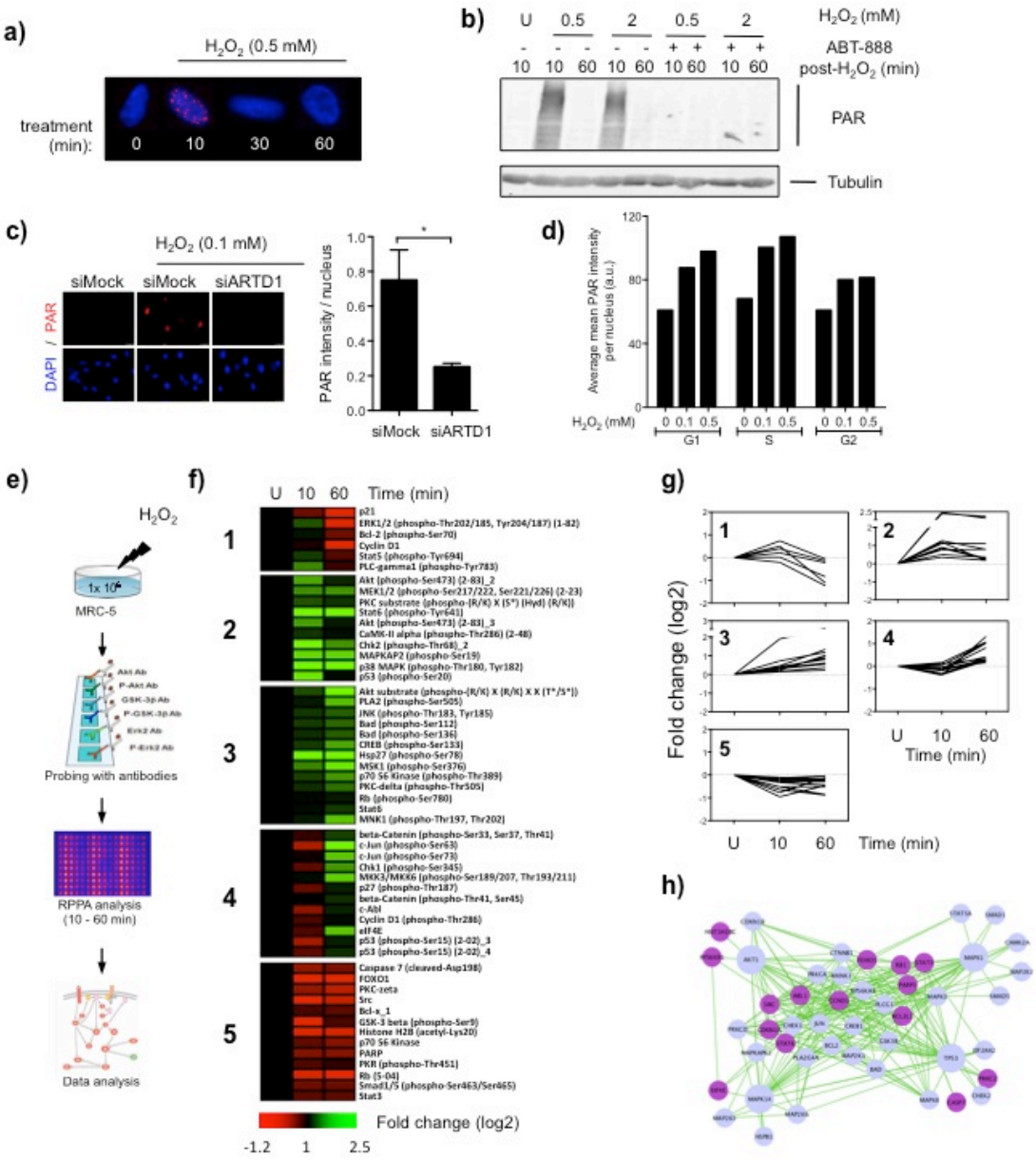
a)
H2O2 (0.5 mM)
treatment (min):
0
10
30
60
b)
U
0.5
2
0.5
2
H2O2 (mM)
ABT-888
10 10 60 10 60 10 60 10 60
post-H2O2 (min)
PAR
Tubulin
c)
H2O2 (0.1 mM)
siMock
siMock
siARTD1
PAR
DAPI
PAR intensity / nucleus
siMock
siARTD1
d)
Average mean PAR intensity per nucleus (a.u.)
H2O2 (mM)
0 0.1 0.5 0 0.1 0.5 0 0.1 0.5
G1
S
G2
e)
H2O2
1x 10^4
MRC-5
Probing with antibodies
RPPA analysis
(10 - 60 min)
Data analysis
f)
U 10 60 Time (min)
1
2
3
4
5
Fold change (log2)
-1.2 1 2.5
g)
Fold change (log2)
U 10 60 Time (min)
h)

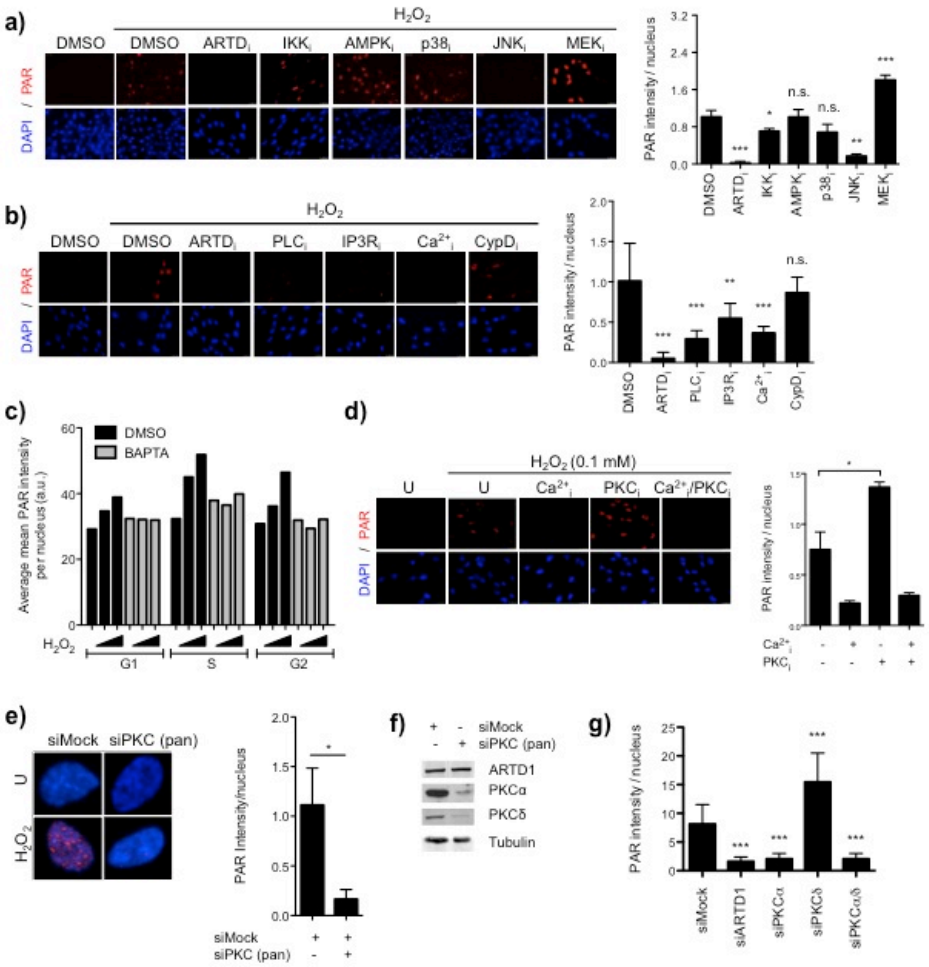
a)
H_2O_2
DMSO
DMSO
ARTD$_i$
IKK$_i$
AMPK$_i$
p38$_i$
JNK$_i$
MEK$_i$
PAR / DAPI
PAR intensity / nucleus
n.s.
b)
H_2O_2
DMSO
DMSO
ARTD$_i$
PLC$_i$
IP3R$_i$
Ca$^{2+}_i$
CypD$_i$
PAR / DAPI
PAR intensity / nucleus
n.s.
c)
DMSO
BAPTA
Average mean PAR intensity per nucleus (a.u.)
H_2O_2
G1
S
G2
d)
H_2O_2 (0.1 mM)
U
U
Ca$^{2+}_i$
PKC$_i$
Ca$^{2+}_i$/PKC$_i$
PAR / DAPI
PAR intensity / nucleus
e)
siMock
siPKC (pan)
U
H_2O_2
PAR intensity/nucleus
f)
siMock
siPKC (pan)
ARTD1
PKCα
PKCδ
Tubulin
g)
PAR intensity / nucleus
siMock
siARTD1
siPKCα
siPKCδ
siPKCαδ

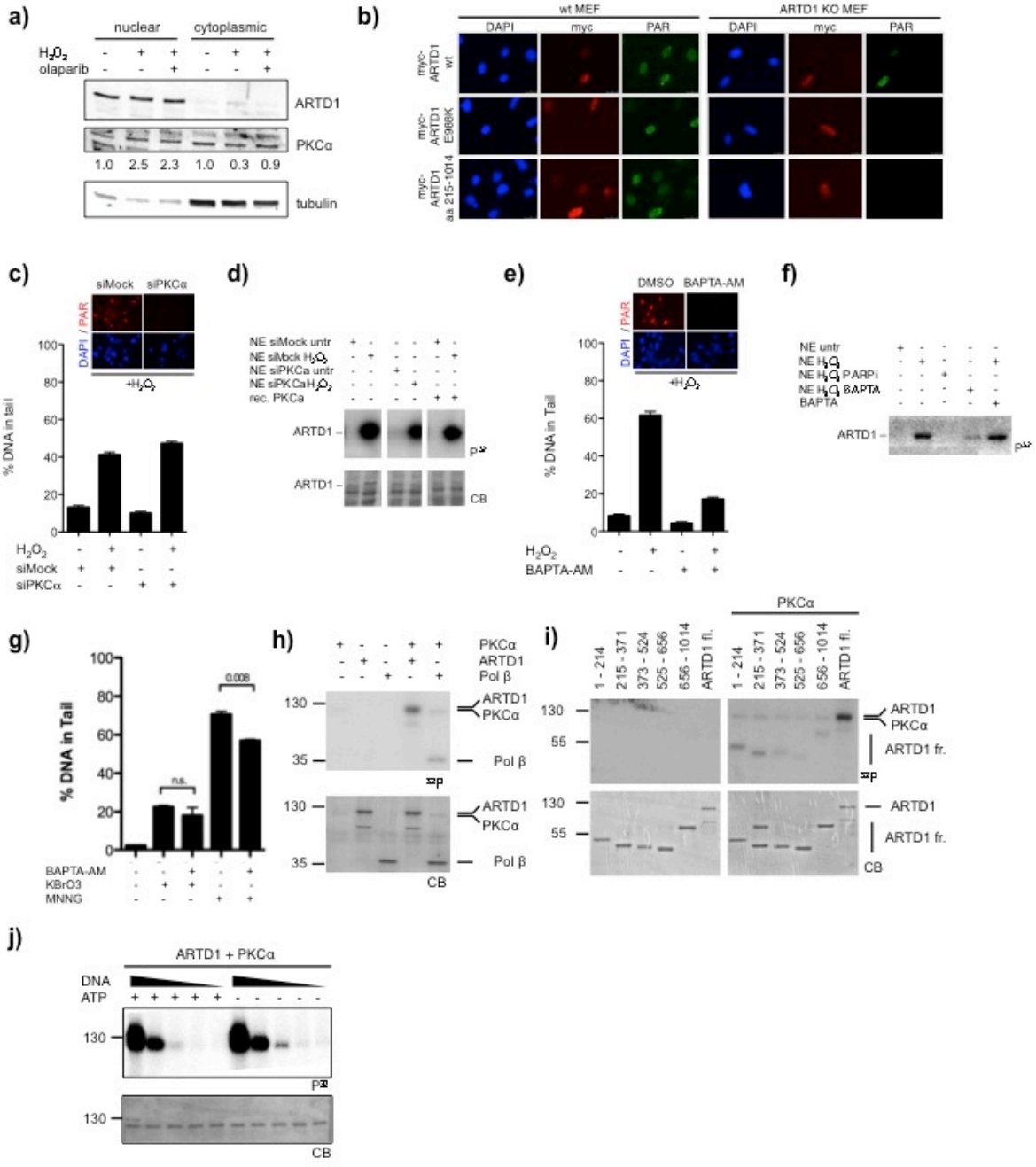
a)
nuclear
cytoplasmic
H2O2
olaparib
ARTD1
PKCα
1.0 2.5 2.3 1.0 0.3 0.9
tubulin
b)
wt MEF
ARTD1 KO MEF
DAPI
myc
PAR
myc-ARTD1 wt
myc-ARTD1 E988K
myc-ARTD1 aa 215-1014
c)
siMock
siPKCα
DAPI / PAR
+H2O2
% DNA in tail
H2O2
siMock
siPKCα
d)
NE siMock untr
NE siMock H2O2
NE siPKCa untr
NE siPKCa H2O2
rec. PKCa
ARTD1
PAR
CB
e)
DMSO
BAPTA-AM
% DNA in Tail
f)
NE untr
NE H2O2
NE H2O2 PARPi
NE H2O2 BAPTA
BAPTA
g)
% DNA in Tail
n.s.
0.008
BAPTA-AM
KBrO3
MNNG
h)
PKCα
ARTD1
Pol β
ARTD1 PKCα
Pol β
CB
i)
PKCα
1 - 214
215 - 371
373 - 524
525 - 656
656 - 1014
ARTD1 fl.
ARTD1 PKCα
ARTD1 fr.
ARTD1
j)
ARTD1 + PKCα
DNA
ATP
130
PAR
CB

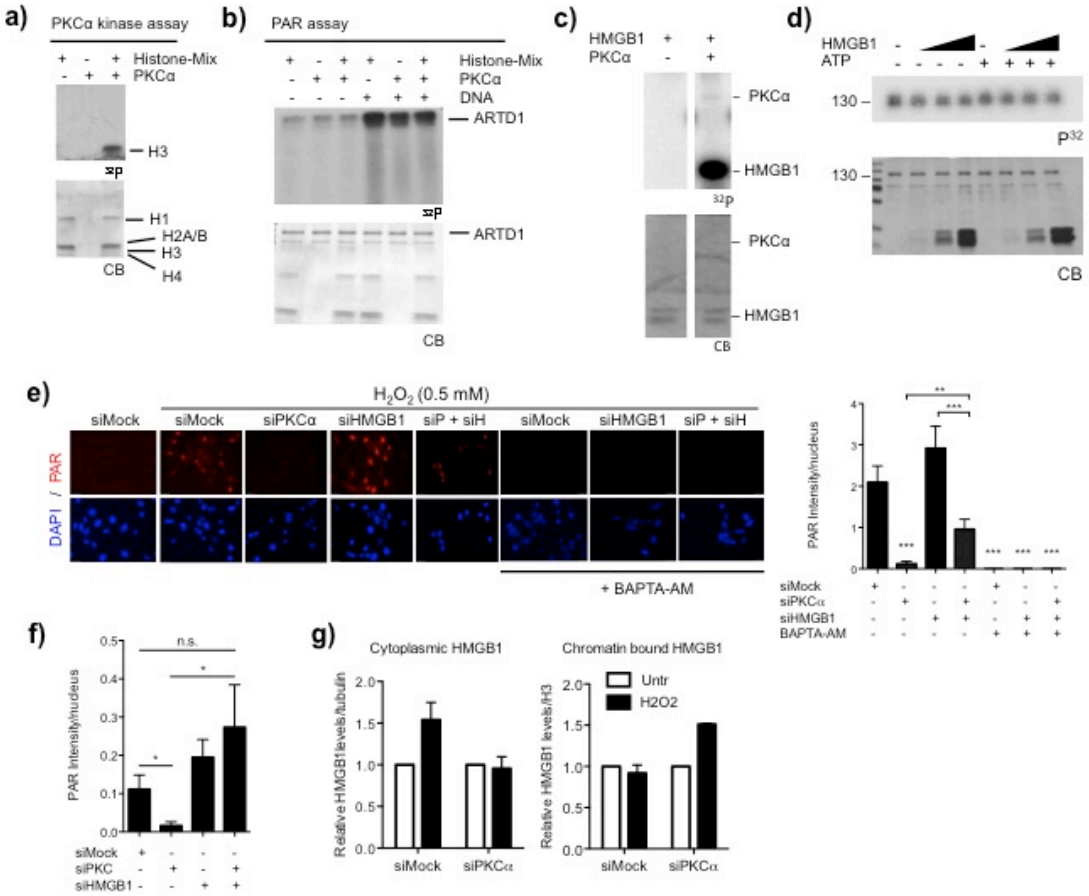
a)
PKCα kinase assay
Histone-Mix
PKCα
H3
H1
H2A/B
H3
H4
CB
b)
PAR assay
Histone-Mix
PKCα
DNA
ARTD1
ARTD1
CB
c)
HMGB1
PKCα
PKCα
HMGB1
PKCα
HMGB1
CB
d)
HMGB1
ATP
130
130
CB
e)
H2O2 (0.5 mM)
siMock
siMock
siPKCα
siHMGB1
siP + siH
siMock
siHMGB1
siP + siH
PAR
DAPI
+ BAPTA-AM
PAR intensity/nucleus
siMock
siPKCα
siHMGB1
BAPTA-AM
f)
n.s.
PAR intensity/nucleus
siMock
siPKC
siHMGB1
g)
Cytoplasmic HMGB1
Chromatin bound HMGB1
Untr
H2O2
Relative HMGB1 levels/tubulin
Relative HMGB1 levels/H3
siMock
siPKCα
siMock
siPKCα

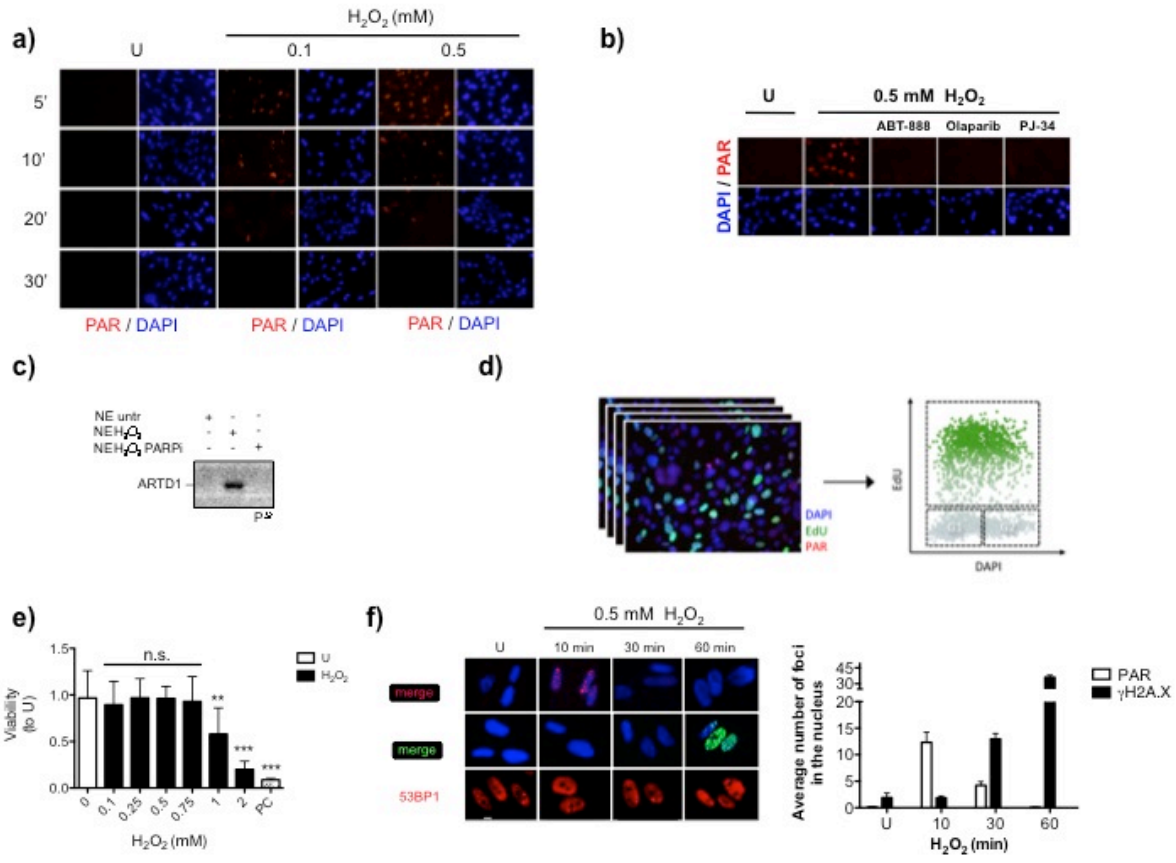
a)
H_2O_2 (mM)
U
0.1
0.5
5'
10'
20'
30'
PAR / DAPI
PAR / DAPI
PAR / DAPI
b)
U
0.5 mM H_2O_2
ABT-888
Olaparib
PJ-34
DAPI / PAR
c)
NE untr
NEH_2O_2
NEH_2O_2 PARPi
ARTD1
PS
d)
DAPI
EdU
PAR
EdU
DAPI
e)
n.s.
U
H_2O_2
Viability (to U)
1.5
1.0
0.5
0.0
**
***
***
0
0.1
0.25
0.5
0.75
1
2
PC
H_2O_2 (mM)
f)
0.5 mM H_2O_2
U
10 min
30 min
60 min
merge
merge
53BP1
Average number of foci in the nucleus
45
30
20
15
10
5
0
PAR
γH2A.X
U
10
30
60
H_2O_2 (min)

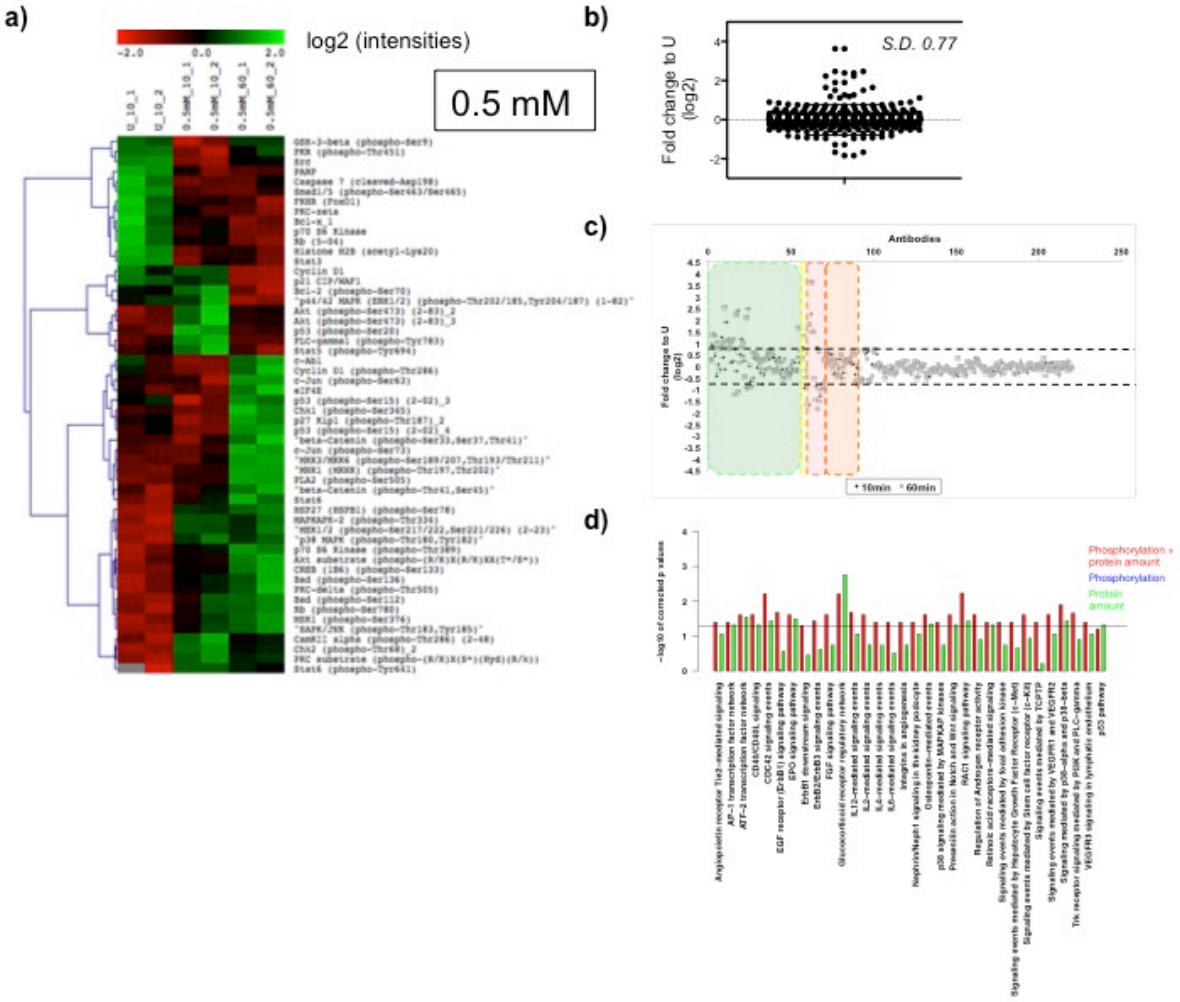
a)
log2 (intensities)
0.5 mM
b)
S.D. 0.77
Fold change to U (log2)
c)
Antibodies
Fold change to U (log2)
10min
60min
d)
-log10 of corrected p values
Phosphorylation + protein amount
Phosphorylation
Protein amount

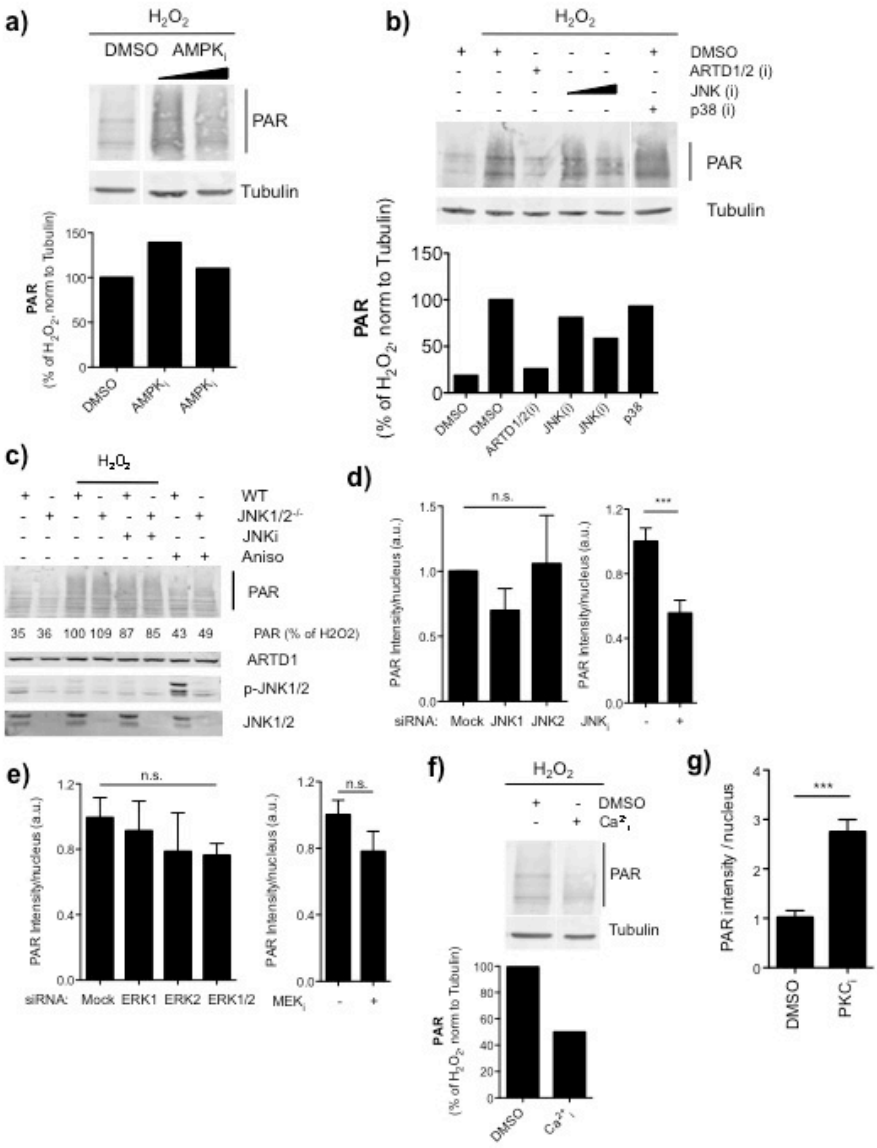
a)
H_2O_2
DMSO
AMPK$_i$
PAR
Tubulin
PAR (% of H_2O_2, norm to Tubulin)
DMSO
AMPK$_i$
AMPK$_i$
b)
H_2O_2
DMSO
ARTD1/2 (i)
JNK (i)
p38 (i)
PAR
Tubulin
PAR (% of H_2O_2, norm to Tubulin)
DMSO
DMSO
ARTD1/2(i)
JNK(i)
JNK(i)
p38
c)
H_2O_2
WT
JNK1/2$^{-/-}$
JNKi
Aniso
PAR
35 36 100 109 87 85 43 49
PAR (% of H2O2)
ARTD1
p-JNK1/2
JNK1/2
d)
n.s.
***
PAR Intensity/nucleus (a.u.)
siRNA: Mock JNK1 JNK2
JNK$_i$
e)
n.s.
n.s.
PAR Intensity/nucleus (a.u.)
siRNA: Mock ERK1 ERK2 ERK1/2
MEK$_i$
f)
H_2O_2
DMSO
Ca^{2+}$_i$
PAR
Tubulin
PAR (% of H_2O_2, norm to Tubulin)
DMSO
Ca^{2+} $_i$
g)
***
PAR intensity / nucleus
DMSO
PKC$_i$

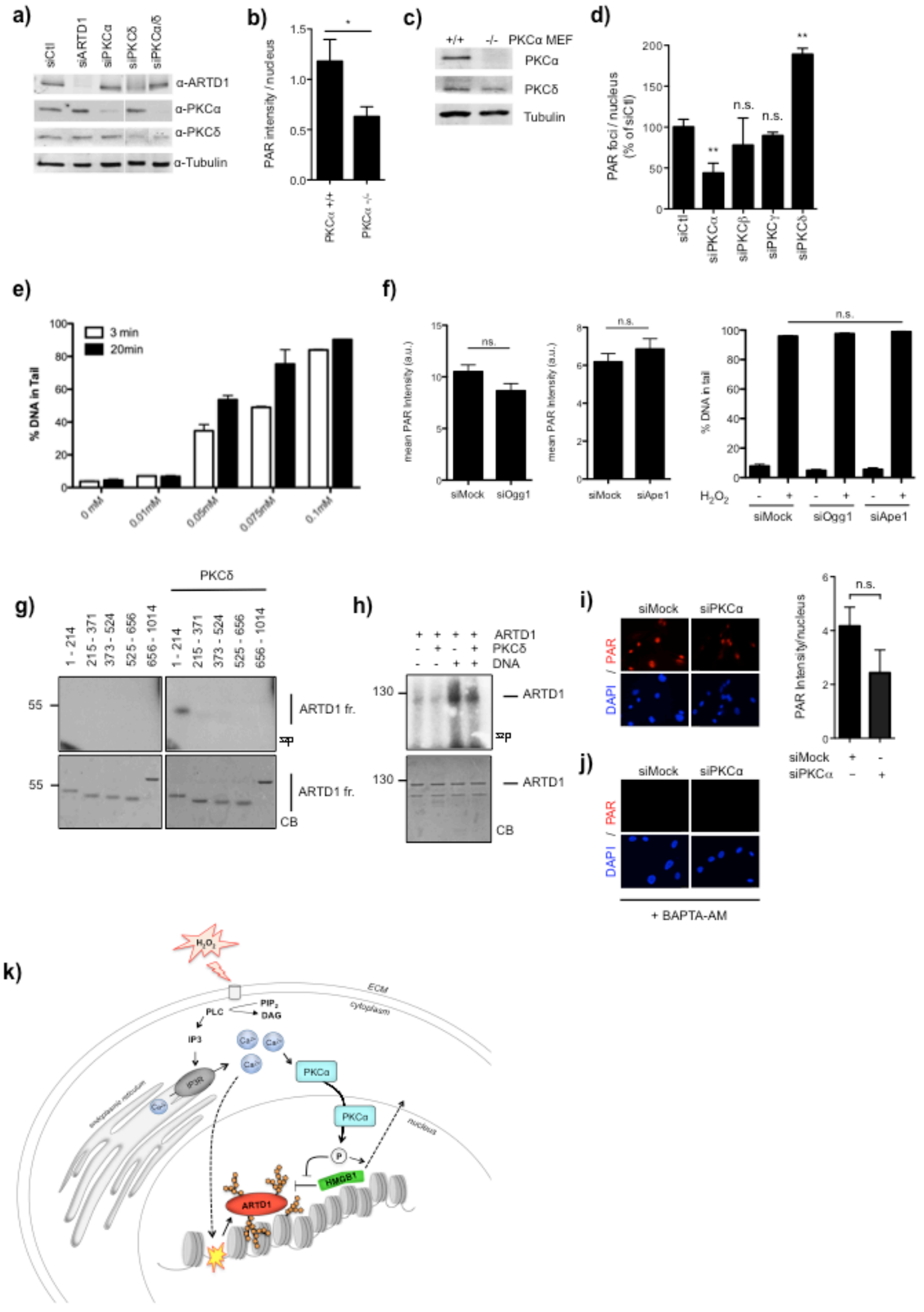
a)
siCtl
siARTD1
siPKCα
siPKCδ
siPKCαδ
α-ARTD1
α-PKCα
α-PKCδ
α-Tubulin
b)
PAR intensity / nucleus
PKCα +/+
PKCα -/-
c)
+/+
-/-
PKCα MEF
PKCα
PKCδ
Tubulin
d)
PAR foci / nucleus (% of siCtl)
n.s.
siCtl
siPKCα
siPKCβ
siPKCγ
siPKCδ
e)
3 min
20min
% DNA in Tail
0 mM
0.01mM
0.05mM
0.075mM
0.1mM
f)
mean PAR intensity (a.u.)
ns.
siMock
siOgg1
siApe1
% DNA in tail
H2O2
g)
PKCδ
1 - 214
215 - 371
373 - 524
525 - 656
656 - 1014
55
ARTD1 fr.
IB
CB
h)
ARTD1
PKCδ
DNA
130
i)
siMock
siPKCα
PAR
DAPI
PAR Intensity/nucleus
j)
+ BAPTA-AM
k)
ECM
cytoplasm
PLC
PIP2
DAG
IP3
Ca2+
PKCα
endoplasmic reticulum
IP3R
nucleus
P
HMGB1
ARTD1

3.2 Published results

3.2.1 ARTD1 Supresses Interleukin 6 Expression by Repressing MLL1-Dependent Histone H3 Trimethylation

MCB
Journals.ASM.org

ARTD1 Suppresses Interleukin 6 Expression by Repressing MLL1-Dependent Histone H3 Trimethylation

Roberta Minotti,[a] Anneli Andersson,[a,b] Michael O. Hottiger[a]

Institute of Veterinary Biochemistry and Molecular Biology, University of Zurich, Zurich, Switzerland[a]; Life Science Zurich Graduate School, Molecular Life Science Program, University of Zurich, Zurich, Switzerland[b]

ADP-ribosyltransferase diphtheria-toxin like 1/poly(ADP-ribose) polymerase 1 (ARTD1/PARP1) is a chromatin-associated protein in the nucleus and plays an important role in different cellular processes such as regulation of gene transcription. ARTD1 has been shown to coregulate the inflammatory response by modulating the activity of the transcription factor nuclear factor κB (NF-κB), the principal regulator of interleukin 6 (IL-6), an important inflammatory cytokine implicated in a variety of diseases such as cancer. However, to what extent and how ARTD1 regulates *IL-6* transcription has not been clear. Here, we show that ARTD1 suppresses lipopolysaccharide (LPS)-induced *IL-6* expression in macrophages, without affecting the recruitment of the NF-κB subunit RelA to the *IL-6* promoter and independent of its enzymatic activity. Interestingly, knockdown of ARTD1 did not alter H3 occupancy but increased LPS-induced trimethylation of histone 3 at lysine 4 (H3K4me3), a hallmark of transcriptionally active genes. We found that ARTD1 mediates its effect through the methyltransferase MLL1, by catalyzing H3K4me3 at the *IL-6* promoter and forming a complex with NF-κB. These results demonstrate that ARTD1 modulates *IL-6* expression by regulating the function of an NF-κB enhanceosome complex, which involves MLL1 and does not require ADP-ribosylation.

Interleukin 6 (IL-6) is an important inflammatory cytokine triggered, e.g., by pathogen-associated molecular patterns (PAMPs) such as bacterial lipopolysaccharide (LPS) (1). Increased IL-6 production is linked to inflammatory diseases such as inflammatory bowel disease, rheumatoid arthritis, mast cell growth proliferation, chronic inflammation, and obesity and to different cancers such as breast, colon, epithelial, or lung cancer (1–6). IL-6 can be released from tumors themselves, or from cancer-associated fibroblasts, and together with other factors thereby creates a tumor-promoting microenvironment (7–9). Understanding the mechanisms how *IL-6* transcription is regulated in different cell types is thus important for diseases such as cancer and inflammatory diseases. While the expression of *IL-6* is principally regulated by the transcription factor nuclear factor κB (NF-κB), epigenetic mechanisms also play an important role in the regulation of *IL-6* gene expression (10–14).

NF-κB is a widely expressed, inducible transcription factor crucial for inflammation, immunity, cell proliferation, and apoptosis (15, 16). In mammalian cells, five members of the NF-κB family exist, forming different homo- or heterodimers (17). The most abundant, best-studied, and "classical" form of NF-κB is a heterodimer consisting of the two subunits p50 and RelA (p65). In unstimulated cells, NF-κB is mostly sequestered in the cytoplasm as an inactive transcription factor complex by its physical association with one of the several inhibitors of NF-κB (IκB). PAMPs induce the classical, canonical pathway, which involves the rapid activation of IκB kinase β (IKKβ), NEMO-dependent phosphorylation and the subsequent degradation of IκBs, and the consequent nuclear translocation of primarily RelA-containing NF-κB heterodimers. As a mechanism to control the inflammatory response, nuclear NF-κB activity is selectively regulated at various levels downstream of activation, including DNA methylation (which depends on the differentiation state of the cell in question), nucleosome positioning, and histone modifications (e.g., histone methylation such as H3K4, H3K4, or H4K27 methylation), and via complex formation with coregulators, including p300/CBP and MLL1 (18–22). MLL1 is a member of the SET1/MLL family of methyltransferases and is known for its crucial functions for homeobox gene expression during development and embryogenesis and for stem cell regulation, as well as for gene transcription in general (23, 24). Interestingly, MLL1-dependent regulation of NF-κB downstream genes, including *IL-6*, has recently been reported (25). Due to these pivotal functions, mutations affecting the *MLL1* gene cause severe diseases and are implicated in acute leukemia in children and adults, with a particularly poor prognosis (26). To prevent fatal malfunction or misregulation of MLL1, multiple mechanisms control its activity in the cell (27). Together, there is a diversity of regulatory mechanisms for the differential activation of NF-κB-dependent target genes within the same cell or the differential activation of the same gene in different cells (20, 28). Furthermore, NF-κB is subject to positive-feedback regulation by cytokines such as IL-6 (29, 30).

ADP-ribosyltransferase diphtheria-toxin like 1/poly(ADP-ribose) polymerase 1 (ARTD1/PARP1) is an abundant nuclear protein that plays key roles in a variety of nuclear processes, including the regulation of transcription (31). ARTD1 possesses an intrinsic enzymatic activity that catalyzes the transfer of ADP-ribose

Received 2 March 2015 **Returned for modification** 25 March 2015
Accepted 25 June 2015
Accepted manuscript posted online 6 July 2015
Citation Minotti R, Andersson A, Hottiger MO. 2015. ARTD1 suppresses interleukin 6 expression by repressing MLL1-dependent histone H3 trimethylation. Mol Cell Biol 35:3189–3199. doi:10.1128/MCB.00196-15.

Address correspondence to Michael O. Hottiger, hottiger@vetbio.uzh.ch.

R.M. and A.A. contributed equally to this article.

Supplemental material for this article may be found at http://dx.doi.org/10.1128/MCB.00196-15.

doi:10.1128/MCB.00196-15

(ADPr) units from NAD (NAD^+) onto target gene regulatory proteins, thereby modulating their activities, functions, and interacting partners (32, 33).

Since its discovery, most studies on ARTD1 have focused on its role in DNA damage detection and repair responses (34). However, over the past decade, the role of ARTD1 in gene regulation has received increasing attention (31). Interestingly, ARTD1 can act as a transcriptional enhancer or as an attenuator. ARTD1 can regulate transcription by binding to nucleosomes and interacts dynamically with different types of chromatin domains to modulate the chromatin structure (34, 35). Nucleosome binding and auto-ADP-ribosylation of ARTD1 has been described as the underlying mechanism for this formation of transcriptionally inactive, dense chromatin (36, 37) and have been implicated in the reciprocal binding of ARTD1 and histone H1 to chromatin (38). ARTD1 has also been shown to covalently modify histone and chromatin-associated nonhistone proteins with poly(ADP-ribose) (PAR) (39, 40). ARTD1 can modulate the activity of nucleosome remodelers through noncovalent mechanisms, as is the case with ALC1 (amplified in liver cancer 1; also known as CHD1L), a macrodomain-containing nucleosome-remodeling enzyme. PAR-dependent interactions between ARTD1 and ALC1 promote nucleosome remodeling by ALC1, as well as recruitment of ALC1 to sites of DNA damage in cells (41, 42). ADP-ribosylation of KDM5B, a histone lysine demethylase acting on H3 lysine 4 trimethylation (H3K4me3), has been shown to block the binding of KDM5B to chromatin and inhibit its demethylase activity (43). This antagonism between ARTD1 and KDM5B helps to explain the high correlation between ARTD1 and H3K4me3 at actively transcribed promoters. The functional interplay between ARTD1 and KDM5B helps to control the chromatin state at ARTD1-regulated promoters for both basal and signal-regulated transcriptional outcomes (43). Finally, ARTD1 may also function as a scaffold protein independent of its catalytic activities, by interacting with and promoting the recruitment of other coregulatory enzymes required for transcription. We were the first to show that ARTD1 directly interacts with the NF-κB subunits and thereby regulates NF-κB-dependent gene expression (44, 45). We found that ARTD1 synergistically coregulates transcription together with known NF-κB transcriptional cofactors such as p300, CARM1, PRMT1 and the Mediator complex (18, 45, 46).

Although the enzymatic activity is not required for the transcriptional activation of transiently transfected NF-κB reporter plasmids by ARTD1 or upon NLRP3 inflammasome-induced ARTD1 cleavage (47), we were able to link ARTD1 and ADP-ribosylation to signaling during inflammation and the expression of adhesion molecules in atherogenesis, as well as cell survival under stress conditions (48). ARTD1 and NF-κB are thus interconnected in the inflammatory response.

At the inflammatory level, we have recently shown that nonapoptotic LPS-induced caspase 7 activation via the NLRP3 inflammasome induces ARTD1 cleavage at the transcriptional start sites (TSS) of distinct NF-κB target genes, including *IL-6*, and thereby causes elevated expression of these genes (49). The molecular mechanism responsible for the repressed *IL-6* expression levels in the presence of ARTD1 was not elucidated, however.

In the present work, we characterized and elucidated the molecular mechanism by which ARTD1 regulates the transcription of *IL-6*. Our results demonstrate that the negative regulation of *IL-6* expression by ARTD1 is independent of its enzymatic activity and does not affect RelA recruitment to the *IL-6* promoter. Instead, we found that ARTD1 is enriched at the *IL-6* promoter and suppresses MLL1-dependent H3K4me3. These results uncover a new mechanism of chromatin remodeling by ARTD1 and its importance for inflammation.

MATERIALS AND METHODS

Cell culture. Mouse leukemic monocyte macrophage cell line (RAW 264.7) was cultured in RPMI medium (Gibco/Invitrogen, Carlsbad, CA) at 37°C. NIH 3T3 and HEK293T cells were cultivated in Dulbecco modified Eagle medium (PAA, Pasching, Austria). Bone marrow-derived macrophages (BMDM) were obtained from bones (femurs and tibias) of wild-type and ARTD1 knockout mice and also cultivated in RPMI medium. The bones were cut from both ends, and bone marrow was flushed out with complete medium using a 1-ml syringe with a 23G needle until the bones were completely white. Cells were resuspended in RPMI medium supplemented with 20% of the supernatant of L929 cells and plated in bacterial dishes for 5 days. Differentiated macrophages were maintained in culture for 2 weeks in RPMI medium supplemented with 5% L929 supernatant. All media were supplemented with 1% (vol/vol) penicillin-streptavidin and 10% (vol/vol) fetal calf serum (Gibco/Invitrogen).

Cells were preincubated with the ARTD1 inhibitors olaparib (1 μM; SelleckChem) and ABT-888 (1 μM; Enzo LifeSciences) for 3 h before LPS (100 ng/ml; Sigma-Aldrich, St. Louis, MO) stimulation. RAW 264.7 macrophages (Raw cells) stably downregulating ARTD1 were generated using viral transduction. Virus expressing an shARTD1 construct were generated in HEK293T cells. Then, 10 μg of shARTD1 plasmid, 6 μg of packaging plasmid, and 3.5 μg of viral envelope plasmid were transfected into HEK293T cells (4×10^6 cells per 10-cm plate) using calcium phosphate. The medium was changed at 6 to 8 h posttransfection, and supernatant containing virus was collected, centrifuged, and filtered (0.45-μm-pore-size cellulose acetate filters) after 3 days. RAW 264.7 cells were seeded 1 day prior to transduction on a 6-well plate (5×10^5 cells per well). Polybrene was added to a final concentration of 4 μg/ml overnight. Subsequently, 1 ml of supernatant containing virus was added per well. The medium was replaced at 8 h postinfection and changed to selective medium after 2 days (puromycin, 2 μg/ml; Invivogen, San Diego, CA). Cells were kept under constant selection.

siRNA transfection. Negative-control AllStars (siMOCK), human siPARP1#6, mouse siPARP1#7, mouse siMLL1#1, mouse siSet7#1, and mouse siRelA#2 were ordered from Qiagen (Hilden, Germany). Cells were seeded at 50% confluence (2×10^5 cells per well) and transfected with 20 nmol of small interfering RNA (siRNA) per well (in six-well plate) with RNAiMAX Lipofectamine (Invitrogen). The experiment was performed 3 days after transfection.

RNA extraction and quantitative real-time PCR (qPCR) analysis. RNA extraction was performed with the NucleoSpin RNA II kit (Macherey-Nagel, Düren, Germany). RNA was quantified with a NanoDrop (Thermo-Fisher Scientific, Waltham, MA), and 2 μg of RNA was reverse transcribed according to the supplier's protocol (high-capacity cDNA reverse transcription kit; Applied Biosystems, Foster City, CA).

qPCRs were performed witha SYBR green SensiMix SYBR Hi-ROX kit (Bioline Reagents, Ltd., London, United Kingdom) and a Rotor-Gene Q 2plex HRM system (Qiagen). See Table S1 in the supplemental material for primer sequences. The relative amounts of each mRNA were normalized to the *RPS12* (mouse) and *RPL28* (human) housekeeping genes.

Cell lysis, SDS-PAGE, and Western blot analysis. Whole-cell extracts were prepared directly on plate by using a Tris lysis buffer (50 mM Tris [pH 8], 500 mM NaCl, 1% Triton X-100, 1 μg of pepstatin/ml, 1 μg of bestatin/ml, 1 μg of leupeptin/ml, 2 mM phenylmethylsulfonyl fluoride). Lysates were homogenized for 10 min at 4°C, followed by a 10-min centrifugation (maximum speed at 4°C) to eliminate cell debris. The protein concentration was quantified by a Bradford assay (Bio-Rad Laboratories, Hercules, CA), and 30 μg of protein extract was separated on a 10 or 7.5% SDS-polyacrylamide gel (120 V). The gel was blotted onto a polyvi-

nylidene difluoride membrane and analyzed using protein-specific antibodies.

Coimmunoprecipitation. Cells were harvested with a scraper and washed once with phosphate-buffered saline (PBS) for 5 min at 900 × *g*. The pellet was resuspended in 400 μl of hypotonic buffer (0.5% NP-40, 85 mM KCl, 5 mM HEPES [pH 7.4]) and directly centrifuged for 10 min at 6,200 × *g* using a cold centrifuge. Next, the pellet was resuspended in 200 μl of nuclear extraction buffer (50 mM Tris-HCl [pH 7.5], 150 mM KCl, 5 mM $MgCl_2$, 0.2 mM EDTA, 20% glycerol, 0.1% NP-40) and sonicated twice for 30 s. The nuclear extract was incubated for 30 min at 4°C with 1 μl of DNase and sonicated again for 30 s, followed by a 10-min centrifugation (4°C and 3,500 × *g*). Proteins were quantified by using a Bradford assay. Immunoprecipitation was carried out with 300 μg of extract at 4°C overnight with 10 μl of monoclonal antihemagglutinin (anti-HA)-agarose beads (Sigma-Aldrich). After overnight incubation, the beads were washed three times with washing buffer (20 mM Tris-HCl [pH 7.5], 0.1 M KCl, 5 mM $MgCl_2$, 0.2 mM EDTA, 10% glycerol, 0.1% Tween), resuspended in 2× Laemmli buffer (20 μl), and boiled for 5 min at 95°C. SDS-PAGE and Western blot analysis were performed as described above.

Immunofluorescence microscopy. Cells were cultured on sterile coverslips (10^5 cells per well in a 24-well-plate) and grown overnight. After treatment with or without H_2O_2 (at 1 mM in fetal calf serum-free medium for 10 min), the cells were fixed (methanol-acetic acid [3:1], 5 min on ice) and washed twice with PBS. The cells were blocked for 30 min in PBS containing 5% milk powder and 0.05% Tween and incubated with 10H PAR antibody (1:350) in the same buffer (1 h at room temperature). Coverslips were incubated with secondary Cy3-conjugated antibody (for 1 h at room temperature in the dark). After being washed with PBS, the coverslips were mounted with Vectashield containing DAPI (4′,6′-diamidino-2-phenylindole; Vector Laboratories, Burlingame, CA). Conventional microscopy was carried out using a Leica DMI 6000B light microscope (Leica Microsystems GmbH, Wetzlar, Germany).

ChIP. Chromatin immunoprecipitation (ChIP) analysis for H3, H3K4me3 and ARTD1 was performed as described previously (54) using magnetic Dynabeads (Life Technologies, Carlsbad, CA). ChIP analysis for p65 was performed as described previously (50), using protein A-agarose-salmon sperm DNA beads (Millipore, Billerica, MA).

Luciferase assay. Cells were transfected with a specific siRNA as described above (2×10^4 cells per well in a 24-well plate). At 1 day after transfection, the medium was changed, and different luciferase constructs were transfected using a TransIT-3T3 transfection kit (Mirus, Madison, WI). A luciferase assay was performed after 48 h using a dual-luciferase reporter assay system (Promega, Madison, WI) according to the supplier's protocol.

Antibodies. The following antibodies were used: PARP1/ARTD1 (H-250 [rabbit]), PARP-1 (C2-10 [mouse]), and p65 (C-20 [rabbit]) from Santa Cruz Biotechnology, Inc. (Dallas, TX); tubulin (mouse) from Sigma-Aldrich; H3K4me3 (rabbit) from Millipore; and histone H3 (rabbit) from Abcam PLS (Cambridge, United Kingdom). MLL1/HRX was obtained from Millipore. Secondary Cy3-conjugated AffiniPure goat anti-mouse antibody was obtained from Jackson ImmunoResearch Laboratories (Suffolk, United Kingdom), and 10H PAR (mouse) antibody was prepared in-house.

RESULTS

ARTD1 negatively regulates LPS-induced *IL-6* expression in a RelA-dependent manner. Stimulation of Raw cells with LPS for 1 or 4 h led to a strong induction of *IL-6* transcript levels as identified by quantitative reverse transcription-PCR (RT-PCR) (Fig. 1A). In shARTD1-treated Raw cells (see Fig. 1A, right panel, for knockdown efficiency), *IL-6* expression levels were comparably induced after 1 h but significantly enhanced at 4 h after LPS stimulation, suggesting that ARTD1 negatively regulates *IL-6* gene expression at this later time point. The observed effect was specific for *IL-6*, since the NF-κB-dependent control gene *IκBα* was not affected by ARTD1 knockdown (Fig. 1A). Selectively enhanced *IL-6* expression (compared to their respective controls) was also observed in LPS-stimulated primary BMDM from *ARTD1* knockout mice (Fig. 1B) and NIH 3T3 fibroblasts treated with siARTD1 (Fig. 1C; see the right-hand panels for knockout and knockdown efficiencies), as well as in siARTD1-treated HEK293T cells stimulated with PMA (Fig. 1D; see the right-hand panel for the induction of RelA nuclear translocation), suggesting that the ARTD1-mediated negative regulation of *IL-6* expression is cell type (and stimulus) independent.

Because of their ease of transfectability, the mechanism of the negative regulatory effect of ARTD1 on *IL-6* expression was further investigated using NIH 3T3 cells. To assess whether the negative regulation by ARTD1 was dependent on NF-κB, experiments with double knockdown of *ARTD1* and *RelA* were performed. Enhanced *IL-6* expression by ARTD1 knockdown in LPS-stimulated NIH 3T3 cells was completely abolished by concomitant downregulation of *RelA* (Fig. 2A), indicating that the negative regulatory effect of ARTD1 on *IL-6* expression was highly dependent on the induction of RelA in these cells. To corroborate these results, reporter assays with a luciferase gene under the control of either the wild-type *IL-6* promoter or a mutated *IL-6* promoter lacking the NF-κB binding site were performed. In line with the analysis of the transcript levels, knockdown of ARTD1 led to enhanced *IL-6* promoter transcriptional activity (Fig. 2B). This effect was not observed when the NF-κB binding site was mutated, confirming that the negative regulatory effect of ARTD1 under these conditions is also RelA-dependent and the chromatinization of the transfected reporter plasmids is sufficient to detect the ARTD1-mediated *IL-6* repression.

ARTD1 negatively regulates *IL-6* expression independent of its enzymatic activity. ARTD1 can regulate gene expression by ADP-ribosylating target proteins (including itself) or by its association with chromatin at the promoters of regulated genes (i.e., independently of its enzymatic activity). To determine whether the enzymatic activity of ARTD1 is required for the observed negative regulatory effect on *IL-6* expression, Raw cells were stimulated with LPS in the absence or presence of the ADP-ribosylation inhibitor olaparib. Again, ARTD1 knockdown lead to enhanced *IL-6* expression, whereas that of *IκBα* remained unaffected (Fig. 2C). Treatment of cells with olaparib, which effectively inhibited H_2O_2-induced PAR formation at the dose used for this experiment (data not shown), neither affected *IL-6* expression in shMOCK cells nor enhanced expression in shARTD1 cells (Fig. 2C), indicating that ADP-ribosylation is not involved in the negative regulatory effect of ADRT1 on *IL-6* expression. Comparable results were obtained with another ADP-ribosylation inhibitor, ABT-888 (Fig. 2D). Together, these results demonstrate that the observed derepression of *IL-6* expression upon knockdown of ARTD1 is neither dependent on ARTD1-mediated ADP-ribosylation nor on that by another ARTD family member.

ARTD1 does not alter the H3 occupancy at the *IL-6* promoter. To investigate whether ARTD1 represses *IL-6* expression indirectly by hampering RelA recruitment to the *IL-6* promoter, LPS-induced recruitment of RelA to the *IL-6* and *IκBα* promoters (100 bp upstream of the TSS was compared in shMOCK and shARTD1-treated Raw cells. The biphasic recruitment of RelA to the *IL-6* promoter (i.e., immediate within 1 h and late at 4 h after stimulation) was not different between shMOCK and shARTD1-treated cells in regard to timing and extent (Fig. 3A). The ARTD1-

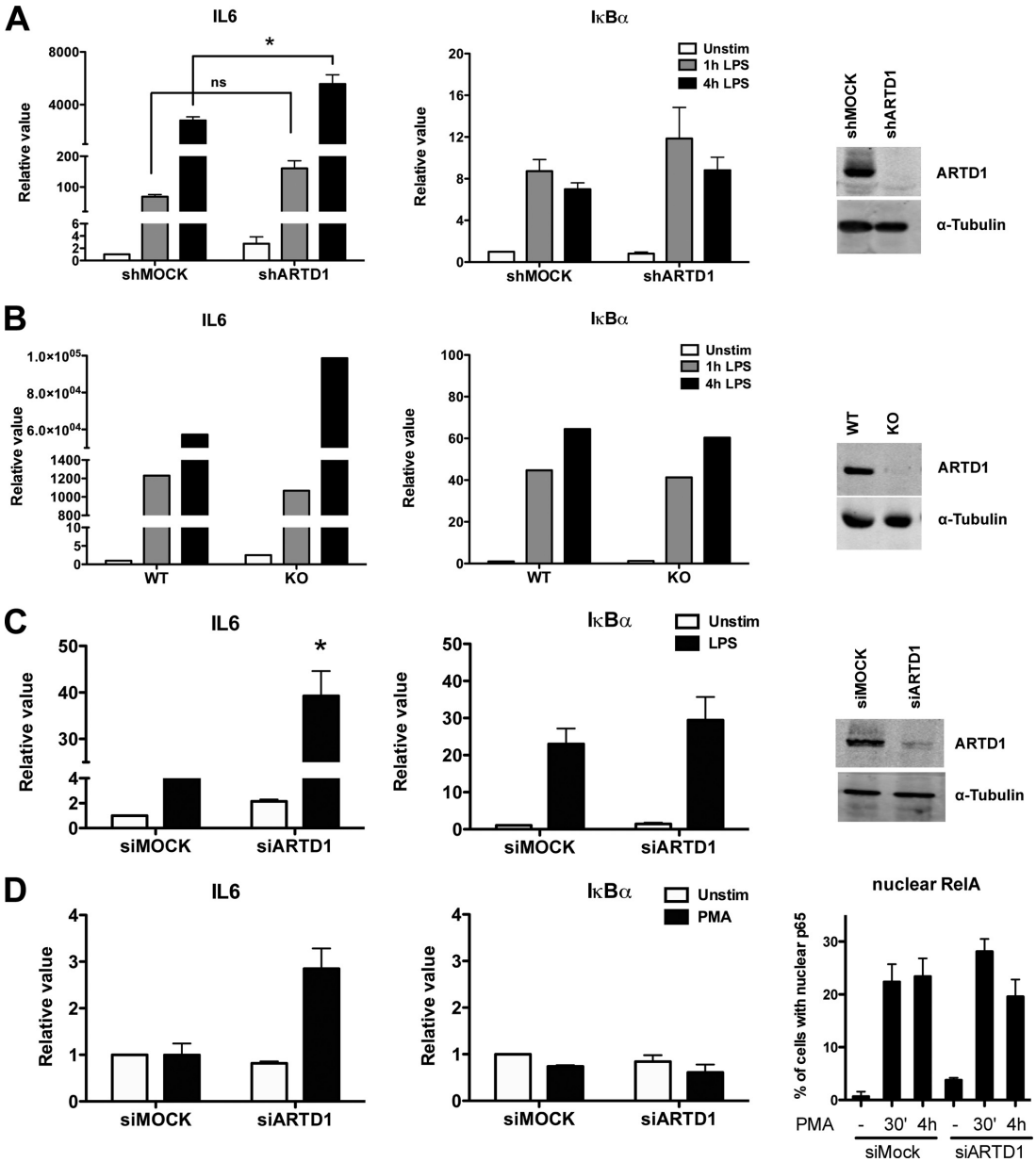

FIG 1 ARTD1 negatively regulates LPS- or PMA-induced *IL-6* expression. *IL-6* and *IκBα* gene expression was quantified by RT-PCR in Raw cells (A), BMDM (B), NIH 3T3 cells (C), and HEK293T cells (D). (A) *IL-6* and *IκBα* expression upon LPS stimulation in Raw cells treated with shRNA specific against ARTD1 ($n = 5$). The right panel shows knockdown efficiency by Western blotting. (B) *IL-6* and *IκBα* expression upon LPS stimulation in BMDM from wild-type and ARTD1 knockout mice (one representative experiment out of three). The right panel demonstrates knockout by Western blotting. (C) *IL-6* and *IκBα* expression upon LPS stimulation in NIH 3T3 cells treated with siRNA specific against ARTD1 ($n = 3$ or 4). The right panel shows knockdown efficiency by Western blotting. (D) *IL-6* and *IκBα* expression upon PMA stimulation in HEK293T cells treated with siRNA specific against ARTD1 ($n = 2$). The right panel demonstrates induction of p65 by PMA (quantitative representation of immunofluorescence analysis). The data are presented as means ± the standard deviations (SD) and were analyzed by one-way analysis of variance (ANOVA), followed by Bonferroni's *post hoc* test. *, $P < 0.05$.

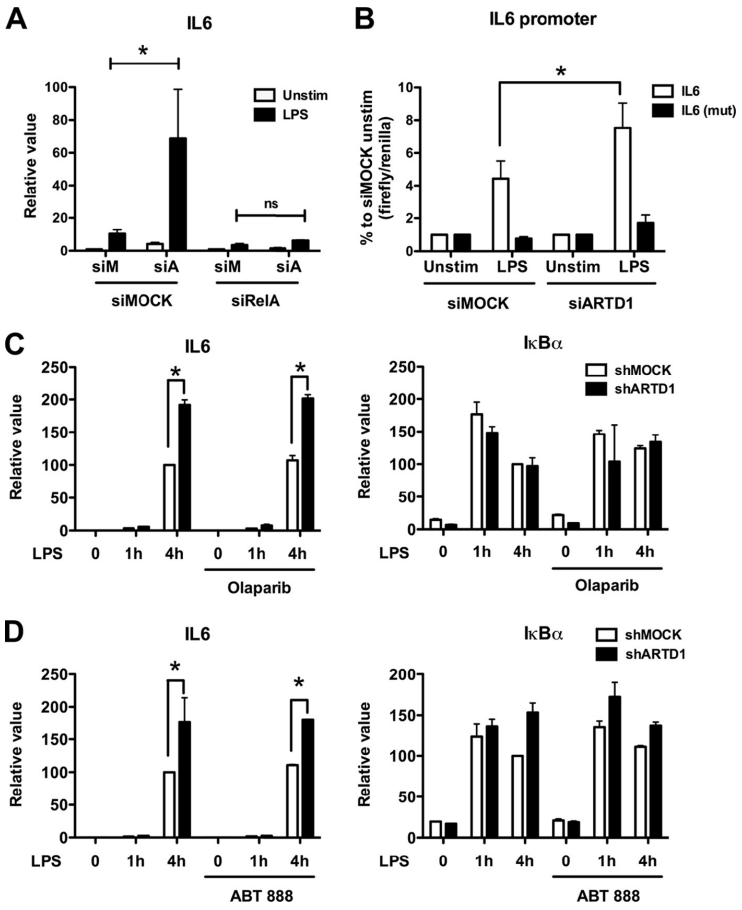

FIG 2 ARTD1 negatively regulates *IL-6* expression in a p65-dependent manner and independent of its enzymatic activity. (A) *IL-6* expression upon ARTD1 and RelA knockdown in NIH 3T3 cells stimulated with LPS or not stimulated ($n = 3$). (B) Expression of the luciferase reporter under the control of *IL-6* promoter (after 4 h of LPS stimulation or unstimulated) in NIH 3T3 cells ($n = 3$). (C) *IL-6* and *IκBα* expression upon olaparib treatment (1 μM) in Raw cells ($n = 2$). (D) *IL-6* and *IκBα* expression upon ABT-888 treatment (1 μM) in Raw cells ($n = 2$). The data are presented as means ± the SD and were analyzed by one-way ANOVA, followed by Bonferroni's *post hoc* test. *, $P < 0.05$.

dependent negative regulation of *IL-6* expression was therefore not due to an effect on RelA recruitment to the *IL-6* promoter.

Alternatively, as a chromatin-associated factor, ARTD1 may exert its regulatory function through the modulation of the chromatin state at the TSS of the *IL-6* gene. To address the function of ARTD1 as a chromatin regulator at the promoter of *IL-6*, ChIP experiments were performed to analyze the H3 occupancy at the *IL-6* and *IκBα* promoters. These analyses revealed that the chromatin at the *IL-6* promoter was strongly enriched (at least 3-fold) in histone H3 compared to that at the *IκBα* promoter in shMOCK-treated cells (Fig. 3B), suggesting a more compact chromatin state at the *IL-6* promoter (51). The H3 occupancy in shARTD1-treated Raw cells under basal conditions (i.e., untreated) was not significantly reduced compared to shMOCK-treated cells in the first 100 bp upstream of the TSS of the *IL-6* promoter but also not further upstream and even downstream in the gene body (Fig. 3C). Upon LPS stimulation, the measured H3 content was also not significantly changed between shARTD1 and shMOCK cells (Fig. 3D), suggesting that ARTD1 affects IL-6 expression unlikely by altering the histone occupancy around the TSS.

ARTD1 regulates *IL-6* expression through the H3K4me3 levels at the *IL-6* promoter. The results obtained thus far indicate that ARTD1 negatively regulates *IL-6* expression independent of H3 recruitment or its enzymatic activity. However, ARTD1 may exert its regulatory function through the modulation of the histone modifications at the TSS of the *IL-6* gene. The higher occupancy of H3 at the *IL-6* promoter compared to the *IκBα* promoter (Fig. 3B) suggests that a H3 modification may be required to induce a more permissive chromatin state. H3K4me3 is a mark that is associated with active gene expression (52). We therefore eluci-

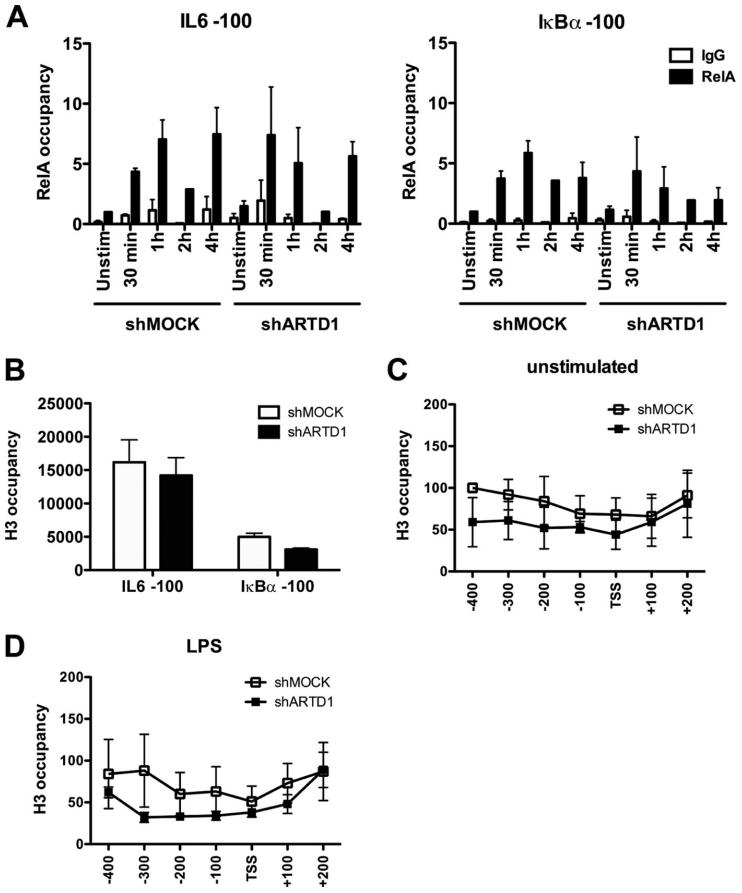

FIG 3 ARTD1 helps to maintain H3 at the *IL-6* promoter. (A) Effect of ARTD1 knockdown on p65 occupancy on *IL-6* and *IκBα* promoters upon LPS stimulation in Raw cells ($n = 3$). (B to D) H3 occupancy at the *IL-6* and *IκBα* promoters in Raw cells under unstimulated conditions (shMOCK and shARTD1) (B and C) or after 4 h of LPS treatment (D) ($n = 3$). The data are presented as mean ± the SD.

dated whether ARTD1 inhibits H3K4me3 at the *IL-6* promoter, thereby keeping the chromatin in a nonpermissive state. To study this possibility, ChIP experiments for H3K4me3 were performed and the *IL-6* and *IκBα* promoters analyzed in detail. Upon *ARTD1* knockdown and LPS stimulation, the relative occupancy of H3K4me3 100 bp upstream of the TSS of the *IL-6* promoter was strongly increased, while no significant changes were observed at the *IκBα* promoter (Fig. 4A). More detailed analysis revealed that the strongest effects on relative H3K4me3 levels upon ARTD1 downregulation and LPS stimulation were observed between the TSS and 200 bp upstream (Fig. 4B), which corresponds to the location of the NF-κB response element. The increased H3K4me3 was observed at the 4-h time point, supporting the gene expression data and suggesting that ARTD1 represses H3K4me3 levels at the NF-κB binding site of the *IL-6* promoter, thereby repressing *IL-6* gene expression.

MLL1 is responsible for the H3K4me3 at the *IL-6* promoter and interacts with NF-κB. To identify the responsible H3K4 methyltransferase at the *IL-6* TSS and to investigate a potential antagonistic effect with ARTD1, Set7/9 and MLL1 were knocked down by siRNA in NIH 3T3 cells in the presence or absence of ARTD1 (Fig. 5A; see the right-hand panels for the knockdown efficiencies). Whereas the enhanced *IL-6* gene expression observed in siARTD1-treated cells was unaffected by knockdown of the methyltransferase Set7/9, it was rescued by knocking down MLL1, suggesting that MLL1 is the methyltransferase responsible for enhanced H3K4me3 formation at the *IL-6* promoter upon knockdown of ARTD1 (Fig. 5A). The expression of *IκBα* was neither significantly affected by siARTD1 nor by siMLL1 treatment. The H3K4me3 could be also altered by a reduced activity of the histone demethylase KDM5B (43). However, knockdown of KDM5B did not lead to increased expression of *IL-6* in either shMOCK or shARTD1 cells (Fig. 5B). Furthermore, knockdown of MLL1 but not of Set7/9 led to a significantly reduced H3K4me3 at the *IL-6* promoter after LPS stimulation, whereas that at the control promoter *IκBα* was unaffected (Fig. 5C). These analyses

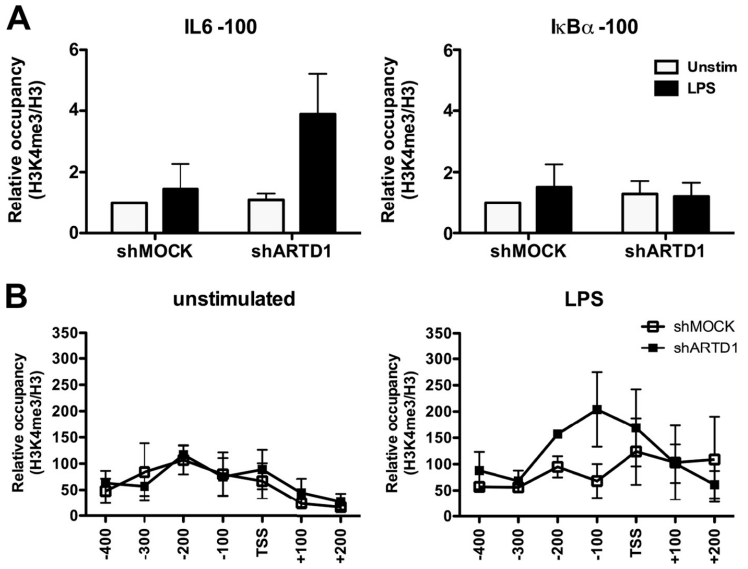

FIG 4 ARTD1 knockdown is associated with increased H3K4me3 occupancy at the *IL-6* promoter in LPS-stimulated cells. H3K4me3 occupancy at the *IL-6* and *IκBα* promoters in Raw cells after 4 h of LPS stimulation (shMOCK and shARTD1) ($n = 3$) is shown.

provide strong evidence that the methyltransferase MLL1 and not Set7/9, or KDM5B regulates H3K4me3 at the *IL-6* promoter in LPS-stimulated cells. The same observation was made when MLL1 was knocked down together with ARTD1, indicating that ARTD1 mediates its effect through MLL1 (Fig. 5D).

To test whether MLL1 forms a complex with NF-κB, complex formation was analyzed in HEK293T cells overexpressing HA-tagged MLL1. Since HEK293T cells lack TLR4 and therefore cannot be stimulated by LPS, cells were stimulated with phorbol myristate acetate (PMA). In HEK293T cells overexpressing MLL1, complex formation of MLL1 with endogenous RelA was detected in chromatin-free nuclear extracts 4 h after stimulation (Fig. 5E). Interestingly, the interaction between RelA and MLL1 was observed in a stimulus-dependent manner and at the same time point when the enhancement of *IL-6* expression by ARTD1 knockdown was the most prominent. Due to the lack of suitable antibodies, the chromatin recruitment of MLL1 could not be analyzed, although others have recently reported that MLL1 is recruited to the chromatin in an NF-κB-dependent manner to regulate NF-κB-mediated gene expression (25).

ARTD1 forms a complex with MLL1 but leaves the *IL-6* promoter in a stimulus-dependent manner. To explain how ARTD1 interferes with MLL1-dependent *IL-6* expression and H3K4me3 at the *IL-6* promoter, *MLL1* expression levels were analyzed. ARTD1 knockdown did neither significantly affect *MLL1* expression nor MLL1 protein levels (Fig. 6A and B), suggesting that ARTD1 may rather be involved in the recruitment of MLL1 to the chromatin or may influence specific protein-protein interactions.

To test, whether ARTD1 forms a complex with MLL1, MLL1 was immunoprecipitated from HEK293T cells overexpressing MLL1 and stimulated for 4 h with PMA. An interaction of MLL1 with endogenous ARTD1 was indeed detected in a stimulus-dependent manner at the same time point as for RelA (i.e., 4 h after stimulation) (Fig. 6C). The detected signal was specific, because ARTD1 knockdown obliterated the signal. Since the negative regulation of *IL-6* expression by ARTD1 could not be explained by an altered recruitment of RelA (Fig. 3A) and the chromatin recruitment of MLL1 could not be analyzed, we investigated whether the chromatin recruitment of ARTD1 is changed during LPS stimulation. ChIP experiments with LPS-stimulated Raw cells revealed that ARTD1 was time-dependently released from the promoters of both *IL-6* and *IκBα* upon LPS stimulation (Fig. 6D), suggesting that LPS stimulation changes the occupancy of ARTD1 at different chromatin loci.

In summary, we describe MLL1 as a new transcriptional coactivator of NF-κB and an additional molecular mechanism by which ARTD1 coregulates NF-κB-dependent transcription, namely, by the regulation of H3K4me3 through MLL1 and independent of ARTD1's enzymatic activity.

DISCUSSION

ADP-ribosylation and in particular ARTD1 have been implicated in many different and distinct cellular and biological processes (31). One of the most important functions of ARTD1 is the coregulation of inflammatory gene expression by direct modulation of transcriptional regulators or indirectly through alterations of the chromatin state (31).

Here, we elucidated the mechanism by which ARTD1 conveys a nonpermissive chromatin state at the *IL-6* promoter, by interfering with MLL1-dependent H3K4me3 upon LPS stimulation. Interestingly, expression of the gene encoding the NF-κB inhibitor IκBα and other housekeeping genes was not ARTD1 dependent, which may be due to different chromatin architecture at the

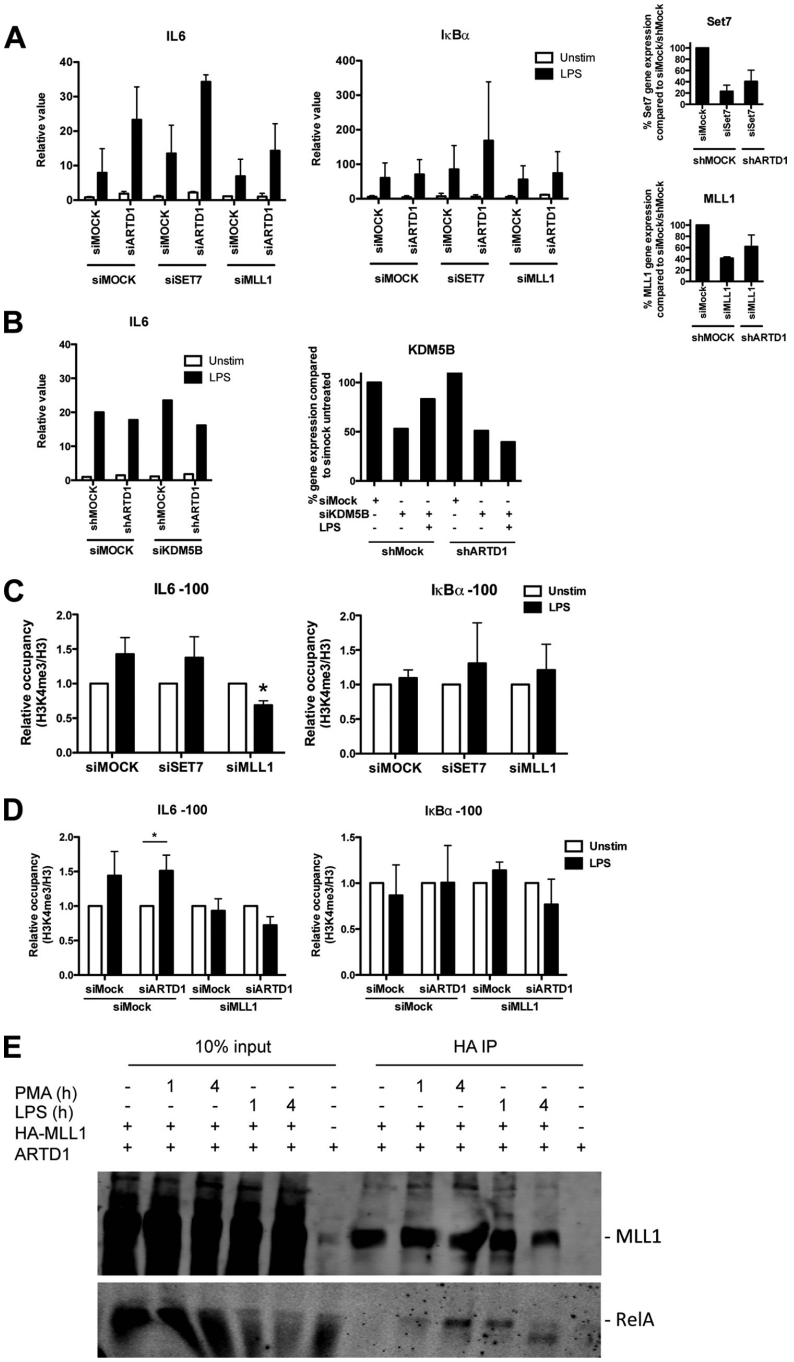

FIG 5 MLL1 regulates *IL-6* expression and H3K4me3 levels at the *IL-6* promoter. (A) *IL-6* and *IκBα* expression upon combined knockdown of ARTD1 and either SET7 or MLL1 in NIH 3T3 cells after 4 h of LPS stimulation ($n = 3$). The rightmost panels show the knockdown efficiency of siRNA treatment against *SET7* and *MLL1* by qPCR analysis. (B, left) *IL-6* expression upon combined knockdown of ARTD1 and KDM5B in NIH 3T3 cells after 4 h of LPS stimulation ($n = 1$).

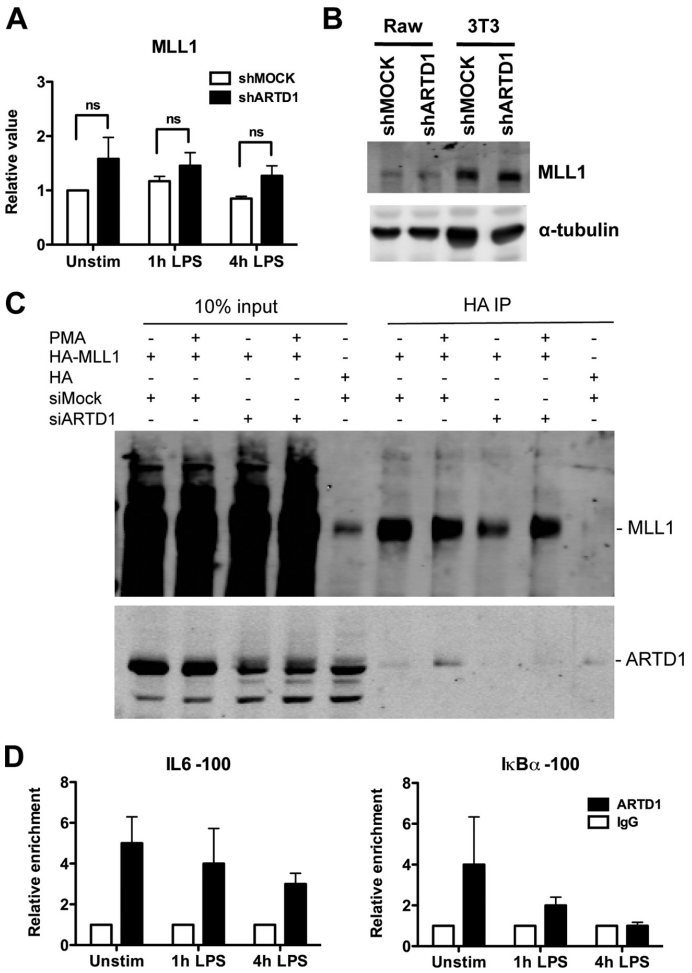

FIG 6 MLL1 interacts with ARTD1 and p65 after LPS stimulation. (A and B) MLL1 gene (A) and protein (B) expression in shMOCK and shARTD1-treated Raw cells ($n = 5$ each). (C) MLL1 and ARTD1 coimmunoprecipitation in HEK293T cells overexpressing MLL1 and pretreated with siMOCK or siARTD1 (4 h PMA). (D) ChIP analysis of ARTD1 occupancy on *IL-6* and *IκBα* promoters in Raw cells ($n = 4$).

promoters of these two genes. The coregulatory function of ARTD1 was not mediated by its enzymatic activity.

The results presented here define the negative regulation of H3K4me3 at the *IL-6* promoter by MLL1 as the mechanism by which ARTD1 modulates *IL-6* expression. Previously, ARTD1 activity was shown to positively regulate transcription via the modification and inhibition of the histone demethylase KDM5B, responsible for the demethylation of H3K4me3 (43). In the present study, knockdown of MLL1 but not of SET7 or KDM5B altered the H3K4me3 of the *IL-6* promoter. It is tempting to speculate that ARTD1, depending on the cellular context, its stimulation, and the availability of its substrate NAD^+, can either repress H3K4me3, through ADP-ribosylation-independent binding to MLL1, or enhance H3K4me3 and therefore gene expression through ADP-ribosylation of KDM5B.

We observed that ARTD1 chromatin association is reduced

(Right) Knockdown efficiency of siRNA treatment against *KDM5B* by qPCR analysis. (C) H3K4me3 occupancy at the *IL-6* and *IκBα* promoters upon knockdown of ARTD1 and either SET7 or MLL1 in NIH 3T3 cells after 4 h of LPS stimulation ($n = 3$). The data are presented as means ± the SD and were analyzed by one-way ANOVA, followed by Bonferroni's *post hoc* test. *, $P < 0.05$. (D) H3K4me3 occupancy at the *IL-6* and *IκBα* promoters upon combined knockdown of ARTD1 and either SET7 or MLL1 in NIH 3T3 cells after 4 h of LPS stimulation ($n = 3$). (E) MLL1 and p65 coimmunoprecipitation in HEK293T cells overexpressing MLL1 (lanes 1 and 4, unstimulated; lane 2, 1 h of PMA; lane 3, 4 h of PMA).

upon LPS treatment after 4 h. Based on our recent studies (49), it is likely that the activation of the inflammasome at this time point is responsible for the proteolytic cleavage of ARTD1 at D214 and its subsequent release from chromatin. Since LPS itself is not expected to activate the inflammasome but to induce the expression of its components, it remains to be elucidated by which mechanism the inflammasome is activated.

According to our study, ARTD1 is bound to the *IL-6* promoter even before stimulation of the cells, likely regulating the compaction and basal expression levels of *IL-6*. Similar to this result, biochemical studies with reconstituted chromatin have shown that in the absence of NAD^+, ARTD1 promotes chromatin compaction independently of its enzymatic activity (53).

Our findings suggest a model in which ARTD1 represses *IL-6* expression by interfering with the MLL1-induced H3K4me3 at the *IL-6* promoter. Upon stimulation of cells, ARTD1 leaves the *IL-6* promoter in a time-dependent manner. Interestingly, ARTD1 forms a complex with MLL1 only at the later time point (4 h, second NF-κB wave), when complex formation of MLL1 with NF-κB is also observed, suggesting that upon eviction of ARTD1, ARTD1 might compete with NF-κB for binding to MLL1, thus allowing only a certain amount of MLL1 to bind to NF-κB and thus damping the MLL1-induced H3K4me3 levels at this later time point. In contrast, in cells lacking ARTD1 or expressing reduced levels of ARTD1, all MLL1 binds to NF-κB and remains associated with the chromatin, resulting in increased H3K4me3 at the *IL-6* promoter and consequently, increased *IL-6* gene expression.

Since we were not able to investigate and quantify the recruitment of MLL1 to the *IL-6* promoter, and the coimmunoprecipitation of MLL1 with NF-κB and/or ARTD1 does not allow us to distinguish whether all three proteins are found in the same complex or in distinct complexes containing MLL1 only associated with NF-κB or ARTD1, additional investigations are required to fully dissect the mechanism by which ARTD1 regulates MLL-1-driven NF-κB-dependent gene expression of *IL-6*, including also in developmental processes, homeobox gene expression or the development of acute leukemia. In this context, it will be of particular interest to investigate the regulation of *IL-6* expression by ARTD1 in cells harboring *MLL1* mutations.

In summary, our experiments have identified the dampening effect of ARTD1 on MLL1-dependent H3K4me3 as a new mechanism regulating the expression of the inflammatory cytokine *IL-6*. Taken together, these data strongly indicate that ARTD1 orchestrates chromatin accessibility and the posttranslational modification of histones indirectly through the interaction with the H3K4 methyltransferase MLL1 and thereby modulates the expression of *IL-6*. This apparently occurs in an ADP-ribosylation-independent manner. These results not only have important implications for our understanding and future analysis of MLL1 functions and *IL-6* regulation but also highlight a potential cross talk between IL-6- and MLL1-induced pathologies.

ACKNOWLEDGMENTS

We thank Robert Roeder (The Rockefeller University, New York, NY) for providing the Flag-HA-tagged MLL1 pcDNA5 clone. We thank Florian Freimoser and Stephan Christen (Institute of Veterinary Biochemistry and Molecular Biology, University of Zurich, Zurich, Switzerland) for editorial assistance and critical input during the writing.

This study was supported in part by the Swiss National Science Foundation (grants 310030B_138667 and 310030_157019), the Kanton of Zurich, and the Novartis Foundation (to M.O.H.).

REFERENCES

1. **Nishimoto N, Kishimoto T.** 2006. Interleukin 6: from bench to bedside. Nat Clin Pract Rheumatol **2:**619–626. http://dx.doi.org/10.1038/ncprheum0338.
2. **Ganapathi MK, Weizer AK, Borsellino S, Bukowski RM, Ganapathi R, Rice T, Casey G, Kawamura K.** 1996. Resistance to interleukin 6 in human non-small cell lung carcinoma cell lines: role of receptor components. Cell Growth Differ **7:**923–929.
3. **Yamaji H, Iizasa T, Koh E, Suzuki M, Otsuji M, Chang H, Motohashi S, Yokoi S, Hiroshima K, Tagawa M, Nakayama T, Fujisawa T.** 2004. Correlation between interleukin 6 production and tumor proliferation in non-small cell lung cancer. Cancer Immunol Immunother **53:**786–792.
4. **Knupfer H, Preiss R.** 2007. Significance of interleukin-6 (IL-6) in breast cancer. Breast Cancer Res Treat **102:**129–135. http://dx.doi.org/10.1007/s10549-006-9328-3.
5. **Bromberg J, Wang T.** 2009. Inflammation and cancer: IL-6 and STAT3 complete the link. Cancer Cell **15:**79–80. http://dx.doi.org/10.1016/j.ccr.2009.01.009.
6. **Iliopoulos D, Hirsch HA, Wang G, Struhl K.** 2011. Inducible formation of breast cancer stem cells and their dynamic equilibrium with non-stem cancer cells via IL-6 secretion. Proc Natl Acad Sci U S A **108:**1397–1402. http://dx.doi.org/10.1073/pnas.1018898108.
7. **Hugo HJ, Lebret S, Tomaskovic-Crook E, Ahmed N, Blick T, Newgreen DF, Thompson EW, Ackland ML.** 2012. Contribution of fibroblast and mast cell (afferent) and tumor (efferent) IL-6 effects within the tumor microenvironment. Cancer Microenviron **5:**83–93. http://dx.doi.org/10.1007/s12307-012-0098-7.
8. **Raz Y, Erez N.** 2013. An inflammatory vicious cycle: fibroblasts and immune cell recruitment in cancer. Exp Cell Res **319:**1596–1603. http://dx.doi.org/10.1016/j.yexcr.2013.03.022.
9. **Servais C, Erez N.** 2013. From sentinel cells to inflammatory culprits: cancer-associated fibroblasts in tumour-related inflammation. J Pathol **229:**198–207. http://dx.doi.org/10.1002/path.4103.
10. **Armenante F, Merola M, Furia A, Palmieri M.** 1999. Repression of the IL-6 gene is associated with hypermethylation. Biochem Biophys Res Commun **258:**644–647. http://dx.doi.org/10.1006/bbrc.1999.0566.
11. **Armenante F, Merola M, Furia A, Tovey M, Palmieri M.** 1999. Interleukin-6 repression is associated with a distinctive chromatin structure of the gene. Nucleic Acids Res **27:**4483–4490. http://dx.doi.org/10.1093/nar/27.22.4483.
12. **Dandrea M, Donadelli M, Costanzo C, Scarpa A, Palmieri M.** 2009. MeCP2/H3meK9 are involved in IL-6 gene silencing in pancreatic adenocarcinoma cell lines. Nucleic Acids Res **37:**6681–6690. http://dx.doi.org/10.1093/nar/gkp723.
13. **Takeuch O, Akira S.** 2011. Epigenetic control of macrophage polarization. Eur J Immunol **41:**2490–2493. http://dx.doi.org/10.1002/eji.201141792.
14. **Tang B, Zhao R, Sun Y, Zhu Y, Zhong J, Zhao G, Zhu N.** 2011. Interleukin-6 expression was regulated by epigenetic mechanisms in response to influenza virus infection or dsRNA treatment. Mol Immunol **48:**1001–1008. http://dx.doi.org/10.1016/j.molimm.2011.01.003.
15. **Li Q, Verma IM.** 2002. NF-κB regulation in the immune system. Nat Rev Immunol **2:**725–734. http://dx.doi.org/10.1038/nri910.
16. **Karin M, Greten FR.** 2005. NF-κB: linking inflammation and immunity to cancer development and progression. Nat Rev Immunol **5:**749–759. http://dx.doi.org/10.1038/nri1703.
17. **Tak PP, Firestein GS.** 2001. NF-κB: a key role in inflammatory diseases. J Clin Invest **107:**7–11. http://dx.doi.org/10.1172/JCI11830.
18. **Hassa PO, Haenni SS, Buerki C, Meier NI, Lane WS, Owen H, Gersbach M, Imhof R, Hottiger MO.** 2005. Acetylation of poly(ADP-ribose) polymerase-1 by p300/CREB-binding protein regulates coactivation of NF-κB-dependent transcription. J Biol Chem **280:**40450–40464. http://dx.doi.org/10.1074/jbc.M507553200.
19. **Mao X, Gluck N, Li D, Maine GN, Li H, Zaidi IW, Repaka A, Mayo MW, Burstein E.** 2009. GCN5 is a required cofactor for a ubiquitin ligase that targets NF-κB/RelA. Genes Dev **23:**849–861. http://dx.doi.org/10.1101/gad.1748409.
20. **Smale ST.** 2010. Selective transcription in response to an inflammatory stimulus. Cell **140:**833–844. http://dx.doi.org/10.1016/j.cell.2010.01.037.

21. **Li H, Wittwer T, Weber A, Schneider H, Moreno R, Maine GN, Kracht M, Schmitz ML, Burstein E.** 2012. Regulation of NF-κB activity by competition between RelA acetylation and ubiquitination. Oncogene **31:** 611–623. http://dx.doi.org/10.1038/onc.2011.253.
22. **Sen N, Paul BD, Gadalla MM, Mustafa AK, Sen T, Xu R, Kim S, Snyder SH.** 2012. Hydrogen sulfide-linked sulfhydration of NF-κB mediates its antiapoptotic actions. Mol Cell **45:**13–24. http://dx.doi.org/10.1016/j.molcel.2011.10.021.
23. **Ansari KI, Mandal SS.** 2010. Mixed lineage leukemia: roles in gene expression, hormone signaling and mRNA processing. FEBS J **277:**1790–1804. http://dx.doi.org/10.1111/j.1742-4658.2010.07606.x.
24. **Hubert A, Henderson JM, Ross KG, Cowles MW, Torres J, Zayas RM.** 2013. Epigenetic regulation of planarian stem cells by the SET1/MLL family of histone methyltransferases. Epigenetics **8:**79–91. http://dx.doi.org/10.4161/epi.23211.
25. **Wang X, Zhu K, Li S, Liao Y, Du R, Zhang X, Shu HB, Guo AY, Li L, Wu M.** 2012. MLL1, a H3K4 methyltransferase, regulates the TNFα-stimulated activation of genes downstream of NF-κB. J Cell Sci **125:**4058–4066. http://dx.doi.org/10.1242/jcs.103531.
26. **Marschalek R.** 2010. Mixed lineage leukemia: roles in human malignancies and potential therapy. FEBS J **277:**1822–1831. http://dx.doi.org/10.1111/j.1742-4658.2010.07608.x.
27. **Zhang P, Bergamin E, Couture JF.** 2013. The many facets of MLL1 regulation. Biopolymers **99:**136–145. http://dx.doi.org/10.1002/bip.22126.
28. **Ramirez-Carrozzi V, Braas D, Bhatt D, Cheng C, Hong C, Doty K, Black J, Hoffmann A, Carey M, Smale S.** 2009. A unifying model for the selective regulation of inducible transcription by CpG islands and nucleosome remodeling. Cell **138:**114–128. http://dx.doi.org/10.1016/j.cell.2009.04.020.
29. **Iliopoulos D, Hirsch H, Struhl K.** 2009. An epigenetic switch involving NF-κB, Lin28, Let-7 MicroRNA, and IL6 links inflammation to cell transformation. Cell **139:**693–706. http://dx.doi.org/10.1016/j.cell.2009.10.014.
30. **Korkaya H, Liu S, Wicha MS.** 2011. Regulation of cancer stem cells by cytokine networks: attacking cancer's inflammatory roots. Clin Cancer Res **17:**6125–6129. http://dx.doi.org/10.1158/1078-0432.CCR-10-2743.
31. **Kraus WL, Hottiger MO.** 2013. PARP-1 and gene regulation: progress and puzzles. Mol Aspects Med **34:**1109–1123. http://dx.doi.org/10.1016/j.mam.2013.01.005.
32. **Rosenthal F, Hottiger MO.** 2014. Identification of ADP-ribosylated peptides and ADP-ribose acceptor sites. Front Biosci (Landmark ed) **19:**1041–1056. http://dx.doi.org/10.2741/4266.
33. **Elser M, Borsig L, Hassa PO, Erener S, Messner S, Valovka T, Keller S, Gassmann M, Hottiger MO.** 2008. Poly(ADP-ribose) polymerase 1 promotes tumor cell survival by coactivating hypoxia-inducible factor-1-dependent gene expression. Mol Cancer Res **6:**282–290. http://dx.doi.org/10.1158/1541-7786.MCR-07-0377.
34. **D'Amours D, Desnoyers S, D'Silva I, Poirier G.** 1999. Poly(ADP-ribosyl)ation reactions in the regulation of nuclear functions. Biochem J **342:**249–268. http://dx.doi.org/10.1042/0264-6021:3420249.
35. **Kraus W, Lis J.** 2003. PARP goes transcription. Cell **113:**677–683. http://dx.doi.org/10.1016/S0092-8674(03)00433-1.
36. **de Murcia G, Huletsky A, Lamarre D, Gaudreau A, Pouyet J, Daune M, Poirier G.** 1986. Modulation of chromatin superstructure induced by poly(ADP-ribose) synthesis and degradation. J Biol Chem **261:**7011–7017.
37. **Kim M, Mauro S, Gévry N, Lis J, Kraus W.** 2004. NAD+-dependent modulation of chromatin structure and transcription by nucleosome binding properties of PARP-1. Cell **119:**803–814. http://dx.doi.org/10.1016/j.cell.2004.11.002.
38. **Krishnakumar R, Gamble M, Frizzell K, Berrocal J, Kininis M, Kraus W.** 2008. Reciprocal binding of PARP-1 and histone H1 at promoters specifies transcriptional outcomes. Science **319:**819–821. http://dx.doi.org/10.1126/science.1149250.
39. **Altmeyer M, Messner S, Hassa PO, Fey M, Hottiger MO.** 2009. Molecular mechanism of poly(ADP-ribosyl)ation by PARP1 and identification of lysine residues as ADP-ribose acceptor sites. Nucleic Acids Res **37:**3723–3738. http://dx.doi.org/10.1093/nar/gkp229.
40. **Messner S, Altmeyer M, Zhao H, Pozivil A, Roschitzki B, Gehrig P, Rutishauser D, Huang D, Caflisch A, Hottiger MO.** 2010. PARP1 ADP-ribosylates lysine residues of the core histone tails. Nucleic Acids Res **38:**6350–6362. http://dx.doi.org/10.1093/nar/gkq463.
41. **Ahel D, Horejsi Z, Wiechens N, Polo SE, Garcia-Wilson E, Ahel I, Flynn H, Skehel M, West SC, Jackson SP, Owen-Hughes T, Boulton SJ.** 2009. Poly(ADP-ribose)-dependent regulation of DNA repair by the chromatin remodeling enzyme ALC1. Science **325:**1240–1243. http://dx.doi.org/10.1126/science.1177321.
42. **Gottschalk A, Timinszky G, Kong S, Jin J, Cai Y, Swanson S, Washburn M, Florens L, Ladurner A, Conaway J, Conaway R.** 2009. Poly(ADP-ribosyl)ation directs recruitment and activation of an ATP-dependent chromatin remodeler. Proc Natl Acad Sci U S A **106:**13770–13774. http://dx.doi.org/10.1073/pnas.0906920106.
43. **Krishnakumar R, Kraus W.** 2010. PARP-1 regulates chromatin structure and transcription through a KDM5B-dependent pathway. Mol Cell **39:**736–749. http://dx.doi.org/10.1016/j.molcel.2010.08.014.
44. **Hassa PO, Hottiger MO.** 1999. A role of poly (ADP-ribose) polymerase in NF-κB transcriptional activation. Biol Chem **380:**953–959.
45. **Hassa PO, Buerki C, Lombardi C, Imhof R, Hottiger MO.** 2003. Transcriptional coactivation of nuclear factor-κB-dependent gene expression by p300 is regulated by poly(ADP)-ribose polymerase-1. J Biol Chem **278:**45145–45153. http://dx.doi.org/10.1074/jbc.M307957200.
46. **Hassa PO, Covic M, Bedford MT, Hottiger MO.** 2008. Protein arginine methyltransferase 1 coactivates NF-κB-dependent gene expression synergistically with CARM1 and PARP1. J Mol Biol **377:**668–678. http://dx.doi.org/10.1016/j.jmb.2008.01.044.
47. **Hassa PO, Covic M, Hasan S, Imhof R, Hottiger MO.** 2001. The enzymatic and DNA binding activity of PARP-1 are not required for NF-κB coactivator function. J Biol Chem **276:**45588–45597. http://dx.doi.org/10.1074/jbc.M106528200.
48. **von Lukowicz T, Hassa PO, Lohmann C, Borén J, Braunersreuther V, Mach F, Odermatt B, Gersbach M, Camici GG, Stähli BE, Tanner FC, Hottiger MO, Lüscher TF, Matter CM.** 2008. PARP1 is required for adhesion molecule expression in atherogenesis. Cardiovasc Res **78:**158–166. http://dx.doi.org/10.1093/cvr/cvm110.
49. **Erener S, Petrilli V, Kassner I, Minotti R, Castillo R, Santoro R, Hassa PO, Tschopp J, Hottiger MO.** 2012. Inflammasome-activated caspase 7 cleaves PARP1 to enhance the expression of a subset of NF-κB target genes. Mol Cell **46:**200–211. http://dx.doi.org/10.1016/j.molcel.2012.02.016.
50. **Saccani S, Pantano S, Natoli G.** 2001. Two waves of nuclear factor κB recruitment to target promoters. J Exp Med **193:**1351–1359. http://dx.doi.org/10.1084/jem.193.12.1351.
51. **Lachner M, O'Carroll D, Rea S, Mechtler K, Jenuwein T.** 2001. Methylation of histone H3 lysine 9 creates a binding site for HP1 proteins. Nature **410:**116–120. http://dx.doi.org/10.1038/35065132.
52. **Santos-Rosa H, Schneider R, Bannister AJ, Sherriff J, Bernstein BE, Emre NC, Schreiber SL, Mellor J, Kouzarides T.** 2002. Active genes are tri-methylated at K4 of histone H3. Nature **419:**407–411. http://dx.doi.org/10.1038/nature01080.
53. **Wacker D, Ruhl D, Balagamwala E, Hope K, Zhang T, Kraus W.** 2007. The DNA binding and catalytic domains of poly(ADP-ribose) polymerase 1 cooperate in the regulation of chromatin structure and transcription. Mol Cell Biol **27:**7475–7485. http://dx.doi.org/10.1128/MCB.01314-07.
54. **Santoro R, Li J, Grummt I.** 2002. The nucleolar remodeling complex NoRC mediates heterochromatin formation and silencing of ribosomal gene transcription. Nat Genet **32:**393–396. http://dx.doi.org/10.1038/ng1010.

Supplemental material

Supplemental Table 1: Primers for qPCR analysis

Primer Name	Sequence
mIL6 for	CTGCAAGAGACTTCCATCCAGTT
mIL6 for	GAAGTAGGGAAGGCCGTGG
hIL6 for	GGCACTGGCAGAAAACAACC
hIL6 rev	GCAAGTCTCCTCATTGAATCC
mRSP12 for	GAAGCTGCCAAAGCCTTAGA
mRSP12 rev	AACTGCAACCAACCACCTTC
hRPL28 for	GCAATTCCTTCCGCTACAAC
hRPL28 rev	TGTTCTTGCGGATCATGTGT
mIκBα for	AAATCTCCAGATGCTACCCGAGAG
mIκBα rev	ATAATGTCAGACGCTGGCCTCCAA
hIκBα for	GCACCTCCACTCCATCCTGAAGG
hIκBα rev	CCATTACAGGGCTCCTGAGCATTG
mIL6 -400 for	AGCCTCTTATTCATGTGTGTGTG
mIL6 -400 rev	CAGCACTTGAGCATGTCTTGA
mIL6 -300 for	TCCCATCAAGACATGCTCAA
mIL6 -300 rev	GGGGCTGATTGGAAACCTTA
mIL6 -200 for	AAGCACACTTTCCCCTTCCT
mIL6 -200 rev	TCATGGGAAAATCCCACATT
mIL6 -100 for	CAATCAGCCCCACCCACTCTGG
mIL6 -100 rev	TTCTTGGTGGGCTCCAGAGCAGAA
mIL6 TSS for	AATGTGGGATTTTCCCATGA
mIL6 TSS rev	GCTCTCTGCCTCACACTCCT

mIL6 +100 for	CTGGCGGAGCTATTGAGACT
mIL6 +100 rev	TGGTTGTCACCAGCATCAGT
mIL6 +200 for	TTTTCTCCACGCAGGAGACT
mIL6 +200 rev	TCCACGATTTCCCAGAGAAC
mIκBα -100 for	AAAGTTCCCTGTGCATGACC
mIκBα -100 rev	CTGGCAGGGGATTTCTCAG
mMLL1 for	ACCCCGGAAGTGCTCGGTCA
mMLL1 rev	GCTCGGCTGAACTCCTGGGC

open Biology

rsob.royalsocietypublishing.org

Research

Cite this article: Kassner I, Andersson A, Fey M, Tomas M, Ferrando-May E, Hottiger MO. 2013 SET7/9-dependent methylation of ARTD1 at K508 stimulates poly-ADP-ribose formation after oxidative stress. Open Biol 3: 120173. http://dx.doi.org/10.1098/rsob.120173

Received: 3 December 2012
Accepted: 11 September 2013

Subject Area:
cellular biology/molecular biology

Keywords:
ADP-ribosylation, lysine methylation, PARP-1, protein regulation, SET7/9

Author for correspondence:
Michael O. Hottiger
e-mail: hottiger@vetbio.uzh.ch

Electronic supplementary material is available at http://dx.doi.org/10.1098/rsob.120173.

Royal Society Publishing
Informing the science of the future

SET7/9-dependent methylation of ARTD1 at K508 stimulates poly-ADP-ribose formation after oxidative stress

Ingrid Kassner[1,2], Anneli Andersson[1,2], Monika Fey[1], Martin Tomas[3,4], Elisa Ferrando-May[3] and Michael O. Hottiger[1]

[1]Institute of Veterinary Biochemistry and Molecular Biology, and [2]Life Science Zurich Graduate School, Molecular Life Science Program, University of Zurich, Winterthurerstrasse 190, 8057 Zurich, Switzerland
[3]Department of Biology, Bioimaging Center, and [4]Department of Physics, Center for Applied Photonics, University of Konstanz, Universitätstrasse 10, 78464 Konstanz, Germany

1. Summary

ADP-ribosyltransferase diphtheria toxin-like 1 (ARTD1, formerly PARP1) is localized in the nucleus, where it ADP-ribosylates specific target proteins. The post-translational modification (PTM) with a single ADP-ribose unit or with polymeric ADP-ribose (PAR) chains regulates protein function as well as protein–protein interactions and is implicated in many biological processes and diseases. SET7/9 (Setd7, KMT7) is a protein methyltransferase that catalyses lysine monomethylation of histones, but also methylates many non-histone target proteins such as p53 or DNMT1. Here, we identify ARTD1 as a new SET7/9 target protein that is methylated at K508 *in vitro* and *in vivo*. ARTD1 auto-modification inhibits its methylation by SET7/9, while auto-poly-ADP-ribosylation is not impaired by prior methylation of ARTD1. Moreover, ARTD1 methylation by SET7/9 enhances the synthesis of PAR upon oxidative stress *in vivo*. Furthermore, laser irradiation-induced PAR formation and ARTD1 recruitment to sites of DNA damage in a SET7/9-dependent manner. Together, these results reveal a novel mechanism for the regulation of cellular ARTD1 activity by SET7/9 to assure efficient PAR formation upon cellular stress.

2. Background

ADP-ribosyltransferase diphtheria toxin-like 1 (ARTD1, formerly named PARP1, [1]) is a nuclear protein that post-translationally modifies proteins by transferring the ADP-ribose moiety from NAD^+ to specific amino acid residues of target proteins. It is the best described member of the ADP-ribosyltransferase (ART) protein family, which currently comprises 22 human enzymes [1]. ARTD1 is not only the main nuclear ART, but also the primary acceptor for polymeric ADP-ribose (PAR). ARTD1 can be ADP-ribosylated at specific lysine residues and is also modified by acetylation and sumoylation between the amino acid residues 481 and 525 [2–4]. Protein modification with a single ADP-ribose unit or with PAR chains regulates protein function and is implicated in biological processes such as transcriptional control, cell differentiation or cell-cycle regulation [5,6]. Many cellular functions of ARTD1 are

brought about by complex formation with partner proteins or the ADP-ribosylation of target proteins in the cell nucleus [5,7]. For example, histones or transcription factors are poly-ADP-ribosylated (PARylated) by ARTD1, which causes concomitant changes in chromatin structure and DNA metabolism [8,9].

Genotoxic and cellular stresses activate ARTD1 enzyme activity [10]. However, the detailed upstream mechanisms leading to the activation of ARTD1 and the involvement of PTMs-modulating ARTD1 activity are little understood. *In vitro*, the DNA-dependent interaction between the amino-terminal DNA-binding domain and the catalytic domain of ARTD1 increased *V*max and decreased the *Km* for NAD^+ [4]. The amount of DNA in this study was kept at a saturating 1 : 1 ratio (DNA : ARTD1 dimer). It is currently not clear whether ARTD1 activity and the subsequent PAR formation under non-saturating DNA levels depend on additional regulatory mechanisms.

SET7/9 (also called Setd7 or KMT7) was discovered as a histone methyltransferase that causes monomethylation of histone 3 lysine 4 (H3K4me1) [11] and is thereby involved in the regulation of euchromatic gene expression [12–14]. However, SET7/9 has only weak activity on nucleosomes [15], which implies that the main targets of the enzyme are non-histone proteins. In agreement with this hypothesis, numerous non-histone proteins such as Dnmt1 (reduction in stability), p53 (activation and stabilization), TAF10 (increased affinity for polymerase II), oestrogen receptor α (activation and stabilization), pRb, p65, MyoD and Tat protein of HIV1 are methylated by SET7/9 [16–24]. In addition, a recent study identified up to 90 new non-histone SET7/9 target peptides and a strong methylation of free H2A and H2B tails [25]. This promiscuous targeting of different substrates by SET7/9 suggests a low specificity of the enzyme. SET7/9 knockout mice are viable and fertile and loss of SET7/9 does not seem to impair p53-dependent cell-cycle arrest or apoptosis following DNA damage [26,27], although SET7/9 was originally thought to regulate p53 activity in human cells [16]. SET7/9 preferentially modifies positively charged amino acid regions and methylates the last lysine residue in the motif [K>R] [S>KYARTPN] [K] [25]. Peptides that do not perfectly match this sequence can be methylated to a lesser extent. In cells, a strong interaction of acceptor proteins with the SET7/9 methyltransferase might stimulate the transfer of a methyl group to weak target sites. Hence, a weaker methylation does not have to imply a lower biological importance [25].

SET7/9-mediated monomethylation of non-histone proteins is a reversible PTM that can be removed by demethylases such as the lysine-specific demethylase 1 (LSD1) [28,29] and likely also by the close homologue LSD2. Both proteins are flavin-dependent demethylases that are specific for mono- and dimethylated lysines and which are part of histone modification complexes that control cell-specific gene expression [30,31].

The study presented here identifies ARTD1 as a new SET7/9 target protein that is methylated at K508, which enhances PAR synthesis upon oxidative stress. Similarly, SET7/9 also affected PAR synthesis and ARTD1 recruitment to sites of DNA damage *in vivo* upon laser irradiation. These results define methylation of ARTD1 by SET7/9 as an additional regulatory element for cellular ADP-ribosylation and ARTD1 enzymatic activity.

3. Results and discussion

3.1. ARTD1 is methylated *in vitro* and *in vivo* at K508 by SET7/9

Based on methylation profile searches and preliminary experiments, it was hypothesized that SET7/9 directly methylates ARTD1. To determine whether SET7/9 indeed modifies ARTD1, biochemical *in vitro* methylation assays with purified proteins were performed. SET7/9 methylated the known substrate histone H3 as well as full-length ARTD1, while neither GST nor ARTD2, another member of the ARTD family, was modified (figure 1*a*). To localize the modification site, purified ARTD1 fragments covering the whole amino acid sequence were methylated by SET7/9 *in vitro* (figure 1*b*). The potential SET7/9 modification site(s) in ARTD1 could be narrowed down to the auto-modification domain (AD) consisting of amino acids 373–524, which was strongly methylated *in vitro*, while all other tested ARTD1 fragments (containing the DNA-binding (DBD), WGR or catalytic (CAT) domains) were not methylated (figure 1*b*). *In silico* analysis identified lysine 508 (K508) as the putative target site as it was the only lysine residue within this region matching the published [KR] [STA] [K(me)] consensus motif for SET7/9-dependent methylation [18]. Mutation of K508 to arginine (K508R) indeed abolished SET7/9-dependent methylation of full-length ARTD1 (figure 1*c*). ARTD1 K508 was confirmed as the target residue of SET7/9 by mass spectrometric analysis of recombinant ARTD1 (373–524) *in vitro* methylated by SET7/9 (see electronic supplementary material, figure S1*a*,*b*). To confirm methylation of ARTD1 K508 in cells, a polyclonal antibody against a synthetic human ARTD1 peptide containing monomethylated K508 was generated. The anti-meARTD1 antibody specifically recognized the monomethylated peptide (see electronic supplementary material, figure S1*c*) and full-length ARTD1 that was methylated by SET7/9 *in vitro* (see electronic supplementary material, figure S1*d*), while the methylation-deficient K508R mutant was not detected (figure 1*d*). *In vivo*, the same antibody specifically detected the methylation of ARTD1 in cells overexpressing SET7/9 (figure 1*e*,*f*). The antibody did not detect methylation of overexpressed mouse ARTD1 in mouse cells, which was most probably owing to sequence differences between human and mouse ARTD1 at the methylation site.

These results defined ARTD1 as a new target for SET7/9-dependent methylation *in vitro* and *in vivo* and identified K508 as the main target site for SET7/9-dependent methylation of ARTD1.

3.2. ARTD1 auto-modification inhibits its methylation by SET7/9

Interestingly, the SET7/9 target residue K508 lies within a heavily modified region (aa 486–524) of the ARTD1 AD domain that comprises five acetylation and three ADP-ribosylation sites as well as one lysine residue that can be sumoylated (see electronic supplementary material, figure S2). Modification of ARTD1 with SUMO did not affect its ADP-ribosylation activity, but completely abrogated p300-mediated acetylation of ARTD1, revealing an intriguing crosstalk of sumoylation and acetylation on ARTD1 [2]. Crosstalk between different PTMs of the same modified amino acid residue has been documented in particular for modifications comprising the histone code [32–34]. It was

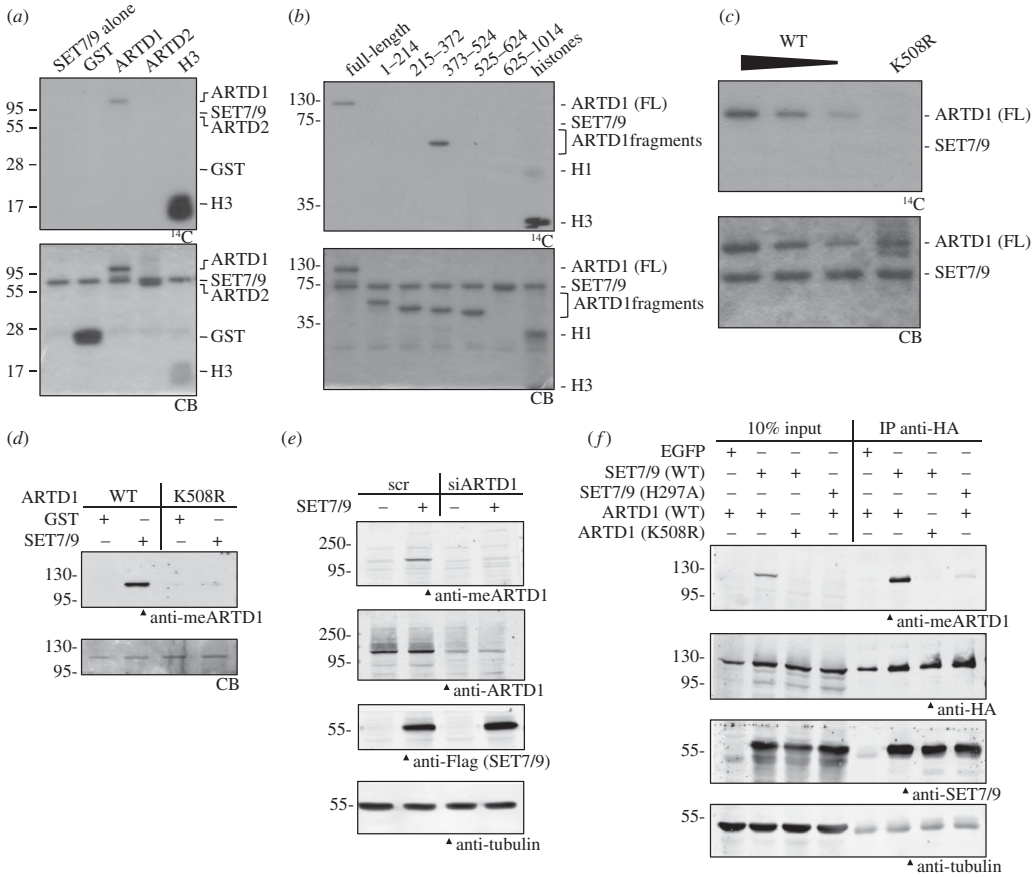

Figure 1. ARTD1 is methylated at K508 by SET7/9 *in vitro* and *in vivo*. (*a*) GST, ARTD1, ARTD2 and H3 were incubated with SET7/9 and ^{14}C-labelled SAM in an *in vitro* methylation assay, separated by SDS-PAGE and analysed by autoradiography (^{14}C). Coomassie blue (CB) stained gels are shown below. (*b*) Full-length ARTD1 and fragments covering the whole protein were incubated in an *in vitro* methylation assay and analysed by autoradiography. (*c*) Decreasing amounts of WT ARTD1 and K508R ARTD1 were methylated by SET7/9 and analysed by autoradiography. (*d*) An antibody directed against a peptide carrying the methylated lysine residue of ARTD1 was generated and tested in a western blot with *in vitro* methylated ARTD1 WT and K508R. (*e*) U2OS cells were transfected with scrambled siRNA (scr) or siRNA directed against ARTD1. One day later, cells were transfected with an empty vector or with a plasmid containing WT *SET7/9*. Whole cell extracts were analysed by western blot on day 3 after knockdown using the same antibody as in (*d*). (*f*) U2OS cells were co-transfected with HA-ARTD1 (WT or K508R) and EGFP or Flag-HA-SET7/9 (WT or H297A). After immunoprecipitation with an anti-HA antibody, whole cell extracts and IP samples were analysed by western blotting with the indicated antibodies. All experiments were repeated at least twice, gave a similar result, and one representative blot is shown.

thus tested whether there is crosstalk between PARylation, acetylation and SET7/9-dependent methylation of ARTD1 *in vitro*. Prior stimulation of recombinant ARTD1 with DNA in the presence of NAD$^+$ and subsequent auto-modification completely inhibited methylation by SET7/9 (figure 2*a*). Inhibition of ADP-ribosylation by 3-aminobenzamide from the beginning (3-AB; +) reverted this effect on ARTD1 methylation, while 3-AB addition after auto-modification, but before addition of SET7/9 (3-AB; ±), still resulted in markedly decreased methylation (figure 2*a*). Consequently, these experiments suggested that auto-ADP-ribosylation of ARTD1, but not a possible ADP-ribosylation of SET7/9 by ARTD1, prevented subsequent methylation. The sharp band of methylated ARTD1 running at the height of unmodified ARTD1 strengthened the conclusion that SET7/9 only methylated ARTD1 that was not or only slightly ADP-ribosylated.

By contrast, auto-PARylation of ARTD1 was not impaired by prior methylation of ARTD1 as indicated by the smear of methylated ARTD1 upon incubation with cold NAD$^+$ and DNA (figure 2*b*). Similarly, methylation of the 373–524 ARTD1 fragment by SET7/9 did not affect subsequent acetylation by p300 (figure 2*c*(i)). The experiment was controlled with the enzymatically inactive H297A SET7/9 mutant and methylation of ARTD1 was confirmed in a parallel experiment using ^{14}C-SAM (figure 2*c*(ii)).

These results suggested that SET7/9-dependent methylation of ARTD1 is influenced by ARTD1 auto-modification, while neither PARylation itself nor acetylation by p300 is impaired by the methyl-modification of K508.

3.3. SET7/9-dependent methylation stimulates ARTD1 activity

In order to test the hypothesis that SET7/9 regulates the enzymatic activity of ARTD1 *in vivo*, we first confirmed

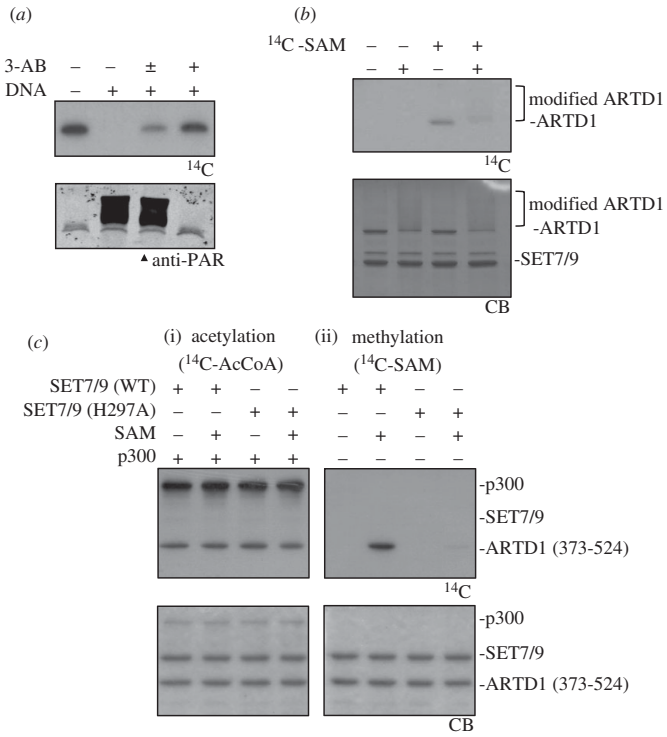

Figure 2. ARTD1 methylation by SET7/9 does not influence its PARylation or acetylation but is inhibited by ARTD1 auto-modification. (*a*) Recombinant ARTD1 was methylated by SET7/9 after ADP-ribosylation in the presence or absence of DNA and 3-AB. ±: 3-AB was added after the ADP-ribosylation reaction. (*b*) ARTD1 was first incubated with SET7/9 in the presence or absence of ^{14}C-SAM and afterwards incubated with activating DNA and cold NAD^+ to allow auto-modification. (*c*) ARTD1 (373–524) was first incubated with WT SET7/9 or an enzymatic dead mutant (H297A) in the presence of cold SAM and afterwards acetylated with p300 and ^{14}C-AcCoA (i). Methylation was controlled with ^{14}C-SAM (ii). All experiments were repeated at least twice, gave a similar result, and one representative blot is shown.

that both enzymes are localized in the nucleus of U2OS cells. While ARTD1 was only present in the nucleus and enriched in the nucleoli, SET7/9 was localized throughout the cell except in the nucleoli (see electronic supplementary material, figure S3*a*). Next, Flag-tagged wild-type (WT) SET7/9 was overexpressed and PAR formation following oxidative stress by H_2O_2 was determined (see figure 3*a* and electronic supplementary material, figure S3*b*). PAR formation was indeed increased upon overexpression of WT SET7/9 (lanes 2 and 5), even in unstimulated cells (lane 2), while the enzymatically inactive SET7/9 mutant H297A did not cause this effect (lanes 3 and 6). To prove that SET7/9 stimulated PAR formation, we analysed mouse fibroblasts lacking SET7/9. Upon H_2O_2 stimulation, SET7/9-knockout MEFs showed significantly reduced PAR staining and lower PAR-synthesizing activity as compared with the WT control cells (see figure 3*b*,*c* and electronic supplementary material, figure S3*c*), suggesting that SET7/9 regulates PAR formation *in vivo*. This was also confirmed by SET7/9 knockdown in U2OS cells (see electronic supplementary material, figure S4*a*,*b*). Following oxidative stress by H_2O_2, siSET7/9-treated cells formed less PAR than cells transfected with a control siRNA (see figure 3*d* and electronic supplementary material, figure S4*c*). To further analyse the influence of SET7/9 on ARTD1 enzymatic activity in cells, nuclear extracts (NEs) from siRNA-treated U2OS cells (control siRNA or siRNA directed against SET7/9 or ARTD1) were prepared and auto-ADP-ribosylation of ARTD1 was tested *in vitro* in the presence or absence of exogenous DNA. Downregulation of SET7/9 reduced the basal ARTD1 activity to levels only slightly above those in siARTD1 cells (in the absence of exogenous DNA, figure 3*e*; electronic supplementary material, figure S4*d*). This effect was also seen, but to a lesser extent, when ARTD1 activity was stimulated by an excess of exogenous DNA, suggesting that SET7/9 methylation regulates ARTD1, especially in the absence of a strong stimulus.

These results suggested that SET7/9-dependent methylation stimulates ARTD1-dependent PAR formation in U2OS cells.

3.4. SET7/9-dependent methylation of ARTD1 at K508 regulates ADP-ribosylation *in vivo*

To elucidate whether SET7/9-dependent methylation of ARTD1 at K508 is directly responsible for the observed influence of SET7/9 on ARTD1-dependent PAR formation *in vivo*, *ARTD1*−/− MLFs were stably genetically complemented with WT ARTD1 or with two methylation-deficient mutants (K508A and K508R). The WT and the mutant proteins were comparably expressed in the NEs, but not detectable in the cytoplasmic extracts (CEs) or the vector control (pRRL) (figure 4*a*). NEs containing WT or mutant ARTD1 were incubated with radioactively labelled NAD^+, but without exogenous DNA, and ARTD1 auto-ADP-ribosylation was assessed. The methylation-deficient ARTD1 mutants K508A and K508R exhibited markedly reduced activity in comparison with the WT control (see figure 4*b* and electronic supplementary material, figure S5*a*). Upon addition

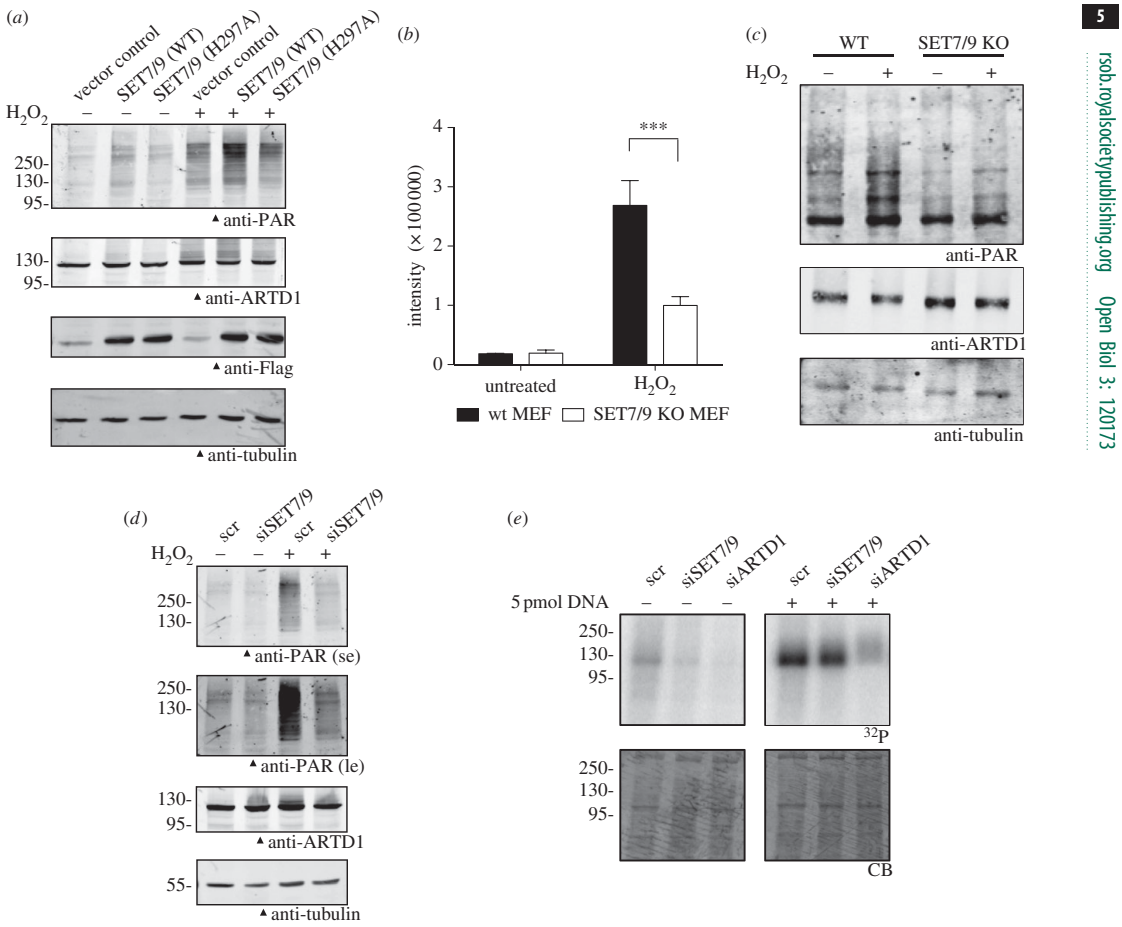

Figure 3. SET7/9-dependent methylation increases ARTD1 activity in cells. (*a*) After overexpression of Flag-SET7/9 WT or H297A, U2OS cells were treated with or without 1 mM H_2O_2 for 5 min and PAR formation was analysed by western blot. (*b*) H_2O_2-induced PAR formation was analysed by immunofluorescence in SET7/9 KO and WT MEFs. The intensity of the anti-PAR-stained cells was quantified. (*c*) H_2O_2-induced PAR formation in SET7/9 KO and WT MEFs was analysed as in (*a*). (*d*) U2OS cells were transfected with scrambled siRNA (scr) or siRNA targeting SET7/9. Three days after knockdown, H_2O_2-induced PAR formation was analysed as in (*a*). Short and long exposures (se and le, respectively) of the anti-PAR blot are shown. (*e*) ARTD1 activity was analysed in NEs from U2OS cells after knockdown of SET7/9 and ARTD1 for 3 days by radioactive ADP-ribosylation assays. All experiments were repeated at least twice, gave a similar result, and one representative blot is shown. Quantifications are shown in the electronic supplementary material, figures S3*b* and S4*c*,*d*.

of excess DNA, the methylation-deficient ARTD1 proteins K508A and K508R still exhibited reduced enzymatic activity, but the effect was less pronounced as compared with conditions without exogenous DNA (see figure 4*b* and electronic supplementary material, figure S5*b*), again pointing at a SET7/9 methylation effect on ARTD1 activation.

This indicated that the methylation-deficient ARTD1 mutants (K508A and K508R) are enzymatically less active and provided further evidence that SET7/9-dependent methylation of ARTD1 at K508 affects its activity.

3.5. Mutation of K508 affects ARTD1 recruitment to damaged chromatin

The results described above suggested that SET7/9-dependent methylation of ARTD1 at K508 regulates its enzymatic activity at basal conditions of low levels of DNA damage and in response to oxidative stress (figures 1*c* and 4*b*). We hypothesized that SET7/9-dependent methylation may influence ARTD1 activity by affecting its interaction with chromatin, but SET7/9 downregulation had no effect on the extraction of ARTD1 under different salt concentrations (see electronic supplementary material, figure S5*c*), suggesting that the affinity of ARTD1 to undamaged chromatin was not changed. However, methylation by SET7/9 may prime ARTD1 for efficient recruitment to sites of DNA damage. In order to study whether ARTD1 methylation affects its recruitment to sites of DNA damage *in vivo*, cells expressing EGFP-tagged WT and methylation-deficient ARTD1 were analysed by localized femtosecond laser irradiation [35]. This method allows studying the kinetics of the recruitment of proteins to sites of DNA damage. The nature of the lesion can be influenced via the irradiation wavelength: at 775 nm, both DNA strand breaks and UV photoproducts are generated, while at 1050 nm mainly DNA strand breaks are produced [35]. Irradiation with a wavelength of

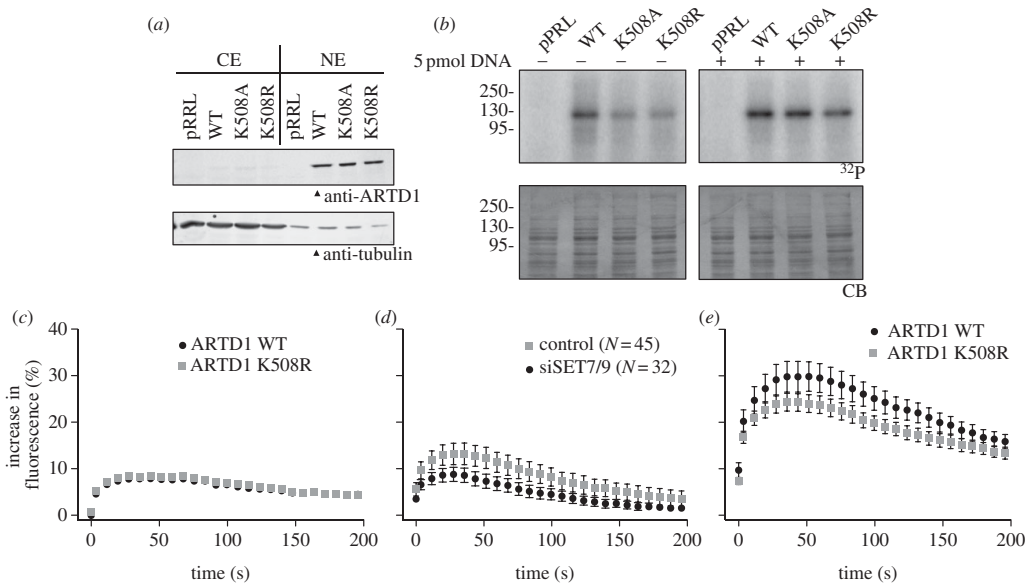

Figure 4. Methylation-deficient ARTD1 is less active and less efficiently recruited to sites of local DNA damage induced by femtosecond laser irradiation. (*a*) ARTD1 knockout MLFs were stably complemented with WT ARTD1 or two methylation-deficient mutants. Cells were then fractionated and CEs and NEs were analysed by western blot. (*b*) ARTD1 activity in NE from (*a*) was analysed by radioactive PAR assays in the absence or presence of 5 pmol-activating DNA. Experiments in A and B were repeated twice with a similar outcome and one representative blot is shown. Quantifications are shown in the electronic supplementary material, figure S5*a*,*b*. (*c*) Recruitment of WT and K508R ARTD1 to sites of local DNA damage induced by femtosecond laser irradiation at $\lambda = 1050$ nm. (*d*) Recruitment of macroH2A1.1-EGFP to sites of local DNA damage induced by femtosecond laser irradiation at $\lambda = 1050$ nm. (*e*) Recruitment of WT and K508R ARTD1 to sites of DNA damage by femtosecond laser irradiation at $\lambda = 775$ nm.

1050 nm caused similar recruitment of WT and K508R ARTD1 (figure 4*c*) and the release of WT and K508R ARTD1 from the irradiated sites was comparable (data not shown), suggesting that methylation did not affect recruitment to sites of DNA damage. However, laser microirradiation of live cells [36] caused significantly lower recruitment of GFP-labelled macroH2A1.1 in siSET7/9 cells as compared with WT (figure 4*d*), which is indicative of reduced PAR synthesis or different ADP-ribose structures. In contrast to irradiation with 1050 nm, femtosecond pulses at $\lambda = 775$ nm caused lower recruitment of the K508R ARTD1 mutant (figure 4*e*). It is thus possible that SET7/9 differentially affects ARTD1 stimulation depending on the stress level and type of induced DNA damage. In summary, these findings show that SET7/9-dependent methylation stimulates ARTD1 enzymatic activity in response to both oxidative and DNA stress.

4. Conclusion

The results presented here suggest that SET7/9 methylates ARTD1 *in vivo* and *in vitro* at lysine K508. The residue K508 was identified as the target site for SET7/9-dependent methylation by site-directed mutagenesis and mass spectrometry, as well as with a specific polyclonal antibody raised against this methylated site. Methylation of ARTD1 by SET7/9 did not prevent its consecutive ADP-ribosylation, but affected ARTD1 recruitment to sites of local DNA damage *in vivo*. Prior auto-ADP-ribosylation of ARTD1 impaired its methylation by SET7/9. Knockdown of SET7/9 or the expression of methylation-deficient ARTD1 in cells lacking WT ARTD1 caused reduced PAR formation *in vitro* and *in vivo*. Moreover, overexpression of SET7/9, but not of its enzymatically inactive mutant enhanced PAR formation in untreated (basal) and H_2O_2-treated cells. These findings identify ARTD1 as a new SET7/9 methylation target and reveal a previously unknown mechanism for the regulation of ARTD1 activity in cells.

The stimulatory effect of ARTD1 methylation on PAR formation was most apparent if no exogenous DNA was added to the reactions that were performed with NEs of SET7/9 knockdown cells or of cells genetically complemented with a methylation-deficient ARTD1 mutant (the NEs may contain low amounts of endogenous DNA). The effect was much weaker under conditions of saturating DNA concentrations (DNA : ARTD1 dimer ratio greater than 1). Methylation by SET7/9 may thus represent a priming step that precedes and facilitates the activation of ARTD1 by DNA or comprises a DNA damage independent ARTD1 co-regulatory mechanism. We have already provided evidence that DNA double strand breaks are recognized and bound by the DBD of ARTD1, which subsequently leads to binding to the CAT domain, induces structural changes within the catalytic cleft, increases the affinity for NAD^+ and stabilizes reaction intermediates [4]. The identified SET7/9-dependent methylation site at K508 of ARTD1 lies within the central AD [4]. It is at the first glance surprising that ARTD1 is methylated in the AD and not in one of the zinc fingers of the DNA-binding domain or in the catalytic domain of ARTD1, but nevertheless affected in its enzymatic activity. However, the AD harbours the ADP-ribose acceptor sites indicating that this domain has to enter the catalytic cleft of ARTD1 to be

subsequently modified. SET7/9-dependent methylation may sensitize ARTD1 for auto-modification by stabilizing the AD in the catalytic domain of ARTD1 under non-genotoxic conditions or in the presence of minimal DNA damage (fewer DNA lesions compared with ARTD1 molecules). Alternatively, methylation might induce structural changes, which affect the binding of the DBD to the CAT, and thus sensitize the enzyme for a special type of DNA damage (see below). Likewise, methylated ARTD1 could exhibit higher affinity for its substrate NAD^+, and therefore show increased catalytic activity. Based on this hypothesis, methylation of ARTD1 at K508 by SET7/9 serves as a sensitization step that assures basal ARTD1 stimulation to assure PAR formation upon oxidative stress. The fact that we observed a similar effect of SET7/9 on the irradiation-induced PAR formation does not necessarily imply a similar regulatory mechanism. However, in order to compare such regulatory mechanisms and to study ARTD1 stimulation by SET7/9 mechanistically, structural analyses would be required.

The AD represents a PTM hotspot that is also modified by ADP-ribosylation, acetylation and sumoylation [2–4]. Interestingly, prior auto-modification of recombinant ARTD1 inhibited subsequent methylation by SET7/9 most probably through steric hindrance (figure 2*a*), which is in agreement with earlier studies providing evidence that the adjacent lysines 498, 521 and 524 are the acceptor sides for ADP-ribose [4]. Similarly, a synthetic ARTD1 peptide acetylated at K508 could not be methylated by SET7/9 (see electronic supplementary material, figure S5*d*). However, the SET7/9-mediated methylation of ARTD1 did not inhibit its auto-ADP-ribosylation, indicating that the methylation would not interfere with the positioning of this domain into the catalytic domain. The functional relevance of this crosstalk needs to be further defined. It is intriguing to speculate that ARTD1 auto-modification would hamper K508 methylation to avoid an additional enhancement of its activity through this modification. Moreover, this could explain the inefficiency of SET7/9-dependent methylation to further activate already stimulated ARTD1 and hints again at a sensitization function of SET7/9 for ARTD1 under non-stimulatory conditions.

The presence of SET7/9 had no influence on the overall affinity of ARTD1 for (undamaged) chromatin *in vivo*. By contrast, different recruitment of WT and K508R ARTD1 to sites of local damage in the nucleus was observed. Interestingly, WT and K508R ARTD1 showed similar recruitment to DNA lesions induced with a wavelength of 1050 nm, while a clear reduction was observed for the mutant after treatment with laser pulses at 775 nm (figure 4*c*,*e*). This effect was likely owing to the UV photoproducts generated at 775 nm or to other differences in the types of lesion induced by 775 nm versus 1050 nm irradiation. The latter wavelength mainly induces DNA strand breaks but achieves a lower overall level of damage than 775 nm at the irradiation conditions used here [35]. Alternatively, a higher affinity for a certain type of lesion or chromatin alteration (qualitative difference) of the methylated ARTD1 protein, as compared with the unmethylated or the non-methylatable mutant, could also contribute to this behaviour.

The methylation of ARTD1 *in vivo* is very difficult to detect. This indicates either low endogenous levels of ARTD1 K508 methylation or further di- and trimethylation at this residue by other methyl transferases. Here, SET7/9 strongly affected ARTD1 activity in the presence of low amounts of DNA and upon stimulation by H_2O_2, although we do not know whether this was due to oxidative damage of the DNA. ARTD1 and its enzymatic activity are also important for chromatin compaction [7,37]. An increased ARTD1 activity might lead to a more open chromatin, allowing subsequent histone modifications (epigenetic events) changing the chromatin status and structure. Furthermore, our studies provide evidence for the involvement of SET7/9 in the oxidative stress response of the cell. Whether SET7/9 is similarly required for the response to other signals (e.g. N-methyl-N′-nitro-N-nitrosoguanidine or phorbol 12-myristate 13-acetate) remains to be investigated. The fact that SET7/9 is not required for cell-cycle arrest or p53 stabilization in mice suggests that the methylation-dependent stimulation of PAR formation is not required for these aspects but serves for other, yet to be identified, signalling pathways. Most importantly, the results presented here may indicate DNA-damage independent induction of ARTD1 activity *in vivo* and suggest that ARTD1 methylation stimulates ADP-ribosylation in response to other cellular stresses that do not necessarily involve DNA damage [5].

5. Material and methods

5.1. Plasmids and protein expression

pGEX-SET7/9 (52–366) and pcDNA3-SET7/9 (full-length/WT and H297A) were kindly provided by D. Reinberg (Howard Hughes Medical Institute, NYU School of Medicine, New York, NY, USA). pcDNA4-Flag-HA-SET7/9 was created by subcloning SET7/9 into pcDNA4. pCMV-HA-PARP1 and pRRL-vectors as described previously [2]. All point mutations were inserted by site-directed mutagenesis. The construct encoding macroH2A-EGFP was kindly provided by A. Ladurner (Department of Physiological Chemistry, Ludwig-Maximilians Universität (LMU) Munich, Munich, Germany).

The baculovirus expression vector BacPak8 (Clontech, Mountain View, CA, USA) was used for the expression of recombinant proteins in Sf21 insect cells, as described previously [38]. Recombinant GST-tagged proteins were expressed in *Escherichia coli*. All recombinant proteins were purified by a one-step affinity chromatography using ProBond resin (Invitrogen, Zug, Switzerland) for His-tagged and glutathione sepharose (GE Healthcare, Zurich, Switzerland) for GST-tagged proteins, according to the manufacturer's recommendations.

5.2. Antibodies and siRNAs

The following antibodies were used for immunoblotting: rabbit PARP-1 (H-250, Santa Cruz, Heidelberg, Germany); rabbit poly(ADP-ribose) (LP96–10, BD Biosciences, Allschwil, Switzerland); rabbit SET7/9 (no. 2815, Cell Signalling); mouse Flag (M2, Sigma-Aldrich, Buchs, Switzerland); mouse tubulin (T6199, Sigma); rabbit PARP (mono methyl K508) (ab92986) was generated in collaboration with Abcam (Cambridge, UK) using a synthetic ARTD1 peptide containing the methylated lysine residue (LSKKSK(me1)GQVKE).

The following FlexiTube siRNAs (QIAGEN, Hombrechtikon, Switzerland) were used in RNAi experiments: AllStars Negative Control, Hs_SET7_3 and Hs_PARP1_6.

5.3. Tissue culture and transfections

U2OS cells were cultured in Dulbecco's modified eagle medium (PAA Laboratories, Pasching, Austria) supplemented with 10% FCS and penicillin/streptomycin. MLFs were cultured in the same medium supplemented in addition with non-essential amino acids (Gibco/Invitrogen). The SET7/9 knockout MEFs were obtained from Colby Zaph and were previously described [26]. Transfections with the indicated plasmids were performed with TransIT-LT1 (Mirus Bio, Madison, WI, USA) according to the manufacturer's instructions and cells were harvested after 48 h. Knockdown was achieved by reverse transfection of 16 nM siRNA using RNAiMAX (Invitrogen) according to the manufacturer's protocol. Cells were harvested after 3 days. Cells were treated with 1 mM H_2O_2 in PBS containing 1 mM $MgCl_2$ for 10 min and with 0.5 µM Adr in normal medium.

Complementation of ARTD1 knockout MLFs was achieved by retroviral transduction with pRRL-myc-PARP1 vectors containing a blasticidine resistance marker or the corresponding empty vector. Generation of viruses and transduction of cells were done as described earlier [39].

5.4. *In vitro* methylation assays

A 1 µg substrate protein was incubated with 1 µg bacterially purified GST-SET7/9 in the presence of 0.03 µCi [^{14}C]-SAM (PerkinElmer) or 0.8 mM cold SAM (Sigma-Aldrich) in methylation buffer (50 mM Tris–HCl pH8.0, 50 mM NaCl, 10% glycerol, 1 mM PMSF and 1 mM DTT) or PAR buffer (see section below) for 1 h at 30°C. Reactions were stopped by boiling in 10× SDS-loading buffer and separated by SDS-PAGE. Gels were stained with Coomassie blue, incubated in 1 M sodium salicylate for 20 min, dried and exposed on X-ray films at −80°C. For mass spectrometric analysis, ARTD1 fragment 373–524 was methylated as described above, separated by SDS-PAGE, excised from the gel and digested with Glu-C. Peptides were analysed by MALDI-MS.

5.5. Sequential *in vitro* modification assays

Sequential ADP-ribosylation and methylation assays were performed in PAR buffer (50 mM Tris–HCl, 4 mM $MgCl_2$, 250 µM DTT, 1 mg ml^{-1} pepstatin, 1 mg ml^{-1} bestatin and 1 mg ml^{-1} leupeptin). A 10 pmol recombinant ARTD1 was methylated with 1 µg recombinant GST-SET7/9 as described above. The ADP-ribosylation was then started by addition of 5 pmol-activating DNA and 400 µM cold NAD^+ (Sigma, after methylation with [^{14}C]-SAM) or 100 µM NAD^+ spiked with [^{32}P]-NAD^+ (Perkin Elmer, after methylation with cold SAM). ADP-ribosylation reactions were incubated for 5 min at 30°C, stopped by addition of 10× SDS-loading buffer and proteins were separated by SDS-PAGE. Hot methylation/ADP-ribosylation was assayed by autoradiography of the Coomassie stained, dried gels, whereas cold modifications were controlled by immunoblotting with the indicated antibodies.

In the reverse experiment, 10 pmol ARTD1 was first incubated with activating DNA and 100 µM NAD^+ for 5 min on ice. 3-AB (Sigma-Aldrich) was added in a concentration of 8 mM to stop the ADP-ribosylation before the methylation was started by addition of 1 µg SET7/9 and [^{14}C]-SAM. The activating DNA used in all assays was an annealed double-stranded oligomer (5′-GGAATTCC-3′). For sequential methylation/acetylation, 1 µg ARTD1 fragment (373–524) was methylated as described above. Acetylation was then started by addition of 20 µl HAT reaction mix (50 mM Tris–HCl pH 8.0, 50 mM NaCl, 10% glycerol, 1 mM DTT, 1 mM sodium butyrate, 1 mM PMSF, 0.5 µg p300 and 75 µM [^{14}C]-AcCoA) and allowed to proceed for 1 h at 30°C.

5.6. Cellular extracts and ARTD1 activity assays

Whole cell extracts were prepared in lysis buffer (50 mM Tris–HCl pH7.5, 400 mM NaCl, 1%Triton and 25 mM NaF), and chromatin fractions were prepared as described elsewhere [40].

NEs from U2OS cells and complemented MLFs were generated as described earlier [41,42]. Five microgram NEs were incubated in 30 µl reaction buffer (50 mM Tris–HCl, 4 mM $MgCl_2$, 1 mg ml^{-1} pepstatin, 1 mg ml^{-1} bestatin, 1 mg ml^{-1} leupeptin and 250 nM [^{32}P]-NAD^+ (0.1–0.2 µCi)) in the absence or presence of 5 pmol-activating DNA for 20 min at 30°C. Proteins were separated by SDS-PAGE, and ADP-ribosylation was analysed by autoradiography. Quantifications were done using the software ImageQuant. Alternatively, ADP-ribosylation assays were performed with cold NAD^+ and modification was assessed by western blotting with anti-PAR antibody.

5.7. Induction of local DNA damage and imaging set-up

Local DNA damage was induced by femtosecond laser irradiation, and recruitment of fluorescently tagged proteins was recorded as described previously using an LSM 5 Pascal confocal microscope [35,43]. Briefly, cells were irradiated with femtosecond laser pulses through a 40× oil immersion lens with a numerical aperture of 1.3 (EC-Plan-Neo-Fluar, Carl Zeiss) along a 6 µm track within the nucleus, followed by fluorescence imaging at 488 nm. The maximum peak irradiance in the focal plane was 330 GW cm^{-2} (pulse duration 200 fs, repetition rate 40 MHz) for excitation at 775 nm and 1200 GW cm^{-2} (pulse duration 85 fs, repetition rate 107 MHz) at 1050 nm. Time series of fluorescence images were quantified with ImageJ (http://rsb.info.nih.gov/ij) as described [43,44].

Acknowledgements. We thank D. Reinberg (Howard Hughes Medical Institute, NYU School of Medicine, New York, NY, USA) for providing SET7/9 plasmids and A. Ladurner (Ludwig-Maximilians Universität München, München, Germany) for the macroH2A1.1-EGFT construct. S. Flott from Abcam is acknowledged for support during the generation of the anti-meARTD1 antibody. C. Zaph (The University of British Columbia, Vancouver, Canada) is acknowledged for sending SET7/9 knockout MEFs. The laser recruitment experiments were carried out with the support of A. Leitenstorfer (University of Konstanz, Germany) as a Euro-BioImaging Proof-of-Concept Study. We are grateful to F. Freimoser and all the members of the Institute of Veterinary Biochemistry and Molecular Biology (University of Zurich, Switzerland) for helpful advice and discussions. The Functional Genomics Center Zurich (FGCZ) is acknowledged for mass spectrometric analyses.

Funding statement. This work was supported by the Swiss National Science Foundation grant no. 310030B-138667 and the Kanton of Zurich (both to M.O.H.).

References

1. Hottiger MO, Hassa PO, Lüscher B, Schüler H, Koch-Nolte F. 2010 Toward a unified nomenclature for mammalian ADP-ribosyltransferases. *Trends Biochem. Sci.* **35**, 208–219. (doi:10.1016/j.tibs.2009.12.003)
2. Messner S, Schuermann D, Altmeyer M, Kassner I, Schmidt D, Schär P, Müller S, Hottiger MO. 2009 Sumoylation of poly(ADP-ribose) polymerase 1 inhibits its acetylation and restrains transcriptional coactivator function. *FASEB J.* **23**, 3978–3989. (doi:10.1096/fj.09-137695)
3. Hassa PO, Haenni SS, Buerki C, Meier NI, Lane WS, Owen H, Gersbach M, Imhof R, Hottiger MO. 2005 Acetylation of poly(ADP-ribose) polymerase-1 by p300/CREB-binding protein regulates coactivation of NF-κB-dependent transcription. *J. Biol. Chem.* **280**, 40 450–40 464. (doi:10.1074/jbc.M507553200)
4. Altmeyer M, Messner S, Hassa PO, Fey M, Hottiger MO. 2009 Molecular mechanism of poly(ADP-ribosyl)ation by PARP1 and identification of lysine residues as ADP-ribose acceptor sites. *Nucleic Acids Res.* **37**, 3723–3738. (doi:10.1093/nar/gkp229)
5. Hassa PO, Haenni S, Elser M, Hottiger MO. 2006 Nuclear ADP-ribosylation reactions in mammalian cells: where are we today and where are we going? *Microbiol. Mol. Biol. Rev.* **70**, 789–829. (doi:10.1128/MMBR.00040-05)
6. Ji Y, Tulin A. 2010 The roles of PARP1 in gene control and cell differentiation. *Curr. Opin. Genet. Dev.* **20**, 512–518. (doi:10.1016/j.gde.2010.06.001)
7. Schreiber V, Dantzer F, Ame J-C, De Murcia G. 2006 Poly(ADP-ribose): novel functions for an old molecule. *Nat. Rev. Mol. Cell Biol.* **7**, 517–528. (doi:10.1038/nrm1963)
8. D'Amours D, Desnoyers S, D'Silva I, Poirier G. 1999 Poly(ADP-ribosyl)ation reactions in the regulation of nuclear functions. *Biochem. J.* **342**, 249–268. (doi:10.1042/0264-6021:3420249)
9. Ueda K, Kawaichi M, Okayama H, Hayaishi O. 1979 Poly(ADP-ribosy)ation of nuclear proteins. Enzymatic elongation of chemically synthesized ADP-ribose-histone adducts. *J. Biol. Chem.* **254**, 679–687.
10. Luo X, Kraus WL. 2012 On PAR with PARP: cellular stress signaling through poly(ADP-ribose) and PARP-1. *Genes Dev.* **26**, 417–432. (doi:10.1101/gad.183509.111)
11. Wang H, Cao R, Xia L, Erdjument-Bromage H, Borchers C, Tempst P, Zhang Y. 2001 Purification and functional characterization of a histone H3-lysine 4-specific methyltransferase. *Mol. Cell* **8**, 1207–1217. (doi:10.1016/S1097-2765(01)00405-1)
12. Brasacchio D *et al.* 2009 Hyperglycemia induces a dynamic cooperativity of histone methylase and demethylase enzymes associated with gene-activating epigenetic marks that coexist on the lysine tail. *Diabetes* **58**, 1229–1236. (doi:10.2337/db08-1666)
13. Deering TG, Ogihara T, Trace AP, Maier B, Mirmira RG. 2009 Methyltransferase Set7/9 maintains transcription and euchromatin structure at islet-enriched genes. *Diabetes* **58**, 185–193. (doi:10.2337/db08-1150)
14. Li Y, Reddy MA, Miao F, Shanmugam N, Yee JK, Hawkins D, Ren B, Natarajan R. 2008 Role of the histone H3 lysine 4 methyltransferase, SET7/9, in the regulation of NF-kappaB-dependent inflammatory genes. Relevance to diabetes and inflammation. *J. Biol. Chem.* **283**, 26 771–26 781. (doi:10.1074/jbc.M802800200)
15. Wang H *et al.* 2001 Methylation of histone H4 at arginine 3 facilitating transcriptional activation by nuclear hormone receptor. *Science* **293**, 853–857. (doi:10.1126/science.1060781)
16. Chuikov S *et al.* 2004 Regulation of p53 activity through lysine methylation. *Nature* **432**, 353–360. (doi:10.1038/nature03117)
17. Kurash J, Lei H, Shen Q, Marston W, Granda B, Fan H, Wall D, Li E, Gaudet F. 2008 Methylation of p53 by Set7/9 mediates p53 acetylation and activity *in vivo*. *Mol. Cell* **29**, 392–400. (doi:10.1016/j.molcel.2007.12.025)
18. Couture JF, Collazo E, Hauk G, Trievel RC. 2006 Structural basis for the methylation site specificity of SET7/9. *Nat. Struct. Mol. Biol.* **13**, 140–146. (doi:10.1038/nsmb1045)
19. Ea C, Baltimore D. 2009 Regulation of NF-κB activity through lysine monomethylation of p65. *Proc. Natl Acad. Sci. USA* **105**, 18 972–18 977. (doi:10.1073/pnas.0910439106)
20. Munro S, Khaire N, Inche A, Carr S, La Thangue N. 2010 Lysine methylation regulates the pRb tumour suppressor protein. *Oncogene* **29**, 2357–2367. (doi:10.1038/onc.2009.511)
21. Pagans S *et al.* 2010 The Cellular lysine methyltransferase Set7/9-KMT7 binds HIV-1 TAR RNA, monomethylates the viral transactivator Tat, and enhances HIV transcription. *Cell Host Microbe* **7**, 234–244. (doi:10.1016/j.chom.2010.02.005)
22. Kouskouti A, Scheer E, Staub A, Tora L, Talianidis I. 2004 Gene-specific modulation of TAF10 function by SET9-mediated methylation. *Mol. Cell* **14**, 175–182. (doi:10.1016/S1097-2765(04)00182-0)
23. Subramanian K, Jia D, Kapoor-Vazirani P, Powell DR, Collins RE, Sharma D, Peng J, Cheng X, Vertino PM. 2008 Regulation of estrogen receptor alpha by the SET7 lysine methyltransferase. *Mol. Cell* **30**, 336–347. (doi:10.1016/j.molcel.2008.03.022)
24. Tao Y, Neppl RL, Huang ZP, Chen J, Tang RH, Cao R, Zhang Y, Jin SW, Wang DZ. 2011 The histone methyltransferase Set7/9 promotes myoblast differentiation and myofibril assembly. *J. Cell Biol.* **194**, 551–565. (doi:10.1083/jcb.201010090)
25. Dhayalan A, Kudithipudi S, Rathert P, Jeltsch A. 2011 Specificity analysis-based identification of new methylation targets of the SET7/9 protein lysine methyltransferase. *Chem. Biol.* **18**, 111–120. (doi:10.1016/j.chembiol.2010.11.014)
26. Lehnertz B, Rogalski JC, Schulze FM, Yi L, Lin S, Kast J, Rossi FM. 2011 p53-dependent transcription and tumor suppression are not affected in Set7/9-deficient mice. *Mol. Cell* **43**, 673–680. (doi:10.1016/j.molcel.2011.08.006)
27. Campaner S, Spreafico F, Burgold T, Doni M, Rosato U, Amati B, Testa G. 2011 The methyltransferase Set7/9 (Setd7) is dispensable for the p53-mediated DNA damage response *in vivo*. *Mol. Cell* **43**, 681–688. (doi:10.1016/j.molcel.2011.08.007)
28. Huang J *et al.* 2007 p53 is regulated by the lysine demethylase LSD1. *Nature* **449**, 105–108. (doi:10.1038/nature06092)
29. Wang J *et al.* 2009 The lysine demethylase LSD1 (KDM1) is required for maintenance of global DNA methylation. *Nat. Genet.* **41**, 125–129. (doi:10.1038/ng.268)
30. Karytinos A, Forneris F, Profumo A, Ciossani G, Battaglioli E, Binda C, Mattevi A. 2009 A novel mammalian flavin-dependent histone demethylase. *J. Biol. Chem.* **284**, 17 775–17 782. (doi:10.1074/jbc.M109.003087)
31. Shi Y, Lan F, Matson C, Mulligan P, Whetstine JR, Cole PA, Casero RA. 2004 Histone demethylation mediated by the nuclear amine oxidase homolog LSD1. *Cell* **119**, 941–953. (doi:10.1016/j.cell.2004.12.012)
32. Lee JS, Smith E, Shilatifard A. 2010 The language of histone crosstalk. *Cell* **142**, 682–685. (doi:10.1016/j.cell.2010.08.011)
33. van Attikum H, Gasser SM. 2009 Crosstalk between histone modifications during the DNA damage response. *Trends Cell Biol.* **19**, 207–217. (doi:10.1016/j.tcb.2009.03.001)
34. Yang X-J, Seto E. 2008 Lysine acetylation: codified crosstalk with other posttranslational modifications. *Mol. Cell* **31**, 449–461. (doi:10.1016/j.molcel.2008.07.002)
35. Trautlein D, Deibler M, Leitenstorfer A, Ferrando-May E. 2010 Specific local induction of DNA strand breaks by infrared multi-photon absorption. *Nucleic Acids Res.* **38**, e14. (doi:10.1093/nar/gkp932)
36. Timinszky G *et al.* 2009 A macrodomain-containing histone rearranges chromatin upon sensing PARP1 activation. *Nat. Struct. Mol. Biol.* **16**, 923–929. (doi:10.1038/nsmb.1664)
37. Krishnakumar R, Kraus W. 2010 PARP-1 regulates chromatin structure and transcription through a KDM5B-dependent pathway. *Mol. Cell* **39**, 736–749. (doi:10.1016/j.molcel.2010.08.014)
38. Hassa PO, Buerki C, Lombardi C, Imhof R, Hottiger MO. 2003 Transcriptional coactivation of nuclear factor-κB-dependent gene expression by p300 is regulated by poly(ADP)-ribose polymerase-1. *J. Biol. Chem.* **278**, 45 145–45 153. (doi:10.1074/jbc.M307957200)
39. El-Andaloussi N *et al.* 2006 Arginine methylation regulates DNA polymerase β. *Mol. Cell* **22**, 51–62. (doi:10.1016/j.molcel.2006.02.013)
40. Todorov IT, Attaran A, Kearsey SE. 1995 BM28, a human member of the MCM2–3–5 family, is displaced from chromatin during DNA replication.

J. Cell Biol. **129**, 1433–1445. (doi:10.1083/jcb.129.6.1433)

41. Felzien LK, Woffendin C, Hottiger MO, Subbramanian RA, Cohen EA, Nabel GJ. 1998 HIV transcriptional activation by the accessory protein, VPR, is mediated by the p300 co-activator. *Proc. Natl Acad. Sci. USA* **95**, 5281–5286. (doi:10.1073/pnas.95.9.5281)
42. Perkins ND, Agranoff AB, Duckett CS, Nabel GJ. 1994 Transcription factor AP-2 regulates human immunodeficiency virus type 1 gene expression. *J. Virol.* **68**, 6820–6823.
43. Camenisch U, Trautlein D, Clement FC, Fei J, Leitenstorfer A, Ferrando-May E, Naegeli H. 2009 Two-stage dynamic DNA quality check by xeroderma pigmentosum group C protein. *EMBO J.* **28**, 2387–2399. (doi:10.1038/emboj.2009.187)
44. Clement FC, Kaczmarek N, Mathieu N, Tomas M, Leitenstorfer A, Ferrando-May E, Naegeli H. 2011 Dissection of the xeroderma pigmentosum group C protein function by site-directed mutagenesis. *Antioxid. Redox Signal.* **14**, 2479–2490. (doi:10.1089/ars.2010.3399)

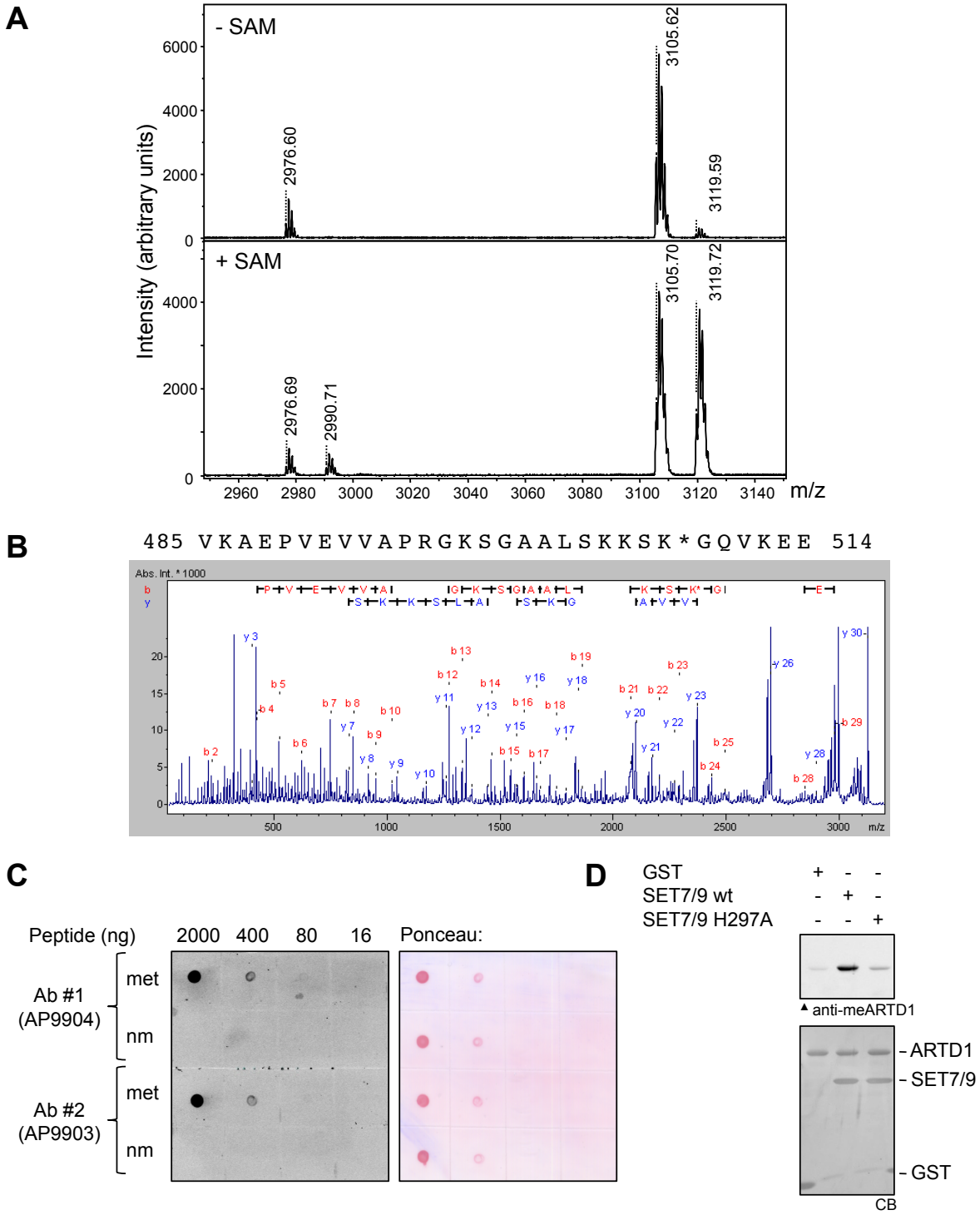

Supplementary Figure 1. (A) Mass spectrometric analysis of recombinant ARTD1 (373-524) incubated with SET7/9 in presence and absence of SAM. (B) MS/MS scan of ion with m/z 3119.72 according to ARTD1 peptide 485 – 514 identifying lysine 508 as the methylated residue. (C) Dot blot with ARTD1 peptides (503-513) not methylated (nm) and methylated (met) at K508 at the indicated concentrations. Two different antibody batches were tested. (D) Validation of a peptide specific antibody directed against monomethylated K508 in ARTD1. A specific signal for K508 ARTD1 methylation was observed upon *in vitro* methylation with WT SET7/9.

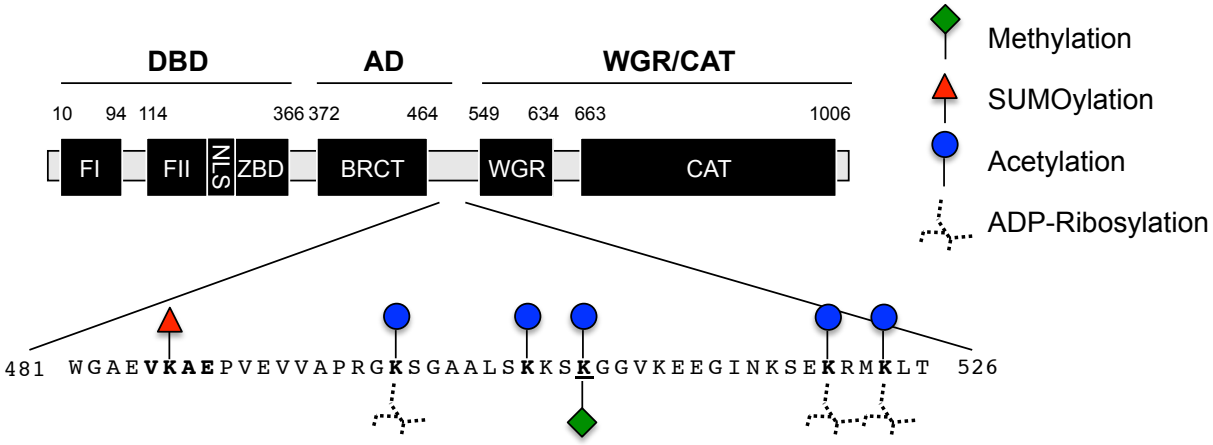

Supplementary Figure 2. Schematic representation of the ARTD1 domain structure and the important methylation, sumoylation, acetylation and ADP-ribosylation sites in the automodification domain of ARTD1.

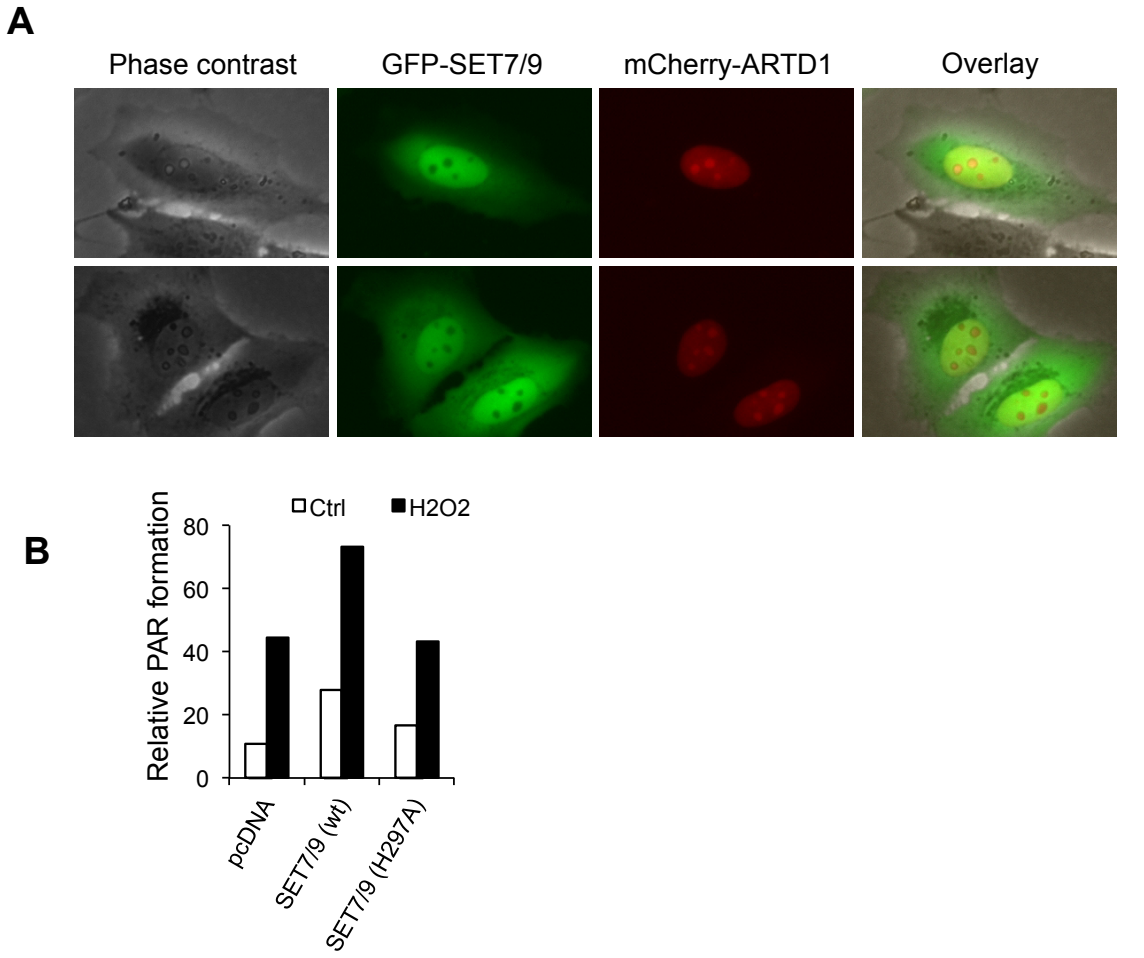

Supplementary Figure 3. (A) U2OS cells expressing GFP-tagged SET7/9 and mCherry-tagged ARTD1 were analyzed by fluorescence microscopy. (B) H_2O_2-induced PAR formation was quantified after overexpression of Flag-SET7/9 WT or H297A. The corresponding western blot is shown in Fig. 3A. (C) WT and SET7/9 KO MEFs were treated for 10 min with 1 mM H_2O_2 and PAR formation was analyzed by immunofluorescence.

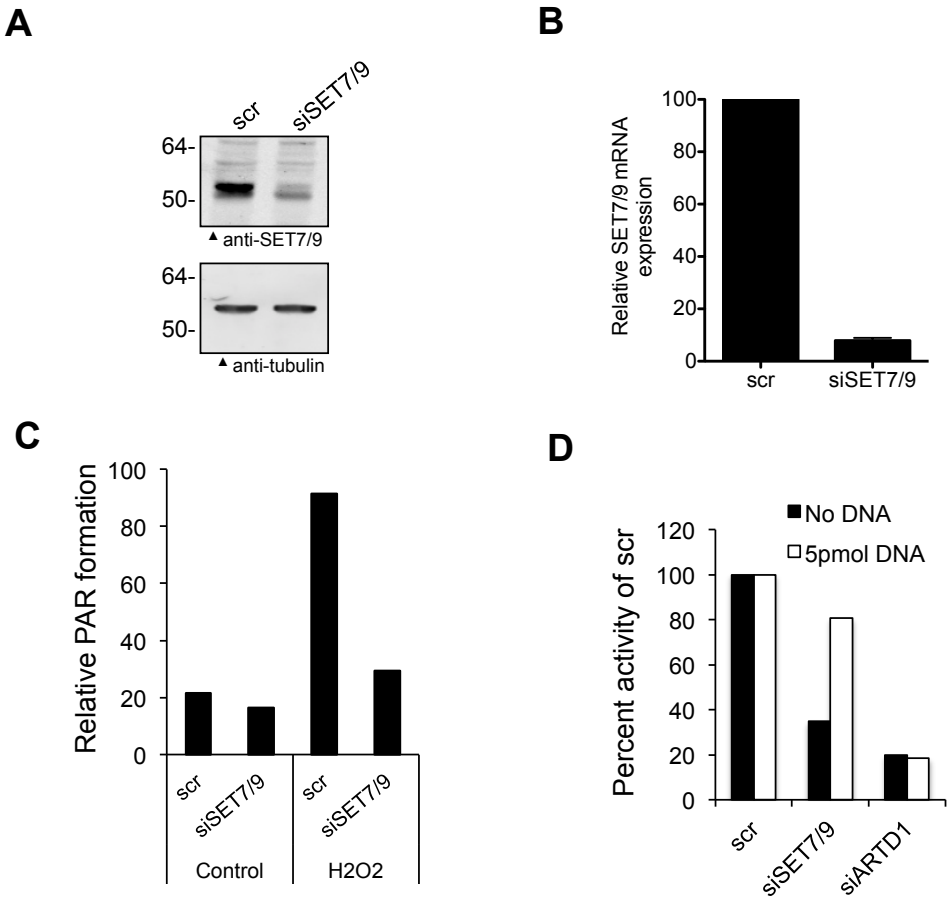

Supplementary Figure 4. (A) U2OS cells were transfected with scrambled siRNA (scr) or siRNA targeting SET7/9. (B) Effect of SET7/9 depletion by siRNA treatment on SET7/9 mRNA levels. The mean of three quantifications and the standard error of the mean are shown. (C-D) U2OS cells were transfected with scrambled siRNA (scr) or siRNA targeting SET7/9. Quantifications of blots shown in Figs. 3D-E. (C) Three days after knockdown, the cells were treated with or without 1 mM H_2O_2 for 5 min and PAR formation was quantified. (D) ARTD1 activity was quantified in nuclear extracts from U2OS cells after knockdown of SET7/9 and ARTD1 for three days.

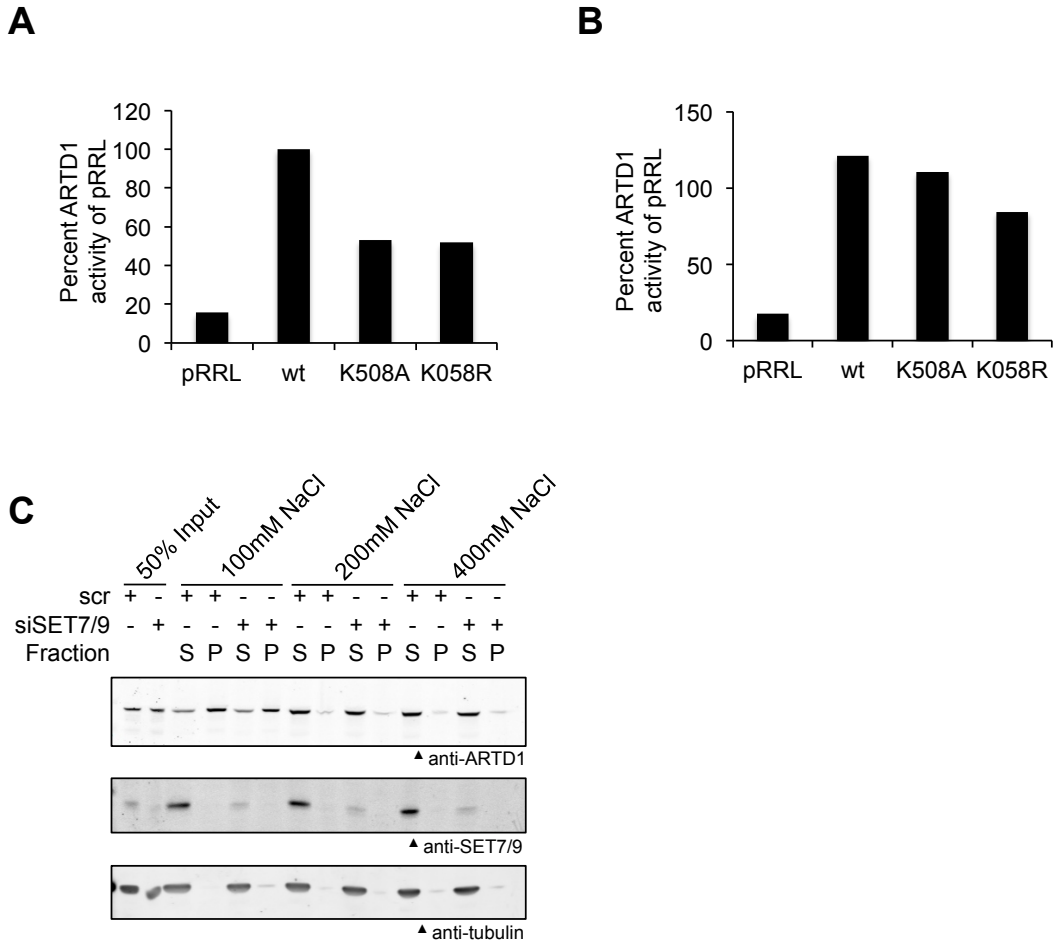

D

Detected modification	Exp. mass	-Ac -SET7/9	-Ac +SET7/9	+Ac -SET7/9	+Ac +SET7/9
None	1548	+	+	-	-
Mono-met	1562	-	+	-	-
Acetyl x3	1674	-	-	+	+
Ac + Met	1688	-	-	-	-

Supplementary Figure 5: (A-B) ARTD1 knockout MLFs were stably complemented with WT ARTD1 or two methylation deficient mutants. Cells were then fractionated and cytoplasmic (CE) and nuclear extracts (NE) were analyzed. Quantifications of western blots shown in Fig. 4B. (A) ARTD1 activity in NE was analyzed by radioactive PAR assay. (B) ARTD1 activity in NE from complemented MLFs as in (A) but in presence of 5 pmol activating DNA. (C) After SET7/9 depletion for three days, ARTD1 affinity to chromatin was tested at different sodium chloride (NaCl) concentrations and analyzed by Western blot. S: supernatant, P: pellet = chromatin bound. (D) Methylation experiment with an ARTD1 peptide and consecutive MS analysis. A synthetic ARTD1 peptide was non-acetylated or acetylated and in vitro methylated with SET7/9. Modifications were detected by MS. Only the non-acetylated peptide was monomethylated in the presence of SET7/9.

5

3.3 Unpublished results

3.3.1 H_2O_2-induced, but not basal PAR formation is dependent on Ca^{2+}

Ca^{2+} has been shown to be important for the induction of PAR formation, something we confirmed upon 10 min H_2O_2 treatment in the manuscript "PKCα controls oxidative stress-induced poly-ADP-ribose formation by phosphorylating HMGB1" [92, 93]. To study whether basal levels of PAR are also dependent on calcium, we pre-treated HeLa-cells with the calcium chelator BAPTA-AM, followed by 10 min of H_2O_2. Basal levels of PAR could be detected in HeLa cells by immunofluorescence (IF), using a different antibody (enzo) than in the manucscript, and the levels were strongly increased upon 10 min of H_2O_2 (Figure 6a,b). Interestingly, the basal PAR formation, which can be reduced by PARPi, was not changed upon treatment with BAPTA-AM. In contrast, the H_2O_2-induced PAR was reduced to basal levels in the presence of BAPTA-AM, suggesting that a calcium-dependent induction of PAR was specifically observed only upon H_2O_2 treatment.

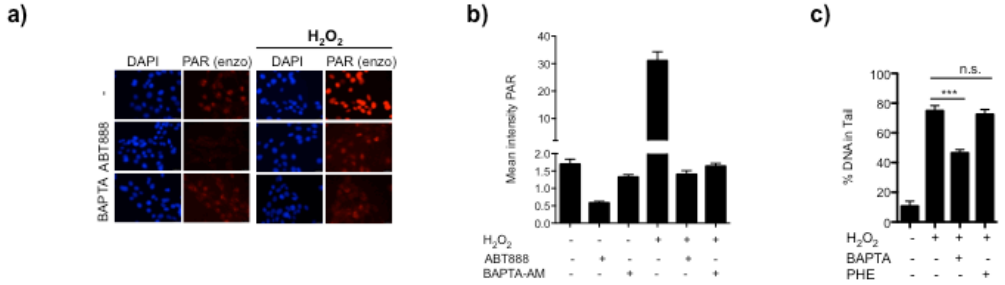

Figure 6. Calcium-induced PAR-formation. a) HeLa cells were pre-incubated with 10 µM ABT888 or 10 µM BAPTA-AM for 60 min, followed by 0.1 mM H_2O_2 for 10 min. IF was performed using anti-PAR (enzo). **b)** Intensity from a) quantified using ImageJ. **c)** MEFs were pre-incubated for 30 min with 5 µM BAPTA-AM or 5 µM 1,10-phenanthroline, followed by 0.1 mM H_2O_2 for 10 min. An alkaline comet assay was performed to visualize DNA-breaks and AP-sites (lesions), 75 comets/condition was quantified. n.s $p>0.05$, *$p<0.05$, **$p<0.01$, ***$p<0.001$, +/- SEM.

It has been suggested that BAPTA-AM could directly inhibit the transition metal ion-mediated Fenton reaction at the site of DNA, and thereby reduce the H_2O_2-induced DNA lesions, which would lead to a reduction of PAR formation [226]. To exclude this, we incubated mouse embryonic fibroblasts (MEFs) with BAPTA-AM or the iron/copper-chelating agent 1,10-phenanthroline (PHE), followed by H_2O_2-treatment (Figure 6c). We performed an alkaline comet assay and could observe an increase of DNA lesions upon H_2O_2, which could be significantly reduced by BAPTA-AM, but not by PHE. These results strongly suggest that the DNA lesions observed upon H_2O_2 treatment are not due to iron or copper, but are dependent on H_2O_2-induced calcium release and a yet to be defined mechanism.

3.3.2 OGG1 and APE1 do not play a role in H_2O_2-induced PAR formation

The role of Ca^{2+} in the induction of DNA breaks upon H_2O_2 treatment could not only be due to direct breaks on the DNA backbone, but also be mediated by Ca^{2+}-dependent DNA-glycosylases and endonucleases due to the oxidatively damaged bases [1, 4]. The most studied DNA-glycosylase, OGG1, is Ca^{2+}-dependent and has been shown to interact with ARTD1 upon oxidative damage [227]. To investigate whether OGG1 is involved in H_2O_2-induced DNA lesions, OGG1 KO and wt MEF were treated with H_2O_2 for 10 min. Using the alkaline comet assay, only a minor reduction of DNA lesions could be observed in the OGG1 KO MEFs as compared to wt MEFs (Figure 7a). Although, when depleting OGG1 of MEFs using siRNA, no difference as compared to the MEFs treated with scrambled siRNA (siMock) in H_2O_2-induced DNA lesions was observed. To investigate whether the AP-lyase APE1 is involved in H_2O_2-induced DNA lesions, *Ape1* was knocked down in MEFs, followed by treatment with H_2O_2, but no decrease in DNA lesions could be observed (Figure 7b). However, this does not rule out an involvement of OGG1 and APE1 in the

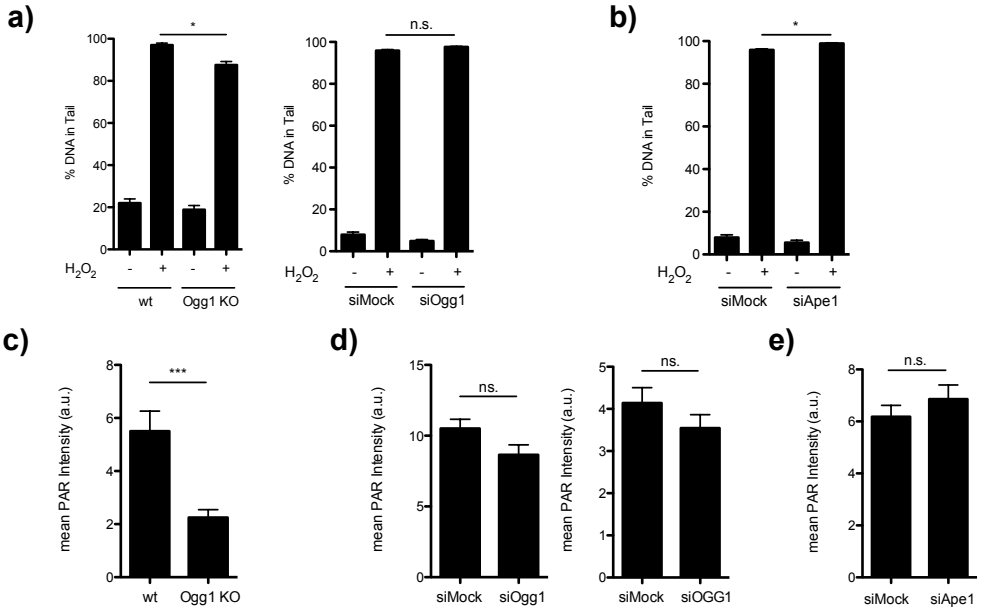

Figure 7. H_2O_2-induced DNA lesions and PAR-formation upon KO or kd of DNA-glycosylases or AP-lyases. **a)** Alkaline comet assay in OGG1 KO and wt MEFs *(left)* or MEFs transfected with siRNA against *Ogg1* or mock, treated with 0.1 mM H_2O_2 for 10 min. **b)** Performed as in a), using siRNA against *Ape1* in MEFs. **c)** OGG1 KO and wt MEFs were treated with 0.1 mM H_2O_2 for 10 min, before fixed with methanol/acetic acid and immunostained with anti-PAR (10H). **d)** siRNA-mediated knockdown of *Ogg1* in MEFs (*left)* and MRC-5 cells *(right)*, was followed by 0.5 mM H_2O_2 for 10 min, 48 h post-transfection. IF as in c). **e)** Performed as in d) using siRNA against *Ape1* in MEFs. PAR intensity was quantified using ImageJ. *p<0.05, **p<0.01, ***p<0.001, +/- SEM.

induction of PAR formation. To further investigate that, we treated OGG1 KO and wt MEF with H_2O_2 and measured the intensity of PAR using IF. An attenuated PAR formation could be observed in OGG1 KO, as compared to that in the wt MEFs

(Figure 7c). Although, when knocking down OGG1 in MEFs using siRNA, no difference as compared to the MEFs treated with scrambled siRNA (siMock) in H_2O_2-induced PAR formation could be observed (Figure 7d). The same was observed when knocking down OGG1 in the human cell line MRC-5, suggesting that the transient removal of OGG1 is not sufficient to reduce H_2O_2-induced PAR formation. Thus, another mechanism must be responsible for the H_2O_2-induced PAR formation. Furthermore, the influence of APE1 on H_2O_2-induced PAR formation was addressed by knocking down APE1 in MEFs, followed by treatment with H_2O_2. However, PAR formation was equally increased in siApe1 and siMock-treated MEFs, showing that APE1 is also not involved in H_2O_2-induced PAR formation (Figure 7e). This indicates that the breaks induced upon H_2O_2 are possibly caused by other DNA-glycosylases or endonucleases.

3.3.3 XPF, XPG, FEN1 and FAN1 do not play a role in H_2O_2-induced PAR formation.

ARTD1 has also been described to bind nicked DNA and single-stranded overhangs, and its involvement in stalled replication fork resolution and homologous recombination (HR) has been suggested [54, 95, 228]. Several endonucleases that recognize structural DNA features and are involved in other repair pathways than BER could potentially be involved in H_2O_2-induced PAR formation. We therefore performed knockdown of XPF (cleaves 3' flaps), XPG, FEN1 and FAN1 (cleaves 5' flaps) [229-231] in MEFs, and subsequently treated them with H_2O_2. No influence on H_2O_2-induced PAR formation could be observed upon knockdown of these factors, as compared to siMock (Figure 8a), indicating that XPF, XPG, FEN1 and FAN1 do not play a role in H_2O_2-induced PAR formation. MUS81 is an endonuclease involved in HR, and resolves D-loops and Holliday junctions [229]. Upon knockdown of MUS81,

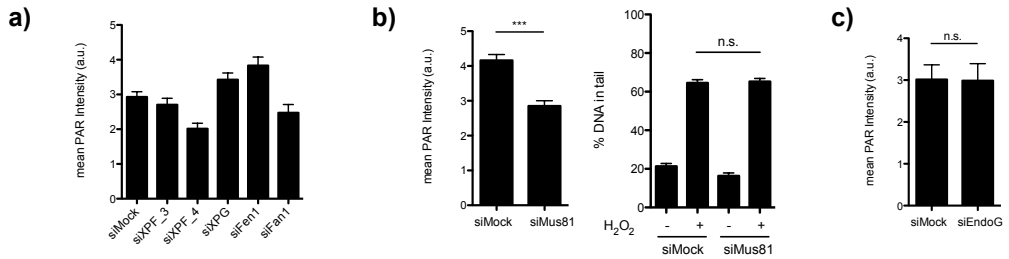

Figure 8. H_2O_2-induced PAR-formation and DNA lesions after knockdown of endonucleases. a) MEFs were transfected with siRNA against XPF, XPG, FEN1, FAN1, or mock. After 48 h MEFs were treated with 0.5 mM H_2O_2 for 10 min, before fixed with methanol/acetic acid and immunostained with anti-PAR (10H). **b)** Performed as in a), using siRNA against MUS81. Alkaline comet assay performed in MEFs transfected with siRNA against MUS81, after treatement with 0.1 mM H_2O_2 for 10 min. **c)** Performed as in a) using siRNA against EndoG. PAR intensity was quantified using ImageJ. n.s. $p>0.05$, *$p<0.05$, **$p<0.01$, ***$p<0.001$, +/- SEM.

a weakly attenuated PAR formation upon H_2O_2 was detected, as compared to siMock, although no effect was seen on the DNA lesions (Figure 8b), suggesting that MUS81 is not involved in H_2O_2-induced DNA lesion formation.

The endonuclease G (EndoG) is located in the mitochondrial intracellular space, and translocates to the nucleus upon oxidative stress to mediate apoptosis [232]. To investigate the role of EndoG in H_2O_2-induced PAR formation, we knocked it down in MEFs, followed by H_2O_2 treatment. The knockdown showed no effect on PAR formation, as compared to siMock (Figure 8c), suggesting that EndoG is not involved in the regulation of H_2O_2-induced PAR formation.

Together, these results provide evidence that out of the tested endonucleases, only MUS81 influences H_2O_2-induced PAR formation, and interestingly, the levels of H_2O_2-induced PAR formation cannot be directly correlated to the levels of H_2O_2-induced DNA lesions, since none of the tested enzymes affected DNA tail formation.

3.3.4 Knockdown of NEIL3 leads to attenuated H_2O_2-induced PAR formation

Four other DNA-glycosylases are also known to remove oxidative damaged bases. NTH1 and NEIL1-3, from which NEIL1 and NTH1 have a very overlapping lesion-recognition, and the lack of NEIL1 has been shown to reduce oxidative stress-induced PAR formation [1, 233]. We therefore chose to investigate the role of NEIL1-3 in H_2O_2-induced PAR formation. Interestingly, when NEIL1, NEIL2 or NEIL3 were knocked down by siRNA in MEFs and cells subsequently treated with H_2O_2, no effect was observed for siNeil1 and siNeil2, but an attenuated PAR formation could be observed in siNeil3 MEFs, as compared to siMock (Figure 9a). However, the induced DNA lesions were unchanged upon knockdown of NEIL3, suggesting that NEIL3 influences H_2O_2-induced PAR formation, but not through the regulation of DNA

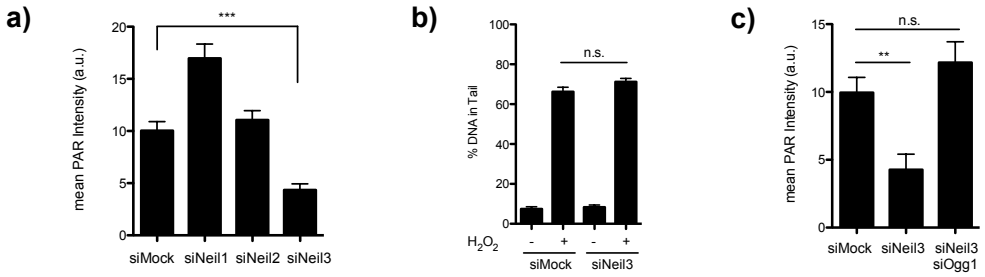

Figure 9. H_2O_2-induced PAR-formation and DNA lesions upon knockdown of Neil1-3. a) MEFs transfected with siRNA against *Neil1*, *Neil2* and *Neil3*. were treated with 0.1 mM H_2O_2 for 10 min, before fixed with methanol/acetic acid and immunostained with anti-PAR (10H). **b)** Alkaline comet assay in MEFs transfected with siRNA against *Neil3* or mock, treated with 0.1 mM H_2O_2 for 10 min. **c)** Performed as in a) using siRNA against *Neil3* and *Ogg1*.

lesions (Figure 9b). To investigate whether the different DNA-glycosylases compensate for each other, a combination of knockdowns was performed, using siRNA against *Ogg1* and *Neil1-3*. Unfortunately, aiming at knocking down all four proteins reduced the knockdown efficiency tremendously and no relevant results were obtained (data not shown). One exception was the double knockdown of OGG1 and NEIL3, which showed a good efficiency, but surprisingly resulted in an increase in H_2O_2-induced PAR formation, as compared to NEIL3 knockdown alone (Figure 9c). This suggests that the knockdown of OGG1 rescues the reduced levels of H_2O_2-induced PAR formation caused by knockdown of NEIL3 and that these two proteins functionally interact. Taken together, NEIL3 is important for optimal PAR formation upon oxidative stress, although the NEIL3-dependent excision of oxidative lesions does not seem to be responsible for the observed effect on PAR formation.

3.3.5 Ionomycin induces PAR formation in a Ca^{2+}-dependent, but DNA-independent manner

Considering the major influence of calcium on PAR formation after H_2O_2-treatment, we were wondering if increased Ca^{2+} levels alone could activate PAR formation and if so, whether ARTD1 is the main responsible enzyme. To increase intracellular levels of Ca^{2+} in an H_2O_2-independent manner, we treated MEFs with the ionophore ionomycin. An induction of PAR formation upon ionomycin could be observed. To determine whether the induced PAR formation was ARTD1 dependent, we knocked down ARTD1 before we performed the same experiment. Knockdown of ARTD1 completely abrogated PAR formation upon ionomycin treatment (Figure 10a,b). This suggests that increased levels of intracellular Ca^{2+} lead to the activation of ARTD1.

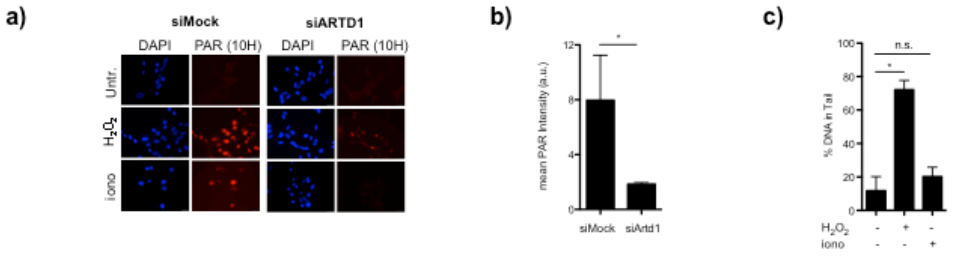

Figure 10. Ionomycin-induced PAR-formation. a) MEFs were transfected with ARTD1 siRNA or with a mock control, and 48 h after transfection incubated with either 0.5 mM H_2O_2 or 1 µM ionomycin for 10 min in FCS-free medium containing 3.6 mM Ca^{2+}. IF was performed using anti-PAR (10H). **b)** Quantification of the ionomycin induced PAR-formation in b). **c)** Alkaline comet assay of MEFs treated with 0.1 mM H_2O_2 or 1 µM ionomycin for 10 min. n.s. $p>0.05$, *$p<0.05$, **$p<0.01$, ***$p<0.001$, +/- SEM.

To investigate if the enhanced Ca^{2+} levels could activate ARTD1 in a DNA damage-independent manner, we performed an alkaline comet assay with ionomycin-treated cells. There was no significant induction of DNA lesions upon treatment with ionomycin (Figure 10c), suggesting that ionomycin-induced PAR formation is independent of DNA lesions.

3.3.6 ARTD1 in lysates from wild-type cells is activated by lysates from ARTD1 knockout cells

Several publications have described how stimulation-induced modification of ARTD1 or protein interactions can activate ARTD1, in a DNA-independent manner [96, 97, 141]. We intended to investigate whether upon 10 min of H_2O_2 treatment, a nuclear soluble signal is induced, which DNA-independently activates ARTD1 *in vitro*. By adding nuclear extracts (NEs) from H_2O_2-treated ARTD1 KO MEFs to NEs from untreated wt MEFs, we could study the activation of ARTD1 *in vitro*. NEs from untreated or H_2O_2-treated MEFs were pre-incubated with DNase I to digest potential contaminating DNA fragments, subsequently incubated with NAD^{p32}, and analyzed by autoradiography. No ADP-ribosylation activity was detected in the NEs from untreated wt MEFs, but was strongly induced in NEs from H_2O_2-treated wt MEFs presumably in an ARTD1-dependent manner, since no ADP-ribosylation was detected in NEs from ARTD1 KO MEFs (Figure 11a). Surprisingly, ARTD1 in NEs from untreated wt MEF was activated upon co-incubation with ARTD1 KO NEs, independent of H_2O_2 treatment (Figure 11b).

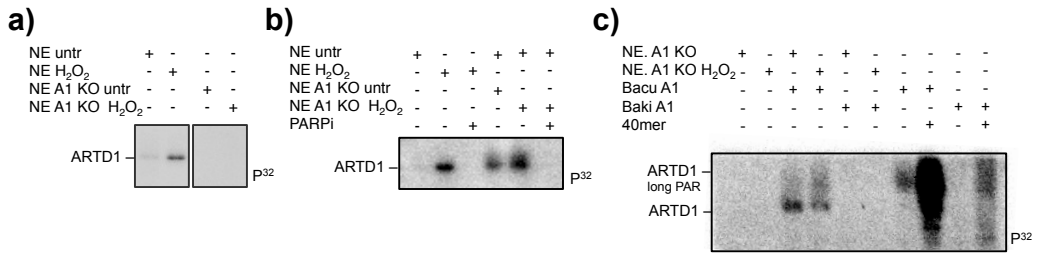

Figure 11. ARTD1 activity in nuclear extracts. a) ARTD1 KO and wt MEFs were treated with 0.5 mM H_2O_2 for 10 min or left untreated, before harvested. Nuclear extracts were prepared and 10 ug extract incubated *in vitro* with NAD^{p32}, before exposed on a phosphoscreen for autoradiographic analysis. **b)** Performed as in a). *In vitro* assay performed in the presence or absence of PARPi ABT888. **c)** Performed as in a), in the presence or absence of Bacu ARTD1, Baki ARTD1 and activating DNA (40mer).

To rule out that the observed activation of ARTD1 could be due to a DNA contamination, the wt NEs were substituted with recombinant ARTD1, purified either from baculo (Bacu A1) or bacterial cells (Baki A1). Even though both of the

recARTD1s were activated upon addition of DNA, only the bacu A1 was activated by the NEs (Figure 11c), indicating a DNA-independent mode of activation by the NEs of ARTD1 KO MEFs.

3.3.7 Inhibition of HDAC and MSK1 does not affect H_2O_2-induced PAR formation

It has recently been reported that acetylation and phophorylation of histone H2A can positively influence PAR formation [138]. To investigate whether the acetylation of histones is involved in the H_2O_2-induced PAR formation, we pre-incubated MEFs with HDAC inhibitors before treating with H_2O_2 for 10 min (Figure 12a). We detected a marked increase in nuclear acetyl-lysine upon HDAC inhibitor, but the PAR formation was comparable before to the tested condition, suggesting that histone hyperacetylation does not influence H_2O_2-induced PAR formation.

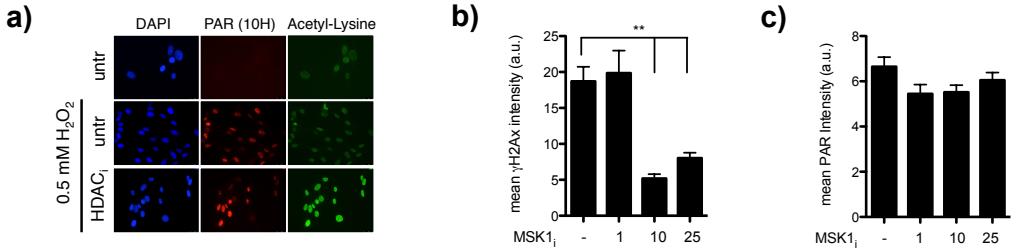

Figure 12. a) MEFs were pre-incubated for 1 h with 1 µM $HDAC_i$ (TSA), followed by 0.5 mM H_2O_2 for 10 min. Immunofluorescent staining was performed using anti-PAR (10H) and anti-AcetylLysine (pan). **b)** MEFs were incubated with 1, 10 or 25 µM $MSK1_i$ (H-89) for 30 min before treated with 0.5 mM H_2O_2 for 60 min. Cells were fixed in Methanol Acetic acid and stained against γH2AX. **c)** performed as in b), but only 10 min H_2O_2 treatment and stained against PAR (10H). Intensity measured using ImageJ. n.s. $p>0.05$, *$p<0.05$, **$p<0.01$, ***$p<0.001$, +/- SEM.

To investigate a possible role of MSK1-mediated histone phosphorylation on H_2O_2-induced PAR formation, we incubated MEFs with the MSK1 inhibitor H-89 before treating them with H_2O_2. The inhibition of MSK1 was efficient, as measured by the MSK1 target γH2AX phophorylation (Figure 12b), but had no influence on the H_2O_2-induced PAR formation (Figure 12c), indicating that the H_2O_2-induced phosphorylation of γH2AX by MSK1 does not regulate H_2O_2-induced PAR formation.

3.3.8 ARTD1 ADP-ribosylates HMGB1 between amino acid 121-126

Several groups have described HMGB1 to be ADP-ribosylated by ARTD1 [36, 186], although, a modification site was so far not identified and the role of other ARTDs not investigated. Knowing the ADP-ribosylation site on HMGB1 would allow further investigations regarding the physiological function of ADP-ribosylated HMGB1. To investigate whether another nuclear ARTD beside ARTD1, such as ARTD2, or a

MARylating ARTD, ARTD10, would modify HMGB1, an *in vitro* ADP-ribosylation assay was performed using purified recombinant protein. ARTD1, 2 or 10, was incubated with HMGB1, and NAD^{p32}, and further analyzed by autoradiography (Figure 13a). Only ARTD1, but not ARTD2 and ARTD10, modified HMGB1 under the tested conditions.

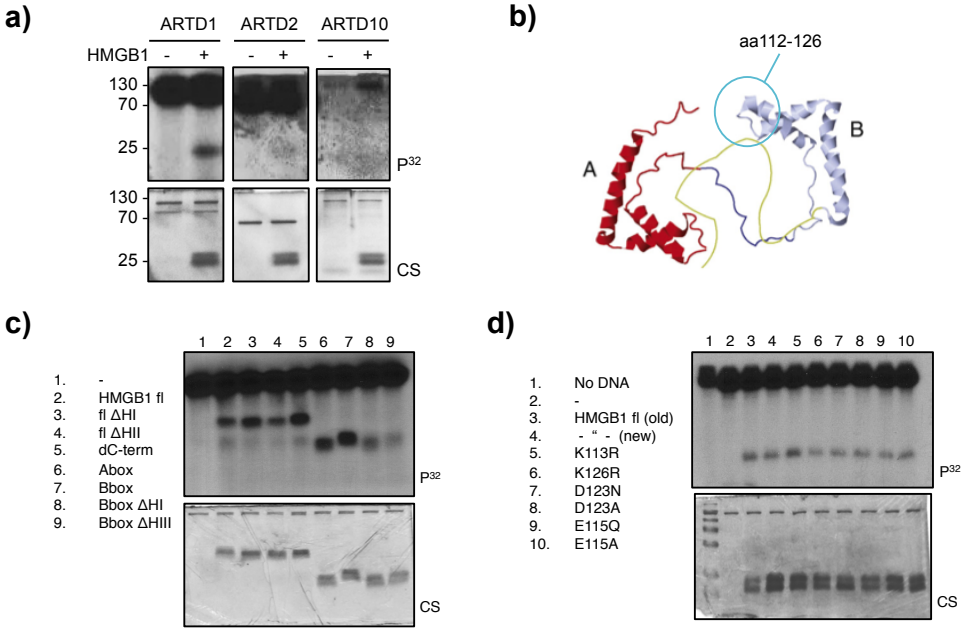

Figure 13. ARTD1-dependent ADP-ribosylation of HMGB1. a) *In vitro* ADP-ribosylation assay. Recombinant ARTD1, ARTD2 or ARTD10 was incubated with HMGB1 and NAD^{p32}. ARTD1 was incubated in the presence of activating DNA (40mer) for 15 min at 30°C. ARTD2 and ARTD10 was incubated for 1h at 30°C. **b)** The 3D structure of HMGB1. A-box in red, B-box in purple and the C-tail oin green. The localization of the peptide identified by MS-analysis is circled in blue. [153] **c)** *In vitro* ADP-ribosylation assay. ARTD1, NAD^{p32} and 40mer was incubated together with fl HMGB1, HMGB1 fragments or HMGB1 deletion mutatants for 15 min at 30°C. **d)** Performed as in c), using HMGB1 containing point-mutations at indicated amino acids.

Using mass spectrometry methods recently developed by our group, modified HMGB1 was detected from *in vitro* ADP-ribosylation assay, as well as in lysates from cells treated with H_2O_2. Several ADP-ribosylated peptides were found, and the most abundantly detected ADP-ribsoylated peptide was matched to the DNA-intercalating sequence on the B-box of HMGB1, between amino acids (aa) 112-126 (Figure 13b [153]). We deleted parts of this sequence, either the last five aa in helix I (ΔHI), or the first six aa in the helix II (ΔHII), in the full-length (fl) HMGB1 or in the B-box alone. Using these constructs, in parallel with fl HMGB1, HMGB1 lacking the C-terminal, and the A-box and B-box alone, we performed an *in vitro* ADP-ribosylation assay (Figure 13c). An increased modification of HMGB1 lacking the C-terminal tail was observed (lane 5), likely due to better accessibility to the modification site. Both the A-box and B-box were modified by ARTD1 *in vitro*, although the signal was stronger for the B-box (lane 6 and 7). While the fl ΔHI

mutant (lane 3) showed no significant difference in modification compared to fl wt, a partial reduction of HMGB1 modification could be observed in the fl ΔHII mutant (lane 4) and an even stronger reduction for the B-box ΔHII mutant (lane 9). These data indicate that HMGB1 was mainly modified between aa 121-126, but has additional acceptor sites *in vitro*. To investigate whether any of the known ARTD1 acceptor sites in the identified peptide (K, E or D) is the main site of ADP-ribosylation of HMGB1, six different point mutations were generated and subsequently modified by ARTD1 in the presence of NAD^{p32}. The strongest reduction of ADP-ribosylation was observed with the K126R mutant (lane 6) confirming our previous findings that the main modification-site of HMGB1 resides within aa121-126 (Figure 13d). This indicates that several ADP-ribosylation acceptor sites of HMGB1 are modified by ARTD1 *in vitro*, and K126 seems to be the major acceptor site.

3.3.9 ARTD1 regulates HMGB1 nuclear release upon LPS, but not upon H_2O_2 treatment

Next, we investigated if ARTD1 and HMGB1 interact also *in vivo*, and whether this interaction is H_2O_2-dependent. We overexpressed HA-ARTD1 and GFP-HMGB1 in HEK293 cells and performed an immunoprecipitation (IP) anti-HA with nuclear extracts from untreated or H_2O_2-stimulated cells (Figure 14a). An interaction between ARTD1 and HMGB1 could be observed in the untreated cells, however the interaction was lost upon H_2O_2 treatment (lane 11 and 12), suggesting that ARTD1 and HMGB1 interact *in vivo*, but that H_2O_2 treatment abolishes that interaction. ARTD1-dependent nuclear release of HMGB1 has been described in several recent publications, upon different stimuli such as LPS, MNNG and H_2O_2 [36, 187, 188]. To confirm these data, we pre-incubated RAW 264.7 cells (RAWs) with olaparib before treatment for 16 h with LPS followed by 3 h with ATP. The supernatant of the cells was collected, concentrated and subsequently analyzes by WB. In this setting, we could detect HMGB1 released into the medium in an ADP-ribosylation-dependent manner (i.e. reduced by PARPi) (Figure 14b). This suggests that ADP-ribsylation is indeed required for the LPS/ATP-induced release of HMGB1.

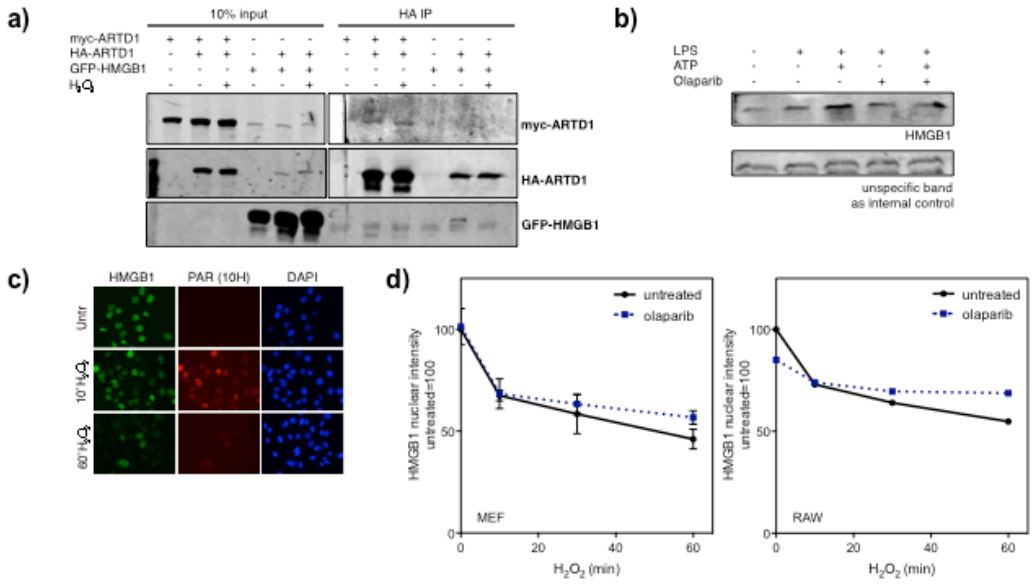

Figure 14. LPS- and H_2O_2-induced HMGB1-release. a) Overexpression of GFP-HMGB1, HA-ARTD1 and myc-ARTD1 (as positive control) in HEK293. 48 h post-transfection cells were treated with 1 mM H_2O_2 for 10 min, followed by a nuclear extraction and an IP anti-HA. IP and 10% input were loaded on SDS-PAGE, and WB anti-ARTD1 (*upper lane of input*), anti-myc, anti-HA, and anti-HMGB1 was performed. **b)** RAW 264.7 cells were pre-incubated with olaparib for 1.5 h before treated with LPS for 16 h, followed by 3 h ATP. The medium was collected, filtered (45 µm) and concentrated through 9 kDa spin-columns, loaded on SDS-PAGE and blotted anti-HMGB1. **c)** MEFs were treated with 0.5 mM H_2O_2 for 10 or 60 min, fixed with 4% PFA and immunostained with anti-HMGB1 and anti-PAR (10H). **d)** MEFs and RAWs were treated with 0.5 mM H_2O_2 for 10, 30 or 60 min, fixed with 4% PFA and immunostained with anti-HMGB1. The signal intensity of nuclear HMGB1 was quantified using ImageJ.

Moreover, we were interested to investigate whether short time stimulation with H_2O_2 would also lead to HMGB1 release in a ADP-ribosylation-dependent manner, since most other published studies focused on later time-points, e.g. 0.5-3 h. Therefore MEFs were treated for 10 or 60 min H_2O_2, followed by IF against HMGB1. We could observe a partial reduction of nuclear HMGB1 staining at 10 min, followed by a further reduction after 60 min H_2O_2 (Figure 14c). PAR formation could be detected after 10, but not 60 min, as expected. Interestingly, the cells that sustain high HMGB1 levels upon 10 min H_2O_2 treatment also show high levels of PAR formation. This could be due to kinetics of PAR formation and imply that the cells without nuclear HMGB1 might already have passed the maximal intensity of H_2O_2-induced PAR formation.

To investigate whether the H_2O_2-induced release of HMGB1 was due to ADP-ribosylation, we incubated MEFs and RAWs with PARPi (olaparib) followed by 10, 30 or 60 min H_2O_2 treatment, and analyzed the HMGB1 release by IF and subsequent quantification of the nuclear HMGB1 intensity. Olaparib pre-incubation had no influence on the release of nuclear HMGB1 after 10 min of H_2O_2, however, upon longer exposure to H_2O_2, e.g. 60 min, the release of nuclear HMGB1 was slightly

attenuated in the presence of olaparib (Figure 14d). Conclusively, ADP-ribosylation does not play a role in the release of nuclear HMGB1 upon 10 min H_2O_2-treatment, but influence the HMGB1 release upon extended H_2O_2-stimulation.

3.3.10 Regulation of IP-10 gene expression by ARTD1 and HMGB1

Transcription of NF-κB-dependent genes has been described to be dependent on ARTD1, although independent of its enzymatic activity [208, 214]. Additionally, HMGB1 can influence the binding of NF-κB dimers to the chromatin and thereby modulate transcription of NF-κB-dependent genes [178]. We therefore aimed to investigate whether ARTD1 and HMGB1 co-regulate the same genes. By stimulating MEFs with LPS for 1 h, and analyzing *IL-6* and *IP-10* gene expression using qRT-PCR we observed an induced expression of both *IL-6* and *IP-10* (Figure 15a, b).

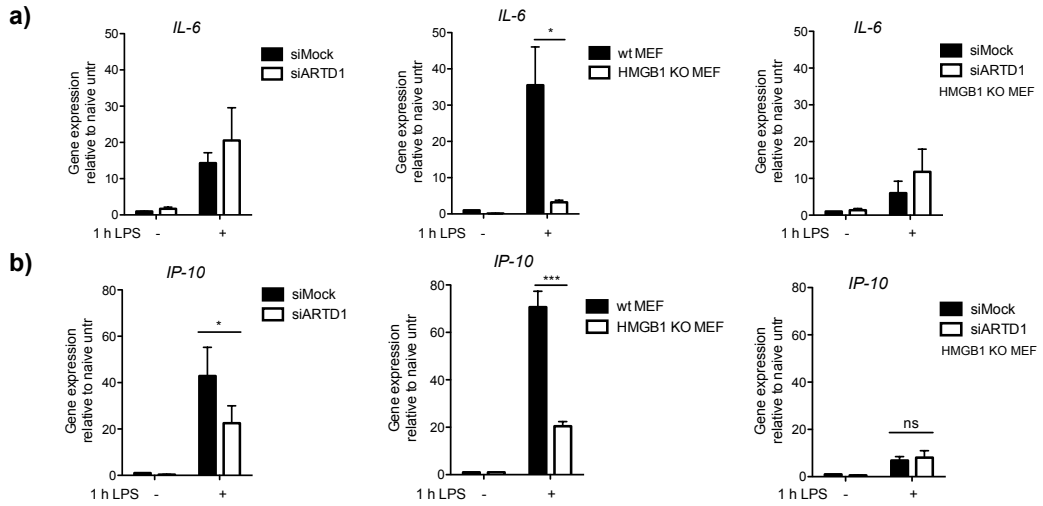

Figure 15. Regulation of LPS-induced *IL-6* and *IP-10* gene expression by ARTD1 and HMGB1. Wt or HMGB1 KO MEFs were treated siRNA against ARTD1 or mock, and stimulated for 1 h LPS, 48 h post-transfection. Gene expression of *IL-6* **a)** and *IP-10* **b)** was measured using qRT-PCR.

Knocking down ARTD1 in wt MEFs, showed a slightly enhanced *IL-6* expression, while HMGB1 KO MEFs showed significantly suppressed *IL-6* expression as compared to wt. Upon knockdown of ARTD1 in HMGB1 KO MEFs, the slight increase in *IL-6* expression was still observed. These data indicate that ARTD1 and HMGB1 independently regulate *IL-6* expression. The LPS-induced *IP-10* gene expression was attenuated both in wt MEFs with a knockdown of ARTD1 as well as in non-transfected HMGB1 KO MEFs, as compared to wt. The knockdown of ARTD1 in HMGB1 KO MEFs showed no additive effect on LPS-induced *IP-10* gene expression. Taken together, these data suggest that ARTD1 and HMGB1 regulate LPS-induced *IP-10*, but not *IL*-6, gene expression through a common mechanism.

Additionally, we investigated the contribution of ARTD1 and HMGB1 in the TNFα-induced *IP-10* gene expression, and compared it to *MIP-2* gene expression, by the knockdown of ARTD1, HMGB1 or both proteins by siRNA. Upon 5 h TNFα treatment we observed an induced expression of *IP-10*, which was reduced in both ARTD1 and HMGB1 siRNA treated cells, confirming the results achieved upon LPS-stimulation (Figure 16a). The *MIP-2* expression was reduced upon HMGB1 knockdown, but no effect could be observed upon ARTD1 knockdown, indicating that ARTD1 is not involved in *MIP-2* gene regulation and thus the co-regulation between ARTD1 and HMGB1 is gene specific.

To analyze the contribution of ARTD1 activity on *IP-10* gene expression, the siRNA-treated cells were pre-incubated with PARPi (olaparib) before stimulated with TNFα (Figure 16a). An enhanced TNFα-induced *IP-10* expression could be observed in siMock cells, while *MIP-2* expression levels were unaffected. Thus, the stimulating effect on *IP-10* expression by olaparib is likely mediated via ARTD1 and its co-regulation with HMGB1, considering that their knockdown abolished the enhanced *IP-10* expression caused by olaparib.

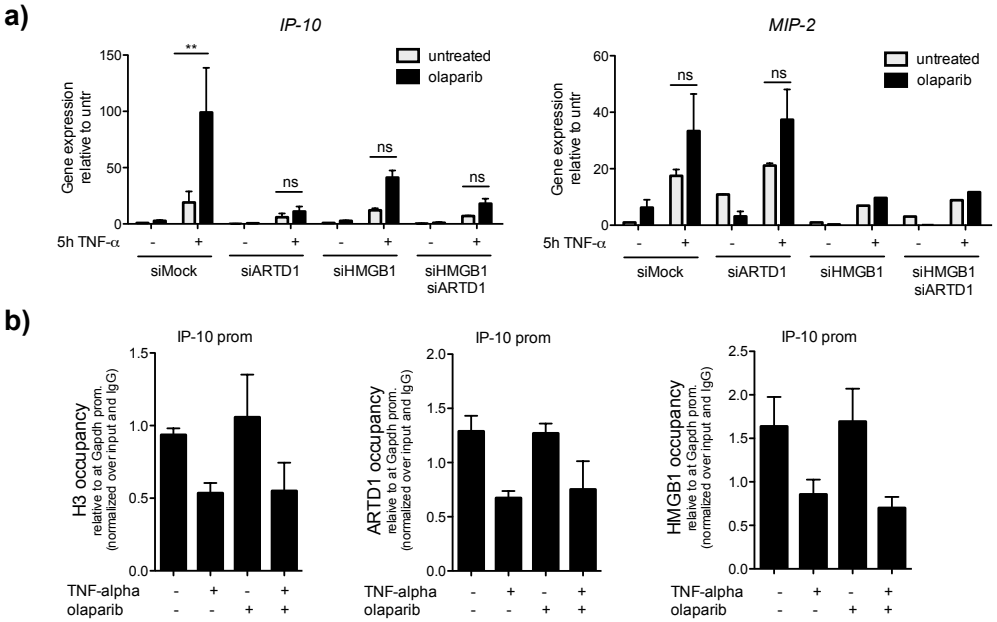

Figure 16. Regulation of *IP-10* gene expression by ARTD1 and HMGB1. a) MEFs were transfected with siRNA against ARTD1, HMGB1 or both combined. After 48 h cells were pre-incubated with 10 μM olaparib for 30 min, before treated with 40 ng/μl TNF-α for 5 h. mRNA was extracted and *IP-10* and *MIP-2* gene expression levels measured by qRT-PCR. **b)** MEFs were pre-incubated with 10 μM olaparib for 30 min, before treated with 40 ng/μl TNF-α for 5 h. ChIP against H3, ARTD1 anf HMGB1 was performed, followed by qPCR analyses of the IP-10 promoter sequence. n.s. $p>0.05$, *$p<0.05$, **$p<0.01$, ***$p<0.001$, +/- SEM.

Since excessive PARylation has been described to repel modified proteins from the chromatin [82, 140], a possible explanation of the observed positive regulatory effects of ARTD1 and HMGB1 and negative regulatory effect of ADP-ribosylation on *IP-10* expression, is that ARTD1 and HMGB1 are required at the *IP-10* promoter for high transcription efficiency, but are repelled upon ADP-ribosylation. To test this hypothesis, we performed ChIP analyses of H3, ARTD1 and HMGB1 at the *IP-10* promoter of TNFα-treated MEFs, in the absence or presence of olaparib (Figure 16b). Upon stimulation, a reduction of H3, ARTD1 and HMGB1 occupancy on the *IP-10* promoter was observed, however independent of ADP-ribosylation. The enhancing effect of *IP-10* expression by PARPi is most likely due to the second wave of transcription, or secondary inflammatory effects, since the increase in gene expression is not significant upon 1 h TNFα. However, through which pathway this occurs needs further investigation.

3.3.11 LPS-induced endotoxin tolerance in MEFs and RAWs is independent of HMGB1, ARTD1, and ADP-ribosylation, under tested cell culture conditions

Inflammation, when uncontrolled, can lead to extensive tissue damage and develop into sepsis, metabolic diseases, autoimmune diseases and cancer [198]. The inflammatory response thus needs to be tightly regulated. One mechanism that promotes anti-inflammatory signaling during such conditions is endotoxin tolerance (ET) [234]. Cells exposed to low concentrations of endotoxin (e.g. LPS) can enter into a transient unresponsive state in which they are unable to respond to further endotoxin challenges. The molecular mechanism underlying induction-process of ET is not known in detail, however multiple studies have revealed the involvement of TLR-signaling, micro-RNAs, NF-κB dimer-formation as well as chromatin remodeling, such as increased levels of H1 and H3K9me3, in the establishment of ET [235]. HMGB1 was proposed to be an important player in the chromatin remodeling during ET [236]. Considering the interaction of HMGB1 with ARTD1, and ARTD1's role in inflammatory transcription and chromatin remodeling, we investigated their involvement in the regulation of ET.

To induce tolerance in a cell culture system, we treated cells with LPS for 16 h, before re-challenging them with LPS another hour. The induced gene expression upon 1 h of LPS in naïve cells was then compared to the gene expression upon 1 h of LPS in tolerant cells. We performed the tolerance protocol with RAW (Figure 17a)

and MEF cells (not shown) and compared the expression of various inflammatory genes. The three example-genes shows three different tolerance profiles; *IL-6* expression was tremendously enhanced upon 16 h LPS treatment and still inducible, *IP-10* showed no expression upon 16 h LPS and was additionally no longer inducible, and *IκBα* showed a similar response in naïve and tolerant cells (Figure 17a). This expression profile was the same in MEFs and RAWs, and we decided to focus on *IP-10* expression, considering the typical ET profile represented by this gene.

To confirm previous findings [236], we first induced ET in HMGB1 KO or wt

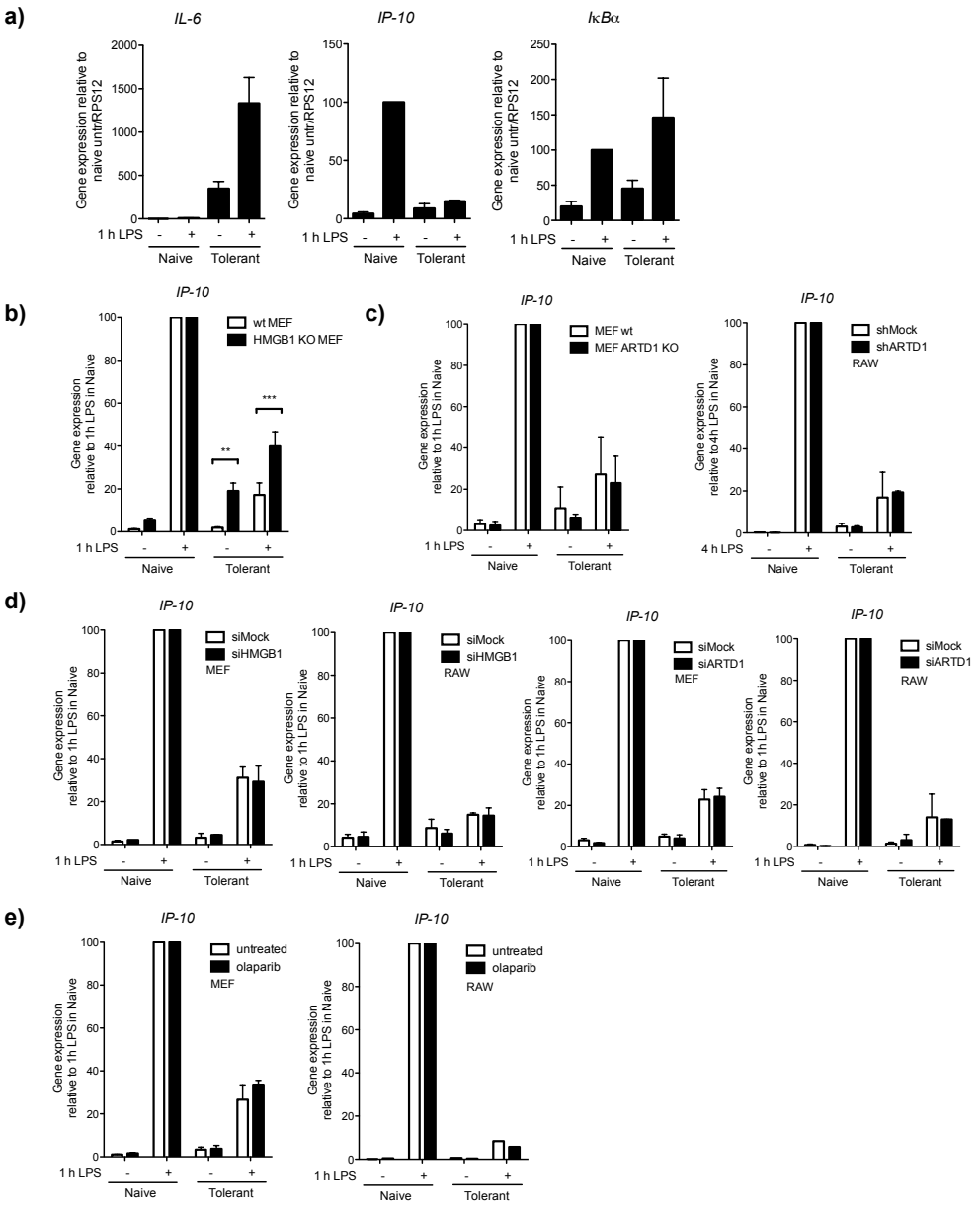

Figure 17. The influence of HMGB1, ARTD1 and ADP-ribosylation on *IP-10* gene expression in endotoxin tolerance. a) RAWs treated with 16 h of 0.1 µg/µl LPS (Tolerant) or left untreated (Naive), before re-challanged with 1 h of 0.1 µg/µl LPS. mRNA was purified and the gene expression levels measured using qRT-PCR. Expression levels normalized to housekeeping gene *RPS12* and 1 h LPS in Naive cells set to 100. **b)** performed as in a), using HMGB1 KO and wt MEFs. **c)** performed as in a) using ARTD1 KO and wt MEFs and RAWs transfected with shRNA against ARTD1. **d)** performed as in a) using MEFs and RAWs transfected with siRNA against HMGB1 or ARTD1. **e)** performed as in a), using MEFs and RAWs untreated or treated with 10 µM olaparib for 30 min pre-tolerance-induction.

MEFs and compared the *IP-10* gene expression after 1 h of LPS in naïve and tolerant cells (Figure 17b). We observed an increased expression of *IP-10* in tolerant cells, representing a loss of ET, which suggested that HMGB1 is required for setting or keeping cells in a tolerant state. Next, the role of ARTD1 in ET was examined by performing the ET protocol in ARTD1 KO and wt MEFs, or RAWs with a shRNA-mediated knockdown of ARTD1 (Figure 17c). The ARTD1-lacking tolerant cells exhibited the same levels of *IP-10* expression as their corresponding mock or wt tolerant cells, suggesting that the stable lack of ARTD1 does not influence ET.

To investigate whether we observe the same effect with transiently knockdown HMGB1 and ARTD1, we performed the same experiment in siRNA-mediated HMGB1- and ARTD1-depleted MEFs or RAWs (Figure 17d). No effect on *IP-10* gene expression in tolerant cells could be observed upon knockdown of HMGB1 or ARTD1, as compared to siMock. This implies that the effect observed using HMGB1 KO MEFs was more likely due to changes in the proteome of these cells or adaptation of the chromatin to the constitutive lack of HMGB1, rather than a direct role of HMGB1. Our obtained results differ from the literature, where one publication states that the knockdown of HMGB1 increases *TNF-α* gene expression in tolerant THP-1 cells [236]. However, cell type, species and the analyzed target gene, can influence the outcome of a study, which is likely the cause of the observed differences between our studies and the already published one [236].

Furthermore, we aimed to elucidate whether ADP-ribosylation could play a role in the induction of an ET state and therefore treated MEFs and RAWs with olaparib for 1 h pre-tolerance induction (Figure 17e). The *IP-10* gene expression was identical in olaparib pre-treated and non-pre-treated tolerant cells, suggesting that ADP-ribosylation is not involved in the induction of ET. These data clearly provide evidence that neither HMGB1, ADP-ribosylation, nor ARTD1 affect the induction of ET under the tested cell culture conditions.

3.3.12 H_2O_2 can induce an ET-like state, however independent of ADP-ribosylation and ARTD1

We further investigated whether treatment of cells with H_2O_2 could induce a similar tolerance as the LPS-induced ET. Therefore, the cells were exposed to 1 mM H_2O_2 for 10 min, the medium was exchanged and the cells were incubated for 4 h, followed by 1 h of LPS treatment. The same genes as for LPS-induced ET were studied and

interestingly, they all showed a similar tolerance profile as upon ET (Figure 18a). To elucidate the role of ADP-ribosylation in H_2O_2-induced tolerance, we pre-treated MEFs and RAWs with olaparib before inducing tolerance (Figure 18b). Surprisingly, the *IP-10* expression in H_2O_2-induced tolerant cells was not affected by olaparib pre-treatment, suggesting that ADP-ribosylation does not play a role in H_2O_2-induced tolerance. Next, the role of ARTD1 as a protein in H_2O_2-induced tolerance was investigated by the transient knockdown of ARTD1 in MEFs and stably in RAWs (Figure 18c). No difference in *IP-10* gene expression could be observed between tolerant siARTD1 cells and the tolerant siMock cells, indicating that H_2O_2 can induce an ET-like state, however, independently of ADP-ribosylation and ARTD1.

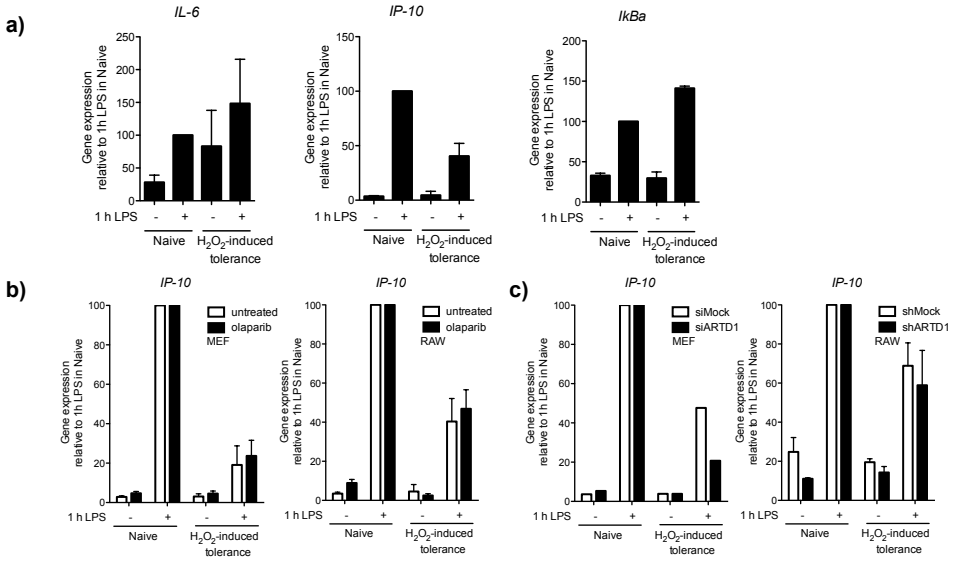

Figure 18. The influence of ADP-ribosylation and ARTD1 on *IP-10* gene expression during H_2O_2-induced tolerance. a) MEFs were treated with 1 mM H_2O_2 for 10 min (H_2O_2-induced tolerance) or left untreated (Naive), following medium replacement and 4 h incubation, before challanged with 0.1 µg/µl LPS for 1 h. mRNA was purified and the gene expression levels measured using qRT-PCR. Expression levels normalized to housekeeping gene *RPS12* and 1 h LPS in Naive cells set to 100. **b)** performed as in a), using MEFs and RAWs untreated or treated with 10 µM olaparib for 30 min pre-tolerance-induction. **c)** performed as in a) using MEFs transfected with siRNA against ARTD1 and RAWs stably transfected with shRNA against ARTD1.

4 Discussion and Perspectives

4.1 Investigations of Ca^{2+} in H_2O_2-induced DNA lesions

We could show, in Andersson et al. that the Ca^{2+}-dependent kinase PKCα is required for H_2O_2-induced PAR formation. Additionally, the importance of Ca^{2+}-signaling in the induction of DNA lesions and the activation of ARTD1 was shown in our study, which has previously been described by others [93, 106, 237]. Ca^{2+}-mediated PAR formation upon oxidative stress is commonly described to be due to the Ca^{2+}-induced release of ROS from mitochondria. Surprisingly, the ROS scavenger NAC showed no effect on either H_2O_2-induced PAR or DNA lesion formation (previous data from our lab). The ability of the Ca^{2+} chelator BAPTA-AM to reduce the H_2O_2-induced DNA lesions by interfering with the transition metal ion-mediated Fenton reaction at the site of DNA has been suggested [226]. Although, another group could observe reduced DNA lesion formation using the two other Ca^{2+} chelators EGTA and Quin-2 [92]. Furthermore, we could demonstrate that BAPTA-AM, but not the iron/copper-chelator PHE, reduced H_2O_2-induced DNA lesions, indicating the crucial role of Ca^{2+}, but not transition metals in H_2O_2-induced DNA lesion formation (Figure 6c). Such a Ca^{2+}-dependent induction of DNA lesions could be through the activation of Ca^{2+}-dependent DNA-glycosylases or endonucleases. An interaction of ARTD1 with several DNA-glycosylases and endonucleases has been described [227, 233, 238]. Additionally, AP sites have been described to activate ARTD1 [239, 240]. In some cases, as for OGG1 and NEIL1, the interaction has already been shown to enhance the activity of ARTD1 [227, 233]. We addressed the role of DNA-glycosylases and endonucleases in H_2O_2-induced DNA lesions by knockdown experiments in cells upon H_2O_2 treatment. The obtained data clearly show that the main BER factors OGG1 and APE1, as well as the other tested DNA-glycosylase NEIL3 and endonuclease MUS81, are not involved in the H_2O_2-induced DNA lesions (Figure 7, 8, 9). Although we found no effect of the single knockdowns of several endonucleases on H_2O_2-induced lesions, multiple knockdowns simultaneously could potentially affect the Ca^{2+}-induced DNA lesions, indicating that different enzymes together might contribute to the observed DNA lesions. In contrast, Ca^{2+} has been described to specifically regulate DNA conformation at $d(TG/AC)_n$ repeats under physiological concentrations by binding to DNA [241]. One could speculate that elevated nuclear levels of Ca^{2+} would result in enhanced binding of Ca^{2+} to DNA, which consequently

could cause DNA distortions and strand-breaks. This would indicate a direct mode of DNA lesion formation by elevated Ca^{2+} concentrations as a result of H_2O_2 treatment. The targeting of Ca^{2+} to $d(TG/AC)_n$ repeats suggests a specific targeting of Ca^{2+}-induced DNA lesions to repetitive sequences, such as satellite DNA or retrotransposons [242, 243].

4.2 NEIL3 plays a role in H_2O_2-induced PAR formation

Interestingly, we could show how MEFs lacking NEIL3 exhibited reduced PAR formation upon H_2O_2 treatment, although no effect on the DNA lesions was detected (Figure 9a,b). However, the levels of DNA lesions induced by NEIL3 could be low, and therefore not detectable by the alkaline comet assay, but still induce PAR formation. Additionally, to dissect the role of NEIL3 in H_2O_2-induced DNA lesions, the differential impact on SSB and oxidative lesions upon knockdown of NEIL3 should be investigated by the use of a different pH in the alkaline comet assay [244]. NEIL3 specifically recognizes single-stranded DNA, and shows no activity towards 8-oxoG [245]. It is not yet known if the activity of NEIL3 upon H_2O_2-treatment is Ca^{2+}-dependent, but a Ca^{2+}-dependent NEIL3 activity upon H_2O_2-treatment would imply that ARTD1 is activated by a highly specific DNA lesion upon oxidative stress. Moreover, a colocalization of NEIL3 and PAR foci in H_2O_2-treated cells would further suggest that the specific PAR foci detected by IF upon H_2O_2 are due to NEIL3-induced lesions.

The fact that the knockdown of OGG1 in cells lacking NEIL3 rescues PAR formation (Figure 9c), implies a compensation mechanism via an increased activity of NEIL1 or NEIL2 [1, 246]. These DNA-glycoylases can excise 8-oxoG, which is heavily induced upon H_2O_2, and could potentially compensate for OGG1. They can also excise similar lesions as NEIL3, thus leading us to speculate that upon their enhanced activity, they could additionally compensate for the lack of NEIL3. A combination of knockdowns using siRNA against multiple DNA glycosylases, as suggested for endonucleases above, or the use of DNA glycosylase inhibitors, which would target several enzymes simultaneously, would address the crosstalk and compensation between them [1, 246, 247]. The compensatory mechanisms between the different DNA glycosylases, as well as how specific lesions activate ARTD1

differently, would greatly deepen our knowledge on H_2O_2-induced, Ca^{2+}-mediated PAR formation.

4.3 PAR formation is activated independently of DNA lesions

We show that PAR formation induced by H_2O_2 treatment is dependent on Ca^{2+}, but the basal PAR levels under untreated conditions are not (Figure 6a, b). The basal PAR levels vary between cell lines, and could be activated by ARTD1 complex formation, PTMs or interactions with DNA, lipids or proteins [75, 95, 97, 98, 248, 249]. Basal PAR formation has recently been suggested to be due to complex formation with NuA4-complex, an ATPase chromatin-remodeling complex containing a histone acetyltransferase as well as helicase activity, suggesting an activation of PAR upon chromatin remodeling [249]. Additionally, the interaction with CTCF has been shown to activate ARTD1 in the absence of stimulation, and could be found at hundreds of sites throughout the chromatin [113, 145]. These modes of basal ARTD1 activity-regulation suggest the involvement of low PARylation levels in transcriptional activity and other nuclear functions on a non-induced level.

An interesting question is whether this basal pre-ADP-ribosylated serves as priming ARTD1 to be further activated (i.e. extension of MARylated to PARylated), and if increased levels of intracellular Ca^{2+} alone could further activate ARTD1. We show indeed that increased intracellular levels of Ca^{2+} by the treatment with ionomycin can activate ARTD1-dependent PAR formation, independent of DNA lesions (Figure 10). This suggests that Ca^{2+} not only induces DNA lesions, but can also activate ARTD1 in a different manner. One alternative would be that Ca^{2+}-dependent kinases activate ARTD1 directly by phosphorylation or indirectly via further signaling. However, by knocking down Ca^{2+}-dependent CaMKII, which has previously been described to modulate ARTD1 activity, we could not observe an influence on H_2O_2-induced PAR formation (data not shown) [106, 237]. We show, in our submitted manuscript Andersson et al., that the Ca^{2+}-dependent kinase PKCα is required for PAR formation, but not responsible for the activation of ARTD1, and that the MAPKs, which were previously shown to modulate ARTD1 activity, are not involved in the PAR formation induced after 10 min of H_2O_2 treatment [97, 98, 101]. Additionally, we show, and others have shown, that phosphorylation by certain isoforms of PKC can act inhibitory on ARTD1 activity [103, 104]. The phosphatase

calcineurin is regulated by Ca^{2+} and could potentially be a regulator of ARTD1 activity by dephosphorylating these inhibitory phospho-residues [250]. Furthermore, increased Ca^{2+} levels and subsequent calcineurin activation has recently been described to be important for the activity of Brg1 ATPase of the SWI/SNF chromatin remodeling enzyme, described to be a calcineurin substrate [250]. As we have shown that the chromatin architectural protein HMGB1 controls the H_2O_2-induced PAR formation, one could speculate that the Ca^{2+}-induced changes in chromatin remodeling by SWI/SNF could be important for the induction of PAR formation.

Moreover, we found that NEs from ARTD1 KO MEFs activate ARTD1 in NEs from wt MEFs, also in the absence of treating the cells with H_2O_2 (Figure 11). The activation of ARTD1 in wt NEs by NEs lacking ARTD1 could be explained by an activating signal normally repressed by ARTD1, or a PARylation-repressor normally under the control of ARTD1 (Figure 19). One such PARylation repressor could be PARG or ARH3, which in wt cells balances the activity of ARTD1, while

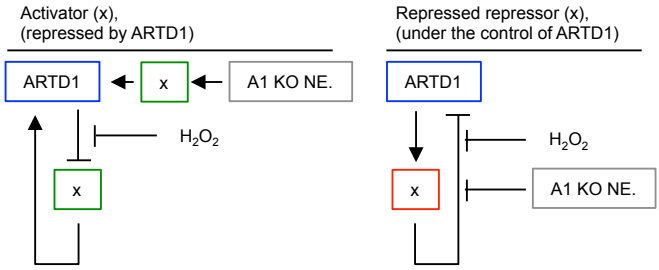

Figure 19. Schematic explanation of two hypothetical modes how NEs from ARTD1 KO MEFs can activate ARTD1 in wt NEs.

ARTD1 KO NEs could contain a repressor of these hydrolases due to the very low PAR levels [71, 251]. To address this, NEs from cells lacking PARG and/or ARH3 could be used together with the ARTD1 KO NEs. Additionally, future studies should be performed addressing the effect of Ca^{2+} on PARG and ARH3 activity *in vivo*, as the Ca^{2+}-dependent activation of PAR formation could be due to the repression of hydrolases to allow 'primed' ARTD1 full activity. The repression of hydrolases could be a Ca^{2+}-dependent, but DNA lesion independent mode of ARTD1 activation.

4.4 ARTD1 activity is controlled by HMGB1 via PKCα-mediated phosphorylation during oxidative stress

H_2O_2-induced PAR formation was found to be strongly dependent on Ca^{2+}, as well as the Ca^{2+}-dependent kinase PKCα (Andersson et al. submitted). Surprisingly, the

phosphorylation of ARTD1 by this kinase did not affect ADP-ribosylation *in vitro*. However, we discovered that the histone-like protein HMGB1 controls ARTD1 activity, and PKCα-mediated phosphorylation of HMGB1 is required to allow full activation of PAR formation by H_2O_2. Nevertheless, by which mechanism HMGB1 controls ARTD1 activity, and how the phosphorylation of HMGB1 induces PAR formation, needs further investigation. This thesis shows that HMGB1 and ARTD1 interact *in vivo*. However, upon H_2O_2 treatment, the interaction is lost (Figure 13a). This implies that either the activation of ARTD1 leads to their dissociation, or another H_2O_2-induced signaling event, e.g. phosphorylation, interferes with the interaction between ARTD1 and HMGB1. When incubating HMGB1 with ARTD1 *in vitro*, no effect was observed on DNA-induced PAR formation by ARTD1. However, it would be interesting to investigate whether the interaction of HMGB1 and ARTD1 *in vivo* in the presence of chromatin leads to the repression of ARTD1 activity. HMGB1 and ARTD1 were reported to compete for the same site of the nucleosome as well as to certain structures of DNA, and unphosphorylated HMGB1 could thereby act as a block for ARTD1 DNA-binding and subsequent activation [95, 159, 162, 172]. Previous reports have shown that PKC phosphorylates HMGB1, which changes its localization, DNA-binding preference and DNA-bending ability [180, 189, 190]. We could also show a decreased H_2O_2-induced chromatin release of HMGB1 upon PKCα knockdown, and the release of HMGB1 from the chromatin and nucleus upon PKC-mediated phosphorylation would allow full activity of ARTD1.

Alternatively, the enhanced DNA bending activity by HMGB1 upon PKCα-mediated phosphorylation could be involved in the activation of ARTD1. HMGB1-mediated DNA bending has been described to be involved in several processes, such as the recruitment of transcription factors, the initiation of chromatin remodelers and the enabling of DNA repair factor binding to DNA [165, 175, 252]. The v-like structure in DNA, formed by HMGB1 upon bending, facilitates the binding of chromatin remodelers to nucleosomal DNA and has been shown to facilitate the sliding of nucleosomes [165, 253]. This way of increasing the accessibility to nucleosomal DNA could be important for the activation of ARTD1 e.g. upon DNA break formation at nucleosomal DNA.

To find the mechanism by which PKCα regulates PAR formation through HMGB1, we would need to confirm the phosphorylation sites of HMGB1 by PKCα *in vivo*, upon H_2O_2-induced oxidative stress. Identifying the PKCα-specific

phosphorylation sites on HMGB1 by mass spectrometry would allow the cloning of HMGB1 phosphorylation mutants, and thereby a tool to study PKCα-mediated phosphorylation of HMGB1 and its functional consequences on chromatin changes and in H_2O_2-induced PAR formation *in vivo*.

Taken together, we could show that PKCα-mediated phosphorylation of HMGB1 regulates ARTD1 activity. The phosphorylation leads to a partial chromatin release of HMGB1, which could contribute to the enhanced PAR formation, although the change in chromatin affinity of phosphorylated HMGB1 could potentially also play a role. This reveals a regulation of ARTD1 by chromatin structure and composition, which has only been shown before *in vitro* [94]. Future studies to shed light onto how the chromatin surrounding affects ARTD1 would be of very high interest, both regarding its enzymatic activity in response to oxidative stress, and its function as a co-regulator of transcription upon stimulation with other stimuli, such as LPS (see below).

4.5 PKCα-mediated chromatin phosphorylation could regulate ARTD1 activity

Whether the HMGB1 phosphorylation by PKCα *in vivo*, in the chromatin context, affects the ARTD1 activity alone remains to be determined. There is also the possibility that PKCα regulates other chromatin-associated proteins in addition to HMGB1 that influence H_2O_2-induced PAR formation, such as heterochromatin protein (HP) 1. Chromatin-associated ADP-ribosylation upon H_2O_2 treatment is mainly detected at areas with an increased amount of H3K9me3 (submitted data from our lab), a heterochromatic mark that can be bound by HP1 [127]. A recent study shows how the specificity of HP1 for tri- as opposed to unmethylated H3K9 requires phosphorylation by CK2 [254]. Whether PKCα phosphorylates HP1 is not yet known, but it would be interesting to investigate whether the recruitment of phosphorylated HP1 to H3K9me3 is involved in H_2O_2-induced PAR formation. HP1 can be recruited to sites of DNA-damage within seconds, independently of repair factors, and has additionally been described to bind oxidative DNA lesions [255]. ARTD1 has been shown to interact with HP1, which could be a potential way of ARTD1-activation at sites of DNA-damage within heterochromatic regions [256].

Another protein often associated with heterochromatic regions and target of phosphorylation is the linker histone H1 [115]. Phosphorylation of H1 has been

described to lead to its release from chromatin and result in cellular proliferation [130, 140]. However, its influence on ARTD1 activity is not yet known. H1 and ARTD1 bind to overlapping sites on chromatin, at the dyad axis where the DNA exits the nucleosome, and have been shown to be mutually exclusive on the chromatin [94, 257]. Furthermore, histone H1 can be removed by HMGB1 from the chromatin [169], and should this removal require phosphorylation of HMGB1 by PKCα, it could serve to enhance the accessibility for ARTD1 binding to these sites and be another mean of PKCα to influence ARTD1 activation.

The PKCα-mediated phosphorylation of histones *in vitro* had no effect on ARTD1 activity (Andersson et al.), but could potentially still play a more important role in the context of chromatin *in vivo*. In Drosophila, acetylated H2A in combination with JIL-1-mediated phosphorylation of H2Av leads to the activation of ARTD1 [138]. However, we have shown that neither histone hyperacetylation upon HDAC inhibitor treatment, nor inhibition of MSK1, the JIL-1 mouse analogue, has an effect on H_2O_2-induced PAR formation (Figure 11). Although, the phosphorylation of H2A by other kinases, such as PKCα, could potentially regulate ARTD1 upon oxidative stress.

4.6 ADP-ribosylation of HMGB1

We additionally demonstrated that HMGB1 is ADP-ribosylated by ARTD1 and that the main acceptor site is between aa 121-126 (Figure 13). To further investigate the modification site on HMGB1 and the functional relevance of ADP-ribosylated HMGB1, overexpression of HMGB1 ADP-ribosylation deficient point-mutations and wild-type with a subsequent IP of HMGB1 from cells upon LPS or H_2O_2 stimulation could be performed and analyzed by mass spectrometry. Due to recent technical advances in our lab for these techniques [32, 33], significant ADP-ribosylation sites upon various stimuli would be possible to determine. Using these and previous hits, stimulus-specific ADP-ribosylation deficient mutants of HMGB1 could be generated, and used to study the effect of the ADP-ribosylation under oxidative stress and inflammatory conditions. The site-specific mutagenesis of HMGB1, K126R, has revealed a decrease of approximately 30% in ARTD1-mediated ADP-ribosylation *in vitro* (Figure 13d), and this mutant could thus be used for further studies *in vivo*. However, to obtain a stronger reduction of ADP-ribosylation, and since R has also

been suggested as ADP-ribosylation acceptor sites, mutagenesis of other amino acids and to alanine (A), could serve as a better tool to investigate the effect of ADP-ribosylation of HMGB1 *in vivo*. Although, the risk of a distorted protein structure in this important DNA-intercalating protein region needs to be kept in mind [151].

4.7 The effect of HMGB1 ADP-ribosylation

There is a high level of circulating HMGB1 in serum from sepsis patients, and HMGB1 has been described as a major cause of sepsis [217, 258]. ARTD1 KO mice, as well as mice treated with PARPi are resistant towards septic shock, and show a reduction in circulating pro-inflammatory cytokines [211]. ARTD1-dependent ADP-ribosylation of HMGB1 has been described to promote the release of HMGB1 upon stimulation of cultured cells with inflammatory stimuli [36, 188], something we have confirmed by the decreased LPS/ATP-dependent HMGB1 release in the presence of PARPi (Figure 14b). As PARPi have been suggested to be protective against sepsis, measuring the serum-levels of HMGB1 in LPS-challenged ARTD1 KO or PARPi-treated mice would tell us whether the observation made in cell culture is reproduced *in vivo*. Additionally, overexpressing an HMGB1 ADP-ribosylation-deficient mutant in HMGB1 KO mice, as well as treating HMGB1 KO mice with PARPi, and measure LPS-induced cytokines and the incident of sepsis would be of great interest to elucidate the function of HMGB1 ADP-ribosylation in sepsis and septic shock.

Further investigations on the hydrolase responsible for the removal of ADP-ribosyaltion from HMGB1 *in vitro* and follow-up studies *in vivo* would be interesting and could tell more about the biological function of the modification. The various ADP-ribosylation hydrolases have been reported to have different amino acid specificities and different localizations [52, 64-67]. The localization of the responsible hydrolase would hint whether HMGB1 is de-modified before it is released from the nucleus, in the cytoplasm, or in endosomes and thereby reveal the dynamics and function of the modification.

The HMGB1 released from cells during inflammation is found to be oxidized, and functions comparable to a cytokine [224, 225]. In the ADP-ribosylation assays, only the oxidized HMGB1 seems to be modified by ARTD1 (Figure 13) [259, 260]. This shows that PTM of HMGB1 depends on its redox-state. It also implies that the ADP-ribosylation of HMGB1 upon inflammatory stimulation could be initiated by the

change in intracellular redox-state and thereby signal oxidative stress to the extracellular environment [224].

Together, these studies reveal an important regulatory function of ARTD1 activity on HMGB1 localization suggesting that these two proteins are able to regulate each other, and that the kinetics and the type of stimulus regulate the dynamics of their interactions. HMGB1 controls the activity of ARTD1 upon H_2O_2-treatment, while ARTD1 seems to regulate the localization of HMGB1 upon prolonged LPS stimulation, suggesting that ARTD1 in certain conditions can contribute to the removal of its own repressor.

4.8 Regulation of *IL-6* transcription by MLL1 and ARTD1

We could show that ARTD1 is regulating LPS-induced p65-dependent transcription of *IL-6* by repressing MLL1 and subsequently reduce H3K4me3 at the promoter of *IL-6* (Minotti et al.). This demonstrates the ability of ARTD1 to influence the chromatin-composition and the resulting gene expression. The regulation of MLL1 by ARTD1 was independent of its enzymatic activity. However, in previous publications ARTD1 has been shown to ADP-ribosylate KDM5B, thus inactivating it, and subsequently leading to up-regulation of H3K4me3 at active promoters [35]. The differential regulation of H3K4me3 could be explained by the presence or absence of a local ARTD1 activating signal, such as topoisomerase IIβ-induced breaks [140, 261]. Topoisomerase IIβ has been described to be activated upon demethylation of H3K9me2/3 and H3K4me2 by the lysine-specific demethylases KDM1A and KDM4A [262]. Upon demethylation by KDM1A (oxidase) and KDM4A (dioxygenase) in the presence of Fe^{2+}, local oxidation occur, which damages the DNA [263]. This could imply that ARTD1 is only activated on a certain subset of gene promoters to inhibit the demethylation of H3K4me3 and prolong gene expression, while on other promoters, the mode of action is repressory due to the lack of ARTD1 activating signal.

To investigate whether the described regulation of MLL1 by ARTD1 can be observed for several inflammatory genes, and whether it is specific for NF-κB target genes, ChIP-seq analyses of ARTD1 and H3K4me3 upon LPS-stimulation could be performed and compared to H3K4me3 in ARTD1 KO and MLL1 KO cells. Verification of the ARTD1 and MLL1 regulated genes by qPCR would provide

further insights into ARTD1-mediated gene regulation through the inhibition of MLL1-mediated histone methylation.

The methyltransferase SET7/9 is responsible for the mono-methylation of H3K4, which is one of the histone-marks at poised/active enhancer regions [264, 265]. Interaction between SET7/9 and p65 was observed in monocytes upon TNFα-stimulation, and SET7/9 enhances TNFα-dependent gene transcription by mediating H3K4me1 and by competing with histone-deaceylases and precluding H3K9me3 [266, 267]. We have shown how SET7/9 mono-methylates ARTD1 to enhance its activity (Kassner et al.). Thus, another potential distinction whether ARTD1 becomes enzymatically activated or not, at the enhancers or promoters of ARTD1-regulated genes, could be the methylation of ARTD1 by SET7/9. Whether SET7/9 can regulate the activity of ARTD1 upon inflammatory stimuli, and what effect this would have on gene expression, would need to be further investigated. One approach would be to overexpress an ARTD1 K508 mono-methylation mutant in ARTD1 KO cells, to treat the cells with inflammatory stimuli, and to compare the inflammatory gene response to that of ARTD1 KO cells complemented with wt ARTD1. Additionally, studying H3K4me3 and MLL1 occupancy at promoters of ARTD1-regulated genes in the presence of K508 mutant or wt ARTD1, would tell us whether mono-methylation of ARTD1 can direct ARTD1's enhancing or repressor effect on H3K4me3.

4.9 Co-regulation of *IP-10* by ARTD1 and HMGB1

We provide evidence that ARTD1 and HMGB1 co-regulate *IP-10*, but not *IL-6* or *MIP-2* gene expression upon LPS- and TNFα-stimulation of MEFs (Figure 15, 16). This suggests that ARTD1 and HMGB1 both have common, but also separate regulatory functions on NF-κB-dependent genes.

Due to the role of ARTD1 in regulating H3K4me3 at the promoters of stimulus-regulated genes [35, 268], it would be interesting to investigate the levels of H3K4me3 at the *IP-10*-promoter site, and whether this histone mark changes upon knockdown of HMGB1, but also the knockdown of ARTD1. HMGB1 is known to facilitate the recruitment of transcription factors, but also chromatin remodelers, which could be crucial for gene expression [165, 175, 176, 178]. The co-regulation of *IP-10* by HMGB1 and ARTD1 could be due to an HMGB1-dependent recruitment of additional factors, such as chromatin remodelers or acetyltransferases needed for

ARTD1's function as a cofactor of NF-κB, and could additionally explain the gene specificity [269]. Further interaction studies upon LPS-stimulation between ARTD1, HMGB1, chromatin remodelers and other NF-κB cofactors would provides us further evidence regarding such a possible mechanism.

Both ARTD1 and HMGB1 bind to the linker DNA at the exit/entry point of the nucleosomes, comparable to histone H1, and have both been described to be able to displace H1 from the chromatin [140, 168]. If this displacement is activated upon inflammatory stimuli, this could promote a more accessible chromatin around the regulatory sites of the NF-κB-dependent genes, and subsequently enhance transcription. Not only the linker histone H1 was shown to be displaced by HMGB1, but also the movement and displacement of core histones is facilitated by HMGB1 [164-166]. HMGB1 has also been described to facilitate nucleosome sliding, nucleosome assembly/disassembly, and interact with the histone chaperone FACT, implying that the incorporation of histone variants, specific for active transcription, could be influenced by HMGB1 [161, 162, 270]. Taken together, this suggests that HMGB1 might facilitate a remodeling of the chromatin to allow NF-κB binding and cofactor association, including ARTD1, and subsequent induced gene expression.

4.10 H_2O_2-induced tolerance is specific for certain inflammatory genes

We could show that not only LPS induces a tolerant state in MEFs and RAWs, but also the stimulation with H_2O_2 for 10 min induces a tolerance effect on *IP-10*, but not *IL-6* gene expression (Figure 18). The fact that we can observe an endotoxin tolerance (ET)-like state upon H_2O_2-treatment suggests that oxidative stress has a highly relevant function in the modulation of the initial inflammatory response. The stimulation with H_2O_2 changes the oxidative state of the cell and induces various signaling pathways, which in turn activate inflammatory signaling [271]. H_2O_2 was also described to have an inhibitory effect on NF-κB activation and nuclear translocation, but since the different NF-κB-dependent genes showed different tolerance induction, this is likely not what we observed [273]. H_2O_2-stimulation activates also Akt, IKK, the MAPK pathway and protein phosphatases which can all lead to activation of the NF-κB pathway and the expression of cytokines [272]. This in turn could contribute to the induction of a tolerance-like state in a similar manner as by LPS [273]. It has been shown that the MAPK p38 and JNK are important for

IP-10 gene expression [274, 275], and p38 and ERK1/2, but not JNK, are important for *IL-6* gene expression [276-278]. Thus, one could speculate that the gene specificity for the induced tolerance by H_2O_2 could be due to a specific activation of JNK, which would lead to *IP-10* gene expression but also subsequent silencing. The silencing of genes during ET is reported to be due to a chromatin rearrangement at the promoters of the inflammatory genes, thus the specificity of tolerance induction could be due to the nucleosome occupancy and promoter environment at different genes [269, 279]. MAPKs can regulate HATs and HDACs, which are required to promote transcription, but also for the induction of tolerance at specific genes [280, 281]. Additionally, the induction of the NF-κB subunit RelB, which is increased upon ET, has been shown to be regulated by JNK, indicating an important role of this MAPK in regulating H_2O_2-induced ET [282, 283].

ET has been thought of as a protective mechanism against septic shock and ischemia, but is also associated with high risks of secondary infections [234]. That H_2O_2 can induce an ET-like state suggests that increased cellular metabolism, leading to increased ROS, could modulate the inflammatory responsiveness of cells as well. This provides an additional link between the cellular metabolic state and inflammation. Moreover, these results indicate that also exposure to ROS by exogenous sources, such as smoke or UV, could lead to a higher risk of unresolved infections and increased severity of inflammatory diseases, due to ROS induced tolerance.

5 References

1. Dizdaroglu, M., *Substrate specificities and excision kinetics of DNA glycosylases involved in base-excision repair of oxidative DNA damage.* Mutation Research/Fundamental and Molecular Mechanisms of Mutagenesis, 2003. **531**(1-2): p. 109-126.
2. Collins, A.R., *Oxidative DNA damage, antioxidants, and cancer.* BioEssays : news and reviews in molecular, cellular and developmental biology, 1999. **21**(3): p. 238-46.
3. Veal, E.A., A.M. Day, and B.A. Morgan, *Hydrogen peroxide sensing and signaling.* Molecular cell, 2007. **26**(1): p. 1-14.
4. Cooke, M.S., et al., *Oxidative DNA damage: mechanisms, mutation, and disease.* FASEB journal : official publication of the Federation of American Societies for Experimental Biology, 2003. **17**(10): p. 1195-214.
5. Stadtman, E.R. and R.L. Levine, *Protein oxidation.* Annals of the New York Academy of Sciences, 2000. **899**: p. 191-208.
6. Marnett, L.J., *Lipid peroxidation-DNA damage by malondialdehyde.* Mutation research, 1999. **424**(1-2): p. 83-95.
7. Olinski, R., Z. Nackerdien, and M. Dizdaroglu, *DNA-protein cross-linking between thymine and tyrosine in chromatin of gamma-irradiated or H2O2-treated cultured human cells.* Archives of biochemistry and biophysics, 1992. **297**(1): p. 139-43.
8. Forman, H.J., *Use and abuse of exogenous H2O2 in studies of signal transduction.* Free radical biology & medicine, 2007. **42**(7): p. 926-32.
9. Guo, Z., R. Deshpande, and T.T. Paull, *ATM activation in the presence of oxidative stress.* Cell cycle, 2010. **9**(24): p. 4805-11.
10. Hajnoczky, G., et al., *Control of apoptosis by IP(3) and ryanodine receptor driven calcium signals.* Cell calcium, 2000. **28**(5-6): p. 349-63.
11. Berridge, M.J., M.D. Bootman, and H.L. Roderick, *Calcium signalling: dynamics, homeostasis and remodelling.* Nature reviews. Molecular cell biology, 2003. **4**(7): p. 517-29.
12. Crabtree, G.R., *Generic signals and specific outcomes: signaling through Ca2+, calcineurin, and NF-AT.* Cell, 1999. **96**(5): p. 611-4.
13. Smith, M.R., et al., *Overexpression of phosphoinositide-specific phospholipase Cgamma in NIH 3T3 cells promotes transformation and tumorigenicity.* Carcinogenesis, 1998. **19**(1): p. 177-85.
14. Berridge, M.J., P. Lipp, and M.D. Bootman, *The versatility and universality of calcium signalling.* Nature reviews. Molecular cell biology, 2000. **1**(1): p. 11-21.
15. Tarasov, A.I., E.J. Griffiths, and G.A. Rutter, *Regulation of ATP production by mitochondrial Ca(2+).* Cell calcium, 2012. **52**(1): p. 28-35.
16. Dizdaroglu, M., et al., *Free radical-induced damage to DNA: mechanisms and measurement.* Free radical biology & medicine, 2002. **32**(11): p. 1102-15.
17. Rolseth, V., et al., *Loss of Neil3, the major DNA glycosylase activity for removal of hydantoins in single stranded DNA, reduces cellular proliferation and sensitizes cells to genotoxic stress.* Biochimica et biophysica acta, 2013. **1833**(5): p. 1157-64.
18. Sancar, A., et al., *Molecular mechanisms of mammalian DNA repair and the DNA damage checkpoints.* Annual review of biochemistry, 2004. **73**: p. 39-85.
19. Mladenov, E., Iliakis, G., *The Pathways of Double-Strand Break Repair*, in *DNA Repair - On the Pathways to Fixing DNA Damage and Errors.*2011.
20. Krokan, H.E., R. Standal, and G. Slupphaug, *DNA glycosylases in the base excision repair of DNA.* The Biochemical journal, 1997. **325 (Pt 1)**: p. 1-16.
21. Prakash, A., et al., *Structural investigation of a viral ortholog of human NEIL2/3 DNA glycosylases.* DNA repair, 2013. **12**(12): p. 1062-71.
22. Matsumoto, Y., et al., *Escherichia coli Nth and human hNTH1 DNA glycosylases are involved in removal of 8-oxoguanine from 8-oxoguanine/guanine mispairs in DNA.* Nucleic acids research, 2001. **29**(9): p. 1975-81.
23. Hassa, P.O. and M.O. Hottiger, *The diverse biological roles of mammalian PARPS, a small but powerful family of poly-ADP-ribose polymerases.* Frontiers in bioscience : a journal and virtual library, 2008. **13**: p. 3046-82.
24. Collier, R.J., *Understanding the mode of action of diphtheria toxin: a perspective on progress during the 20th century.* Toxicon : official journal of the International Society on Toxinology, 2001. **39**(11): p. 1793-803.

25. Holbourn, K.P., C.C. Shone, and K.R. Acharya, *A family of killer toxins. Exploring the mechanism of ADP-ribosylating toxins.* The FEBS journal, 2006. **273**(20): p. 4579-93.
26. Messner, S., et al., *PARP1 ADP-ribosylates lysine residues of the core histone tails.* Nucleic acids research, 2010. **38**(19): p. 6350-62.
27. Hassa, P.O., et al., *Nuclear ADP-ribosylation reactions in mammalian cells: where are we today and where are we going?* Microbiology and molecular biology reviews : MMBR, 2006. **70**(3): p. 789-829.
28. Hottiger, M.O., et al., *Toward a unified nomenclature for mammalian ADP-ribosyltransferases.* Trends in biochemical sciences, 2010. **35**(4): p. 208-19.
29. Hottiger, M.O., *Nuclear ADP-Ribosylation and Its Role in Chromatin Plasticity, Cell Differentiation, and Epigenetics.* Annual review of biochemistry, 2015. **84**: p. 227-63.
30. Tanaka, M., et al., *Separation of oligo(adenosine diphosphate ribose) fractions with various chain lengths and terminal structures.* Biochemistry, 1977. **16**(7): p. 1485-89.
31. Rosenthal, F., et al., *Identification of distinct amino acids as ADP-ribose acceptor sites by mass spectrometry.* Methods in molecular biology, 2011. **780**: p. 57-66.
32. Rosenthal, F., et al., *Optimization of LTQ-Orbitrap Mass Spectrometer Parameters for the Identification of ADP-Ribosylation Sites.* Journal of proteome research, 2015.
33. Jungmichel, S., et al., *Proteome-wide identification of poly(ADP-Ribosyl)ation targets in different genotoxic stress responses.* Molecular cell, 2013. **52**(2): p. 272-85.
34. Berti, M., et al., *Human RECQ1 promotes restart of replication forks reversed by DNA topoisomerase I inhibition.* Nature structural & molecular biology, 2013. **20**(3): p. 347-54.
35. Krishnakumar, R. and W.L. Kraus, *PARP-1 regulates chromatin structure and transcription through a KDM5B-dependent pathway.* Molecular cell, 2010. **39**(5): p. 736-49.
36. Ditsworth, D., W.X. Zong, and C.B. Thompson, *Activation of poly(ADP)-ribose polymerase (PARP-1) induces release of the pro-inflammatory mediator HMGB1 from the nucleus.* The Journal of biological chemistry, 2007. **282**(24): p. 17845-54.
37. Houtkooper, R.H., et al., *The secret life of NAD+: an old metabolite controlling new metabolic signaling pathways.* Endocrine reviews, 2010. **31**(2): p. 194-223.
38. Ryu, K.W., D.S. Kim, and W.L. Kraus, *New facets in the regulation of gene expression by ADP-ribosylation and poly(ADP-ribose) polymerases.* Chemical reviews, 2015. **115**(6): p. 2453-81.
39. Revollo, J.R., A.A. Grimm, and S. Imai, *The NAD biosynthesis pathway mediated by nicotinamide phosphoribosyltransferase regulates Sir2 activity in mammalian cells.* The Journal of biological chemistry, 2004. **279**(49): p. 50754-63.
40. Canto, C., K.J. Menzies, and J. Auwerx, *NAD(+) Metabolism and the Control of Energy Homeostasis: A Balancing Act between Mitochondria and the Nucleus.* Cell metabolism, 2015. **22**(1): p. 31-53.
41. Conforti, L., et al., *Reducing expression of NAD+ synthesizing enzyme NMNAT1 does not affect the rate of Wallerian degeneration.* The FEBS journal, 2011. **278**(15): p. 2666-79.
42. Rajamohan, S.B., et al., *SIRT1 promotes cell survival under stress by deacetylation-dependent deactivation of poly(ADP-ribose) polymerase 1.* Molecular and cellular biology, 2009. **29**(15): p. 4116-29.
43. Bai, P., et al., *PARP-1 inhibition increases mitochondrial metabolism through SIRT1 activation.* Cell metabolism, 2011. **13**(4): p. 461-8.
44. Vyas, S., et al., *Family-wide analysis of poly(ADP-ribose) polymerase activity.* Nature communications, 2014. **5**: p. 4426.
45. Loseva, O., et al., *PARP-3 is a mono-ADP-ribosylase that activates PARP-1 in the absence of DNA.* The Journal of biological chemistry, 2010. **285**(11): p. 8054-60.
46. Rippmann, J.F., K. Damm, and A. Schnapp, *Functional characterization of the poly(ADP-ribose) polymerase activity of tankyrase 1, a potential regulator of telomere length.* Journal of molecular biology, 2002. **323**(2): p. 217-24.
47. Aguiar, R.C., et al., *B-aggressive lymphoma family proteins have unique domains that modulate transcription and exhibit poly(ADP-ribose) polymerase activity.* The Journal of biological chemistry, 2005. **280**(40): p. 33756-65.
48. Timinszky, G., et al., *A macrodomain-containing histone rearranges chromatin upon sensing PARP1 activation.* Nature structural & molecular biology, 2009. **16**(9): p. 923-9.
49. Pleschke, J.M., et al., *Poly(ADP-ribose) binds to specific domains in DNA damage checkpoint proteins.* The Journal of biological chemistry, 2000. **275**(52): p. 40974-80.

50. Ahel, I., et al., *Poly(ADP-ribose)-binding zinc finger motifs in DNA repair/checkpoint proteins.* Nature, 2008. **451**(7174): p. 81-5.
51. Hottiger, M.O., *ADP-ribosylation of histones by ARTD1: an additional module of the histone code?* FEBS letters, 2011. **585**(11): p. 1595-9.
52. Hottiger, M.O., *SnapShot: ADP-Ribosylation Signaling.* Molecular cell, 2015. **58**(6): p. 1134-1134 e1.
53. Popp, O., et al., *Site-specific noncovalent interaction of the biopolymer poly(ADP-ribose) with the Werner syndrome protein regulates protein functions.* ACS chemical biology, 2013. **8**(1): p. 179-88.
54. Min, W., et al., *Poly(ADP-ribose) binding to Chk1 at stalled replication forks is required for S-phase checkpoint activation.* Nature communications, 2013. **4**: p. 2993.
55. Fahrer, J., et al., *Quantitative analysis of the binding affinity of poly(ADP-ribose) to specific binding proteins as a function of chain length.* Nucleic acids research, 2007. **35**(21): p. e143.
56. Breslin, C., et al., *The XRCC1 phosphate-binding pocket binds poly (ADP-ribose) and is required for XRCC1 function.* Nucleic acids research, 2015. **43**(14): p. 6934-44.
57. Altmeyer, M., et al., *Liquid demixing of intrinsically disordered proteins is seeded by poly(ADP-ribose).* Nature communications, 2015. **6**: p. 8088.
58. Realini, C.A. and F.R. Althaus, *Histone shuttling by poly(ADP-ribosylation).* The Journal of biological chemistry, 1992. **267**(26): p. 18858-65.
59. Gottschalk, A.J., et al., *Poly(ADP-ribosyl)ation directs recruitment and activation of an ATP-dependent chromatin remodeler.* Proceedings of the National Academy of Sciences of the United States of America, 2009. **106**(33): p. 13770-4.
60. Ahel, D., et al., *Poly(ADP-ribose)-dependent regulation of DNA repair by the chromatin remodeling enzyme ALC1.* Science, 2009. **325**(5945): p. 1240-3.
61. Wielckens, K., et al., *DNA fragmentation and NAD depletion. Their relation to the turnover of endogenous mono(ADP-ribosyl) and poly(ADP-ribosyl) proteins.* The Journal of biological chemistry, 1982. **257**(21): p. 12872-7.
62. Alvarez-Gonzalez, R. and F.R. Althaus, *Poly(ADP-ribose) catabolism in mammalian cells exposed to DNA-damaging agents.* Mutation research, 1989. **218**(2): p. 67-74.
63. Brochu, G., G.M. Shah, and G.G. Poirier, *Purification of poly(ADP-ribose) glycohydrolase and detection of its isoforms by a zymogram following one- or two-dimensional electrophoresis.* Analytical biochemistry, 1994. **218**(2): p. 265-72.
64. Oka, S., J. Kato, and J. Moss, *Identification and characterization of a mammalian 39-kDa poly(ADP-ribose) glycohydrolase.* The Journal of biological chemistry, 2006. **281**(2): p. 705-13.
65. Rosenthal, F., et al., *Macrodomain-containing proteins are new mono-ADP-ribosylhydrolases.* Nature structural & molecular biology, 2013. **20**(4): p. 502-7.
66. Barkauskaite, E., et al., *The recognition and removal of cellular poly(ADP-ribose) signals.* The FEBS journal, 2013. **280**(15): p. 3491-507.
67. Jankevicius, G., et al., *A family of macrodomain proteins reverses cellular mono-ADP-ribosylation.* Nature structural & molecular biology, 2013. **20**(4): p. 508-14.
68. Hottiger, M.O., *Poly(ADP-ribose) polymerase inhibitor therapeutic effect: are we just scratching the surface?* Expert opinion on therapeutic targets, 2015. **19**(9): p. 1149-52.
69. Wahlberg, E., et al., *Family-wide chemical profiling and structural analysis of PARP and tankyrase inhibitors.* Nature biotechnology, 2012. **30**(3): p. 283-8.
70. Hassa, P.O. and M.O. Hottiger, *The functional role of poly(ADP-ribose)polymerase 1 as novel coactivator of NF-kappaB in inflammatory disorders.* Cellular and molecular life sciences : CMLS, 2002. **59**(9): p. 1534-53.
71. Burkle, A. and L. Virag, *Poly(ADP-ribose): PARadigms and PARadoxes.* Molecular aspects of medicine, 2013. **34**(6): p. 1046-65.
72. Feng, F.Y., et al., *Chromatin to Clinic: The Molecular Rationale for PARP1 Inhibitor Function.* Molecular cell, 2015. **58**(6): p. 925-34.
73. Hopkins, T.A., et al., *Mechanistic Dissection of PARP1 Trapping and the Impact on in vivo Tolerability and Efficacy of PARP Inhibitors.* Molecular cancer research : MCR, 2015.
74. Giansanti, V., et al., *PARP inhibitors: new tools to protect from inflammation.* Biochemical pharmacology, 2010. **80**(12): p. 1869-77.
75. Qin, W.D., et al., *Poly(ADP-ribose) polymerase 1 inhibition protects against low shear stress induced inflammation.* Biochimica et biophysica acta, 2013. **1833**(1): p. 59-68.

76. Kauppinen, T.M., et al., *Inhibition of poly(ADP-ribose) polymerase suppresses inflammation and promotes recovery after ischemic injury.* Journal of cerebral blood flow and metabolism : official journal of the International Society of Cerebral Blood Flow and Metabolism, 2009. **29**(4): p. 820-9.
77. Vyas, S., et al., *A systematic analysis of the PARP protein family identifies new functions critical for cell physiology.* Nature communications, 2013. **4**: p. 2240.
78. Wang, Z.Q., et al., *PARP is important for genomic stability but dispensable in apoptosis.* Genes & development, 1997. **11**(18): p. 2347-58.
79. Wang, Z.Q., et al., *Mice lacking ADPRT and poly(ADP-ribosyl)ation develop normally but are susceptible to skin disease.* Genes & development, 1995. **9**(5): p. 509-20.
80. Shall, S. and G. de Murcia, *Poly(ADP-ribose) polymerase-1: what have we learned from the deficient mouse model?* Mutation research, 2000. **460**(1): p. 1-15.
81. Kraus, W.L. and M.O. Hottiger, *PARP-1 and gene regulation: progress and puzzles.* Molecular aspects of medicine, 2013. **34**(6): p. 1109-23.
82. Wacker, D.A., et al., *The DNA binding and catalytic domains of poly(ADP-ribose) polymerase 1 cooperate in the regulation of chromatin structure and transcription.* Molecular and cellular biology, 2007. **27**(21): p. 7475-85.
83. Altmeyer, M., et al., *Molecular mechanism of poly(ADP-ribosyl)ation by PARP1 and identification of lysine residues as ADP-ribose acceptor sites.* Nucleic acids research, 2009. **37**(11): p. 3723-38.
84. D'Amours, D., et al., *Poly(ADP-ribosyl)ation reactions in the regulation of nuclear functions.* The Biochemical journal, 1999. **342 (Pt 2)**: p. 249-68.
85. Langelier, M.F., et al., *Structural basis for DNA damage-dependent poly(ADP-ribosyl)ation by human PARP-1.* Science, 2012. **336**(6082): p. 728-32.
86. Chapman, J.D., et al., *Mapping PARP-1 auto-ADP-ribosylation sites by liquid chromatography-tandem mass spectrometry.* Journal of proteome research, 2013. **12**(4): p. 1868-80.
87. Gradwohl, G., et al., *The second zinc-finger domain of poly(ADP-ribose) polymerase determines specificity for single-stranded breaks in DNA.* Proceedings of the National Academy of Sciences of the United States of America, 1990. **87**(8): p. 2990-4.
88. Ali, A.A., et al., *The zinc-finger domains of PARP1 cooperate to recognize DNA strand breaks.* Nature structural & molecular biology, 2012. **19**(7): p. 685-92.
89. Mortusewicz, O., et al., *Feedback-regulated poly(ADP-ribosyl)ation by PARP-1 is required for rapid response to DNA damage in living cells.* Nucleic acids research, 2007. **35**(22): p. 7665-75.
90. Woodhouse, B.C., et al., *Poly(ADP-ribose) polymerase-1 modulates DNA repair capacity and prevents formation of DNA double strand breaks.* DNA repair, 2008. **7**(6): p. 932-40.
91. Ju, B.G., et al., *A topoisomerase IIbeta-mediated dsDNA break required for regulated transcription.* Science, 2006. **312**(5781): p. 1798-802.
92. Virag, L., et al., *Requirement of intracellular calcium mobilization for peroxynitrite-induced poly(ADP-ribose) synthetase activation and cytotoxicity.* Molecular pharmacology, 1999. **56**(4): p. 824-33.
93. Bentle, M.S., et al., *Calcium-dependent modulation of poly(ADP-ribose) polymerase-1 alters cellular metabolism and DNA repair.* The Journal of biological chemistry, 2006. **281**(44): p. 33684-96.
94. Kim, M.Y., et al., *NAD+-dependent modulation of chromatin structure and transcription by nucleosome binding properties of PARP-1.* Cell, 2004. **119**(6): p. 803-14.
95. Lonskaya, I., et al., *Regulation of poly(ADP-ribose) polymerase-1 by DNA structure-specific binding.* The Journal of biological chemistry, 2005. **280**(17): p. 17076-83.
96. Berger, F., C. Lau, and M. Ziegler, *Regulation of poly(ADP-ribose) polymerase 1 activity by the phosphorylation state of the nuclear NAD biosynthetic enzyme NMN adenylyl transferase 1.* Proceedings of the National Academy of Sciences of the United States of America, 2007. **104**(10): p. 3765-70.
97. Cohen-Armon, M., et al., *DNA-independent PARP-1 activation by phosphorylated ERK2 increases Elk1 activity: a link to histone acetylation.* Molecular cell, 2007. **25**(2): p. 297-308.
98. Zhang, S., et al., *c-Jun N-terminal kinase mediates hydrogen peroxide-induced cell death via sustained poly(ADP-ribose) polymerase-1 activation.* Cell death and differentiation, 2007. **14**(5): p. 1001-10.

99. Yoo, Y.D., et al., *Fibroblast growth factor regulates human neuroectoderm specification through ERK1/2-PARP-1 pathway.* Stem cells, 2011. **29**(12): p. 1975-82.
100. Liu, L., et al., *Lipopolysaccharide activates ERK-PARP-1-RelA pathway and promotes nuclear factor-kappaB transcription in murine macrophages.* Human immunology, 2012. **73**(5): p. 439-47.
101. Kauppinen, T.M., et al., *Direct phosphorylation and regulation of poly(ADP-ribose) polymerase-1 by extracellular signal-regulated kinases 1/2.* Proceedings of the National Academy of Sciences of the United States of America, 2006. **103**(18): p. 7136-41.
102. Wright, R.H., et al., *CDK2-dependent activation of PARP-1 is required for hormonal gene regulation in breast cancer cells.* Genes & development, 2012. **26**(17): p. 1972-83.
103. Hegedus, C., et al., *Protein kinase C protects from DNA damage-induced necrotic cell death by inhibiting poly(ADP-ribose) polymerase-1.* FEBS letters, 2008. **582**(12): p. 1672-8.
104. Bauer, P.I., et al., *Inhibition of DNA binding by the phosphorylation of poly ADP-ribose polymerase protein catalysed by protein kinase C.* Biochemical and Biophysical Research Communications, 1992. **187**(2): p. 730-6.
105. Gagne, J.P., et al., *Proteomic investigation of phosphorylation sites in poly(ADP-ribose) polymerase-1 and poly(ADP-ribose) glycohydrolase.* Journal of proteome research, 2009. **8**(2): p. 1014-29.
106. Ju, B.G., et al., *Activating the PARP-1 sensor component of the groucho/ TLE1 corepressor complex mediates a CaMKinase IIdelta-dependent neurogenic gene activation pathway.* Cell, 2004. **119**(6): p. 815-29.
107. Kolthur-Seetharam, U., et al., *Control of AIF-mediated cell death by the functional interplay of SIRT1 and PARP-1 in response to DNA damage.* Cell cycle, 2006. **5**(8): p. 873-7.
108. Canto, C., A.A. Sauve, and P. Bai, *Crosstalk between poly(ADP-ribose) polymerase and sirtuin enzymes.* Molecular aspects of medicine, 2013. **34**(6): p. 1168-201.
109. Kraus, W.L., *Transcriptional control by PARP-1: chromatin modulation, enhancer-binding, coregulation, and insulation.* Current opinion in cell biology, 2008. **20**(3): p. 294-302.
110. Olabisi, O.A., et al., *Regulation of transcription factor NFAT by ADP-ribosylation.* Molecular and cellular biology, 2008. **28**(9): p. 2860-71.
111. Zaniolo, K., et al., *Regulation of poly(ADP-ribose) polymerase-1 (PARP-1) gene expression through the post-translational modification of Sp1: a nuclear target protein of PARP-1.* BMC molecular biology, 2007. **8**: p. 96.
112. Pavri, R., et al., *PARP-1 determines specificity in a retinoid signaling pathway via direct modulation of mediator.* Molecular cell, 2005. **18**(1): p. 83-96.
113. Hassa, P.O., et al., *Acetylation of poly(ADP-ribose) polymerase-1 by p300/CREB-binding protein regulates coactivation of NF-kappaB-dependent transcription.* The Journal of biological chemistry, 2005. **280**(49): p. 40450-64.
114. Tsompana, M. and M.J. Buck, *Chromatin accessibility: a window into the genome.* Epigenetics & chromatin, 2014. **7**(1): p. 33.
115. Margueron, R. and D. Reinberg, *Chromatin structure and the inheritance of epigenetic information.* Nature reviews. Genetics, 2010. **11**(4): p. 285-96.
116. Cedar, H. and Y. Bergman, *Linking DNA methylation and histone modification: patterns and paradigms.* Nature reviews. Genetics, 2009. **10**(5): p. 295-304.
117. Uysal, F., G. Akkoyunlu, and S. Ozturk, *Dynamic expression of DNA methyltransferases (DNMTs) in oocytes and early embryos.* Biochimie, 2015. **116**: p. 103-13.
118. Pombo, A. and N. Dillon, *Three-dimensional genome architecture: players and mechanisms.* Nature reviews. Molecular cell biology, 2015. **16**(4): p. 245-57.
119. Biterge, B. and R. Schneider, *Histone variants: key players of chromatin.* Cell and tissue research, 2014. **356**(3): p. 457-66.
120. Li, G. and D. Reinberg, *Chromatin higher-order structures and gene regulation.* Current Opinion in Genetics & Development, 2011. **21**(2): p. 175-86.
121. Chakravarthy, S. and K. Luger, *The histone variant macro-H2A preferentially forms "hybrid nucleosomes".* The Journal of biological chemistry, 2006. **281**(35): p. 25522-31.
122. Clausell, J., et al., *Histone H1 subtypes differentially modulate chromatin condensation without preventing ATP-dependent remodeling by SWI/SNF or NURF.* PloS one, 2009. **4**(10): p. e0007243.
123. Kouzarides, T., *Chromatin modifications and their function.* Cell, 2007. **128**(4): p. 693-705.

124. Taddei, A., et al., *The effects of histone deacetylase inhibitors on heterochromatin: implications for anticancer therapy?* EMBO reports, 2005. **6**(6): p. 520-4.
125. Zhang, P., E. Bergamin, and J.F. Couture, *The many facets of MLL1 regulation.* Biopolymers, 2013. **99**(2): p. 136-45.
126. McCarthy, N., *Leukaemia: MLL makes friends and influences.* Nature reviews. Cancer, 2010. **10**(8): p. 529.
127. Saksouk, N., E. Simboeck, and J. Dejardin, *Constitutive heterochromatin formation and transcription in mammals.* Epigenetics & chromatin, 2015. **8**: p. 3.
128. Margueron, R. and D. Reinberg, *The Polycomb complex PRC2 and its mark in life.* Nature, 2011. **469**(7330): p. 343-9.
129. Pedersen, M.T. and K. Helin, *Histone demethylases in development and disease.* Trends in cell biology, 2010. **20**(11): p. 662-71.
130. Kamieniarz, K., et al., *A dual role of linker histone H1.4 Lys 34 acetylation in transcriptional activation.* Genes & development, 2012. **26**(8): p. 797-802.
131. Yun, M., et al., *Readers of histone modifications.* Cell research, 2011. **21**(4): p. 564-78.
132. Kassner, I., et al., *Crosstalk between SET7/9-dependent methylation and ARTD1-mediated ADP-ribosylation of histone H1.4.* Epigenetics & chromatin, 2013. **6**(1): p. 1.
133. Wood, C., et al., *Post-translational modifications of the linker histone variants and their association with cell mechanisms.* The FEBS journal, 2009. **276**(14): p. 3685-97.
134. Ogata, N., K. Ueda, and O. Hayaishi, *ADP-ribosylation of histone H2B. Identification of glutamic acid residue 2 as the modification site.* The Journal of biological chemistry, 1980. **255**(16): p. 7610-5.
135. El-Khamisy, S.F., et al., *A requirement for PARP-1 for the assembly or stability of XRCC1 nuclear foci at sites of oxidative DNA damage.* Nucleic acids research, 2003. **31**(19): p. 5526-33.
136. Das, B.B., et al., *PARP1-TDP1 coupling for the repair of topoisomerase I-induced DNA damage.* Nucleic acids research, 2014. **42**(7): p. 4435-49.
137. Tulin, A. and A. Spradling, *Chromatin loosening by poly(ADP)-ribose polymerase (PARP) at Drosophila puff loci.* Science, 2003. **299**(5606): p. 560-2.
138. Thomas, C.J., et al., *Kinase-Mediated Changes in Nucleosome Conformation Trigger Chromatin Decondensation via Poly(ADP-Ribosyl)ation.* Molecular cell, 2014.
139. Erener, S., et al., *Inflammasome-Activated Caspase 7 Cleaves PARP1 to Enhance the Expression of a Subset of NF-kappaB Target Genes.* Molecular cell, 2012.
140. Ju, B.G., *A Topoisomerase II -Mediated dsDNA Break Required for Regulated Transcription.* Science, 2006. **312**(5781): p. 1798-1802.
141. Guastafierro, T., et al., *CCCTC-binding factor activates PARP-1 affecting DNA methylation machinery.* The Journal of biological chemistry, 2008. **283**(32): p. 21873-80.
142. Caiafa, P., T. Guastafierro, and M. Zampieri, *Epigenetics: poly(ADP-ribosyl)ation of PARP-1 regulates genomic methylation patterns.* FASEB journal : official publication of the Federation of American Societies for Experimental Biology, 2009. **23**(3): p. 672-8.
143. De Vos, M., et al., *Poly(ADP-ribose) polymerase 1 (PARP1) associates with E3 ubiquitin-protein ligase UHRF1 and modulates UHRF1 biological functions.* The Journal of biological chemistry, 2014. **289**(23): p. 16223-38.
144. Guetg, C., et al., *Inheritance of silent rDNA chromatin is mediated by PARP1 via noncoding RNA.* Molecular cell, 2012. **45**(6): p. 790-800.
145. Yu, W., et al., *Poly(ADP-ribosyl)ation regulates CTCF-dependent chromatin insulation.* Nature genetics, 2004. **36**(10): p. 1105-10.
146. Zhao, H., et al., *PARP1- and CTCF-Mediated Interactions between Active and Repressed Chromatin at the Lamina Promote Oscillating Transcription.* Molecular cell, 2015.
147. Farrar, D., et al., *Mutational analysis of the poly(ADP-ribosyl)ation sites of the transcription factor CTCF provides an insight into the mechanism of its regulation by poly(ADP-ribosyl)ation.* Molecular and cellular biology, 2010. **30**(5): p. 1199-216.
148. Ong, C.T., et al., *Poly(ADP-ribosyl)ation regulates insulator function and intrachromosomal interactions in Drosophila.* Cell, 2013. **155**(1): p. 148-59.
149. Hock, R., et al., *HMG chromosomal proteins in development and disease.* Trends in cell biology, 2007. **17**(2): p. 72-9.
150. Bustin, M., *Revised nomenclature for high mobility group (HMG) chromosomal proteins.* Trends in biochemical sciences, 2001. **26**(3): p. 152-3.

151. Stros, M., D. Launholt, and K.D. Grasser, *The HMG-box: a versatile protein domain occurring in a wide variety of DNA-binding proteins.* Cellular and molecular life sciences : CMLS, 2007. **64**(19-20): p. 2590-606.
152. Bustin, M., R.B. Hopkins, and I. Isenberg, *Immunological relatedness of high mobility group chromosomal proteins from calf thymus.* The Journal of biological chemistry, 1978. **253**(5): p. 1694-9.
153. Stros, M., *HMGB proteins: interactions with DNA and chromatin.* Biochimica et biophysica acta, 2010. **1799**(1-2): p. 101-13.
154. Weir, H.M., et al., *Structure of the HMG box motif in the B-domain of HMG1.* The EMBO journal, 1993. **12**(4): p. 1311-9.
155. Read, C.M., et al., *Solution structure of a DNA-binding domain from HMG1.* Nucleic acids research, 1993. **21**(15): p. 3427-36.
156. Scaffidi, P., T. Misteli, and M.E. Bianchi, *Release of chromatin protein HMGB1 by necrotic cells triggers inflammation.* Nature, 2002. **418**(6894): p. 191-5.
157. Falciola, L., et al., *High mobility group 1 protein is not stably associated with the chromosomes of somatic cells.* The Journal of cell biology, 1997. **137**(1): p. 19-26.
158. Hughes, E.N., B.N. Engelsberg, and P.C. Billings, *Purification of nuclear proteins that bind to cisplatin-damaged DNA. Identity with high mobility group proteins 1 and 2.* The Journal of biological chemistry, 1992. **267**(19): p. 13520-7.
159. Bianchi, M.E., M. Beltrame, and G. Paonessa, *Specific recognition of cruciform DNA by nuclear protein HMG1.* Science, 1989. **243**(4894 Pt 1): p. 1056-9.
160. Isackson, P.J., et al., *Preferential affinity of high molecular weight high mobility group non-histone chromatin proteins for single-stranded DNA.* The Journal of biological chemistry, 1979. **254**(13): p. 5569-72.
161. Ueda, T., et al., *Acidic C-tail of HMGB1 is required for its target binding to nucleosome linker DNA and transcription stimulation.* Biochemistry, 2004. **43**(30): p. 9901-8.
162. Watson, M., et al., *Characterization of the interaction between HMGB1 and H3--a possible means of positioning HMGB1 in chromatin.* Nucleic acids research, 2014. **42**(2): p. 848-59.
163. Pil, P.M., C.S. Chow, and S.J. Lippard, *High-mobility-group 1 protein mediates DNA bending as determined by ring closures.* Proceedings of the National Academy of Sciences of the United States of America, 1993. **90**(20): p. 9465-9.
164. Paull, T.T., M.J. Haykinson, and R.C. Johnson, *The nonspecific DNA-binding and -bending proteins HMG1 and HMG2 promote the assembly of complex nucleoprotein structures.* Genes & development, 1993. **7**(8): p. 1521-34.
165. Bonaldi, T., et al., *The DNA chaperone HMGB1 facilitates ACF/CHRAC-dependent nucleosome sliding.* The EMBO journal, 2002. **21**(24): p. 6865-73.
166. Joshi, S.R., et al., *Nucleosome dynamics: HMGB1 relaxes canonical nucleosome structure to facilitate estrogen receptor binding.* Nucleic acids research, 2012. **40**(20): p. 10161-71.
167. Celona, B., et al., *Substantial histone reduction modulates genomewide nucleosomal occupancy and global transcriptional output.* PLoS biology, 2011. **9**(6): p. e1001086.
168. Cato, L., et al., *The interaction of HMGB1 and linker histones occurs through their acidic and basic tails.* Journal of molecular biology, 2008. **384**(5): p. 1262-72.
169. Thomas, J.O. and K. Stott, *H1 and HMGB1: modulators of chromatin structure.* Biochemical Society transactions, 2012. **40**(2): p. 341-6.
170. Reddy, M.C., J. Christensen, and K.M. Vasquez, *Interplay between human high mobility group protein 1 and replication protein A on psoralen-cross-linked DNA.* Biochemistry, 2005. **44**(11): p. 4188-95.
171. Yusein-Myashkova, S., I. Ugrinova, and E. Pasheva, *Non-histone protein HMGB1 inhibits the repair of cisplatin damaged DNA in NIH-3T3 murine fibroblasts.* BMB reports, 2013.
172. Lange, S.S., M.C. Reddy, and K.M. Vasquez, *Human HMGB1 directly facilitates interactions between nucleotide excision repair proteins on triplex-directed psoralen interstrand crosslinks.* DNA repair, 2009. **8**(7): p. 865-72.
173. Prasad, R., et al., *HMGB1 is a cofactor in mammalian base excision repair.* Molecular cell, 2007. **27**(5): p. 829-41.
174. Jiao, Y., H.C. Wang, and S.J. Fan, *Growth suppression and radiosensitivity increase by HMGB1 in breast cancer.* Acta pharmacologica Sinica, 2007. **28**(12): p. 1957-67.
175. McKinney, K. and C. Prives, *Efficient specific DNA binding by p53 requires both its central and C-terminal domains as revealed by studies with high-mobility group 1 protein.* Molecular and cellular biology, 2002. **22**(19): p. 6797-808.

176. Rowell, J.P., et al., *HMGB1-facilitated p53 DNA binding occurs via HMG-Box/p53 transactivation domain interaction, regulated by the acidic tail.* Structure, 2012. **20**(12): p. 2014-24.
177. Livesey, K.M., et al., *p53/HMGB1 complexes regulate autophagy and apoptosis.* Cancer research, 2012. **72**(8): p. 1996-2005.
178. Agresti, A., et al., *HMGB1 interacts differentially with members of the Rel family of transcription factors.* Biochemical and Biophysical Research Communications, 2003. **302**(2): p. 421-426.
179. Ramachandran, C., et al., *Phosphorylation of high-mobility-group proteins by the calcium-phospholipid-dependent protein kinase and the cyclic AMP-dependent protein kinase.* The Journal of biological chemistry, 1984. **259**(21): p. 13495-503.
180. Youn, J.H. and J.S. Shin, *Nucleocytoplasmic shuttling of HMGB1 is regulated by phosphorylation that redirects it toward secretion.* Journal of immunology, 2006. **177**(11): p. 7889-97.
181. Ugrinova, I., et al., *In vivo acetylation of HMG1 protein enhances its binding affinity to distorted DNA structures.* Biochemistry, 2001. **40**(48): p. 14655-60.
182. Bonaldi, T., et al., *Monocytic cells hyperacetylate chromatin protein HMGB1 to redirect it towards secretion.* The EMBO journal, 2003. **22**(20): p. 5551-60.
183. Ito, I., J. Fukazawa, and M. Yoshida, *Post-translational methylation of high mobility group box 1 (HMGB1) causes its cytoplasmic localization in neutrophils.* The Journal of biological chemistry, 2007. **282**(22): p. 16336-44.
184. Wu, F., et al., *High mobility group box 1 protein is methylated and transported to cytoplasm in clear cell renal cell carcinoma.* Asian Pacific journal of cancer prevention : APJCP, 2013. **14**(10): p. 5789-95.
185. Tanuma, S. and G.S. Johnson, *ADP-ribosylation of nonhistone high mobility group proteins in intact cells.* The Journal of biological chemistry, 1983. **258**(7): p. 4067-70.
186. Poirier, G.G., et al., *Adenosine diphosphate ribosylation of chicken-erythrocyte histones H1, H5 and high-mobility-group proteins by purified calf-thymus poly(adenosinediphosphate-ribose) polymerase.* European journal of biochemistry / FEBS, 1982. **127**(3): p. 437-42.
187. Yang, Z., et al., *PARP-1 mediates LPS-induced HMGB1 release by macrophages through regulation of HMGB1 acetylation.* Journal of immunology, 2014. **193**(12): p. 6114-23.
188. Davis, K., et al., *Poly(ADP-ribosyl)ation of high mobility group box 1 (HMGB1) protein enhances inhibition of efferocytosis.* Molecular medicine, 2012. **18**: p. 359-69.
189. Oh, Y.J., et al., *HMGB1 is phosphorylated by classical protein kinase C and is secreted by a calcium-dependent mechanism.* Journal of immunology, 2009. **182**(9): p. 5800-9.
190. Ugrinova, I., S. Zlateva, and E. Pasheva, *The effect of PKC phosphorylation on the "architectural" properties of HMGB1 protein.* Molecular biology reports, 2012. **39**(11): p. 9947-53.
191. Kang, H.J., et al., *Non-histone nuclear factor HMGB1 is phosphorylated and secreted in colon cancers.* Laboratory Investigation, 2009. **89**(8): p. 948-959.
192. Shin, J.H., et al., *Ethyl pyruvate inhibits HMGB1 phosphorylation and release by chelating calcium.* Molecular medicine, 2014. **20**: p. 649-57.
193. Passalacqua, M., et al., *Secretion and binding of HMG1 protein to the external surface of the membrane are required for murine erythroleukemia cell differentiation.* FEBS letters, 1997. **400**(3): p. 275-9.
194. Ugrinova, I., I.G. Pashev, and E.A. Pasheva, *Post-synthetic acetylation of HMGB1 protein modulates its interactions with supercoiled DNA.* Molecular biology reports, 2008. **36**(6): p. 1399-1404.
195. Ugrinova, I., I.G. Pashev, and E.A. Pasheva, *Nucleosome binding properties and Co-remodeling activities of native and in vivo acetylated HMGB-1 and HMGB-2 proteins.* Biochemistry, 2009. **48**(27): p. 6502-7.
196. Bianchi, M.E. and A.A. Manfredi, *How macrophages ring the inflammation alarm.* Proceedings of the National Academy of Sciences of the United States of America, 2014. **111**(8): p. 2866-7.
197. Lu, B., et al., *JAK/STAT1 signaling promotes HMGB1 hyperacetylation and nuclear translocation.* Proceedings of the National Academy of Sciences of the United States of America, 2014. **111**(8): p. 3068-73.
198. Barton, G.M., *A calculated response: control of inflammation by the innate immune system.* The Journal of clinical investigation, 2008. **118**(2): p. 413-20.

199. Medzhitov, R., *Origin and physiological roles of inflammation.* Nature, 2008. **454**(7203): p. 428-35.
200. Hayden, M.S. and S. Ghosh, *Shared principles in NF-kappaB signaling.* Cell, 2008. **132**(3): p. 344-62.
201. Lawrence, T., *The nuclear factor NF-kappaB pathway in inflammation.* Cold Spring Harbor perspectives in biology, 2009. **1**(6): p. a001651.
202. Gerondakis, S., et al., *NF-kappaB control of T cell development.* Nature immunology, 2014. **15**(1): p. 15-25.
203. Hoffmann, A., G. Natoli, and G. Ghosh, *Transcriptional regulation via the NF-kappaB signaling module.* Oncogene, 2006. **25**(51): p. 6706-16.
204. Hayden, M.S. and S. Ghosh, *NF-kappaB, the first quarter-century: remarkable progress and outstanding questions.* Genes & development, 2012. **26**(3): p. 203-34.
205. Millet, P., C. McCall, and B. Yoza, *RelB: an outlier in leukocyte biology.* Journal of leukocyte biology, 2013.
206. Razani, B., A.D. Reichardt, and G. Cheng, *Non-canonical NF-kappaB signaling activation and regulation: principles and perspectives.* Immunological reviews, 2011. **244**(1): p. 44-54.
207. Natoli, G., *NF-kappaB and chromatin: ten years on the path from basic mechanisms to candidate drugs.* Immunological reviews, 2012. **246**(1): p. 183-92.
208. Hassa, P.O., et al., *Protein arginine methyltransferase 1 coactivates NF-kappaB-dependent gene expression synergistically with CARM1 and PARP1.* Journal of molecular biology, 2008. **377**(3): p. 668-78.
209. Handschick, K., et al., *Cyclin-dependent kinase 6 is a chromatin-bound cofactor for NF-kappaB-dependent gene expression.* Molecular cell, 2014. **53**(2): p. 193-208.
210. Gao, Z., et al., *Coactivators and corepressors of NF-kappaB in IkappaB alpha gene promoter.* The Journal of biological chemistry, 2005. **280**(22): p. 21091-8.
211. Oliver, F.J., et al., *Resistance to endotoxic shock as a consequence of defective NF-kappaB activation in poly (ADP-ribose) polymerase-1 deficient mice.* The EMBO journal, 1999. **18**(16): p. 4446-54.
212. Hassa, P.O. and M.O. Hottiger, *A role of poly (ADP-ribose) polymerase in NF-kappaB transcriptional activation.* Biological chemistry, 1999. **380**(7-8): p. 953-9.
213. Kameoka, M., et al., *Evidence for regulation of NF-kappaB by poly(ADP-ribose) polymerase.* The Biochemical journal, 2000. **346 Pt 3**: p. 641-9.
214. Hassa, P.O., et al., *The enzymatic and DNA binding activity of PARP-1 are not required for NF-kappa B coactivator function.* The Journal of biological chemistry, 2001. **276**(49): p. 45588-97.
215. Kauppinen, T.M., L. Gan, and R.A. Swanson, *Poly(ADP-ribose) polymerase-1-induced NAD(+) depletion promotes nuclear factor-kappaB transcriptional activity by preventing p65 de-acetylation.* Biochimica et biophysica acta, 2013. **1833**(8): p. 1985-91.
216. Andersson, U., et al., *High mobility group 1 protein (HMG-1) stimulates proinflammatory cytokine synthesis in human monocytes.* The Journal of experimental medicine, 2000. **192**(4): p. 565-70.
217. Wang, H., *HMG-1 as a Late Mediator of Endotoxin Lethality in Mice.* Science, 1999. **285**(5425): p. 248-251.
218. Tsung, A., et al., *The nuclear factor HMGB1 mediates hepatic injury after murine liver ischemia-reperfusion.* The Journal of experimental medicine, 2005. **201**(7): p. 1135-43.
219. Goldstein, R.S., et al., *Elevated high-mobility group box 1 levels in patients with cerebral and myocardial ischemia.* Shock, 2006. **25**(6): p. 571-4.
220. Rickenbacher, A., et al., *Fasting protects liver from ischemic injury through Sirt1-mediated downregulation of circulating HMGB1 in mice.* Journal of hepatology, 2014. **61**(2): p. 301-8.
221. Pullerits, R., et al., *High mobility group box chromosomal protein 1, a DNA binding cytokine, induces arthritis.* Arthritis and rheumatism, 2003. **48**(6): p. 1693-700.
222. Tsung, A., S. Tohme, and T.R. Billiar, *High-mobility group box-1 in sterile inflammation.* Journal of internal medicine, 2014. **276**(5): p. 425-43.
223. Hori, O., et al., *The receptor for advanced glycation end products (RAGE) is a cellular binding site for amphoterin. Mediation of neurite outgrowth and co-expression of rage and amphoterin in the developing nervous system.* The Journal of biological chemistry, 1995. **270**(43): p. 25752-61.

224. Schiraldi, M., et al., *HMGB1 promotes recruitment of inflammatory cells to damaged tissues by forming a complex with CXCL12 and signaling via CXCR4.* The Journal of experimental medicine, 2012. **209**(3): p. 551-63.
225. Venereau, E., et al., *Mutually exclusive redox forms of HMGB1 promote cell recruitment or proinflammatory cytokine release.* The Journal of experimental medicine, 2012. **209**(9): p. 1519-28.
226. Jornot, L., H. Petersen, and A.F. Junod, *Hydrogen peroxide-induced DNA damage is independent of nuclear calcium but dependent on redox-active ions.* The Biochemical journal, 1998. **335 (Pt 1)**: p. 85-94.
227. Noren Hooten, N., et al., *Poly(ADP-ribose) polymerase 1 (PARP-1) binds to 8-oxoguanine-DNA glycosylase (OGG1).* The Journal of biological chemistry, 2011. **286**(52): p. 44679-90.
228. Bryant, H.E., et al., *PARP is activated at stalled forks to mediate Mre11-dependent replication restart and recombination.* The EMBO journal, 2009. **28**(17): p. 2601-15.
229. Minocherhomji, S. and I.D. Hickson, *Structure-specific endonucleases: guardians of fragile site stability.* Trends in cell biology, 2014. **24**(5): p. 321-7.
230. Grasby, J.A., et al., *Unpairing and gating: sequence-independent substrate recognition by FEN superfamily nucleases.* Trends in biochemical sciences, 2012. **37**(2): p. 74-84.
231. Zhang, J. and J.C. Walter, *Mechanism and regulation of incisions during DNA interstrand cross-link repair.* DNA repair, 2014. **19**: p. 135-42.
232. Lee, J.S., et al., *CHIP has a protective role against oxidative stress-induced cell death through specific regulation of endonuclease G.* Cell death & disease, 2013. **4**: p. e666.
233. Noren Hooten, N., et al., *Coordination of DNA repair by NEIL1 and PARP-1: a possible link to aging.* Aging, 2012. **4**(10): p. 674-85.
234. Biswas, S.K. and E. Lopez-Collazo, *Endotoxin tolerance: new mechanisms, molecules and clinical significance.* Trends in immunology, 2009. **30**(10): p. 475-87.
235. Foster, S.L. and R. Medzhitov, *Gene-specific control of the TLR-induced inflammatory response.* Clinical immunology, 2009. **130**(1): p. 7-15.
236. El Gazzar, M., et al., *Chromatin-specific remodeling by HMGB1 and linker histone H1 silences proinflammatory genes during endotoxin tolerance.* Molecular and cellular biology, 2009. **29**(7): p. 1959-71.
237. Midorikawa, R., Y. Takei, and N. Hirokawa, *KIF4 motor regulates activity-dependent neuronal survival by suppressing PARP-1 enzymatic activity.* Cell, 2006. **125**(2): p. 371-83.
238. Prasad, R., et al., *DNA polymerase beta -mediated long patch base excision repair. Poly(ADP-ribose)polymerase-1 stimulates strand displacement DNA synthesis.* The Journal of biological chemistry, 2001. **276**(35): p. 32411-4.
239. Prasad, R., et al., *Mammalian Base Excision Repair: Functional Partnership between PARP-1 and APE1 in AP-Site Repair.* PloS one, 2015. **10**(5): p. e0124269.
240. Khodyreva, S.N., et al., *Apurinic/apyrimidinic (AP) site recognition by the 5'-dRP/AP lyase in poly(ADP-ribose) polymerase-1 (PARP-1).* Proceedings of the National Academy of Sciences of the United States of America, 2010. **107**(51): p. 22090-5.
241. Dobi, A. and D. v Agoston, *Submillimolar levels of calcium regulates DNA structure at the dinucleotide repeat (TG/AC)n.* Proceedings of the National Academy of Sciences of the United States of America, 1998. **95**(11): p. 5981-6.
242. Treco, D. and N. Arnheim, *The evolutionarily conserved repetitive sequence d(TG.AC)n promotes reciprocal exchange and generates unusual recombinant tetrads during yeast meiosis.* Molecular and cellular biology, 1986. **6**(11): p. 3934-47.
243. Benet, A., G. Molla, and F. Azorin, *d(GA x TC)(n) microsatellite DNA sequences enhance homologous DNA recombination in SV40 minichromosomes.* Nucleic acids research, 2000. **28**(23): p. 4617-22.
244. Tice, R.R., et al., *Single cell gel/comet assay: guidelines for in vitro and in vivo genetic toxicology testing.* Environmental and molecular mutagenesis, 2000. **35**(3): p. 206-21.
245. Liu, M., et al., *Structural characterization of a mouse ortholog of human NEIL3 with a marked preference for single-stranded DNA.* Structure, 2013. **21**(2): p. 247-56.
246. Jacobs, A.L. and P. Schar, *DNA glycosylases: in DNA repair and beyond.* Chromosoma, 2012. **121**(1): p. 1-20.
247. Jacobs, A.C., et al., *Inhibition of DNA glycosylases via small molecule purine analogs.* PloS one, 2013. **8**(12): p. e81667.

248. Chen, Y., et al., *Acyl-CoA-binding domain containing 3 modulates NAD+ metabolism through activating poly(ADP-ribose) polymerase 1.* The Biochemical journal, 2015. **469**(2): p. 189-98.
249. Krukenberg, K.A., et al., *Basal activity of a PARP1-NuA4 complex varies dramatically across cancer cell lines.* Cell reports, 2014. **8**(6): p. 1808-18.
250. Nasipak, B.T., et al., *Opposing calcium-dependent signalling pathways control skeletal muscle differentiation by regulating a chromatin remodelling enzyme.* Nature communications, 2015. **6**: p. 7441.
251. Shieh, W.M., et al., *Poly(ADP-ribose) polymerase null mouse cells synthesize ADP-ribose polymers.* The Journal of biological chemistry, 1998. **273**(46): p. 30069-72.
252. Lange, S.S., D.L. Mitchell, and K.M. Vasquez, *High mobility group protein B1 enhances DNA repair and chromatin modification after DNA damage.* Proceedings of the National Academy of Sciences of the United States of America, 2008. **105**(30): p. 10320-5.
253. Osmanov, T., I. Ugrinova, and E. Pasheva, *The chaperone like function of the nonhistone protein HMGB1.* Biochemical and Biophysical Research Communications, 2013. **432**(2): p. 231-5.
254. Nishibuchi, G., et al., *N-terminal phosphorylation of HP1alpha increases its nucleosome-binding specificity.* Nucleic acids research, 2014. **42**(20): p. 12498-511.
255. Luijsterburg, M.S., et al., *Heterochromatin protein 1 is recruited to various types of DNA damage.* The Journal of cell biology, 2009. **185**(4): p. 577-86.
256. Quenet, D., et al., *The histone subcode: poly(ADP-ribose) polymerase-1 (Parp-1) and Parp-2 control cell differentiation by regulating the transcriptional intermediary factor TIF1beta and the heterochromatin protein HP1alpha.* FASEB journal : official publication of the Federation of American Societies for Experimental Biology, 2008. **22**(11): p. 3853-65.
257. Krishnakumar, R., et al., *Reciprocal binding of PARP-1 and histone H1 at promoters specifies transcriptional outcomes.* Science, 2008. **319**(5864): p. 819-21.
258. Klune, J.R., et al., *HMGB1: endogenous danger signaling.* Molecular medicine, 2008. **14**(7-8): p. 476-84.
259. Polanska, E., S. Pospisilova, and M. Stros, *Binding of histone H1 to DNA is differentially modulated by redox state of HMGB1.* PloS one, 2014. **9**(2): p. e89070.
260. Stros, M., et al., *Histone H1 Differentially Inhibits DNA Bending by Reduced and Oxidized HMGB1 Protein.* PloS one, 2015. **10**(9): p. e0138774.
261. Lehmann, M., et al., *ARTD1-induced poly-ADP-ribose formation enhances PPARgamma ligand binding and co-factor exchange.* Nucleic acids research, 2015. **43**(1): p. 129-42.
262. Zuchegna, C., et al., *Mechanism of retinoic acid-induced transcription: histone code, DNA oxidation and formation of chromatin loops.* Nucleic acids research, 2014. **42**(17): p. 11040-55.
263. Perillo, B., et al., *DNA oxidation as triggered by H3K9me2 demethylation drives estrogen-induced gene expression.* Science, 2008. **319**(5860): p. 202-6.
264. Natoli, G., S. Ghisletti, and I. Barozzi, *The genomic landscapes of inflammation.* Genes & development, 2011. **25**(2): p. 101-6.
265. Keating, S.T. and A. El-Osta, *Transcriptional regulation by the Set7 lysine methyltransferase.* Epigenetics, 2013. **8**(4): p. 361-72.
266. Li, Y., et al., *Role of the histone H3 lysine 4 methyltransferase, SET7/9, in the regulation of NF-kappaB-dependent inflammatory genes. Relevance to diabetes and inflammation.* The Journal of biological chemistry, 2008. **283**(39): p. 26771-81.
267. Nishioka, K., et al., *Set9, a novel histone H3 methyltransferase that facilitates transcription by precluding histone tail modifications required for heterochromatin formation.* Genes & development, 2002. **16**(4): p. 479-89.
268. Minotti, R., A. Andersson, and M.O. Hottiger, *ARTD1 Suppresses Interleukin 6 Expression by Repressing MLL1-Dependent Histone H3 Trimethylation.* Molecular and cellular biology, 2015. **35**(18): p. 3189-99.
269. Wang, V.Y., et al., *The transcriptional specificity of NF-kappaB dimers is coded within the kappaB DNA response elements.* Cell reports, 2012. **2**(4): p. 824-39.
270. Rhoades, A.R., S. Ruone, and T. Formosa, *Structural features of nucleosomes reorganized by yeast FACT and its HMG box component, Nhp6.* Molecular and cellular biology, 2004. **24**(9): p. 3907-17.
271. Gloire, G. and J. Piette, *Redox regulation of nuclear post-translational modifications during NF-kappaB activation.* Antioxidants & redox signaling, 2009. **11**(9): p. 2209-22.

272. Morgan, M.J. and Z.G. Liu, *Crosstalk of reactive oxygen species and NF-kappaB signaling.* Cell research, 2011. **21**(1): p. 103-15.
273. Oliveira-Marques, V., et al., *Role of hydrogen peroxide in NF-kappaB activation: from inducer to modulator.* Antioxidants & redox signaling, 2009. **11**(9): p. 2223-43.
274. Wong, C.K., et al., *Role of p38 MAPK and NF-kB for chemokine release in coculture of human eosinophils and bronchial epithelial cells.* Clinical and experimental immunology, 2005. **139**(1): p. 90-100.
275. Shen, Q., R. Zhang, and N.R. Bhat, *MAP kinase regulation of IP10/CXCL10 chemokine gene expression in microglial cells.* Brain research, 2006. **1086**(1): p. 9-16.
276. Son, Y.H., et al., *Roles of MAPK and NF-kappaB in interleukin-6 induction by lipopolysaccharide in vascular smooth muscle cells.* Journal of cardiovascular pharmacology, 2008. **51**(1): p. 71-7.
277. Olsnes, C., J. Olofsson, and H.J. Aarstad, *MAPKs ERK and p38, but not JNK phosphorylation, modulate IL-6 and TNF-alpha secretion following OK-432 in vitro stimulation of purified human monocytes.* Scandinavian journal of immunology, 2011. **74**(2): p. 114-25.
278. Zauberman, A., et al., *Stress activated protein kinase p38 is involved in IL-6 induced transcriptional activation of STAT3.* Oncogene, 1999. **18**(26): p. 3886-93.
279. Smale, S.T., *Selective transcription in response to an inflammatory stimulus.* Cell, 2010. **140**(6): p. 833-44.
280. Whitmarsh, A.J., *Regulation of gene transcription by mitogen-activated protein kinase signaling pathways.* Biochimica et biophysica acta, 2007. **1773**(8): p. 1285-98.
281. McCall, C.E., et al., *Gene-specific epigenetic regulation in serious infections with systemic inflammation.* Journal of innate immunity, 2010. **2**(5): p. 395-405.
282. McCall, C.E., et al., *Epigenetics, bioenergetics, and microRNA coordinate gene-specific reprogramming during acute systemic inflammation.* Journal of leukocyte biology, 2011. **90**(3): p. 439-46.
283. Wang, X. and G.E. Sonenshein, *Induction of the RelB NF-kappaB subunit by the cytomegalovirus IE1 protein is mediated via Jun kinase and c-Jun/Fra-2 AP-1 complexes.* Journal of virology, 2005. **79**(1): p. 95-105.

6 Acknowledgements

First, I would like to thank my doctoral thesis supervisor Prof. Michael Hottiger, for giving me the chance to perform my doctoral thesis in his laboratory, and for his many ideas, advices and support.

Further, I would like to thank my thesis committee members Prof. Anne Müller, PD Dr. Hans-Dietmar Beer and Prof. Marco Bianchi, for valuable input during my committee meetings. Additionally, many thanks to Dr. Stephan Christen, for his great help with writing and structuring the manuscripts. Acknowledgments goes to Prof. Bernhard Lüscher, who kindly agreed to be the external reviewer of this thesis.

Thanks to all members of the IVBMB and CABMM for support, equipment, suggestions and discussions, as well as a great working atmosphere. Many thanks to former and present members of the Hottiger lab, I enjoyed to work with you. The scientific input has been great, everyone has been extremely helpful, and we had lots of fun times.

Special thanks to the extended hood; Flo, Schelli, Eveli, Fridi, Matthias and Natasa, for making me feel at home in Zürich, always making me laugh and for help through difficult times. Thank you Linda, for many conversations about science and life, and for your wise advises. Thanks to my ZUF-ladies for your energy, our adventures, and for refreshing and distracting my mind when needed. Thank you Dani, for your caring support and patience throughout these past years.

Last but not least, many thanks and lots of love goes to family and friends at home in Sweden and other places of Europe, caring for me no matter what, no matter when, no matter where.

7 Curriculum Vitae

Personal information

Surname:	ANDERSSON
Name:	Anneli Elisabeth
Address:	Hardturmstr. 124a, CH-8005 Zurich
Phone:	+41-774373902
Email:	anneli.andersson@uzh.ch
Date of Birth:	4th June 1985
Place of Birth:	Stenungsund, Sweden
Nationality:	Swedish

Education

April 2011 – present

Doctoral Studies in Molecular Biology

- Institute of Veterinary Biochemistry and Molecular Biology, University of Zürich, Switzerland
- Ph.D Program in Molecular Life Sciences, LSZGS
  Thesis title: HMGB1 Controls ARTD1 during Stress Signaling

September 2006 – March 2011

Academic Studies, Master of Science

- University of Lund, Sweden
- Field of study: Biotechnology
- Degree: Master of Science
- Thesis title: Simultaneous determination of glucose and lactose in whole blood for clinical monitoring using a thermal biosensor

September 2009 – July 2010

Student exchange year

- Science de la vie, EPFL, Lausanne

September 2001 – June 2004

Secondary School

- Nösnäsgymnasiet, Stenungsund, Sweden
- Student degree, Natural Sciences

Grants

July 2014	Travel reimbursement of the MLS Ph.D program for the Cold Spring Harbor meeting on The PARP Family & Friends; Gene Regulations and Beyond.
September 2013	Travel reimbursement of the MLS Ph.D program for the Spetses Summer School on Chromatin and Systems Biology.

List of Publications

Minotti, R.*, **Andersson, A.***, & Hottiger, M. O. (2015). ARTD1 Supresses Interleukin 6 Expression by Repressing MLL1-Dependent Histone H3 Trimethylation. *Molecular and Cellular Biology,* **35** (18): 3189-99 *equal contribution

Chen, Q., **Andersson, A.,** Mecklenburg, M. & Xie, B. (2015). A biosensing strategy for the rapid detection and classification of antibiotic resistance. *Biosensors and Bioelectronics,* **73**: 251-5

Kassner, I., **Andersson, A.,** Fey, M., Tomas, M., Ferrando-May, E. & Hottiger, M.O. (2013). SET7/9-dependent methylation of ARTD1 at K508 stimulates poly-ADP-ribose formation after oxidative stress. *Open Biology,* **3** (10): 120173

Chen, Y., **Andersson, A**., Mecklenburg, M., Xie, B. & Zhou, Y. (2011). Dual-signal analysis eliminates requirement for milk sample pretreatment. *Biosensors and Bioelectronics,* **29** (1): 115-8

Ballmer-Hofer, K., **Andersson, A. E.**, Ratcliffe, L. E. & Berger, P. (2011). Neuropilin-1 promotes VEGFR-2 trafficking through Rab11 vesicles thereby specifying signal output. *Blood,* **118** (3): 816-826